Title

ASPECTS OF QUANTUM FIELD THEORY

ISBN

9798190929355

Author

Li, Yanyan

Publication Date

2026-09-11

Peer reviewed|Thesis/dissertation

UNIVERSITY OF CALIFORNIA
Los Angeles

ASPECTS OF QUANTUM FIELD THEORY

A dissertation submitted in partial satisfaction
of the requirements for the degree
Doctor of Philosophy in Physics

by

Yanyan Li

2026

ABSTRACT OF THE DISSERTATION

ASPECTS OF QUANTUM FIELD THEORY

by

Yanyan Li
Doctor of Philosophy in Physics
University of California, Los Angeles, 2026
Professor Thomas Dumitrescu, Chair

This dissertation is a collection of work on several aspects of quantum field theory, including the worldsheet dynamics of vortex strings, non-invertible symmetries and their holographic realizations, and quantum field theory in non-integer spacetime dimensions.

In Chapter 2, we study string excitations and the effective worldsheet action of Abrikosov–Nielsen–Olesen vortex strings in the four-dimensional Abelian Higgs model. We analyze fluctuations around the vortex and determine the worldsheet spectrum. Interestingly, we find a light dilaton in the type-I regime and a light axion in the type-II regime. By integrating out the massive modes, we compute the $\mathcal{O}(K^4)$ Wilson coefficients of the effective string action and compare the resulting theory with flux-tube S-matrix bootstrap constraints and Yang–Mills confining strings. We also discuss the implications of this comparison for the dual superconductor picture of confinement.

In Chapter 3, we study non-invertible defects in two-dimensional S_N orbifold CFTs. We construct universal defects which do not depend on the details of the seed CFT and hence exist in any orbifold CFT. Additionally, we investigate non-universal defects arising from the topological defects of the seed CFT. We argue that there exist universal defects that are non-trivial in the large-N limit, making them relevant for the $\mathrm{AdS}_3/\mathrm{CFT}_2$ correspondence. We then focus on $\mathrm{AdS}_3 \times S^3 \times \mathcal{M}_4$ with one unit of NS–NS flux and propose an explicit

realization of these defects on the worldsheet. We also calculate the entanglement entropy in symmetric orbifold CFTs in the presence of topological defects.

In Chapter 4, we revisit the old problem of analytically continuing quantum field theories to fractional dimension $d \in \mathbb{C}$. We observe that common theories such as QCD and QED have branch cuts in the complex d plane. In particular, many operators in their low-energy CFTs have OPEs and scaling dimensions that jump as a function of d.

The dissertation of Yanyan Li is approved.

Michael Gutperle

Eric D'Hoker

Per Kraus

Thomas Dumitrescu, Committee Chair

University of California, Los Angeles

2026

To my parents

TABLE OF CONTENTS

LIST OF FIGURES

LIST OF TABLES

ACKNOWLEDGMENTS

I would first like to thank my advisor, Thomas Dumitrescu, for his constant guidance, support, and encouragement throughout my Ph.D. I have learned a lot from Thomas, both about physics and from the way he approaches research, explains ideas, and gives talks. His precision, attention to detail and high standards have strongly influenced the way I work. When a problem seemed too difficult, he encouraged me to understand what made it difficult rather than shy away from it, which changed the way I face hard problems. I am grateful for everything he taught me and for all the time and care he has given me.

I have been very lucky to work with Diego Delmastro, Amey Gaikwad, Michael Gutperle, Julio Parra-Martinez, Dikshant Rathore, and Konstantinos Roumpedakis. I am grateful for everything I learned from them. I am especially grateful to Michael and Julio for the time they spent working with me, for everything they taught me, and for their advice and encouragement at important moments, which meant a lot to me.

I would also like to thank the faculty in the UCLA group, especially Zvi Bern, Eric D'Hoker, Per Kraus, Mikhail Solon, and Ryan Thorngren, for their guidance, support, and many insightful discussions, and for making the group such a stimulating place to be.

I would also like to thank Diego Medrano and Pedro Vieira for an earlier collaboration. I am especially grateful to Pedro for the opportunity to work on an interesting project, for his support, and for everything I learned from him. I am also grateful to Pedro and Timothy Hsieh for hosting me as a visitor at Perimeter Institute during my Ph.D. applications. I am very grateful to Chi-Ming Chang for hosting me as a visitor at Tsinghua University during part of the first year of my Ph.D., during the pandemic.

I am also very grateful to the many fellow postdocs and graduate students who have been part of the UCLA group during my time here, including Adar, Amey, Anna, Callum, Calvin, Chris, Christina, Diego, Dikshant, Enrico, Giulia, Jack, Konstantinos, Lukas, Luis, Matteo, Michael, Niccolò, Nick, Noah, Paokuan, Pierluigi, Po-Shen, Ranveer, Richard, Ruben, Seol-hwa, Sriram, Stephen, Suzanne, Sven, Theo, Trevor, Tushar, Yifan, and Zhengdi. I greatly enjoyed our many discussions and conversations, both in and outside of physics, and all the time we spent together over the years. It was a real pleasure to have them around.

I am also deeply grateful to all my friends outside the UCLA group for their friendship, support, advice, encouragement, and companionship. In particular, I would like to thank Baiyun, Guoqing, Ivana, Jiachen, Kasia, Katie, Keyou, Ruochen, Ruoshui, Shuqian, Xiaoyu, Yang, and Yongjia. Their support has meant a lot to me and helped me through many difficult moments over the years.

I am grateful for the financial support provided by the UCLA Department of Physics and Astronomy, the Mani L. Bhaumik Institute for Theoretical Physics, the Robert Finkelstein Fellowship in Theoretical Physics at UCLA, the U.S. Department of Energy (currently under Award No. DE-SC0009937), and the Simons Collaboration on Global Categorical Symmetries.

Finally, I would like to thank my parents and my family for their unconditional love and support throughout my life, for always being willing to listen to my worries and frustrations and to share in my joys, for always being proud of me, and for giving me the courage and confidence to follow my own path.

CONTRIBUTION OF AUTHORS

Chapter 2 reviews ongoing work in collaboration with Thomas Dumitrescu and Amey Gaikwad. Chapter 3 reports on joint work with Michael Gutperle, Dikshant Rathore, and Konstantinos Roumpedakis [6, 7]. Chapter 4 reports on joint work with Diego Delmastro and Dikshant Rathore [8].

VITA

2011–2015	B.S. in Physics, Lanzhou University.
2015–2018	M.Sc. Physics, Lanzhou University.
2018–2019	M.Sc. Physics, Perimeter Institute and University of Waterloo.
2020–2026	Ph.D. Physics, University of California, Los Angeles (Expected).

PUBLICATIONS

Thomas T. Dumitrescu, Amey Gaikwad, **Yan-Yan Li**, "Effective Action of Long Magnetic Flux Tubes," Forthcoming.

Diego Delmastro, **Yan-Yan Li**, Dikshant Rathore, "Does QFT make sense in non-integer dimensions?," arXiv:2607.05338 (2026).

Michael Gutperle, **Yan-Yan Li**, Dikshant Rathore, Konstantinos Roumpedakis, "A note on entanglement entropy and topological defects in symmetric orbifold CFTs," JHEP 09 (2024) 010, arXiv:2406.10967.

Michael Gutperle, **Yan-Yan Li**, Dikshant Rathore, Konstantinos Roumpedakis, "Non-invertible symmetries in S_N orbifold CFTs and holography," JHEP 09 (2024) 110, arXiv:2405.15693.

William Donnelly, Elise LePage, **Yan-Yan Li**, Andre Pereira, Vasudev Shyam, "Quantum corrections to finite radius holography and holographic entanglement entropy," JHEP 05

(2020) 006, arXiv:1909.11402.

Wen-Di Guo, Shao-Wen Wei, **Yan-Yan Li**, Yu-Xiao Liu, “Complexity growth rates for AdS black holes in massive gravity and $f(R)$ gravity,” arXiv:1703.10468.

Yan-Yan Li, Yu-Peng Zhang, Wen-Di Guo, Yu-Xiao Liu, “Fermion localization mechanism with derivative geometrical coupling on branes,” arXiv:1701.02429.

CHAPTER 1

Introduction

Understanding strongly coupled quantum field theories remains one of the central challenges in theoretical physics. Many fundamental questions, including renormalization-group flows and infrared phases, the fate of symmetries, and possible dualities, are difficult to answer directly from the microscopic theory. A broad range of analytic and numerical approaches provide complementary perspectives on strongly coupled systems. Among these, extended objects provide a particularly useful probe. They are ubiquitous in quantum field theory, and their rich structures offer important insights into strongly coupled and non-perturbative phenomena. The problems studied in this dissertation focus in particular on the dynamics of long strings and on topological defects as realizations of generalized symmetries, with applications to confinement, holography, and duality. We also investigate quantum field theory in non-integer spacetime dimensions as a complementary perspective.

We first turn to the worldsheet dynamics of long strings and their connection to confinement, which we study in Chapter 2. A hallmark of confinement is the formation of flux tubes, or confining strings, which at long distances behave as weakly coupled strings described by effective string theory. A long-standing open question is whether such flux tubes admit a UV-complete worldsheet description. While lattice simulations, integrability, and bootstrap analyses have revealed rich structures, analytic control remains limited, motivating the study of more tractable models.

In this spirit, the Abelian Higgs model provides a semiclassical laboratory for studying the dynamics of long strings. Its Abrikosov–Nielsen–Olesen (ANO) vortex strings carry quantized magnetic flux and can be studied semiclassically. At sufficiently low energies, their worldsheet dynamics are described by the translational Nambu–Goldstone modes. The leading dynamics are governed by the universal Nambu–Goto action, while higher-derivative corrections contain model-dependent Wilson coefficients that encode information about the underlying four-dimensional theory [9, 10].

We systematically study the effective string theory of ANO vortex strings in the four-dimensional Abelian Higgs model. We analyze the fluctuation spectrum, including the translational zero modes and massive excitations such as the dilaton, axion, and higher-spin modes, and determine their couplings to the translational Goldstone modes. By integrating out the massive excitations, we derive their contributions to the first non-universal $\mathcal{O}(K^4)$ higher-curvature corrections to the effective string action.

The resulting Wilson coefficients place the Abelian Higgs model within the space allowed by the flux-tube S-matrix bootstrap [3, 4, 11] and make it possible to compare its worldsheet dynamics directly with expectations for Yang–Mills confining strings. Interestingly, the analysis reveals an inversion relative to confining-string expectations: the light axion appears in the repulsive type-II regime, while the attractive type-I regime contains a light dilaton. This indicates that the minimal Abelian Higgs model is not a compelling dual description of Yang–Mills confining strings. At the same time, it provides a controlled setting for studying effective string dynamics and develops a framework that can be generalized to more complicated theories. This comparison clarifies the relation between ANO vortex strings and Yang–Mills confining strings and motivates extending the analysis to softly broken Seiberg–Witten theory [12, 13], where the dual superconductor picture is realized more directly.

We next turn to non-invertible symmetries and topological defects, which we study in Chapter 3. In recent years, generalized and non-invertible symmetries have provided valuable insights into the dynamics of quantum field theories [14–16]. At the core of these generalizations is the realization of symmetries as extended topological operators. Unlike ordinary symmetry operators, their fusion need not be group-like, leading to a richer algebraic structure and new constraints on quantum field theories. This naturally raises the question of how such generalized symmetry structures are realized in holographic duals.

Symmetric orbifold CFTs provide a particularly useful setting for addressing these questions. They are constructed by taking N copies of a seed CFT and gauging the permutation group S_N [17]. Gauging this non-abelian symmetry gives rise to a universal class of non-invertible topological defects whose existence does not depend on the detailed dynamics of the seed theory. In addition, topological defects of the seed theory give rise to non-universal defects in the orbifold theory.

Symmetric orbifold CFTs are also important in $\mathrm{AdS}_3/\mathrm{CFT}_2$. They exhibit large-$N$ factorization and, for suitable seed theories, admit a holographic description in terms of string theory on $\mathrm{AdS}_3 \times S^3 \times \mathcal{M}_4$. In particular, the symmetric orbifold point is related to a tensionless string background with one unit of NS–NS flux [18–21]. This makes it natural to ask which non-invertible defects remain nontrivial at large N and whether they admit a direct realization in the dual string theory.

We construct the universal defects and study their fusion properties, defect Hilbert spaces, and Ward identities. We also investigate non-universal defects inherited from topological defects of the seed theory. We identify universal defects that remain nontrivial at large N and propose a worldsheet realization of them as topological defects in the dual tensionless string theory. This provides a concrete setting for studying non-invertible symmetries in holography. We also study entanglement entropy in symmetric orbifold CFTs in the presence of both universal and non-universal topological defects, providing an additional observable that probes their structure and a possible holographic observable.

We finally turn to quantum field theory in non-integer spacetime dimensions, which we study in Chapter 4. Analytic continuation in the spacetime dimension is familiar from dimensional regularization and the ϵ-expansion. More conceptually, it provides a way to connect quantum field theories defined in different integer dimensions and to ask in what sense they can be regarded as members of the same family.

A natural question is whether one can define a family of QFTs, labeled by $d \in \mathbb{C}$, that agrees with the corresponding theories at several distinct integer dimensions, rather than only in an infinitesimal neighborhood of a particular integer value of d. This question is interesting both for practical reasons, such as dimensional regularization, and for understanding how physical phenomena and operator data evolve as the spacetime dimension is varied.

In Chapter 4, we revisit this problem and show that even vector-like theories such as QCD and QED encounter important subtleties. The main obstruction to a naive analytic continuation is the existence of low-rank exceptions: identities that hold only at special integer dimensions can cause correlation functions and operator data to change qualitatively as d is varied. As a result, expressions that are analytic at generic d need not reproduce the correct theory at low integer dimensions.

We study these effects explicitly in interacting gauge theories using large-N_f methods. Low-rank isomorphisms can make operators that transform differently at generic d become equivalent at special integer dimensions, allowing them to mix and leading to branch points in the complex d plane. Consequently, there is in general no single analytic expression for an operator dimension that reproduces the correct answer at every integer dimension. Instead, the continuation naturally develops multiple analytic branches. In particular, we find that common theories such as QCD and QED have branch cuts in the complex d plane, and that scaling dimensions and OPE data can jump as functions of d.

CHAPTER 2

Effective Action of Long Magnetic Vortex Strings

2.1 Review of Effective String Theory

Given a gapped 3+1d QFT, we consider the low-energy modes of an infinite, stable string of tension T. The string is nearly straight, with a weakly-curved worldsheet relative to the string scale,

$$\ell_s = \frac{1}{\sqrt{T}} \ . \tag{2.1.1}$$

A perfectly straight string spontaneously brakes the 3+1d Poincaré symmetry as follows,

$$\mathrm{ISO}(3,1) \quad \longrightarrow \quad \mathrm{ISO}(1,1) \times SO(2) \ . \tag{2.1.2}$$

Here $\mathrm{ISO}(1,1)$ is the Poincaré symmetry along the 1+1d worldsheet, while $SO(2)$ rotates the plane transverse to the string. This leads to two massless Nambu–Goldstone bosons (NGBs) on the worldsheet, which describe its transverse fluctuations. Generically, they are the only massless excitations on the string,[1] and their low-energy effective field theory on the worldsheet is often referred to as effective string theory (see [9, 10] for a review). It takes the form a suitable derivative expansion, constrained by locality and the symmetries of the problem. The latter are conveniently described by viewing the worldsheet, with coordinates $\sigma^\alpha (\alpha = 0, 1)$, as an embedded, oriented surface $X^\mu(\sigma)$ in 3+1d spacetime:

- The global Poincaré symmetry acts on X^μ as it does on the 3+1d spacetime coordinates.

[1] Additional gapless bosons (fermions) naturally arise if the string spontaneously breaks additional continuous (super-) symmetries. They can also arise as a result of fine-tuning, e.g. at the BPS point of the Abelian Higgs model to be discussed below.

- Worldsheet diffeomorphisms, under which $X^\mu(\sigma)$ is as a scalar, are a gauge redundancy.

It is convenient to explicitly fix static gauge,

$$X^0(\sigma^\alpha) = \sigma^0 \ , \qquad X^3(\sigma^\alpha) = \sigma^1 \ , \tag{2.1.3}$$

where the physical degrees of freedom are the two transverse NGBs,[2]

$$X^i(\sigma^\alpha) \ , \qquad i = 1, 2 \ . \tag{2.1.4}$$

Effective string theory is naturally phrased in terms of the extrinsic geometry of the worldsheet; the building blocks are the induced metric $h_{\alpha\beta} = h_{(\alpha\beta)}$ and the extrinsic curvature $K^i_{\alpha\beta} = K^i_{(\alpha\beta)}$, whose covariant definitions are

$$h_{\alpha\beta} \equiv \eta_{\mu\nu}\, \partial_\alpha X^\mu \partial_\beta X^\nu \ , \tag{2.1.5}$$

$$K^\mu_{\alpha\beta} \equiv \nabla_\alpha \partial_\beta X^\mu = K^i_{\alpha\beta} n^\mu_i \ . \tag{2.1.6}$$

Here $\mu = 0, 1, 2, 3$ are bulk Minkowski indices, and $\eta_{\mu\nu} = + - - -$ is the Minkowski metric. The n^μ_i $(i = 1, 2)$ are orthonormal vectors that frame the 2d normal bundle of the worldsheet. Here ∇_α denotes the worldsheet covariant derivative.

In static gauge, the induced metric only depends on derivatives of the physical transverse NGBs in (2.1.4),

$$h_{\alpha\beta} = \eta_{\alpha\beta} + \partial_\alpha X^i \partial_\beta X_i = \eta_{\alpha\beta} - \partial_\alpha X^i \partial_\beta X^i \ , \tag{2.1.7}$$

where $\eta_{\alpha\beta} = \mathrm{diag}(+, -)$ is the flat Minkowski metric on the world sheet, defined using the same conventions as the bulk Minkowski metric $\eta_{\mu\nu} = \mathrm{diag}(+, -, -, -)$. Here we introduce a convention that we use throughout the paper: whenever two repeated normal bundle indices are in the same position, such as the two raised i indices in (2.1.7), they are summed over $i = 1, 2$ without any minus signs from the spatial components of the metric. This serves

[2] Throughout the paper we use lowercase Latin letters $i, j, k, \ldots = 1, 2$ to denote normal bundle indices; Greek letters $\alpha, \beta, \gamma, \ldots = 0, 1$ from the beginning of the alphabet to denote 1+1d worldsheet Lorentz indices; and (only rarely) Greek letters $\mu, \nu, \ldots = 0, 1, 2, 3$ from the middle of the alphabet for 3+1d Lorentz indices.

to make all minus signs coming from our negative spatial metric convention explicit, rather than hiding them in lowered indices such as $X_i = -X^i$.

Following [9], we classify terms in the effective action by their weight, defined as the number of derivatives minus the number of X-fields. Since any possible term in the action has non-negative weight,[3] the derivative expansion can be organized by increasing weight. We will only discuss terms of weight zero, two, and four:[4]

- There is a unique weight zero term: it is the familiar Nambu-Goto action,

$$S^{(0)}_{\rm NG} = -T \int d^2\sigma \sqrt{-h} \ , \tag{2.1.8}$$

  where $h \equiv \det(h_{\alpha\beta})$. The leading-weight equations of motion that follow from it are

$$h^{\alpha\beta} \nabla_\alpha \nabla_\beta X^\mu = h^{\alpha\beta} K^\mu_{\alpha\beta} = 0 \ . \tag{2.1.9}$$

- At weight two, there are two independent invariants, [5]

$$S^{(2)} = \int d^2\sigma \sqrt{-h} \left(c_R R + c_{K^2} (K^i_{\alpha\beta} h^{\alpha\beta})^2 \right) \ . \tag{2.1.10}$$

  Here, R is the worldsheet Ricci scalar constructed out of $h_{\alpha\beta}$. The Gauss-Bonnet theorem implies that the Einstein–Hilbert term is topological in two dimensions and therefore does not contribute to the (local) dynamics. Furthermore, the term $(K^i_{\alpha\beta} h^{\alpha\beta})^2$ is proportional to the Nambu-Goto equations of motion (2.1.9) and can be removed by a field redefinition, at the expense of generating higher-weight terms. Thus, there are effectively no operators to consider at weight two, as emphasized in [9].

- The first nontrivial corrections arise at weight four,

$$S^{(4)} = \int d^2\sigma \sqrt{-h} \left(c_{K^4} K^i_{\alpha\beta} K^{\alpha\beta j} K^i_{\gamma\delta} K^{\gamma\delta j} + c_{R^2} R^2 \right) \ , \tag{2.1.11}$$

---

[3] This follows from 3+1d translations, which act on the X-fields by constant shifts.

[4] The symmetries of the problem do not allow terms with odd weight [9].

[5] An alternative basis at weight two consists of $K^i_{\alpha\beta} K^{i\alpha\beta}$ and $K^{i\alpha}_{\alpha} K^{i\beta}_{\beta}$. The Gauss–Codazzi equation allows us to trade these operators for R and $K^i_{\alpha\beta} K^{i\alpha\beta}$.

where the coefficients c_{K^4} and c_{R^2} are model-dependent and encode information about the ultraviolet (UV) completion. Note that, following the conventions spelled out below (2.1.7), we sum the repeated indices in (2.1.11) $i, j = 1, 2$ without any signs.

2.1.1 Flux-tube S-matrix bootstrap

Having identified c_{R^2} and c_{K^4} as the first model dependent coefficients in the effective string action, it is natural to ask which values are compatible with a consistent ultraviolet completion. The flux-tube S-matrix bootstrap constrains these coefficients by imposing unitarity, crossing symmetry, and analyticity on the scattering amplitudes of the translational Goldstones [3, 4]. The resulting allowed region provides a parameter space in which different microscopic realizations of effective strings may be identified and compared.

In the conventions of [3], the weight-four interactions are parametrized by the dimensionless coefficients α_3 and β_3. They are related to the coefficients in Eq. (2.1.11) through the following linear combinations, with c_{R^2} and c_{K^4} measured in units of $1/T$

$$\alpha_3 = \frac{1}{8} T \left(2c_{R^2} + 3c_{K^4}\right) \ , \qquad \beta_3 = -\frac{1}{8} T \left(2c_{R^2} + c_{K^4}\right) \ . \tag{2.1.12}$$

In this work, we focus on ANO strings in the Abelian Higgs model and compute the Wilson coefficients c_{R^2} and c_{K^4} explicitly, allowing us to place the ANO strings in the (α_3, β_3) bootstrap parameter space. We first show the result in this parameter space. Figure 2.6 shows the trajectory of the fundamental $n = 1$ string as the Abelian Higgs model parameter β, defined in (2.2.4), is varied. In the following sections, we develop the mode analysis used to compute these coefficients, and return to the physical interpretation of the trajectory in Sec. 2.6.

2.2 Abelian Higgs Model

2.2.1 Lagrangian, Vacuum Structure and Symmetries

We study the Abelian Higgs model (AHM) in four spacetime dimensions $(+,-,-,-)$, describing a single complex scalar field ϕ, carrying unit charge under the gauge group $U(1)$. The action is given by

$$S = \int d^4x \left(-\frac{1}{4} F_{\mu\nu}F^{\mu\nu} + (D_\mu \phi)^\dagger D^\mu \phi - \frac{\lambda}{4}(|\phi|^2 - v^2)^2 \right) \ , \tag{2.2.1}$$

where $D_\mu = \partial_\mu + ieA_\mu$ and $F_{\mu\nu} = \partial_\mu A_\nu - \partial_\nu A_\mu$. The strength of the electromagnetic coupling is given by e and λ denotes the strength of the scalar self-coupling. They are both dimensionless constants. The scales in the theory are set by the dimensionful real constant v. We study the theory with $\lambda > 0$, which ensures that the theory undergoes the Higgs mechanism.

The Abelian Higgs model has a unique vacuum. In the infrared, at weak coupling, the theory undergoes Higgs mechanism and the $U(1)$ gauge group is Higgsed down to nothing. The Higgs vacuum is trivial and gapped. The vacuum condition at weak coupling, upto gauge transformations is given by,

$$A_\mu = 0 \ , \qquad \phi = v \ . \tag{2.2.2}$$

The spectrum in the Higgs vacuum consists of a massive vector boson with mass m_V and a massive Higgs boson with mass m_H, given by,

$$m_V^2 = 2e^2v^2 \ , \qquad m_H^2 = \lambda v^2 \ . \tag{2.2.3}$$

We can define a unique dimensionless ratio β given by,

$$\beta = \frac{m_H^2}{m_V^2} = \frac{\lambda}{2e^2} \ . \tag{2.2.4}$$

It is standard to refer to the $\beta < 1$ parameter regime as the type-I regime and $\beta > 1$ as the type-II regime. For the Abelian Higgs model under consideration, $\beta = 1$ is a special point and is referred to as the Bogomol'nyi-Prasad-Sommerfield (BPS point) [22, 23]. We can show that the AHM at the BPS point is the bosonic part of a supersymmetric QED theory [24].

The Abelian Higgs model enjoys a global $U(1)^{(1)}_m$ one form symmetry [25] (the superscript is to identify the symmetry as one-form). The subscript m denotes that the symmetry is magnetic - the objects charged under the symmetry are 't Hooft lines. The associated current and the charge n are given by:

$$*j^{(2)}_m = \frac{ef^{(2)}}{2\pi} \ , \qquad n \equiv \frac{1}{2\pi}\int_{\Sigma_{xy}} da \in \mathbb{Z} \ . \tag{2.2.5}$$

Due to compact nature of the global symmetry group, the charge $n \in \mathbb{Z}$. Conservation of current follows from the Bianchi identity. Finite tension string states are created by acting the 't Hooft line operator on the vacuum. Here, $U(1)^{(1)}_m$ is unbroken in the Higgs vacuum and the strings realize this vacuum at long distances.

2.2.2 Rescaling

It is convenient to rescale the fields according to

$$\phi \to \frac{\phi}{e} \ , \qquad A_\mu \to \frac{1}{e}A_\mu \ , \qquad \widetilde{v} = ev \ . \tag{2.2.6}$$

Under this rescaling, the action becomes

$$S = \frac{1}{e^2}\int d^4x\left(-\frac{1}{4}F_{\mu\nu}F^{\mu\nu} + (D_\mu\phi)^\dagger D^\mu\phi - \frac{\beta}{2}(|\phi|^2 - \widetilde{v}^2)^2\right) \ . \tag{2.2.7}$$

where $D_\mu = \partial_\mu + iA_\mu$ and β is defined in (2.2.4). In what follows, we work with this rescaled action (2.2.7) and set $\widetilde{v} = 1$. The characteristic mass scale of the theory is then ev, and any dimensionful quantity can be restored by dimensional analysis in powers of ev.

This form of the action also makes manifest that the overall factor $1/e^2$ controls the semiclassical expansion, so that e^2 serves as the loop-counting parameter. After canonically normalizing the fluctuations, interaction vertices carry positive powers of e; in general, an n-point interaction is of order e^{n-2}.

2.2.3 String construction

In any flux sector n, there can be many string configurations, but there would be a ground state or lowest energy string expected to be the most stable one. In order to solve for this minimum energy configuration, we need to study PDEs of the Lagrangian (2.2.7) subject to the flux constraint (2.2.5). This can be done, however in this paper, we will be interested in axially symmetric strings where the magnetic flux is collimated along the $z-$direction. This is a very standard simplifying assumption and the PDEs simplify to solving ODEs. For a recent review, see [26].

In this section, we briefly review axially symmetric finite tension strings charged under $U(1)_m^{(1)}$. In the context of the AHM, these strings have been extensively studied in literature. In a non relativistic setting, these string solutions were first discussed in [27] and in a relativistic context in [28]. These string solutions are the Abrikosov-Nielsen-Oleson (ANO) strings. For a comprehensive textbook treatment, see [29, 30] and references therein. See [26] for a recent discussion and review.

While the background string solutions are essentially unchanged in a non relativistic setting, Lorentz symmetry becomes important when formulating the low energy effective action in the string worldsheet. For a cartoon of an axially symmetric string configuration, see figure 2.1.

It is best to work in cylindrical coordinates (r, θ, z). Consider a string aligned along the z-axis, carrying charge n (2.2.5) under $U(1)_m^{(1)}$, referred to as the n-string. Requirement of rotational symmetry [6] requires that the string configuration is also static and extends uniformly along the $z-$axis. The axially symmetric ANO n-string ansatz is given by :

$$\phi(x) = f(r)e^{in\theta} \ , \quad A_\theta = n\alpha(r) \ , \quad A_i = 0 \ \ (i = t, r, z) \ , \quad f(r), \ \alpha(r) : \mathbb{R}_{\geq 0} \to \mathbb{R} \ . \tag{2.2.8}$$

With this in mind, it makes more sense to talk about the string tension T, defined as the energy per unit length of a string, rather than the energy E. They are related by $E = TL$,

[6] For the ANO string, rotational symmetry refers to the preserved diagonal combination of a spatial rotation around the $z-$axis and a compensating global gauge transformation.

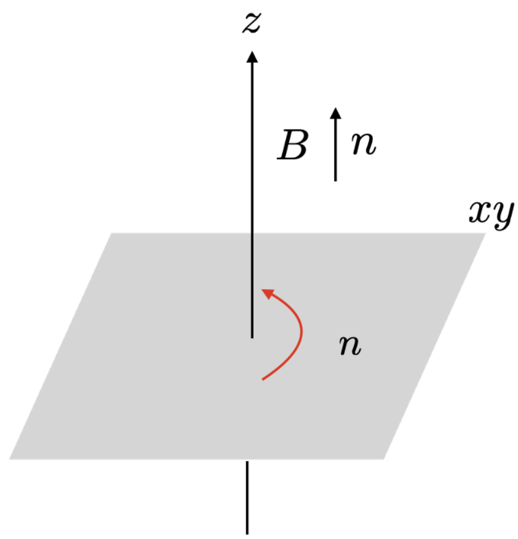

Figure 2.1: A schematic depiction of an axially symmetric ANO vortex carrying $n-$units of conserved magnetic flux along the $z-$axis. The red arrow illustrates the winding of the Higgs field around the vortex. Requiring finite tension fixes the winding number to be n, matching the total magnetic flux carried by the string.

where L is the length of the string. Henceforth in the paper, we will solely talk about the string tension. Additionally, note that only A_θ is activated and the string solution entails magnetic flux F_{12} flowing in the $z-$direction.

The winding of the scalar field is directly correlated with n, the units of flux flowing through the string. This is a consequence of the finite tension requirement. In addition to this, finiteness also sets the boundary conditions for the fields at radial infinity, where the string realizes the Higgs vacuum. Regularity of $A_\theta\,,\phi$ sets the boundary conditions at the origin. Together these imply the following boundary conditions:

$$f(0)=0\ , \qquad \alpha(0)=0\ , \qquad f(\infty)=1\ , \qquad \alpha(\infty)=-1\ . \tag{2.2.9}$$

Substituting the string ansatz into the Hamiltonian for the theory, gives us the following expression for the tension of a string carrying n units of magnetic flux,

$$T_n = 2\pi v^2 \int_0^\infty drr\left(\frac{n^2\alpha'^2}{2r^2} + f'^2 + \frac{f^2n^2}{r^2}(1+\alpha)^2 + \frac{\beta}{2}(f^2-1)^2\right)\ . \tag{2.2.10}$$

Table 2.1: Fundamental string tension T_1 (2.2.10) for 20 values of β in units of $v = 1$.

β	String tension
0.1	4.0150
0.2	4.5610
0.3	4.9296
0.4	5.2159
0.5	5.4533
0.6	5.6576
0.7	5.8379
0.8	6.0000
0.9	6.1475
1	6.2832

β	String tension
2	7.2681
3	7.9225
4	8.4232
5	8.8327
6	9.1811
7	9.4852
8	9.7558
9	9.9998
10	10.2223

To get the equations of motion governing the dynamics of $f(r)\,,\alpha(r)$, we extremize the expression for the string tension (2.2.10), which yields:

$$f'' + \frac{f'}{r} - \frac{n^2(\alpha+1)^2}{r^2} f - \beta f(f^2-1) = 0\ , \tag{2.2.11a}$$

$$\alpha'' - \frac{\alpha'}{r} - 2f^2(\alpha+1) = 0\ . \tag{2.2.11b}$$

These equations do not admit analytic solutions and need to be solved numerically[31]. Analytic solutions can be written down in the infinite flux limit [26]. Consequently, we obtain the behaviour of ANO strings as parameters $n\,,\,\beta$ are varied. We can substitute these numerical solutions into (2.2.10) and obtain the tension of an $n-$string. For the fundamental $n = 1$ string, the tension is tabulated in (2.1) for various values of β.

The BPS point $\beta = 1$ is special and the AHM can be embedded into an $\mathcal{N} = 1$ theory which admits $1/2-$BPS strings. At this point, the following first order equations are true, and in turn imply the full equations of motion (2.2.11),

$$\frac{n}{\sqrt{2}r}\alpha' = \sqrt{\frac{\beta}{2}}(f^2-1)\ , \qquad f' = \frac{n}{r}f(1+\alpha)\ . \tag{2.2.12}$$

The string tension at the BPS point, takes a simple form:

$$T_n = 2\pi v^2 n \ . \tag{2.2.13}$$

For the AHM, the parameter $\beta = m_H^2/m_V^2$ governs the dynamics of the ANO strings. Its most immediate physical consequence is the static interaction between two parallel strings separated by a large distance. This interaction arises from the exchange of the two massive fields of the theory: the Higgs scalar of mass m_H, whose exchange is attractive, and the massive vector of mass m_V, whose exchange is repulsive. At separations large compared to the string width, each field contributes a screened potential set by its mass, and the interaction energy per unit length of two unit-winding strings takes the form

$$\mathcal{U}(d) \ \simeq \ \frac{1}{2\pi}\Big[\, q_V^2\, K_0(m_V d) \ - \ q_S^2\, K_0(m_H d)\Big] , \qquad m_V d,\ m_H d \ \gg \ 1\,, \tag{2.2.14}$$

where K_0 is the modified Bessel function and $q_V, q_S > 0$ are the magnetic and scalar charges of a single string, fixed by the large-distance tails of the profiles $\alpha(r)$ and $f(r)$.[7] Because $K_0(\mu d) \sim \sqrt{\pi/2\mu d}\, e^{-\mu d}$ for large argument, the term with the lighter exchanged field is the longer ranged and controls the sign of the force at large d. In the type-I regime ($\beta < 1$) the Higgs is lighter than the vector, $m_H < m_V$, so the attractive scalar exchange dominates and the strings attract. In the type-II regime ($\beta > 1$) the vector is lighter, $m_V < m_H$, the repulsive exchange dominates, and the strings repel. At the BPS point $\beta = 1$ the two masses coincide, $m_H = m_V$, and the first-order equations (2.2.12) relate the profiles so that the charges are equal, $q_S = q_V$; the attractive and repulsive contributions then cancel identically, and the strings exert no force on one another at any separation. This vanishing of the static force is the origin of the moduli space of static multi-string configurations at critical coupling. See [29] for a textbook treatment.

The same competition controls the stability of an n-string with $n > 1$. The relevant comparison is between a single string of winding n, with tension T_n, and the configuration

[7] Explicitly, the profiles approach the vacuum as $1 - f(r) \sim \frac{q_S}{2\pi} K_0(m_H r)$ and $n\big(1 + \alpha(r)\big) \sim \frac{q_V}{2\pi}\, m_V\, r\, K_1(m_V r)$ at large r, which defines the two charges. The corresponding force per unit length is $\mathcal{F}(d) = -\mathcal{U}'(d) = \frac{1}{2\pi}\big[q_V^2 m_V K_1(m_V d) - q_S^2 m_H K_1(m_H d)\big]$.

of n unit strings infinitely separated from one another, whose total tension is nT_1. The sign of the binding energy $E_b \equiv nT_1 - T_n$ is dictated by the inter-string force. In the type-I regime the strings attract, so they bind: it is energetically favorable for them to coalesce, $T_n < nT_1$, and the n-string is a genuine stable bound state–the minimum-tension configuration carrying n units of flux. In the type-II regime the strings repel, so $T_n > nT_1$, and the n-string is unstable; it lowers its energy by splitting into n fundamental strings that fly apart to infinity, leaving the competing configuration of tension $nT_1 < T_n$. At the BPS point the strings are free, the binding energy vanishes, and $T_n = nT_1$, as follows from the BPS tension (2.2.13); the n-string is then only marginally stable, sitting exactly at threshold, where it can be deformed into separated strings at no cost.

These energetic statements have a direct counterpart in the worldsheet fluctuation spectrum of the n-string, analyzed in Section 2.4. The marginal directions at the BPS point appear there as massless zero modes–the moduli labeling the relative positions of the constituent strings–whereas in the type-II regime these same modes acquire negative mass squared and become tachyonic, the fluctuation-level signal of the decay of the n-string into its separated constituents. Equivalently, in terms of the one-form symmetry $U(1)^{(1)}_m$ under which the string carries charge n, the n-string is a stable, below-threshold bound state in the type-I regime and an unstable, above-threshold state in the type-II regime.

2.3 Perturbing the ANO String

At sufficiently long distances, the dynamics of an ANO string is captured by the Nambu-Goldstone massless modes associated with its broken transverse translations (Also see section 2.1). Fluctuations of the Higgs and gauge fields around the ANO string background (reviewed in section 2.2), give rise to a richer worldsheet spectrum, which in addition to the translational zero modes, also includes normalizable massive bound states localized on the string, and continuum scattering states.

The purpose of this section is to identify this worldsheet spectrum around ANO strings for various values of the parameters λ , e , and n. We do this by expanding the scalar and gauge fields around the classical ANO string background and diagonalizing the quadratic fluctuation operator. The resulting transverse eigenfunctions can be normalizable, associated with localized excitations on the string worldsheet, or non-normalizable, associated with scattering states are smoothly connected with the bulk spectrum . The corresponding eigenvalues of these eigenfunctions gives the worldsheet masses of these excitations.

Concretely, we write

$$\phi(x) = \widetilde{\phi}(r,\theta) + \delta\phi(x) \ , \tag{2.3.1}$$

$$\phi^*(x) = \widetilde{\phi}^*(r,\theta) + \delta\phi^*(x) \ , \tag{2.3.2}$$

$$A_\mu(x) = \widetilde{A}_\mu(r,\theta) + \delta A_\mu(x) \ , \tag{2.3.3}$$

where tildes denote the background solution (2.2.8). Since the minimum energy rotationally symmetric ANO string is static and extends uniformly along the $z-$direction, it is independent of the worldsheet coordinates and hence, the dependence of a fluctuation on (t,z) can be separated from its transverse profile. The fluctuation modes can therefore be chosen with definite worldsheet momentum, reducing the four-dimensional problem to a transverse eigenvalue problem in the (r,θ) plane.

Throughout this section, it is useful to use complex coordinates in the transverse plane,

$$x^\pm = \frac{1}{\sqrt{2}}\, r\, e^{\pm i\theta} \ , \qquad A_+ = \frac{e^{-i\theta}}{\sqrt{2}}\Big(A_r - i\frac{A_\theta}{r}\Big) \ , \qquad A_- = \frac{e^{i\theta}}{\sqrt{2}}\Big(A_r + i\frac{A_\theta}{r}\Big) \ , \tag{2.3.4}$$

so that $A_\pm$ carry definite transverse spin, just like $\partial_\pm$. We use Cartesian coordinates (t,x,y,z), cylindrical coordinates (t,r,θ,z), and complex transverse coordinates (t,x^+,x^-,z) interchangeably. The ANO background gauge field then becomes

$$\widetilde{A}_+ = -\, i\, \frac{n\alpha}{\sqrt{2}\, r}\, e^{-i\theta} \ , \qquad \widetilde{A}_- = i\, \frac{n\alpha}{\sqrt{2}\, r}\, e^{i\theta} \ . \tag{2.3.5}$$

Before turning to the detailed derivation, we summarize the structure of the fluctuation problem. A useful way to organize the fluctuations is to separate the components that transform differently under the symmetries preserved by the string. The scalar fluctuation mixes with the transverse gauge-field components, while the gauge-field components along the string form a separate channel:

$$\text{Dilaton channel:} \quad \delta\Psi^{(D)} \equiv \begin{pmatrix} \delta\phi \\ \delta\phi^* \\ \delta A_+ \\ \delta A_- \end{pmatrix} , \qquad \text{Axion channel:} \quad \delta A_\alpha \ , \tag{2.3.6}$$

where $\alpha \in \{t, z\}$ denotes the worldsheet directions. This terminology is motivated by the worldsheet parity of the physical modes: after imposing the physical constraints, modes in the dilaton channel are even under worldsheet parity, $P_\parallel = +$, while modes in the axion channel are odd, $P_\parallel = -$. Thus the two channels correspond to the two worldsheet-parity sectors of the fluctuation problem. The separation into these two channels follows from the symmetries preserved by the string background, which we review in Sec. 2.3.1.

After gauge fixing, the physical fluctuation problem takes a simple form. The dilaton channel is governed by a coupled operator acting on the scalar fluctuation and the transverse gauge-field components,

$$\mathcal{D}\,\delta\Psi^{(D)} = 0 \ , \tag{2.3.7}$$

together with the gauge constraint (2.3.16). The axion channel is governed by the wave equation for the worldsheet gauge-field components,

$$\left(\Box + 2|\widetilde{\phi}|^2\right)\delta A_\alpha = 0 \ , \qquad \nabla^\alpha \delta A_\alpha = 0 \ . \tag{2.3.8}$$

The role of these equations is to determine which four-dimensional fluctuations become physical fields on the string. After separating the worldsheet dependence and decomposing the transverse profiles into angular-momentum eigenmodes, the two channels reduce to transverse eigenvalue problems,

$$\mathcal{D}_\perp \chi^{(D)}_{m,N_m} = \left(M^{(D)}_{m,N_m}\right)^2 \chi^{(D)}_{m,N_m} \ , \tag{2.3.9}$$

$$\left(-\nabla_i^2 + 2|\widetilde{\phi}|^2\right)\chi^{(A)}_{m,N_m} = \left(M^{(A)}_{m,N_m}\right)^2 \chi^{(A)}_{m,N_m} \ . \tag{2.3.10}$$

Here $m \in \mathbb{Z}$ labels transverse spin, and N_m labels the radial excitation level in a fixed spin sector. The eigenfunctions χ_{m,N_m} describe the transverse profiles of the modes, while the eigenvalues M_{m,N_m} are their masses from the worldsheet point of view. Thus the four-dimensional fluctuation problem becomes a classification of two-dimensional particles living on the string: zero modes, possible massive bound states localized near the core, and continuum scattering states.

The rest of this section derives this structure systematically. In Sec. 2.3.1 we identify the symmetries preserved by the ANO string and use them to classify the fluctuation modes. In Sec. 2.3.2 we discuss the gauge choices needed to isolate the physical modes and derive the quadratic action. We then solve the fluctuation problem in the dilaton channel in Sec. 2.3.3 and in the axion channel in Sec. 2.3.4.

2.3.1 Unbroken symmetries and quantum numbers

The fluctuation operator inherits the symmetries preserved by the ANO string background. These symmetries organize the fluctuation modes into sectors labeled by transverse spin and parity. This classification will be useful both for solving the transverse eigenvalue problem and for identifying the resulting worldsheet particles.

The ANO string lies in a fixed sector of the magnetic one-form symmetry $U(1)^{(1)}_m$, labeled by its flux n. Within this fixed-flux sector, the small fluctuations are classified by the spacetime symmetries preserved by the straight string. These are

$$O(1,1)_\parallel \times O(2)_\perp \ . \tag{2.3.11}$$

The continuous part consists of the worldsheet Poincaré group $ISO(1,1)$ acting on (t,z) and the transverse rotations $SO(2)_\perp$. In addition, the background preserves two discrete reflections. We now spell out the action of these symmetries on the fluctuation fields, since these transformation laws determine the quantum numbers used throughout the spectrum analysis.

- **Transverse rotations $SO(2)_\perp$.** A rotation $R(\alpha) \in SO(2)_\perp$ acts as $\theta \to \theta + \alpha$

and is accompanied by a compensating rigid $U(1)$ gauge transformation under which $\widetilde{\phi} \to e^{-in\alpha}\widetilde{\phi}$ and $\widetilde{A}_\mu \to \widetilde{A}_\mu$, leaving the background invariant. Under this combined action the fluctuations transform as[8]

$$\begin{pmatrix} \delta\phi(\theta) \\ \delta\phi^*(\theta) \\ \delta A_+(\theta) \\ \delta A_-(\theta) \\ \delta A_z(\theta) \\ \delta A_0(\theta) \end{pmatrix} \longmapsto \begin{pmatrix} e^{-in\alpha} & & & & & \\ & e^{in\alpha} & & & & \\ & & e^{i\alpha} & & & \\ & & & e^{-i\alpha} & & \\ & & & & 1 & \\ & & & & & 1 \end{pmatrix} \begin{pmatrix} \delta\phi(\theta+\alpha) \\ \delta\phi^*(\theta+\alpha) \\ \delta A_+(\theta+\alpha) \\ \delta A_-(\theta+\alpha) \\ \delta A_z(\theta+\alpha) \\ \delta A_0(\theta+\alpha) \end{pmatrix} . \tag{2.3.12}$$

The generator of $SO(2)_\perp$ is the transverse spin, which we denote by $m \in \mathbb{Z}$.

- **Transverse parity CR_y.** This transformation combines the spatial reflection $y \mapsto -y$ (equivalently $\theta \mapsto -\theta$) with complex conjugation of the fields. Under CR_y,

$$\begin{pmatrix} \delta\phi(\theta) \\ \delta\phi^*(\theta) \\ \delta A_+(\theta) \\ \delta A_-(\theta) \\ \delta A_z(\theta) \\ \delta A_0(\theta) \end{pmatrix} \longmapsto \begin{pmatrix} 0 & 1 & & & & \\ 1 & 0 & & & & \\ & & 0 & -1 & & \\ & & -1 & 0 & & \\ & & & & -1 & 0 \\ & & & & 0 & -1 \end{pmatrix} \begin{pmatrix} \delta\phi(-\theta) \\ \delta\phi^*(-\theta) \\ \delta A_+(-\theta) \\ \delta A_-(-\theta) \\ \delta A_z(-\theta) \\ \delta A_0(-\theta) \end{pmatrix} . \tag{2.3.13}$$

Its eigenvalues are $P_\perp = \pm 1$, denoting even and odd transverse parity. In what follows we use $P_\perp$ interchangeably for the operator CR_y and for its eigenvalue, the meaning being clear from context. This reflection exchanges the spin-m and spin-$(-m)$ sectors.

- **Worldsheet parity R_z.** This is the reflection $z \mapsto -z$ along the string axis, a

[8] We display only the dependence on the angular coordinate θ, the sole coordinate affected by the $SO(2)_\perp$ transformation; the fluctuations remain functions of all spacetime coordinates. Unspecified entries in the transformation matrices vanish.

worldsheet parity transformation. Under R_z,

$$\begin{pmatrix} \delta\phi(z) \\ \delta\phi^*(z) \\ \delta A_+(z) \\ \delta A_-(z) \\ \delta A_z(z) \\ \delta A_0(z) \end{pmatrix} \longmapsto \begin{pmatrix} 1 & & & & & \\ & 1 & & & & \\ & & 1 & & & \\ & & & 1 & & \\ & & & & -1 & \\ & & & & & 1 \end{pmatrix} \begin{pmatrix} \delta\phi(-z) \\ \delta\phi^*(-z) \\ \delta A_+(-z) \\ \delta A_-(-z) \\ \delta A_z(-z) \\ \delta A_0(-z) \end{pmatrix} . \tag{2.3.14}$$

Its eigenvalues are $P_\parallel = \pm 1$, denoting even and odd worldsheet parity; as with $P_\perp$, we use $P_\parallel$ for both the operator and its eigenvalue.

We now translate these transformation laws into the labels used for the spectrum. The transverse reflection does not commute with the rotations. Instead,

$$CR_y\, R(\alpha)\, CR_y^{-1} = R(-\alpha) \ , \tag{2.3.15}$$

so CR_y maps a spin-m mode to a spin-$(-m)$ mode. Therefore modes with $m \neq 0$ arrange into degenerate $O(2)_\perp$ doublets $\{m, -m\}$. By contrast, the $m = 0$ modes are $O(2)_\perp$ singlets and can be chosen to have definite transverse parity $P_\perp$.

Including the worldsheet parity, the $m = 0$ modes carry the quantum numbers $0^{P_\perp P_\parallel}$. For $|m| \neq 0$, one may either work in a spin-diagonal basis and label the doublets by $m^{P_\parallel}$, or in a parity-diagonal basis and label them by $|m|^{P_\perp P_\parallel}$. Throughout, we take the representative $m > 0$ of each doublet and write $m^{P_\parallel}$, with the partner of spin $-m$ obtained by acting with $P_\perp$.

This symmetry analysis explains the channel decomposition summarized above. As we show in Sec. 2.3.2, the fluctuations $(\delta\phi, \delta\phi^*, \delta A_+, \delta A_-)$ and δA_α decouple: the former constitute the dilaton channel and are even under worldsheet parity, $P_\parallel = +$, while the physical modes of the latter constitute the axion channel and are odd, $P_\parallel = -$. Thus the fluctuation problem splits into two independent worldsheet-parity sectors, which organize both the eigenvalue problems solved below and the worldsheet spectrum analyzed in Sec. 2.4.

2.3.2 Gauge fixing and the quadratic action

Gauge fixing plays an important role in the fluctuation analysis. Around the vortex background, the scalar and gauge-field fluctuations mix, and the gauge redundancy must be removed before identifying the physical worldsheet modes. We will use two gauge choices, adapted to different purposes. The unitary gauge makes the physical spectrum manifest and will be used in the mode analysis below. The background gauge is more convenient for the effective-action calculation in Sec. 2.5; it also matches the gauge choice commonly used in fluctuation analyses of vortices, making contact with previous work more direct.

2.3.2.1 Unitary gauge

We first use a unitary gauge adapted to the vortex background. It is defined by the condition

$$\nabla^i \delta A_i + i\widetilde{\phi}^* \delta\phi - i\widetilde{\phi}\delta\phi^* = 0 \ , \tag{2.3.16}$$

which fixes the gauge redundancy completely. Expanding the action about the ANO background in this gauge gives

$$S_{\mathrm{U}} = -T_n \int d^2\sigma + S_{\mathrm{U}}^{(2)} + S_{\mathrm{U}}^{(3)} + S_{\mathrm{U}}^{(4)} \ , \tag{2.3.17}$$

with the quadratic part[9]

$$S_{\mathrm{U}}^{(2)} = \frac{1}{2e^2} \int d^4x \left[\delta\Psi^{(D)\dagger}\, \mathcal{D}\, \delta\Psi^{(D)} + \delta A_\alpha \left(\Box + 2|\widetilde{\phi}|^2 \right) \delta A^\alpha + (\nabla^\alpha \delta A_\alpha)^2 \right] \ , \tag{2.3.18}$$

where the dilaton-channel fluctuation vector and its conjugate are

$$\delta\Psi^{(D)} = \begin{pmatrix} \delta\phi \\ \delta\phi^* \\ \delta A_+ \\ \delta A_- \end{pmatrix} \ , \qquad \delta\Psi^{(D)\dagger} = \begin{pmatrix} \delta\phi^* & \delta\phi & \delta A_- & \delta A_+ \end{pmatrix} \ . \tag{2.3.19}$$

[9] The gauge-fixing condition holds for physical configurations and may equally be imposed off shell to simplify the action.

The quadratic fluctuation operator takes the form

$$\mathcal{D} = \begin{pmatrix} \mathcal{O} & (1-\beta)\widetilde{\phi}^2 & 2iD_-\widetilde{\phi} & 2iD_+\widetilde{\phi} \\ (1-\beta)\widetilde{\phi}^{*2} & \mathcal{O}^* & -2iD_-\widetilde{\phi}^* & -2iD_+\widetilde{\phi}^* \\ -2iD_+\widetilde{\phi}^* & 2iD_+\widetilde{\phi} & -\Box - 2|\widetilde{\phi}|^2 & 0 \\ -2iD_-\widetilde{\phi}^* & 2iD_-\widetilde{\phi} & 0 & -\Box - 2|\widetilde{\phi}|^2 \end{pmatrix} , \tag{2.3.20}$$

where $D_\pm\widetilde{\phi} = (\partial_\pm + i\widetilde{A}_\pm)\widetilde{\phi}$ and $D_\pm\widetilde{\phi}^* = (\partial_\pm - i\widetilde{A}_\pm)\widetilde{\phi}^*$ are the background covariant derivatives, and

$$\mathcal{O} = -\Box + 2i\widetilde{A}_i\partial_i - \widetilde{A}_i\widetilde{A}_i - \beta(2|\widetilde{\phi}|^2 - 1) - |\widetilde{\phi}|^2 \ . \tag{2.3.21}$$

There are two important consequences of the quadratic action. First, the fluctuation problem separates into the two channels introduced above. The four-component field $\delta\Psi^{(D)}$ and the worldsheet gauge components δA_α do not mix in (2.3.18). This decoupling is the dynamical realization of the symmetry decomposition discussed in Sec. 2.3.1.[10]

Second, the equations of motion must be supplemented by constraints that remove unphysical gauge components. In the dilaton channel, the physical fluctuations are the solutions of

$$\mathcal{D}\,\delta\Psi^{(D)} = 0 \ , \tag{2.3.22}$$

that also obey the gauge condition (2.3.16). In the axion channel, the physical modes obey an additional transversality constraint. The linearized equation for δA_α following from (2.3.18) is

$$\Box\delta A_\alpha - \nabla_\alpha\nabla^\beta\delta A_\beta + 2|\widetilde{\phi}|^2\delta A_\alpha = 0 \ . \tag{2.3.23}$$

Taking its worldsheet divergence yields

$$\left(-\nabla_i^2 + 2|\widetilde{\phi}|^2\right)\nabla^\alpha\delta A_\alpha = 0 \ , \tag{2.3.24}$$

[10] By a *channel* we mean the decomposition into $(\delta\phi, \delta\phi^*, \delta A_+, \delta A_-)$ and δA_α; by a *sector* we mean the further classification by spin within a channel.

and since the operator $-\nabla_i^2 + 2|\widetilde{\phi}|^2$ is positive it has only the trivial kernel, giving the constraint

$$\nabla^\alpha \delta A_\alpha = 0 \ . \tag{2.3.25}$$

Substituting this back into the linearized equation reduces it to the wave equation

$$(\Box + 2|\widetilde{\phi}|^2)\delta A_\alpha = 0 \ . \tag{2.3.26}$$

Thus the physical dilaton modes solve (2.3.22) subject to (2.3.16), while the physical axion modes solve (2.3.26) subject to (2.3.25).

The cubic and quartic terms in $S_{\rm U}$ encode the interactions among the fluctuations,

$$\begin{aligned} S_{\rm U}^{(3)} = \frac{1}{e^2}\int d^4x \, \big[&- i\,\delta A_\mu\,\delta\phi^*\,\nabla^\mu\delta\phi + \delta A_\mu\,\delta A^\mu\,\delta\phi^*\,\widetilde{\phi} \\ &+ \widetilde{A}_\mu\,\delta A^\mu\,\delta\phi^*\,\delta\phi - \beta\,\delta\phi\,\delta\phi\,\delta\phi^*\,\widetilde{\phi}^*\big] + \text{h.c.} \ , \end{aligned} \tag{2.3.27}$$

$$S_{\rm U}^{(4)} = \frac{1}{e^2}\int d^4x \left(\delta A_\mu\,\delta A^\mu\,\delta\phi\,\delta\phi^* - \frac{1}{2}\beta\,\delta\phi^2\,(\delta\phi^*)^2\right) \ , \tag{2.3.28}$$

where "h.c." denotes the Hermitian conjugate of the preceding terms. These interaction terms do not affect the linearized spectrum studied in this section. The cubic vertices (2.3.27) will enter the derivation of the K^4 worldsheet action in Sec. 2.5.

2.3.2.2 Background gauge

For the effective-action calculation in Sec. 2.5, it is convenient to use instead the background gauge [32–34]

$$\partial^\mu \delta A_\mu + (i\delta\phi\widetilde{\phi}^* - i\delta\phi^*\widetilde{\phi}) = 0 \ , \tag{2.3.29}$$

the standard choice in fluctuation analyses around solitonic backgrounds. It corresponds to the R_ξ gauge at $\xi = 1$, with gauge-fixing term

$$\mathcal{L}_{\rm gf} = -\frac{1}{2}\left(\partial_\mu\delta A^\mu + i\,\delta\phi\,\widetilde{\phi}^* - i\,\delta\phi^*\,\widetilde{\phi}\right)^2 \ , \tag{2.3.30}$$

whose virtue is to cancel the derivative mixing between the gauge and scalar fluctuations, rendering the kinetic terms diagonal. Unlike the unitary gauge, this condition leaves a residual gauge freedom, compensated by Faddeev–Popov ghosts with Lagrangian

$$\mathcal{L}_{\rm gh} = \bar{c}\left(-\Box - 2|\widetilde{\phi}|^2 - \delta\phi\,\widetilde{\phi}^* - \delta\phi^*\,\widetilde{\phi}\right) c\ , \tag{2.3.31}$$

where $c, \bar{c}$ are the ghost and anti-ghost fields. Including the gauge-fixing and ghost terms, the action expanded about the ANO background reads

$$S_{\rm B} = -T_n \int d^2\sigma + S^{(2)}_{\rm B} + S^{(3)}_{\rm U} + S^{(4)}_{\rm U} + S^{\rm ghost}\ , \tag{2.3.32}$$

with

$$S^{(2)}_{\rm B} = \frac{1}{e^2}\int d^4x\ \frac{1}{2}\left[(\delta\Psi^{(D)})^\dagger \mathcal{D}\delta\Psi^{(D)} + \delta A_\alpha\left(\Box + 2|\widetilde{\phi}|^2\right)\delta A^\alpha\right]\ , \tag{2.3.33}$$

and

$$S^{\rm ghost} = \frac{1}{e^2}\int d^4x\ \left[-\bar{c}(\Box + 2|\widetilde{\phi}|^2)c + \left(-\bar{c}\delta\phi\,\widetilde{\phi}^* c + \text{h.c.}\right)\right]\ . \tag{2.3.34}$$

The two gauge choices lead to closely related quadratic actions, $S^{(2)}_{\rm U}$ and $S^{(2)}_{\rm B}$, and must give the same gauge-invariant physics. In particular, the dilaton-channel operator $\mathcal{D}$ is the same in the two descriptions, and the worldsheet gauge-field components are governed by the same transverse operator $-\nabla_i^2 + 2|\widetilde{\phi}|^2$. These operators, however, should not be identified directly with the physical spectrum before gauge redundancy is removed. In the unitary-gauge description, the physical subspace is selected directly by imposing the gauge constraint (2.3.16) in the dilaton channel and the transversality condition (2.3.25) in the axion channel. In the background-gauge description, the corresponding projection is implemented by keeping the Faddeev–Popov ghosts and using BRST cohomology. For both this section and the next, we use the unitary gauge, where the physical constraints are imposed directly. We will return to the background gauge in Sec. 2.5, where it is more convenient for deriving the effective action.

2.3.3 Dilaton channel

To determine the full fluctuation spectrum, we must solve the eigenvalue problems in both the dilaton and axion channels. We begin with the dilaton channel. The physical modes are solutions of the transverse eigenvalue problem for $\mathcal{D}_\perp$, subject to the unitary-gauge constraint (2.3.16). We first reduce the four-dimensional linearized equation to a transverse eigenvalue problem, then decompose the modes into transverse-spin sectors, and finally use the resulting eigenfunctions to expand the four-dimensional fluctuations in worldsheet fields.

2.3.3.1 Transverse reduction and spin decomposition

Because the ANO background is independent of (t, z), we exploit the worldsheet translational invariance to separate off the longitudinal dependence,[11]

$$\delta\phi = e^{iMt}\,\delta\phi_\perp(r,\theta)\ , \tag{2.3.35a}$$

$$\delta\phi^* = e^{-iMt}\,\delta\phi^*_\perp(r,\theta)\ , \tag{2.3.35b}$$

$$\delta A_i = e^{iMt}\,\delta A_{i,\perp}(r,\theta)\ , \tag{2.3.35c}$$

where the subscript $\perp$ denotes dependence on the transverse coordinates alone. We set the longitudinal momentum to $p_z = 0$; the general solution is recovered by a Lorentz boost along z. Inserting (2.3.35) into the linearized equations (2.3.22) gives the transverse eigenvalue problem

$$\mathcal{D}_\perp \begin{pmatrix} \delta\phi_\perp \\ \delta\phi^*_\perp \\ \delta A_{+,\perp} \\ \delta A_{-,\perp} \end{pmatrix} = M^2 \begin{pmatrix} \delta\phi_\perp \\ \delta\phi^*_\perp \\ \delta A_{+,\perp} \\ \delta A_{-,\perp} \end{pmatrix}\ , \tag{2.3.36}$$

where $\mathcal{D}_\perp$ is the transverse part of $\mathcal{D}$, obtained by stripping off the worldsheet Laplacian,

$$\mathcal{D} = -\nabla^2_\alpha\, I_{4\times4} - \mathcal{D}_\perp\ , \tag{2.3.37}$$

[11] Since $\mathcal{D}$ commutes with ∂_t, its eigenmodes can be chosen with definite frequency. Only the coupled four-component block must share a common eigenvalue M^2, and hence a common factor e^{iMt}; the ansatz below makes this explicit.

and given explicitly by

$$\mathcal{D}_\perp = \begin{pmatrix} \mathcal{K} & (\beta-1)\widetilde{\phi}^2 & -2iD_-\widetilde{\phi} & -2iD_+\widetilde{\phi} \\ (\beta-1)\widetilde{\phi}^{*2} & \mathcal{K}^* & 2iD_-\widetilde{\phi}^* & 2iD_+\widetilde{\phi}^* \\ 2iD_+\widetilde{\phi}^* & -2iD_+\widetilde{\phi} & -\nabla_i^2+2|\widetilde{\phi}|^2 & 0 \\ 2iD_-\widetilde{\phi}^* & -2iD_-\widetilde{\phi} & 0 & -\nabla_i^2+2|\widetilde{\phi}|^2 \end{pmatrix} , \tag{2.3.38}$$

with all spatial indices lowered, and

$$\mathcal{K} = -\nabla_i^2 - 2i\,\widetilde{A}_i\nabla_i + \widetilde{A}_i^2 + \beta\,(2|\widetilde{\phi}|^2-1) + |\widetilde{\phi}|^2 \,. \tag{2.3.39}$$

We next exploit the transverse rotational symmetry $SO(2)_\perp$, organizing the fields into eigenmodes of angular momentum $m \in \mathbb{Z}$,[12]

$$\delta\phi_\perp = \sum_{m\in\mathbb{Z}} s_m(r)\, e^{i(n+m)\theta} \,, \qquad \delta\phi_\perp^* = \sum_{m\in\mathbb{Z}} s_{-m}^*(r)\, e^{-i(n-m)\theta} \,, \tag{2.3.40a}$$

$$\delta A_{+,\perp} = \sum_{m\in\mathbb{Z}} ig_m(r)\, e^{i(m-1)\theta} \,, \qquad \delta A_{-,\perp} = -\sum_{m\in\mathbb{Z}} ig_{-m}^*(r)\, e^{i(m+1)\theta} \,. \tag{2.3.40b}$$

The factors of $\pm i$ in the expansions of $\delta A_\pm$ are chosen so that the reduced operator is manifestly real, while the pairing of s_m with s_{-m}^* and of g_m with g_{-m}^* makes the complex-conjugation relations among the fields manifest at the level of mode functions; both features streamline the numerical treatment. Inserting (2.3.40) into (2.3.36) decouples the spins, reducing $\mathcal{D}_\perp$ in each spin-m sector to a real radial operator $\mathcal{R}_{(m)}$,

$$\mathcal{R}_{(m)} \begin{pmatrix} s_m \\ s_{-m}^* \\ g_m \\ g_{-m}^* \end{pmatrix} = M^2 \begin{pmatrix} s_m \\ s_{-m}^* \\ g_m \\ g_{-m}^* \end{pmatrix} , \tag{2.3.41}$$

with

$$\mathcal{R}_{(m)} = \begin{pmatrix} D_+ & V & M_1 & M_2 \\ V & D_- & M_2 & M_1 \\ M_1 & M_2 & C_+ & 0 \\ M_2 & M_1 & 0 & C_- \end{pmatrix} , \tag{2.3.42}$$

[12] The phase factors $e^{i(n\pm m)\theta}$ encode the effect of the background winding, ensuring that each term carries definite transverse spin m.

and entries

$$D_{\pm} = -\nabla_r^2 + \frac{(n(\alpha+1) \pm m)^2}{r^2} + f^2 + \beta(2f^2 - 1) \;, \tag{2.3.43a}$$

$$C_{\pm} = -\nabla_r^2 + \frac{(-1 \pm m)^2}{r^2} + 2f^2 \;, \qquad V = (\beta - 1)\, f^2 \;, \tag{2.3.43b}$$

$$M_1 = \sqrt{2}\left(\frac{df}{dr} - \frac{nf}{r}(1+\alpha)\right) \;, \qquad M_2 = -\sqrt{2}\left(\frac{df}{dr} + \frac{nf}{r}(1+\alpha)\right) \;, \tag{2.3.43c}$$

where $\nabla_r^2 \equiv \partial_r^2 + \frac{1}{r}\partial_r$. Together with the angular factors in (2.3.40), the radial eigenfunctions of (2.3.41) furnish a basis of solutions $\chi^{(D)}_{m,N_m}$ of the transverse eigenvalue equation

$$\mathcal{D}_{\perp}\chi^{(D)}_{m,N_m} = \left(M^{(D)}_{m,N_m}\right)^2 \chi^{(D)}_{m,N_m} \;, \tag{2.3.44}$$

where m labels the spin, N_m the radial level, and the superscript D the dilaton channel; we suppress these labels when no confusion arises. Not all of these solutions are physical: the gauge condition (2.3.16) must still be imposed, to which we turn next.

2.3.3.2 Spin sectors, transverse parity, and the gauge constraint

The transverse-parity relation $CR_y\, R(\alpha)\, CR_y^{-1} = R(-\alpha)$ ties the spin-m and spin-$(-m)$ sectors together. At the level of the radial operator,

$$\mathcal{R}_{(-m)} = \mathcal{C}\,\mathcal{R}_{(m)}\,\mathcal{C}^{-1} \;, \qquad \mathcal{C} \equiv \begin{pmatrix} 0 & 1 & 0 & 0 \\ 1 & 0 & 0 & 0 \\ 0 & 0 & 0 & 1 \\ 0 & 0 & 1 & 0 \end{pmatrix} \;, \tag{2.3.45}$$

so that if ζ is an eigenmode of $\mathcal{R}_{(m)}$ with eigenvalue M^2, then $\mathcal{C}\zeta$ is an eigenmode of $\mathcal{R}_{(-m)}$ with the same eigenvalue. It therefore suffices to take $m \geq 0$, the spin-$(-m)$ partner following from $\mathcal{C}$; this is the radial counterpart of the degenerate $O(2)_{\perp}$ doublets. Since $\mathcal{R}_{(m)}$ is real, we may take its eigenvectors real,[13] attaching conjugate coefficients to build complex solutions.

The spin-0 sector is special: there $\mathcal{R}_{(0)}$ commutes with transverse parity,

$$[\mathcal{R}_{(0)}, \mathcal{C}] = 0 \;, \tag{2.3.46}$$

[13] The gauge condition is likewise real and transforms compatibly under $\mathcal{C}$, so this restriction is consistent with the construction of the physical mode basis.

so it decomposes into the two eigenspaces of $\mathcal{C}$, labeled by $P_\perp = \pm$. For a complex mode $(s_0, s_0^*, g_0, g_0^*)^T$ these are

$$P_\perp = + : \quad \begin{pmatrix} \mathrm{Re}\, s_0 \\ \mathrm{Re}\, s_0 \\ \mathrm{Re}\, g_0 \\ \mathrm{Re}\, g_0 \end{pmatrix} , \qquad P_\perp = - : \quad \begin{pmatrix} \mathrm{Im}\, s_0 \\ -\mathrm{Im}\, s_0 \\ \mathrm{Im}\, g_0 \\ -\mathrm{Im}\, g_0 \end{pmatrix} , \tag{2.3.47}$$

and the four-component eigenvalue problem splits into two two-component ones. In the even sector,

$$\begin{pmatrix} D_+ + V & M_1 + M_2 \\ M_1 + M_2 & C_+ \end{pmatrix} \begin{pmatrix} \mathrm{Re}\, s_0 \\ \mathrm{Re}\, g_0 \end{pmatrix} = M^2 \begin{pmatrix} \mathrm{Re}\, s_0 \\ \mathrm{Re}\, g_0 \end{pmatrix} , \tag{2.3.48}$$

and in the odd sector,

$$\begin{pmatrix} D_+ - V & M_1 - M_2 \\ M_1 - M_2 & C_+ \end{pmatrix} \begin{pmatrix} \mathrm{Im}\, s_0 \\ \mathrm{Im}\, g_0 \end{pmatrix} = M^2 \begin{pmatrix} \mathrm{Im}\, s_0 \\ \mathrm{Im}\, g_0 \end{pmatrix} . \tag{2.3.49}$$

We now impose the gauge condition (2.3.16). In the spin-m sector it becomes the radial constraint

$$s_m - s_{-m}^* - \frac{(1 - m + r\partial_r) g_m}{\sqrt{2}\, r f} + \frac{(m + 1 + r\partial_r) g_{-m}^*}{\sqrt{2}\, r f} = 0 . \tag{2.3.50}$$

For $m \neq 0$, this single relation removes one of the four components. It is convenient to pass to the CR_y-covariant combinations $s_m^{(\pm)} = \frac{1}{2}(s_m \pm s_{-m}^*)$ and $g_m^{(\pm)} = \frac{1}{2}(g_m \pm g_{-m}^*)$, in which (2.3.50) determines $g_m^{(+)}$ algebraically; eliminating it leaves the physical spectrum governed by a three-component eigenvalue problem for $(s_m^{(+)}, s_m^{(-)}, g_m^{(-)})$. The covariant basis can be chosen to avoid inverse powers of r near the origin and improve numerical stability. For $m = 0$, the effect of the gauge condition depends on the parity. In the even ($P_\perp = +$) sector it is satisfied automatically, so every solution of (2.3.48) is physical. In the odd ($P_\perp = -$) sector it further restricts the solutions of (2.3.49), reducing that two-component problem to a single radial equation.

In summary, the physical dilaton spectrum is obtained by solving the three-component problem described above for $m > 0$, the even spin-0 problem (2.3.48), and the constrained odd spin-0 problem. The gauge condition removes exactly one unphysical degree of freedom from each spin sector, leaving the physical dilaton modes.

2.3.3.3 Worldsheet fields

The constrained eigenfunctions define the physical transverse profiles of the dilaton-channel worldsheet particles. We denote these profiles by $\chi^{(D)}_{m,N_m}(r,\theta)$, with worldsheet masses $M^{(D)}_{m,N_m}$. The corresponding four-dimensional fluctuation can be expanded in this basis.

Since the radial operators are real, their eigenfunctions may be taken real, and the complex structure is carried entirely by the worldsheet coefficients. For $m \neq 0$, the spin-$\pm m$ sectors are related by complex conjugation and retain complex coefficients, while for $m = 0$ the even and odd subsectors are parametrized by real coefficients, with an explicit factor of i extracted in the odd sector. For the effective-action analysis it is most useful to write this expansion schematically in terms of the associated worldsheet fields,

$$\begin{pmatrix} \delta\phi \\ \delta\phi^* \\ \delta A_+ \\ \delta A_- \end{pmatrix} = \chi^{(D)}_{1,0}\, Y^+(\sigma) + \chi^{(D)}_{-1,0}\, Y^-(\sigma) + \sum_{N_{0,+}} \chi^{(D)}_{0,+,N_{0,+}}\, \varphi^+_{N_{0,+}}(\sigma) + i \sum_{N_{0,-}} \chi^{(D)}_{0,-,N_{0,-}}\, \varphi^-_{N_{0,-}}(\sigma)$$
$$+ \sum_{N_2} \Big(\chi^{(D)}_{2,N_2}\, B^{++}_{N_2}(\sigma) + \chi^{(D)}_{-2,N_2}\, B^{--}_{N_2}(\sigma) \Big) + \cdots \,, \tag{2.3.51}$$

where $Y^\pm$ and $B^{\pm\pm}_{N_2}$ are complex-conjugate pairs of worldsheet fields, while $\varphi^+_{N_{0,+}}$ and $\varphi^-_{N_{0,-}}$ are real. Here $Y^\pm$ are the spin-±1 translational zero modes and φ^+ the worldsheet dilatons, whose spectra are analyzed in Sec. 2.4.

2.3.4 Axion channel

The physical axion modes are the worldsheet gauge components δA_α obeying the wave equation (2.3.26) and the transversality constraint (2.3.25). We first solve the wave equation and then impose the constraint on the polarization. As in the dilaton channel we separate the worldsheet and transverse dependence and expand the transverse profile in angular-momentum eigenmodes,

$$\chi^{(A)}_{m,N_m}(r,\theta) = \chi^{(A)}_{m,N_m}(r)\, e^{im\theta} \ , \tag{2.3.52}$$

where, with a slight abuse of notation, $\chi^{(A)}_{m,N_m}$ denotes both the transverse profile and its radial part. The profile satisfies

$$\left(-\nabla_i^2 + 2|\widetilde{\phi}|^2\right) \chi^{(A)}_{m,N_m}(r,\theta) = \left(M^{(A)}_{m,N_m}\right)^2 \chi^{(A)}_{m,N_m}(r,\theta) \ , \tag{2.3.53}$$

which reduces to the radial equation

$$\left(-\nabla_r^2 + \frac{m^2}{r^2} + 2f^2\right) \chi^{(A)}_{m,N_m}(r) = \left(M^{(A)}_{m,N_m}\right)^2 \chi^{(A)}_{m,N_m}(r) \ . \tag{2.3.54}$$

The full axion fluctuation is then expanded as

$$\delta A_\alpha = \sum_{m\in\mathbb{Z}} \sum\!\!\!\!\!\!\int_{N_m} \int_{-\infty}^{\infty} \widetilde{dk}_z \left[\epsilon_\alpha(k)\, a_{m,N_m}(k)\, \chi^{(A)}_{m,N_m}(r,\theta) e^{-ik\cdot\sigma} + \text{h.c.}\right], \tag{2.3.55}$$

with worldsheet momentum $k_\alpha = \left(\sqrt{(M^{(A)}_{m,N_m})^2 + k_z^2},\, k_z\right)$ and measure $\widetilde{dk}_z \equiv dk_z/(2\pi\sqrt{2k_0})$. The transversality constraint (2.3.25) leaves a single physical worldsheet polarization, normalized as

$$\epsilon_\alpha(k) = \frac{1}{M^{(A)}_{m,N_m}} \epsilon_{\alpha\beta} k^\beta \ , \qquad \epsilon^*_\alpha(k)\epsilon^\alpha(k) = -1 \ . \tag{2.3.56}$$

We use $\epsilon_{01} = 1$ and $\epsilon^{01} = -1$ on the flat worldsheet.

Having constructed the transverse profiles in both channels, we close this section by recording two properties of these bases that underlie the mode expansions (2.3.51) and (2.3.55) and that we use repeatedly in the sequel. The eigenfunctions of (2.3.9) and (2.3.10) are orthonormal in the transverse inner product,

$$\int_0^{2\pi} d\theta \int_0^\infty dr\, r\, \chi^\dagger_{m,N_m}(r,\theta) \chi_{n,N_n}(r,\theta) = \delta_{m,n}\, \delta_{N_m,N_n} \ , \tag{2.3.57}$$

For the full eigenbasis before imposing the physical constraints, completeness on the transverse plane reads

$$\sum_m \sum\!\!\!\!\!\!\int_{N_m} \chi_{m,N_m}(r',\theta') \chi^\dagger_{m,N_m}(r,\theta) = \frac{1}{r}\, \delta(r-r')\, \delta(\theta-\theta')\, \mathbb{I} \ , \tag{2.3.58}$$

where the sum runs over both bound and continuum states, and $\mathbb{I}$ is the identity on the appropriate fluctuation space: $\mathbb{I}_{4\times 4}$ for the dilaton profiles $\chi^{(D)}_{m,N_m}$ and 1 for the axion profiles $\chi^{(A)}_{m,N_m}$. These relations normalize the translational zero modes of the string in Sec. 2.4 and supply the summation rule used to integrate out the massive fluctuations in Sec. 2.5.

2.4 Fluctuation Spectrum

In this section, we analyze the fluctuation spectrum of the ANO string, classifying the modes by their quantum numbers and presenting the corresponding numerical results. The spectrum depends on both the winding number n and the mass ratio β. As discussed in Sec. 2.2.2, dimensionful quantities can be restored by dimensional analysis, and all mass-squared eigenvalues M^2 in the eigenvalue equations (2.3.9) and (2.3.10) are expressed in units of $(ev)^2$.

For *stable strings*, there are three types of fluctuations: (i) zero modes, which lie in the kernel of the second-order transverse fluctuation operator in (2.3.38); (ii) discrete bound states, which are normalizable eigenfunctions describing internal excitations of the string; and (iii) continuum scattering states, which are non-normalizable eigenfunctions. In addition, for strings in the type-II regime, $\beta > 1$, the n-string configuration with $n > 1$ is unstable and tends to decay into n fundamental strings. This instability appears as tachyonic modes with negative energy in the fluctuation spectrum.

The main features of the spectrum can be summarized as follows. Every n-string carries two universal zero modes, the transverse translational Goldstone bosons of spin ± 1. Above these, the low-lying spectrum is organized into two light worldsheet scalars – a 0^{++} *dilaton* and a 0^{--} *axion* – together with a tower of higher-spin bound states. The axion is always present as a bound state, whereas the dilaton and the higher-spin states are bound only in part of the (n, β) plane. At the BPS point $\beta = 1$ the dilaton and axion become degenerate, reflecting the underlying $\mathcal{N} = 1$ supersymmetry, and the spins $1, \ldots, n$ collapse to a set of $2n$ zero modes–the moduli of the multi-string configuration. Moving into the type-II regime

$\beta > 1$ lifts these moduli to negative mass squared; the resulting tachyons signal the decay of the n-string, and the leading instability is the spin-two doublet 2^+. All of these orderings, in the spin m, the winding n, and the coupling β, follow from the centrifugal structure of the radial fluctuation operators.

We begin in section 2.4.1 by classifying the modes according to their quantum numbers. In section 2.4.2 we discuss the zero modes, which arise only in the dilaton channel. Section 2.4.3 then treats the two light scalars, the worldsheet dilaton and axion, and section 2.4.4 the higher-spin tower and the type-II instability. The figures below display the numerical spectra.

2.4.1 Mode Classification

Given the unbroken symmetries $O(1,1)_\parallel \times O(2)_\perp$ discussed in Sec. 2.3.1, the fluctuation spectrum is classified by their quantum numbers. We begin by classifying the modes under the transverse symmetry $O(2)_\perp$. They are labeled by the $SO(2)_\perp$ spin m: for $|m| \neq 0$, the states with spins $\pm m$ are exchanged by the transverse reflection and together form degenerate $O(2)_\perp$ doublets, while for $m = 0$ the modes are $O(2)_\perp$ singlets labeled by the reflection eigenvalue $P_\perp$. In the longitudinal direction, the modes in the rest frame can be further classified by the worldsheet parity $P_\parallel$. Thus, the $m = 0$ modes are labeled by $0^{P_\perp P_\parallel}$, whereas for $|m| \neq 0$ the doublets may be labeled either by $m^{P_\parallel}$ in the spin-diagonal basis or by $|m|^{P_\perp P_\parallel}$ in the parity-diagonal basis. In what follows, for the doublets we will focus on the $m > 0$ modes and denote the corresponding doublets simply by $m^{P_\parallel}$, with the understanding that the partner state with spin $-m$ is obtained by acting with $P_\perp$.

This structure is already visible in the mode expansion and radial eigenvalue equations of the previous section. There, the fluctuations were first decomposed into sectors of definite spin m in the dilaton and axion channels, see (2.3.41) and (2.3.54). In the $m = 0$ sector, the dilaton channel further splits into two decoupled radial eigenvalue equations, (2.3.48) and (2.3.49), corresponding to the 0^{++} and 0^{-+} sectors, respectively, while the physical axion equation (2.3.54) lies in the 0^{--} sector. The decomposition of the radial equations therefore directly matches the quantum number classification of the modes.

For each fixed set of quantum numbers, the fluctuation eigenequations admit scattering states and, in some channels, a discrete tower of bound states labeled by an excitation index N_m. Their corresponding eigenvalues are interpreted as the worldsheet mass squared of these modes, or equivalently as the eigenvalues of the quadratic Casimir of the worldsheet Poincare group $ISO(1,1)$.

2.4.2 Zero Modes

For all strings, there exist two universal zero-eigenvalue modes associated with the spontaneous breaking of translational symmetry in the two transverse directions. These field configurations correspond to gauge-fixed translations of the classical ANO string background (2.2.11), defined by the covariant derivative with the background gauge field [32],

$$\delta_k\phi = \widetilde{D}_k\widetilde{\phi} = \partial_k\widetilde{\phi} + i\widetilde{A}_k\widetilde{\phi} \ , \qquad \delta_k A_j = \widetilde{F}_{kj} \ , \tag{2.4.1}$$

where k labels the two transverse directions. Since they involve only variations of the scalar field $\delta\phi$ and the transverse components of the gauge field δA_i, these modes appear in the dilaton channel. The translational zero modes take the form

$$\chi^{(D)}_{-1,0} = \frac{1}{\sqrt{c_\chi}}\begin{pmatrix} \widetilde{D}_+\widetilde{\phi} \\ \widetilde{D}_+\widetilde{\phi}^* \\ F_{++} \\ F_{+-} \end{pmatrix} = \frac{1}{\sqrt{c_\chi}}\begin{pmatrix} \frac{e^{i\theta(n-1)}(rf'+nf(\alpha+1))}{\sqrt{2}r} \\ \frac{e^{-i\theta(n+1)}(rf'-nf(\alpha+1))}{\sqrt{2}r} \\ 0 \\ \frac{in\alpha'}{r} \end{pmatrix} \tag{2.4.2}$$

$$\chi^{(D)}_{1,0} = \frac{1}{\sqrt{c_\chi}}\begin{pmatrix} \widetilde{D}_-\widetilde{\phi} \\ \widetilde{D}_-\widetilde{\phi}^* \\ F_{-+} \\ F_{--} \end{pmatrix} = \frac{1}{\sqrt{c_\chi}}\begin{pmatrix} \frac{e^{i\theta(n+1)}(rf'-nf(\alpha+1))}{\sqrt{2}r} \\ \frac{e^{-i\theta(n-1)}(rf'+nf(\alpha+1))}{\sqrt{2}r} \\ -\frac{in\alpha'}{r} \\ 0 \end{pmatrix} \tag{2.4.3}$$

These modes are normalizable, and the normalization constant c_χ, chosen to satisfy Eq. (2.3.57), is given by

$$c_\chi = 2\pi\int_0^\infty dr\frac{n^2\alpha'^2 + n^2(\alpha+1)^2f^2 + r^2f'^2}{r} \ . \tag{2.4.4}$$

Using the equations of motion for the vortex background (2.2.11), one can verify that these modes lie in the kernel of the fluctuation operator (2.3.38):

$$\mathcal{D}_\perp \chi^{(D)}_{\pm 1,0} = 0 \tag{2.4.5}$$

and trivially satisfy the gauge constraints (2.3.16).

These two zero modes correspond precisely to the universal Nambu–Goldstone bosons associated with the spontaneous breaking of transverse translational symmetry. They carry spins ± 1 and have $P_\parallel = +$. In the notation introduced above, they form a massless doublet, denoted simply by 1^+.

At the BPS limit, $\beta = 1$, the vortex string background possesses a $2n$-dimensional moduli space [35, 36]. These moduli are identified as the positions of the n vortices in the spatial $xy-$plane. The associated moduli manifest as zero modes in the fluctuation spectrum, giving rise to normalizable modes with spins $\pm 1, \pm 2, \ldots, \pm n$, all in the dilaton channel. These modes form the massless doublets 1^+ , 2^+ , ... , n^+, which describe internal deformations of the multi-string configuration within the moduli space. Away from the BPS point, these modes with spin $|m| > 1$ are no longer massless. In the type-II regime with $\beta > 1$, they acquire a negative mass squared and thus become tachyonic, signaling that the multi-vortex configuration with $n > 1$ is unstable. In contrast, in the type-I regime with $\beta < 1$, these modes remain stable and can be either bound or scattering states, depending on the value of β. We will return to these details below. In the following, unless stated otherwise, zero modes refer to the universal spin-± 1 translational modes of the string.

2.4.3 The Light Scalars: Worldsheet Dilaton and Axion

In addition to the zero modes, the second-order string fluctuation operator admits a massive spectrum consisting of continuum scattering states and, in some sectors, discrete bound states. Its detailed structure depends sensitively on the mass-squared ratio β and the winding number n. In the dilaton channel, the continuum starts at $M^2 = \min\{m_H^2,\, m_V^2\}$, while in the axion channel it starts at $M^2 = m_V^2$. Here m_H^2 and m_V^2 are given in (2.2.3); in units of e^2v^2, they are 2β and 2, respectively. These thresholds are the same in every spin sector, a fact used repeatedly in the analysis below: at large r the profile approaches the Higgs vacuum, $f \to 1$, so the axion equation (2.3.54) reduces to $-\nabla_r^2 + 2$ and the coupled dilaton system to a diagonal form with the same asymptotic potential, fixing the thresholds quoted above independently of the spin. As discussed below, massive discrete bound states are always present in the axion channel, whereas in the dilaton channel their existence depends on the values of β and n.

We begin with the two lightest scalars – the 0^{++} dilaton and the 0^{--} axion, presenting the two channels side by side, since it is their comparison that carries the physics; the higher-spin tower follows in Sec. 2.4.4.

The spin-0 fluctuations decompose into three sectors,[14]

$$0^{++}\,, \qquad 0^{-+}\,, \qquad 0^{--}\,. \tag{2.4.6}$$

The first two arise from the dilaton channel and are governed by Eq. (2.3.48) and the gauge-constrained odd-sector equation, respectively, while the last arises from the axion channel and is governed by Eq. (2.3.54).

The first two arise from the dilaton channel and the last from the axion channel, and we take them in turn. The 0^{++} sector carries a continuum of scattering states with threshold at $M^2 = \min\{2,\, 2\beta\}$ and, throughout the type-I regime and for sufficiently small β in the type-II regime, at least one normalizable bound state—the *worldsheet dilaton*. The range of β over which this bound state exists widens with the winding n; within it, the mass of the lightest state increases with β and decreases with n, while larger n or smaller β can bind additional levels. Beyond this range the sector is purely continuous. The 0^{-+} sector, by contrast, supports no bound states at all: our numerical scan over $\beta \in [0.1, 10]$ and $n = 1, \ldots, 5$ finds only continuum scattering states.

The 0^{--} sector belongs to the axion channel, whose physical modes all carry $P_\parallel = -$; the spin-zero states are odd under both $P_\perp$ and $P_\parallel$ and are the *worldsheet axions*. Here

[14] Since only the axion channel carries $P_\parallel = -$, and $P_\perp$ acts trivially in the axion channel, there is no 0^{+-} sector.

the continuum sets in at $M^2 = 2$, and there is always at least one bound state below it, as expected for an attractive two-dimensional potential well [37]. As in the 0^{++} sector, this lightest axion becomes lighter as n increases or β decreases. The behaviour of both light scalars with β for $n = 1$ is displayed in Fig. 2.2.

It is also instructive to compare the lightest bound states in the 0^{++} dilaton sector and the 0^{--} axion sector. We find that the lightest dilaton is lighter than the lightest axion in the type-I regime, while in the type-II regime the ordering is reversed and the lightest axion becomes lighter. At the BPS point $\beta = 1$, the two masses coincide. This is consistent with the fact that, at the BPS point, the Abelian Higgs model admits an embedding into an $\mathcal{N} = 1$ supersymmetric theory, suggesting a natural relation between these two worldsheet excitations. This comparison of the two masses is shown in Fig. 2.2.

We present numerical results for the lightest bound states in the 0^{++} dilaton sector and the 0^{--} axion sector. For $n = 1$ and representative values of β, we numerically solve the corresponding eigenvalue equations, Eqs. (2.3.48) and (2.3.54), and extract the lowest mass-squared eigenvalues. The spectra plotted below show how the lightest axion and dilaton masses vary with β, including the change in their ordering across the type-I and type-II regimes.

2.4.4 Higher-Spin Modes and the Type-II Instability

In the following discussion, we restrict to the representative with $m > 0$, with the understanding that the partner state with spin $-m$ is generated by $P_\perp$; equivalently, we describe the corresponding degenerate doublets. We now turn to the sectors with $m \geq 1$. In the dilaton channel, these modes have $P_\parallel = +$ and are denoted by m^+, while in the axion channel they have $P_\parallel = -$ and are denoted by m^-.

As in the spin-0 sectors, the spectrum contains a continuum of scattering states, with threshold at $M^2 = \min\{2, 2\beta\}$ in the dilaton channel and $M^2 = 2$ in the axion channel. In addition to the zero modes discussed in Sec. 2.4.2, there may also exist massive bound states, whose detailed structure depends on β and n.

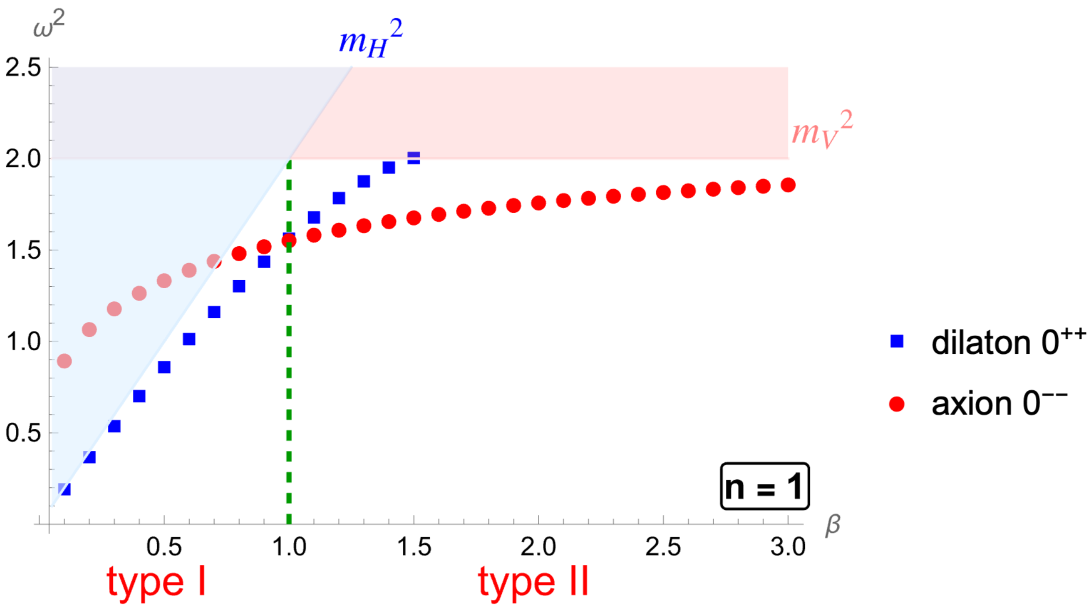

Figure 2.2: Mass squared of the lightest dilaton 0^{++} and axion 0^{--} as a function of β for the fundamental $n = 1$ string. The pink shading marks the region above the axion bound-state threshold m_V^2, while the blue and pink shading together mark the region above the dilaton bound-state threshold $\min\{m_H^2, m_V^2\}$. The green dashed line marks the BPS point $\beta = 1$.

The spins in the window $2 \leq m \leq n$ play a distinguished role, and the dilaton modes m^+ there are the most interesting feature of the higher-spin spectrum. Their lowest state behaves qualitatively differently in the three regimes. At the BPS point $\beta = 1$ it is massless—a modulus of the internal deformations of the multi-string configuration, part of the enlarged moduli space of Sec. 2.4.2. In the type-II regime $\beta > 1$ it acquires negative mass squared and becomes tachyonic, signalling the instability of the cylindrically symmetric $n \geq 2$ vortex under the repulsive inter-string force. In the type-I regime $\beta < 1$ it acquires positive mass and is a stable internal excitation, reflecting the attractive force that binds the constituent strings. The spin-± 1 sector is exceptional: it always contains the universal translational zero modes of Sec. 2.4.2, which remain massless for every β.

Because raising the spin can only raise the mass squared, the leading instability of the type-II n-string is the lowest member of this window, the spin-two doublet 2^+: the tachyons are ordered $M_2^2 \leq M_3^2 \leq \cdots \leq M_n^2 < 0$ for $\beta > 1$, proved for $n = 2$ and confirmed numerically for $n \geq 3$.

Outside this window, for the dilaton modes m^+ and the axion modes m^- with $m > n$, the present numerical scan finds no bound states. The pattern across the whole tower is uniform and traces back to the centrifugal ordering: bound states are favoured, and lighter, at larger n, smaller β, and smaller m, so that the number of levels below threshold falls as the spin is raised and vanishes beyond $m = n$.

We close with the organizing principle behind these trends. The spin m enters the radial fluctuation operators only through non-negative centrifugal terms, so raising the spin can only raise the mass squared, while the winding n and coupling β enter only through the background profile. The orderings in m, n and β—the axion tower rising with $|m|$, the light dilaton and axion crossing at the BPS point, the moduli at spins $1, \ldots, n$, and the spin-two tachyon that controls the type-II instability—are all consequences of this structure.

2.5 Effective String Action: $\mathcal{O}(K^4)$ Curvature Correction

In this section we derive the leading higher-curvature corrections to the Nambu–Goto action for the ANO string by integrating out the massive fluctuation modes of the vortex identified in the previous sections. These corrections appear at weight four in the effective string action, with coefficients determined by the massive worldsheet spectrum and by the cubic couplings of its modes to two zero modes.

2.5.1 Overview

As reviewed in Sec. 2.1, the low-energy dynamics of a long string is described by the Goldstones X^i. In the Abelian Higgs model, these modes are accompanied by a tower of massive modes in the fluctuation spectrum of the vortex. At energies much lower than the massive scale, their leading effect can be viewed as tree-level exchange between pairs of translational zero modes, [15] shown in Fig. 2.3. In the low-energy expansion, this exchange reduces to the leading $\mathcal{O}(K^4)$ corrections to the Nambu–Goto action. This section makes this exchange picture explicit.

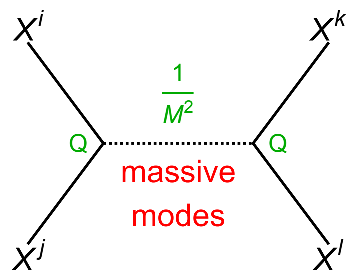

Figure 2.3: Tree-level exchange of a massive worldsheet mode between two pairs of translational zero modes. Integrating out the exchanged mode gives the leading $\mathcal{O}(K^4)$ contribution to the effective string action. At this order, only the 0^{++}, 0^{--}, and 2^+ sectors contribute.

Worldsheet diffeomorphism invariance and spacetime Poincare symmetry strongly restrict which massive sectors can contribute at this order. Only three sectors can appear in the cubic vertices relevant for tree-level exchange: the scalar 0^{++} sector, the pseudoscalar 0^{--} sector, and the spin-two 2^+ sector. Denoting the corresponding worldsheet fields by φ, a, and B_{ij}, their leading couplings to the translational Goldstones take the geometric form [38, 39]

[16]

$$S_\varphi = \int d^2\widetilde{\sigma}\sqrt{-h}\left(\frac{1}{2}(\widetilde{\partial}_\alpha\varphi)^2 - \frac{1}{2}m_\varphi^2\varphi^2 + Q_\varphi\,\varphi R\right), \tag{2.5.1}$$

$$S_a = \int d^2\widetilde{\sigma}\sqrt{-h}\left(\frac{1}{2}(\widetilde{\partial}_\alpha a)^2 - \frac{1}{2}m_a^2 a^2 + Q_a\epsilon^{\beta\gamma}\epsilon_{ij}\,a\,K^i_{\alpha\beta}K^{\alpha\,j}_{\ \gamma}\right), \tag{2.5.2}$$

$$S_B = \int d^2\widetilde{\sigma}\sqrt{-h}\left(\frac{1}{2}(\widetilde{\partial}_\alpha B_{ij})^2 - \frac{1}{2}m_B^2 B_{ij}^2 + Q_B B_{ij}(K^i_{\alpha\beta}K^{\alpha\beta j} - \frac{1}{2}\delta^{ij}R)\right)\ . \tag{2.5.3}$$

Here Q_φ, Q_a, and Q_B are the corresponding cubic couplings.

[15] At low energies the Goldstones X^i are naturally organized into geometric quantities of the worldsheet. Since the first nontrivial corrections to the Nambu–Goto action occur at weight four, the relevant massive-mode sources are quadratic in the extrinsic curvature, schematically $\mathcal{O}(K^2)$. The leading terms of these sources correspond microscopically to cubic vertices involving one massive mode and two zero modes.

[16] Throughout this section, $\widetilde{\sigma}$ and $\widetilde{\partial}$ denote the dimensionful worldsheet coordinates and derivatives, respectively, in order to distinguish them from the dimensionless ones.

Integrating out these massive modes at tree level produces the leading $\mathcal{O}(K^4)$ correction in the effective string action. [17] The resulting terms can be matched to the effective string action in (2.1.8) and (2.1.11). We repeat them here for convenience:

$$S_{\rm eff} = \int d^2\sigma\sqrt{-h}\left[-T + c_{R^2}R^2 + c_{K^4}K^i_{\alpha\beta}K_j^{\alpha\beta}K^i_{\gamma\delta}K_j^{\gamma\delta} + \cdots\right] . \tag{2.5.4}$$

For a single mode in each sector, the contributions are

$$c^{\varphi}_{R^2} = \frac{Q_\varphi^2}{2m_\varphi^2}\ , \qquad c^{a}_{R^2} = -\frac{Q_a^2}{m_a^2}\ , \qquad c^{B}_{R^2} = -\frac{Q_B^2}{4m_B^2}\ , \tag{2.5.5}$$

$$c^{a}_{K^4} = \frac{Q_a^2}{m_a^2}\ , \qquad c^{B}_{K^4} = \frac{Q_B^2}{2m_B^2}\ . \tag{2.5.6}$$

The full coefficients c_{R^2} and c_{K^4} are obtained by summing over all modes in these sectors, including both discrete and scattering states.

In practice, we will not evaluate the continuum contribution mode by mode. Instead, in each symmetry sector the cubic vertex defines a fixed source profile. Using completeness, the full exchange contribution can be rewritten as a matrix element of a power of the inverse transverse fluctuation operator. This is the method used below to obtain the final $\mathcal{O}(K^4)$ coefficients c_{R^2} and c_{K^4}.

To extract these couplings from the Abelian Higgs action, we expand the curvature interactions to leading order in static gauge and introduce the canonically normalized Goldstones

$$Y^i \equiv \sqrt{T}\,X^i\ , \tag{2.5.7}$$

the worldsheet action relevant at this order takes the form

$$S_{\rm ws} \supset \int d^2\widetilde{\sigma}\ \left[-T + \frac{1}{2}(\widetilde{\partial}_\alpha Y^i)^2 + \mathcal{L}_\varphi + \mathcal{L}_a + \mathcal{L}_B\right]\ , \tag{2.5.8}$$

[17] For a massive field φ coupled linearly as $Q_\varphi \varphi J_\varphi$, solving its equation of motion and substituting back gives $\mathcal{L}_{\rm eff} = \frac{1}{2}Q_\varphi^2 J_\varphi(\partial^2 + m_\varphi^2)^{-1}J_\varphi$. At energies well below m_φ, this reduces to $\mathcal{L}_{\rm eff} = \frac{Q_\varphi^2}{2m_\varphi^2}J_\varphi^2 + \mathcal{O}(\partial^2/m_\varphi^4)$.

with

$$\mathcal{L}_\varphi = \frac{1}{2}(\widetilde{\partial}_\alpha \varphi)^2 - \frac{1}{2}m_\varphi^2\varphi^2 + \frac{Q_\varphi}{T}\,\varphi\,\widetilde{\partial}_\alpha\widetilde{\partial}_\beta Y^i\,\widetilde{\partial}^\alpha\widetilde{\partial}^\beta Y^i\ , \tag{2.5.9}$$

$$\mathcal{L}_a = \frac{1}{2}(\widetilde{\partial}_\alpha a)^2 - \frac{1}{2}m_a^2 a^2 + \frac{Q_a}{T}\,a\,\epsilon^{ij}\epsilon^{\alpha\beta}\widetilde{\partial}_\alpha\widetilde{\partial}_\gamma Y^i\,\widetilde{\partial}^\gamma\widetilde{\partial}_\beta Y^j\ , \tag{2.5.10}$$

$$\mathcal{L}_B = \frac{1}{2}(\widetilde{\partial}_\alpha B_{ij})^2 - \frac{1}{2}m_B^2 B_{ij}^2 + \frac{Q_B}{T}\,B_{ij}\left(\widetilde{\partial}_\alpha\widetilde{\partial}_\beta Y^i\,\widetilde{\partial}^\alpha\widetilde{\partial}^\beta Y^j - \frac{1}{2}\delta^{ij}\widetilde{\partial}_\alpha\widetilde{\partial}_\beta Y^k\,\widetilde{\partial}^\alpha\widetilde{\partial}^\beta Y^k\right)\ . \tag{2.5.11}$$

These expressions define the operator basis used below to match the cubic vertices obtained from the Abelian Higgs model.

The rest of the section is organized as follows. In Sec. 2.5.2, we introduce the relevant worldsheet fields, derive their action, and determine the couplings Q_φ, Q_a, and Q_B from the Abelian Higgs model. We then use the completeness relation to obtain the Wilson coefficients c_{R^2} and c_{K^4} for the ANO string in Sec. 2.5.3.

2.5.2 Worldsheet fields and action

We now identify the worldsheet fields and determine their cubic couplings from the Abelian Higgs model. In this section, we work in the background gauge (2.3.29), which simplifies the extraction of the tree-level K^4 correction. This differs from the previous two sections, where we used the unitary gauge to determine the physical spectrum. In the background gauge, the physical and unphysical modes can instead be separated systematically using BRST cohomology. However, we will not need this separation explicitly: by ghost number conservation, the unphysical modes do not contribute to the tree-level exchange between pairs of translational zero modes.

The transverse eigenmodes found in the previous sections provide a good basis for expanding the four-dimensional fluctuations around the ANO vortex. [18] The coefficients of these profiles become two-dimensional fields propagating along the string. As discussed above, we just focus on the translational 1^+ zero modes, the 0^{++} and 2^+ modes in the dilaton channel, and the 0^{--} modes in the axion channel.

[18] The same transverse operators appear in the two gauge choices, while the physical projection is implemented differently, as discussed above.

The relevant fluctuations in the two channels are expanded in transverse eigenmodes of $\mathcal{D}_\perp$ and $-\nabla_i^2 + 2|\widetilde{\phi}|^2$, respectively, as [19]

$$\begin{pmatrix} \delta\phi \\ \delta\phi^* \\ \delta A_+ \\ \delta A_- \end{pmatrix} = e\Bigg[\chi^{(D)}_{1,0}\, Y^+(\sigma) + \chi^{(D)}_{-1,0}\, Y^-(\sigma) + \sum\!\!\!\!\!\!\int_{N_0} \chi^{(D)}_{0,N_0}\, \varphi_{N_0}(\sigma)$$

$$+ \sum\!\!\!\!\!\!\int_{N_2} \Big(\chi^{(D)}_{2,N_2}\, B^{++}_{N_2}(\sigma) + \chi^{(D)}_{-2,N_2}\, B^{--}_{N_2}(\sigma)\Big)\Bigg] + \cdots , \tag{2.5.12}$$

$$\delta A_\alpha = e\, \sum\!\!\!\!\!\!\int_{N_0} \chi^{(A)}_{0,N_0}(r,\theta)\, \frac{1}{M^{(A)}_{0,N_0}}\, \epsilon_{\alpha\beta}\partial^\beta a_{N_0}(\sigma) + \cdots . \tag{2.5.13}$$

[20] The coefficients in these mode expansions realize the worldsheet fields introduced above in the Abelian Higgs model. In the complex basis, the Goldstone and spin-2 fields satisfy

$$(Y^\pm)^* = Y^\mp , \qquad (B^{\pm\pm}_{N_2})^* = B^{\mp\mp}_{N_2} . \tag{2.5.14}$$

The sums run over all modes in the relevant massive sectors, while the ellipses denote modes that will not be needed below.

We now insert the mode expansions (2.5.12) and (2.5.13) into the Abelian Higgs fluctuation action (2.3.32). Keeping the quadratic terms and the cubic terms involving one massive field and two translational zero modes, we obtain the worldsheet action relevant for

[19] While this schematic form of δA_α expansion mirrors the structure of the on-shell mode expansion, care must be taken when using it to compute kinetic terms. In particular, substituting it directly into the kinetic term leads to higher-derivative expressions that are ill-defined off-shell. A well-defined kinetic Hamiltonian instead follows from the properly normalized mode expansion given in Eq. (2.3.55), which yields a canonical Hamiltonian in the axion channel. Once the kinetic structure is fixed in this way, and using the on-shell condition, the schematic expansion may then be used to extract higher-order interactions.

[20] With this convention, the fields Y^i, φ_{N_0}, a_{N_0}, and $B^{ij}_{N_2}$ have canonical quadratic kinetic terms in the reduced worldsheet action. The cubic vertices then carry one explicit power of e.

the tree-level $\mathcal{O}(K^4)$ correction: [21]

$$\int dt\,dz\left[\frac{1}{2}(\partial_\alpha Y^i)^2+\sum_{N_0}\!\!\!\!\!\!\int\left[\frac{1}{2}(\partial_\alpha\varphi_{N_0})^2-\frac{1}{2}(M^{(D)}_{0,N_0})^2\varphi^2_{N_0}+e\,\kappa_{\varphi,N_0}\,\varphi_{N_0}Y^+Y^-\right]\right.$$
$$+\sum_{N_0}\!\!\!\!\!\!\int\left[\frac{1}{2}(\partial_\alpha a_{N_0})^2-\frac{1}{2}(M^{(A)}_{0,N_0})^2a^2_{N_0}+e\,\kappa_{a,N_0}\,\frac{1}{M^{(A)}_{0,N_0}}\,\epsilon_{ij}\epsilon_{\alpha\beta}\,\partial^\beta a_{N_0}\,Y^i\partial^\alpha Y^j\right]$$
$$\left.+\sum_{N_2}\!\!\!\!\!\!\int\left[\frac{1}{2}(\partial_\alpha B_{N_2,ij})^2-\frac{1}{2}(M^{(D)}_{2,N_2})^2B^2_{N_2,ij}+e\,\kappa_{B,N_2}\left(Y^+Y^+B^{--}_{N_2}+Y^-Y^-B^{++}_{N_2}\right)\right]+\cdots\right].\tag{2.5.15}$$

The three sectors in (2.5.15) share the same general structure. In the transverse eigenmode basis, the quadratic worldsheet action is diagonal: the fields φ_{N_0}, a_{N_0}, and $B_{N_2,ij}$ have canonical kinetic terms, with masses given by the corresponding transverse eigenvalues. Each massive mode also couples cubically to a bilinear of translational zero modes. These couplings are given by overlap integrals of the massive mode profiles with the corresponding zero mode bilinear sources:

$$\kappa_{\varphi,N_0}=2\pi\int_0^\infty dr\,r\,\chi^{(D)\dagger}_{0,N_0}(r)\,\zeta_{\varphi XX}(r)\ ,\tag{2.5.16}$$
$$\kappa_{a,N_0}=2\pi\int_0^\infty dr\,r\,\chi^{(A)\dagger}_{0,N_0}(r)\,\zeta_{aXX}(r)\ ,\tag{2.5.17}$$
$$\kappa_{B,N_2}=2\pi\int_0^\infty dr\,r\,\chi^{(D)\dagger}_{2,N_2}(r)\zeta_{BXX}(r)\ ,\tag{2.5.18}$$

Here $\zeta_{\varphi XX}$, ζ_{aXX}, and ζ_{BXX} are the effective radial profiles generated by bilinears of the translational zero modes after summing over the relevant cubic interaction terms. Explicitly,

[21] Here we continue to work in units with $\widetilde{v}=1$. Dimensionful quantities can be restored in powers of ev; for example, the physical masses are evM.

[22]

$$\zeta_{\varphi XX}(r) = \begin{pmatrix} -\dfrac{f\left(3\beta r^2 f'^2 + (\beta-2)n^2 f^2(\alpha+1)^2\right)}{c_\chi r^2} \\ -\dfrac{f\left(3\beta r^2 f'^2 + (\beta-2)n^2 f^2(\alpha+1)^2\right)}{c_\chi r^2} \\ \dfrac{\sqrt{2}n\left(rf'\left[(\alpha+1)(rf'-2f)+2rf\,\alpha'\right]+n^2f^2(\alpha+1)^3\right)}{c_\chi r^3} \\ \dfrac{\sqrt{2}n\left(rf'\left[(\alpha+1)(rf'-2f)+2rf\,\alpha'\right]+n^2f^2(\alpha+1)^3\right)}{c_\chi r^3} \end{pmatrix}, \tag{2.5.19}$$

$$\zeta_{aXX}(r) = \frac{2n\,f'f(\alpha+1)}{r\,c_\chi}\,, \tag{2.5.20}$$

and

$$\zeta_{BXX} = \begin{pmatrix} -\beta f\psi_1^2 - 2\beta f\psi_2\psi_1 + \dfrac{\sqrt{2}(\alpha+1)n\psi_3\psi_1}{r} + \dfrac{\sqrt{2}\psi_3\psi_1}{r} - \sqrt{2}\psi_3\,\psi_1' - \dfrac{\psi_1\,\psi_3'}{\sqrt{2}} \\ -2\beta f\psi_2\psi_1 - \beta f\psi_2^2 + \dfrac{\sqrt{2}(\alpha+1)n\psi_3\psi_2}{r} - \dfrac{\sqrt{2}\psi_3\psi_2}{r} + \sqrt{2}\psi_3\,\psi_2' + \dfrac{\psi_2\,\psi_3'}{\sqrt{2}} \\ -2f\psi_3\psi_2 - 2f\psi_3\psi_1 + \dfrac{\sqrt{2}(\alpha+1)n\psi_2\psi_1}{r} + \dfrac{\psi_2\,\psi_1'}{\sqrt{2}} - \dfrac{\psi_1\,\psi_2'}{\sqrt{2}} \\ \dfrac{\sqrt{2}(\alpha+1)n\psi_2\psi_1}{r} - \dfrac{\psi_2\,\psi_1'}{\sqrt{2}} + \dfrac{\psi_1\,\psi_2'}{\sqrt{2}} \end{pmatrix}, \tag{2.5.21}$$

with

$$\psi_1 = \frac{1}{\sqrt{c_\chi}}\frac{rf' - nf(\alpha+1)}{\sqrt{2}\,r}\,, \quad \psi_2 = \frac{1}{\sqrt{c_\chi}}\frac{rf' + nf(\alpha+1)}{\sqrt{2}\,r}\,, \quad \psi_3 = -\frac{1}{\sqrt{c_\chi}}\frac{n\alpha'}{r}\,. \tag{2.5.22}$$

Although the units with $\widetilde{v}=1$ used in the four-dimensional analysis are convenient, the string tension T provides a more natural scale for the worldsheet action. We therefore restore the dimensionful worldsheet coordinates below. To match the microscopic vertices in (2.5.15) to the effective string couplings in (2.5.9)–(2.5.11), we restore the scale ev, integrate by parts, and use the free equations of motion for the worldsheet fields. The resulting interactions are then written in the same operator basis.

---

[22] This provides a direct check of the selection rule. The angular integral enforces transverse spin conservation, so Y^+Y^- can only couple to spin-zero massive modes. Within this sector, $\zeta_{\varphi XX}$ is orthogonal to the 0^{-+} profiles in (2.3.47), leaving only the 0^{++} modes.

For each mode, the couplings are

$$Q_\varphi = \frac{2\tau(\beta)}{e\left(M_0^{(D)}(\beta)\right)^4}\,\kappa_\varphi(\beta)\ , \tag{2.5.23}$$

$$Q_a = \frac{2\tau(\beta)}{e\left(M_0^{(A)}(\beta)\right)^3}\,\kappa_a(\beta)\ , \qquad\qquad T \equiv \tau(\beta)v^2 \tag{2.5.24}$$

$$Q_B = \frac{4\tau(\beta)}{e\left(M_2^{(D)}(\beta)\right)^4}\,\kappa_B(\beta)\ . \tag{2.5.25}$$

where the dependence on β has been made explicit.

The cubic couplings are well defined for bound states, since they are given by overlap integrals of normalizable profiles. The numerical values of $eQ_{\varphi,0}$ for the lightest dilaton mode are summarized in Table 2.2. For scattering states, however, the eigenfunctions are not normalizable, so individual couplings are not well defined by the overlap formulas above.

2.5.3 Completeness and $\mathcal{O}(K^4)$ Wilsonian coefficients

The contribution of each massive mode to c_{R^2} and c_{K^4} is fixed by its mass and coupling, as reviewed above. Summing over all discrete and continuum dilaton, axion, and spin-two modes then gives the following sum rules:

$$c_{R^2} = c_{R^2}^{\varphi} + c_{R^2}^{a} + c_{R^2}^{B} = \sum\!\!\!\!\!\!\!\int_{N_0} \frac{Q_{\varphi,N_0}^2}{2(evM_{0,N_0}^{(D)})^2} - \sum\!\!\!\!\!\!\!\int_{N_0} \frac{Q_{a,N_0}^2}{(evM_{0,N_0}^{(A)})^2} - \sum\!\!\!\!\!\!\!\int_{N_2} \frac{Q_{B,N_2}^2}{4(evM_{2,N_2}^{(D)})^2}\ , \tag{2.5.26}$$

$$c_{K^4} = c_{K^4}^{a} + c_{K^4}^{B} = \sum\!\!\!\!\!\!\!\int_{N_0} \frac{Q_{a,N_0}^2}{(evM_{0,N_0}^{(A)})^2} + \sum\!\!\!\!\!\!\!\int_{N_2} \frac{Q_{B,N_2}^2}{2(evM_{2,N_2}^{(D)})^2}\ . \tag{2.5.27}$$

However, the scattering modes are non-normalizable, so the corresponding couplings Q are not individually well defined and their contributions to c_{R^2} and c_{K^4} cannot be evaluated mode by mode. Importantly, the completeness relation allows us to perform the continuum sum directly, bypassing this difficulty and obtaining the full contribution. Similar methods have been used in braneworld effective theories [40]. We now explain how this works.

From (2.5.23)–(2.5.27), the tree-level contributions to c_{R^2} and c_{K^4} take the same spectral sum form in each sector,

$$\sum\!\!\!\!\!\!\!\int_N \frac{\kappa_N^2}{M_N^{2s}} \ , \tag{2.5.28}$$

where the integer s and the coefficient κ_N depend on the sector. We retain the four-component radial profiles and sources in the dilaton channel. The angular factors contain no $1/\sqrt{2\pi}$, so (2.3.57) gives $2\pi \int_0^\infty dr\, r\, \chi_N^\dagger(r)\chi_{N'}(r) = \delta_{NN'}$ at fixed spin. No additional radial rescaling is made. Thus, consistently with (2.5.16)–(2.5.18),

$$\kappa_N = 2\pi \int_0^\infty dr\, r\, \chi_N^\dagger(r)\, \zeta(r) \ . \tag{2.5.29}$$

Here $\zeta(r)$ is the zero mode bilinear source and is independent of the excitation level N. For the completeness calculation, $\chi_N(r)$ runs over the full background-gauge eigenbasis at fixed spin of the Hermitian operator $\widehat{\Omega}$,

$$\widehat{\Omega}\chi_N(r) = M_N^2 \chi_N(r) \ . \tag{2.5.30}$$

The operator $\widehat{\Omega}$ is channel dependent: $\widehat{\Omega} = \mathcal{R}_{(m)}$ in the dilaton channel (2.3.41), and $\widehat{\Omega} = -\partial_r^2 + \frac{m^2}{r^2} + 2f^2$ in the axion channel (2.3.54).

We rewrite the source as

$$\zeta(r) = \widehat{\Omega}^s G(r) \ , \tag{2.5.31}$$

where $G(r)$ satisfies boundary conditions for which the boundary terms vanish. If zero modes are present, the inverse is defined on their orthogonal complement, and the source must lie in that subspace.

The overlap coefficient then becomes

$$\begin{aligned} \kappa_N &= 2\pi \int_0^\infty dr\, r\, \chi_N^\dagger(r)\, \widehat{\Omega}^s G(r) \\ &= 2\pi \int_0^\infty dr\, r\, \left(\widehat{\Omega}^s \chi_N(r)\right)^\dagger G(r) \\ &= 2\pi M_N^{2s} \int_0^\infty dr\, r\, \chi_N^\dagger(r)\, G(r) \ , \end{aligned} \tag{2.5.32}$$

where we used the self-adjointness of $\widehat{\Omega}$, the vanishing of the boundary terms, and the eigenvalue equation $\widehat{\Omega}^s \chi_N = M_N^{2s} \chi_N$.

Substituting this result into the spectral sum [23] and using the completeness relation

$$\sum\!\!\!\!\!\!\int_N \chi_N(r)\chi_N^\dagger(\rho) = \frac{1}{2\pi r}\delta(r-\rho)\,\mathbb{I}\ , \tag{2.5.33}$$

where $\mathbb{I}$ is the identity in the fluctuation space of the corresponding channel: $\mathbb{I}_{4\times 4}$ in the dilaton channel and 1 in the axion channel. The sum uses the full eigenbasis at fixed spin; the source $\zeta_{\varphi XX}$ has zero overlap with the odd spin-zero modes. We obtain

$$\sum\!\!\!\!\!\!\int_N \frac{\kappa_N^2}{M_N^{2s}} = 2\pi \int_0^\infty dr\, r\, G^\dagger(r)\zeta(r)\ . \tag{2.5.34}$$

To avoid solving a high-order differential equation in practice, we may instead factor the operator by writing $s = s_1 + s_2$, where $s_1, s_2 \in \mathbb{Z}_{\geq 0}$, and solve

$$\widehat{\Omega}^{s_1} G_1 = \zeta\ , \qquad \widehat{\Omega}^{s_2} G_2 = \zeta\ . \tag{2.5.35}$$

Then the spectral sum becomes

$$\sum\!\!\!\!\!\!\int_N \frac{\kappa_N^2}{M_N^{2s}} = 2\pi \int_0^\infty dr\, r\, G_1^\dagger(r)\, G_2(r)\ , \tag{2.5.36}$$

reducing the differential order involved in the computation.

To summarize, the full spectral sum is obtained by solving for G in (2.5.31), or equivalently for G_1 and G_2 in (2.5.35), and using (2.5.34) or (2.5.36). These expressions include both bound and continuum states without summing over the spectrum mode by mode. Alternatively, the continuum contribution can be isolated by subtracting the discrete bound-state sum from the full result.

We now apply the procedure described above to the three relevant sectors. As discussed

[23] For a real radial basis, $\int_0^\infty dr\, r\, G^\dagger(r)\chi_N(r) = \int_0^\infty dr\, r\, \chi_N^\dagger(r) G(r)$.

above, their contributions to the $\mathcal{O}(K^4)$ Wilson coefficients are

$$c^{\varphi}_{R^2} = \frac{2T^2}{e^4 v^6} \sum\!\!\!\!\!\!\!\int_{N_0} \frac{\kappa^2_{\varphi,N_0}}{(M^{(D)}_{0,N_0})^{10}} \ , \tag{2.5.37}$$

$$c^{a}_{R^2} = -c^{a}_{K^4} = -\frac{4T^2}{e^4 v^6} \sum\!\!\!\!\!\!\!\int_{N_0} \frac{\kappa^2_{a,N_0}}{(M^{(A)}_{0,N_0})^{8}} \ , \tag{2.5.38}$$

$$c^{B}_{K^4} = -2c^{B}_{R^2} = \frac{8T^2}{e^4 v^6} \sum\!\!\!\!\!\!\!\int_{N_2} \frac{\kappa^2_{B,N_2}}{(M^{(D)}_{2,N_2})^{10}} \ . \tag{2.5.39}$$

To rewrite these spectral sums as radial integrals, we define

$$\mathcal{R}^3_{(m=0)} G^{\varphi}_1 = \zeta_{\varphi XX}, \qquad\qquad \mathcal{R}^2_{(m=0)} G^{\varphi}_2 = \zeta_{\varphi XX}, \tag{2.5.40}$$

$$\left(-\partial_r^2 + 2f^2\right)^2 G^a = \zeta_{aXX}, \tag{2.5.41}$$

$$\mathcal{R}^3_{(m=2)} G^{B}_1 = \zeta_{BXX}, \qquad\qquad \mathcal{R}^2_{(m=2)} G^{B}_2 = \zeta_{BXX}. \tag{2.5.42}$$

where $\mathcal{R}_{(m=0)}$ and $\mathcal{R}_{(m=2)}$ are the dilaton channel radial operators in the 0^{++} and 2^+ sectors, respectively, while the axion sector operator is $-\partial_r^2 + 2f^2$. The spectral sums then reduce to

$$c^{\varphi}_{R^2} = \frac{4\pi T^2}{e^4 v^6} \int_0^\infty dr\, r\, G^{\varphi\dagger}_1 G^{\varphi}_2, \tag{2.5.43}$$

$$c^{a}_{R^2} = -c^{a}_{K^4} = -\frac{8\pi T^2}{e^4 v^6} \int_0^\infty dr\, r\, G^{a\dagger} G^{a}, \tag{2.5.44}$$

$$c^{B}_{K^4} = -2c^{B}_{R^2} = \frac{16\pi T^2}{e^4 v^6} \int_0^\infty dr\, r\, G^{B\dagger}_1 G^{B}_2. \tag{2.5.45}$$

We have thus reduced the full contributions of the three sectors to the $\mathcal{O}(K^4)$ Wilson coefficients to a set of radial integrals. In the next section, we evaluate these expressions numerically and examine how the different massive sectors encode the dynamics of the ANO string across the type-I, BPS, and type-II regimes.

β	$eQ_{a,0}$	$evM^{(A)}_{0,0}/\sqrt{T}$
0.1	1.2432	0.4731
0.2	1.2353	0.4846
0.3	1.2295	0.4903
0.4	1.2266	0.4935
0.5	1.2204	0.4956
0.6	1.2148	0.4968
0.7	1.2114	0.4976
0.8	1.2046	0.4980
0.9	1.2013	0.4981
1.0	1.1967	0.4981
2.0	1.1333	0.4928
3.0	1.0841	0.4815
4.0	0.9807	0.4771
5.0	0.8974	0.4697
6.0	0.8107	0.4630
7.0	0.7274	0.4569
8.0	0.6433	0.4513
9.0	0.5587	0.4463
10.0	0.4787	0.4417

β	$eQ_{\varphi,0}$	$evM^{(D)}_{0,0}/\sqrt{T}$
0.1	1.8729	0.2148
0.2	1.5898	0.2813
0.3	1.4549	0.3280
0.4	1.3738	0.3649
0.5	1.3197	0.3956
0.6	1.2815	0.4218
0.7	1.2535	0.4447
0.8	1.2324	0.4648
0.9	1.2148	0.4823
1.0	1.1985	0.4977
1.1	1.1255	0.5101
1.2	1.0744	0.5219
1.3	1.0427	0.5372
1.4	1.0292	0.5404

Table 2.2: Numerical values of the couplings and masses, in units of $\sqrt{T}$, for the lowest axion and dilaton bound states as functions of β for $n = 1$. Most spin-2 dilaton modes are unbound over most of the β range. Here the physical tension and masses are $T = \tau(\beta)\, v^2$ and $M\, ev$.

2.6 Numerical Results and Comparisons

In the previous section, we expressed the $\mathcal{O}(K^4)$ Wilson coefficients as spectral sums over the massive vortex modes. Physically, these coefficients measure how the massive modes of the string affect the curvature response at long distance. Our goal here is to evaluate c_{R^2} and c_{K^4} numerically and understand how the different sectors, including both bound and scattering states, contribute across the type-I, BPS, and type-II regimes. We then compare our determination of the coefficients from the mode analysis with those derived using the Born–Oppenheimer-like approach [1, 2]. We finally compare our results with the bounds on the $\mathcal{O}(K^4)$ Wilson coefficients from the flux-tube S-matrix bootstrap [3], placing the Abelian Higgs model within the broader landscape of effective string theories, and comment on their relation to existing results for Yang–Mills confining strings.

2.6.1 Numerical results

We focus here on the fundamental $n = 1$ string, for which the vortex is stable throughout the full range of β considered. We evaluate the contributions of the bound states to the Wilson coefficients c_{R^2} and c_{K^4} directly from their masses and eigenfunctions, or equivalently from the corresponding couplings Q. The full spectral contributions, including both bound and scattering states, are obtained using the completeness method of Sec. 2.5. An important feature of the results below is that the contributions from scattering states are substantial across a broad range of β, so both bound and scattering states are needed for a complete description.

Figure 2.4 shows the dimensionless combinations of the Wilson coefficients, $e^4v^2c_{R^2}$ and $e^4v^2c_{K^4}$, as functions of β. [24] For c_{R^2}, we show the total contribution from each massive sector, whereas for c_{K^4} we further separate the contributions from bound states and scattering states. The solid curves interpolate the numerical data. We now highlight the main features

[24] Here the Wilson coefficients are written with their dependence on the microscopic parameters e and v explicit. Below, we also express them in worldsheet units using the string tension T, which is more convenient for the low-energy effective worldsheet theory.

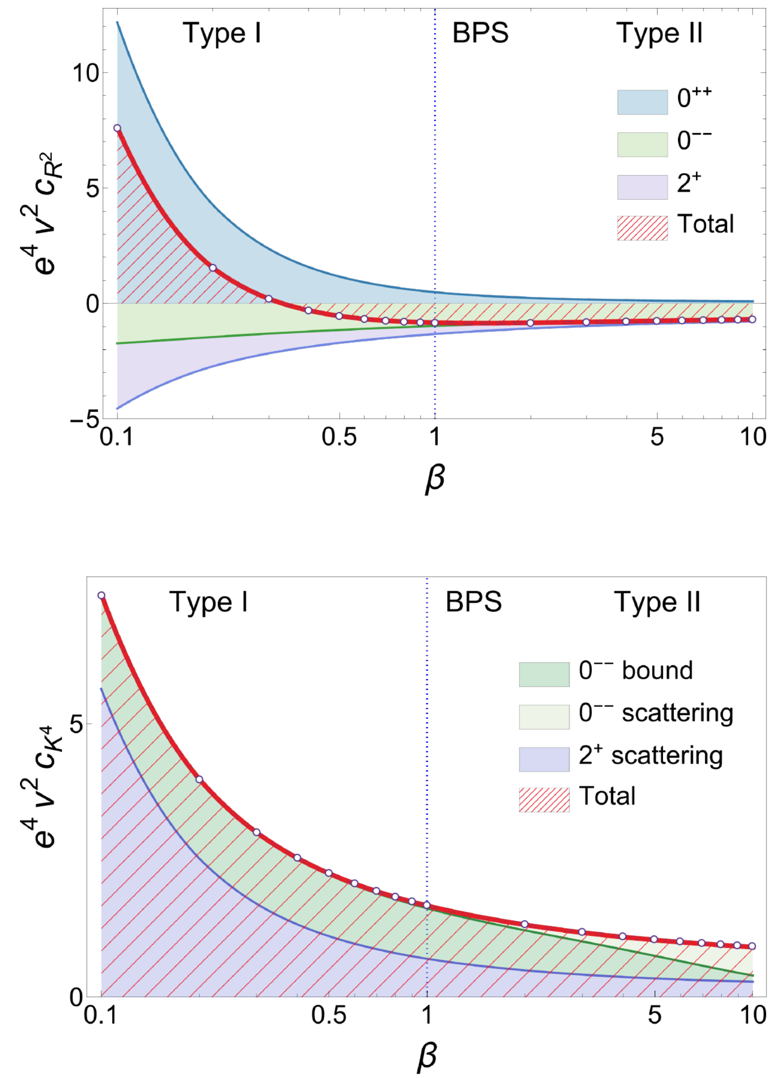

Figure 2.4: Decomposition of the Wilson coefficients for the fundamental $n = 1$ string. The upper plot shows the contributions to c_{R^2} from the 0^{++}, 0^{--}, and 2^{+} sectors in blue, green, and purple, respectively. The lower plot further separates the c_{K^4} contributions into bound states and scattering states: the 2^{+} scattering contribution is shown in purple, while the 0^{--} bound and scattering contributions are shown in dark and light green. The solid curves interpolate the numerical data points. In both plots, the thick red curve gives the total contribution from the massive sectors, while the nearly overlapping dotted curve shows the Born–Oppenheimer result in [1, 2].

of these results.

For c_{R^2}, the positive 0^{++} dilaton contribution dominates in the strongly type-I regime and competes with the negative contributions from the 0^{--} axion and 2^+ sectors. As β increases, the dilaton contribution decreases substantially, while the axion contribution becomes relatively more important, causing the total c_{R^2} to change sign. At large β, the coefficient is dominated by the negative axion contribution.

For c_{K^4}, only the 0^{--} axion and 2^+ sectors contribute, both with positive sign. At small β, the dominant contribution comes from the 2^+ continuum.[25] Its contribution decreases as β increases, while the axion sector becomes progressively more important. Within the axion sector, the contribution from bound states is largest around the BPS region, whereas the contribution from scattering states grows toward large β and eventually dominates.

These trends are closely tied to the structure of the massive spectrum. In the type-I regime, the Higgs is lighter than the vector, so the continuum threshold in the dilaton channel is lower. This enhances the contribution of the dilaton-channel states, including the spin-two continuum, and explains their importance at small β. As β increases, this relative enhancement is lost and the axion sector becomes increasingly important.

The BPS point $\beta = 1$ provides a useful reference between the two regimes. Numerically, the combination $2c_{R^2} + c_{K^4}$ vanishes within our numerical accuracy. The 2^+ contribution cancels identically in this combination, leaving only the 0^{++} dilaton and 0^{--} axion sectors. The cancellation is particularly transparent for the bound states: at the BPS point, the lightest dilaton and axion are degenerate and have equal couplings, as discussed in Sec. 2.4.3, so their contributions to $2c_{R^2} + c_{K^4}$ cancel exactly. This cancellation is therefore consistent with the special BPS structure of the theory and its supersymmetric embedding, in which the string is half-BPS and the dilaton and axion are related by $\mathcal{N} = (0, 2)$ supersymmetry. We will return to this point below when discussing β_3 in the bootstrap picture.

[25] For the fundamental $n = 1$ string, we find no 2^+ bound state over the range of β considered.

2.6.2 Comparison with the Born–Oppenheimer Approach

The $\mathcal{O}(K^4)$ curvature corrections in the Abelian Higgs model were studied in Refs. [1, 2] using a Born–Oppenheimer-like expansion of a weakly curved ANO vortex. In this approach, the transverse vortex string profile is solved for in a slowly varying worldsheet geometry, and its response to the curvature is then used to derive the effective worldsheet action.

The mode analysis developed here provides a complementary description of the same low-energy curvature corrections. After converting the conventions of Refs. [1, 2] to ours, we compare the resulting coefficients c_{R^2} and c_{K^4}.

As shown in Fig. 2.4, the two approaches show close numerical agreement over the full range of β considered, with the dotted Born–Oppenheimer curve nearly overlapping the result from the mode analysis. This provides a nontrivial check of the mode analysis. [26]

At the same time, the mode analysis contains additional information: it resolves the Wilson coefficients into contributions from the different massive sectors and further separates the contributions from bound states and scattering states. This reveals how the underlying dynamics controlling the curvature corrections evolves across different regimes of β.

2.6.3 Bootstrap Bounds and Comparison

Having determined the Wilson coefficients c_{R^2} and c_{K^4}, we can directly locate the ANO strings within the allowed region of the flux-tube S-matrix bootstrap (β_3, α_3) parameter space introduced in Sec. 2.1. For the ANO string, α_3 and β_3 are functions of β with a common overall factor of $1/e^4$. Thus, at fixed e, varying β traces out a trajectory in the bootstrap plane, while varying e radially rescales it. Figure 2.6 shows this trajectory at $e = 1$ for illustration. [27] The main features are as follows:

[26] By the result of [1, 2] we mean values obtained numerically using the formulas developed there, evaluated at the values of β considered here. At the points also considered in [1, 2], the values agree with those reported there, as expected.

[27] Although this value is not parametrically weakly coupled, it provides a convenient normalization for displaying the result.

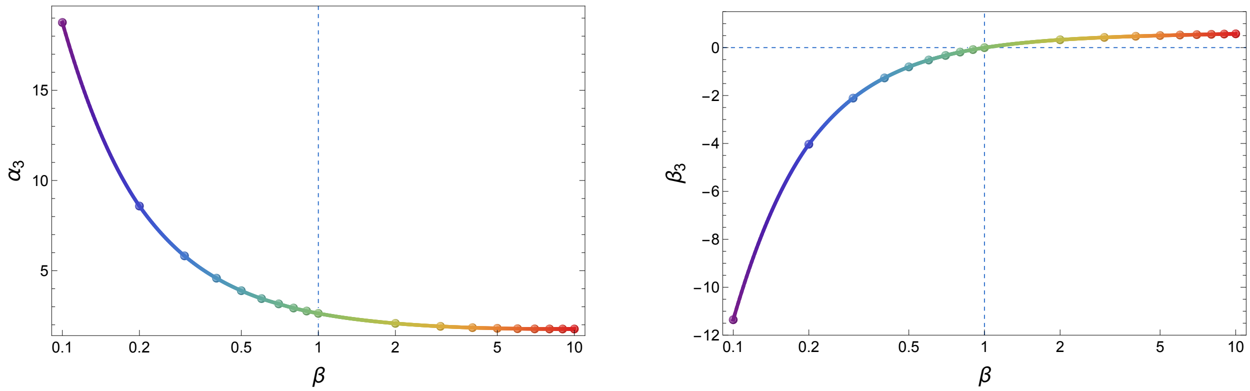

Figure 2.5: Wilson coefficients α_3 and β_3 of the fundamental $n = 1$ ANO string as β is varied. As β increases, α_3 decreases, while β_3 increases and changes sign at the BPS point $\beta = 1$. At larger β, both coefficients vary more slowly and appear to approach constant values.

- As β increases, α_3 decreases, while β_3 increases and changes sign at the BPS point. Since $\beta_3 \propto -(2c_{R^2} + c_{K^4})$, this crossing reflects the BPS cancellation discussed above. The type-I regime lies on the left side of the bootstrap plane, the BPS string lies on the line $\beta_3 = 0$ up to numerical accuracy, and the type-II regime lies on the right. At larger β, both coefficients vary more slowly, suggesting that the ANO string trajectory approaches a limiting point over the range shown.

- The bootstrap boundary has two characteristic branches. The right branch is associated with a sharp worldsheet axion resonance, while the left branch is associated with a sharp dilaton resonance [3, 4]. The ANO trajectory follows the same qualitative pattern: the type-I regime lies on the dilaton side, the BPS point crosses $\beta_3 = 0$, and the type-II regime moves to the axion side. This is consistent with the level crossing of the lightest dilaton and axion masses at the BPS point.

- Varying e instead radially rescales the trajectory. In the weakly coupled regime, the common factor $1/e^4$ makes the coefficients grow as e is decreased, while increasing e moves the trajectory toward the origin. At sufficiently strong coupling, however, the semiclassical calculation is no longer under perturbative control.

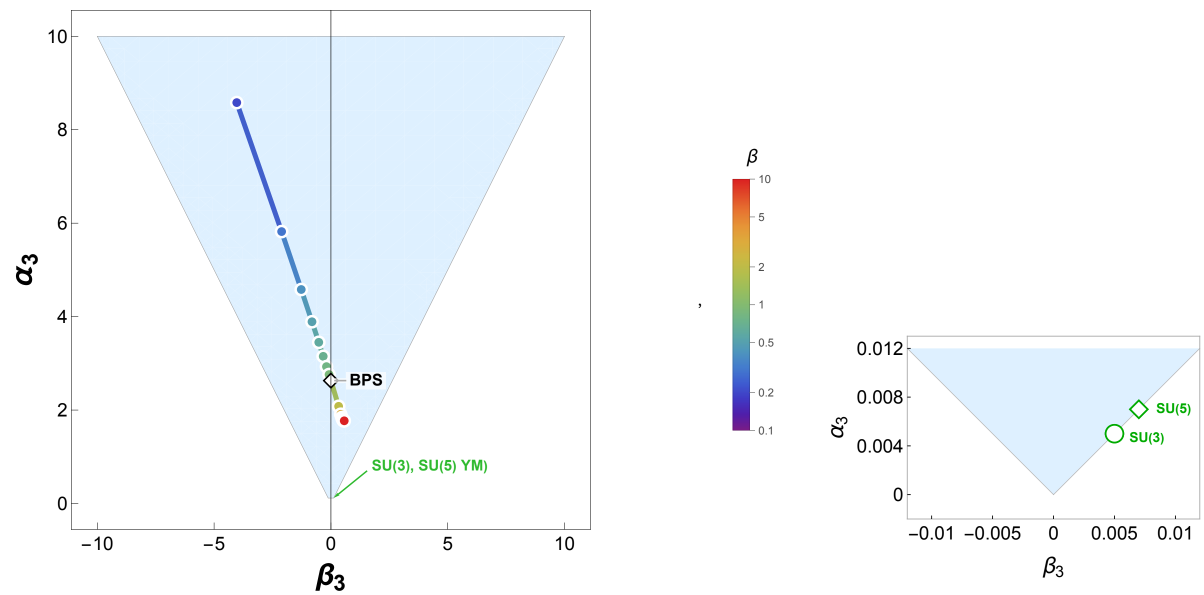

Figure 2.6: Fundamental $n = 1$ ANO strings in the (β_3, α_3) bootstrap parameter space. The blue shaded region is the allowed region [3, 4], bounded by the dilaton branch on the left and the axion branch on the right. The left plot shows the ANO trajectory as β is varied at $e = 1$, with type I strings on the left, the BPS point at $\beta_3 = 0$, and type II strings on the right. The right plot zooms in near the origin, where the $SU(3)$ and $SU(5)$ Yang–Mills estimates lie close to the axion branch.

2.6.3.1 Comparison with Yang–Mills Flux Tubes

It is natural to compare ANO strings with Yang–Mills flux tubes. Such a comparison is motivated by the long-standing dual superconductor picture of confinement, in which confining electric flux tubes are viewed as electric–magnetic duals of ANO vortices [41, 42]. In particular, this picture is realized explicitly in Seiberg–Witten theory, where a soft breaking to $\mathcal{N} = 1$ leads to monopole condensation and confinement, described at low energies by an Abelian Higgs theory [43, 44]. This provides a controlled setting in which the relation between confining flux tubes and ANO vortices can be studied explicitly.

At the level of the effective worldsheet theory, the two systems can be compared in the (α_3, β_3) plane. The $SU(3)$ and $SU(5)$ points shown along the axion branch in Fig. 2.6 schematically indicate where the corresponding Yang–Mills flux tubes may lie in the bootstrap parameter space. This is motivated by lattice measurements of the worldsheet axion, whose mass and coupling are closely matched by the axion resonance on this branch [3, 4].

The Yang–Mills theories lie on the same side of the allowed region as type II ANO strings, consistent with both supporting a relatively light worldsheet axion. However, their string dynamics are quite different: type II ANO strings repel, whereas Yang–Mills confining strings attract and form bound states. This difference creates a tension with the duality, which would suggest broader agreement in the spectrum and string interactions. In this sense, the minimal Abelian Higgs model does not provide a direct microscopic description of the Yang–Mills confining string.

It is worth emphasizing that the Abelian Higgs model captures only a subsector of the softly broken Seiberg–Witten theory. In the full supersymmetric theory, additional bosonic and fermionic fields are present, and these may significantly modify the string dynamics. It would therefore be interesting to extend the present analysis to the full supersymmetric theory and explore the duality from the worldsheet perspective.

2.6.4 $n > 1$ strings

Our analysis has focused on the fundamental $n = 1$ string, for which the string is stable and the translational Goldstones are the only massless worldsheet degrees of freedom throughout the range of β considered. For $n > 1$, the situation depends qualitatively on the regime of β.

In the type-I regime, higher-winding strings are stable, so the mode analysis can be extended to construct a well-defined effective string theory. As n increases, the Wilson coefficients become larger at fixed β and e, moving the ANO string points upward in the bootstrap parameter space. In the type-II regime, by contrast, these strings contain tachyonic fluctuation modes, indicating an instability toward splitting into fundamental vortices. Consequently, there is no well-defined low energy effective action.

At the BPS point, higher-winding strings possess additional zero modes associated with the relative positions of the fundamental strings. The low-energy worldsheet theory must therefore include these additional moduli and cannot be described solely in terms of the two translational Goldstones. It would be interesting to study this enlarged effective action.

CHAPTER 3

Non-Invertible Symmetries in S_N Orbifold CFTs and Entanglement Entropy

3.1 Introduction

In recent years, generalized and non-invertible symmetries in various dimensions have been a very active field of investigation [14–16, 45–98] providing valuable insight into the dynamics of quantum field theories. At the core of these generalizations is the realization of symmetries as (extended) topological operators and vice versa. In this picture, a natural question is to find the holographic dual of these symmetry operators in the bulk. In theories with weakly coupled holographic duals, it has been proposed that boundary topological operators correspond to D-branes in the bulk [99–113] which, in certain limits, can become topological. These proposals are based on anomaly inflow arguments. The goal of this paper is to put forward a proposal for the holographic dual of topological operators in a setup with a strongly coupled bulk theory using the $\mathrm{AdS}_3/\mathrm{CFT}_2$ correspondence.

In two-dimensional conformal field theories (CFT), non-invertible symmetries have a long history starting with the work of Verlinde in rational CFTs [114], the construction of topological defects in terms of projectors [115, 116], the construction of topological duality defects [117, 118], and the topological field theory formulation of RCFTs [119] to name a few. Orbifolds are a powerful way to obtain new CFTs from old ones [120, 121]. In this paper, we focus on the so-called symmetric orbifold CFT, where one takes the tensor product of N copies of a seed CFT $\mathcal{M}$ and gauges the S_N symmetric group [17] that permutes the different copies. A remarkable feature of these theories is that they observe a large-N factorization of correlation functions [122–124], similar to the case of single-trace operators in large-N gauge theories. Proposals for the holographic dual of symmetric orbifold CFTs go back to [125], relating a type IIB $AdS_3 \times S^3 \times \mathcal{M}_4$ background, with $\mathcal{M}_4$ being either K_3 or T^4, to the $\mathcal{N} = (4,4)$ supersymmetric orbifold CFT $\mathcal{M}_4^{\otimes N}/S_N$. This background allows for an exact worldsheet description with only NS-NS flux. However, it has been a challenge to identify the particular background which corresponds to the undeformed $\mathcal{M}_4^{\otimes N}/S_N$ orbifold [126]. Recently, such a dual was found for the $AdS_3 \times S^3 \times \mathcal{M}_4$ background with the minimal $k = 1$ unit of NS-fivebrane flux [18–21, 127].

It is well known that gauging a group-like symmetry leads to a quantum symmetry in the gauged theory [128, 129]. Hence, by construction, an orbifold CFT exhibits a universal set of symmetries arising by the gauging of a discrete group. In the case of interest, the gauging of the non-abelian S_N group leads to a universal set of non-invertible symmetries. In this work, we look at these universal defects in two-dimensional symmetric orbifold CFTs. We construct them by applying the projector construction of Petkova and Zuber [115], and use the modular transformations of the partition function to identify the defect Hilbert spaces of operators on which line-defects can end. Additionally, we propose a realization of the defect operators in terms of non-gauge invariant operators under S_N. These defects, being universal, depend solely on the group theory structure of S_N and not on the specifics of the seed CFT. To illustrate their properties, we examine the simplest example that exhibits non-invertible symmetries, i.e. $N = 3$.

In symmetric orbifold CFTs, universal defects are labeled by the representations of S_N. We study these defects in the large-N limit and analyze which representations remain non-trivial. We argue that these defects correspond to topological defects on the worldsheet and propose an explicit realization. While we verify some of their properties, further investigation is required for a complete realization.

The structure of this chapter is as follows: In section 3.2, we review some background material, in particular non-invertible symmetries in RCFTs and the construction of symmetric orbifold CFTs. In section 3.3, we construct the universal topological line-defect operators in the symmetric orbifold CFTs that realize the Rep(S_N) fusion algebra. We use the modular transformation of the torus partition function with a defect inserted to determine the corresponding defect Hilbert spaces, and we construct the vacuum-state operators in terms of non-gauge invariant twist fields. In section 3.4, we present a detailed example of the S_3 symmetric orbifold. This is one of the simplest examples where non-invertible symmetries arise in CFTs. We determine the lines and defect operators, as well as the Ward identities for two and three-point correlators of twist operators. In section 3.5, we discuss non-universal topological defects, starting with a nontrivial topological defect operator in the seed theory and constructing a "maximally fractional" defect, where all sectors are built on the same seed CFT defect in an S_N invariant manner. We show that such defects are consistent, in the sense that they satisfy the Cardy-Petkova-Zuber [115, 116, 130] conditions. In section 3.6, we discuss some aspects of the large-N limit of these defects, particularly whether a non-invertible defect survives this limit. In section 3.7, we discuss the AdS/CFT dual of the symmetric orbifold [20], which states that the AdS dual is a type IIB string theory on $AdS_3 \times S^3 \times \mathcal{M}_4$ with one unit of NS-NS fivebrane flux. We propose a worldsheet dual of the universal defects and discuss some of their properties. In section 3.8, we calculate the entanglement entropy in the presence of universal and non-universal topological defects. In section 3.9, we close with some discussion of our results and list some open questions and speculations.

3.2 Review

In this section, we review well-known material which will play an important role in the main part of the paper. First, we discuss the construction of Verlinde lines in rational conformal field theories, introducing key concepts of non-invertible symmetries in two-dimensional CFTs. Second, we review the construction of the $\mathcal{M}^{\otimes N}/S_N$ symmetric orbifold CFT, for which we will construct the non-invertible symmetries in following sections.

3.2.1 Non-invertible symmetries in rational CFTs

Let us first look at the construction of topological line-defects in rational conformal field theories (RCFTs). We will restrict our attention to the case of diagonal RCFTs and the Verlinde lines [114] which are in one-to-one correspondence with the chiral primaries. The torus partition function of such an RCFT is given by

$$Z(\tau,\bar{\tau}) = \sum_{i,j} n_{ij}\ \chi_i(\tau)\bar{\chi}_j(\bar{\tau})\ , \tag{3.2.1}$$

where $n_{ij} = \delta_{ij}$ and $\chi_i(\tau)$ denotes the character of a finite irreducible chiral algebra labeled by the representation i. Under the modular S-transformation, the characters transform as $\chi_i(-1/\tau) = \sum_j S_{ij}\ \chi_j(\tau)$. The operator corresponding to a Verlinde line $\mathcal{I}_a$ associated to the chiral primary $|\Phi_a\rangle$ is given by [115, 116]

$$\mathcal{I}_a = \sum_i \frac{S_{ai}}{S_{0i}} P_{i\bar{i}}\ , \tag{3.2.2}$$

where $P_{i\bar{i}}$ is a projector acting on the space spanned by the i-th primary and its descendants:

$$P_{i\bar{i}} = \sum_{n\bar{n}} |i,n\rangle \otimes |i,\bar{n}\rangle\ \langle i,n| \otimes \langle i,\bar{n}|\ \ . \tag{3.2.3}$$

Using the Verlinde formula [114],

$$n^c{}_{ab} = \sum_i \frac{S_{ai}\ S_{bi}\ S^*_{ci}}{S_{0i}}\ , \tag{3.2.4}$$

we can verify that the fusion algebra of the Verlinde lines is isomorphic to that of the chiral primaries,

$$\mathcal{I}_a\,\mathcal{I}_b = \sum_c n^c{}_{ab}\,\mathcal{I}_c\ , \tag{3.2.5}$$

where $n^c{}_{ab}$ is the non-negative integer fusion coefficient, which denotes the multiplicity with which $\mathcal{I}_c$ appears in the fusion product of the defects. Given that the Verlinde lines act as projectors on the modules of the chiral algebra, which includes the Virasoro algebra, they commute with both the holomorphic and anti-holomorphic modes of the stress tensor,

$$L_n\,\mathcal{I}_a = \mathcal{I}_a\ L_n\ , \qquad \bar{L}_n\,\mathcal{I}_a = \mathcal{I}_a\ \bar{L}_n\ , \tag{3.2.6}$$

and are therefore topological. Using the folding trick of [131, 132], the topological defects have a realization as Ishibashi boundary states [130, 133] which characterize $\mathbb{Z}_2$ permutation branes [134–136]. If we start with the folded theory $\mathrm{CFT}_{(1)} \times \overline{\mathrm{CFT}}_{(2)}$, the boundary state defining a $\mathbb{Z}_2$ permutation brane is given by

$$| B_a\rangle\rangle = \sum_i \frac{S_{ai}}{S_{0i}} \sum_n |i,n\rangle_{(1)} \otimes \overline{|i,n\rangle}_{(2)} \sum_m |i,m\rangle_{(2)} \otimes \overline{|i,m\rangle}_{(1)} \ , \tag{3.2.7}$$

such that they obey the following Virasoro gluing conditions:

$$\begin{aligned}
\left(L_k^{(1)} - \bar{L}_{-k}^{(2)}\right) \sum_n |i,n\rangle_{(1)} \otimes \overline{|i,n\rangle}_{(2)} = 0 \ , \\
\left(L_k^{(2)} - \bar{L}_{-k}^{(1)}\right) \sum_m |i,m\rangle_{(2)} \otimes \overline{|i,m\rangle}_{(1)} = 0 \ .
\end{aligned}$$

The quantum dimension of the topological defect operator is the eigenvalue of the defect acting on the CFT vacuum state,

$$\mathcal{I}_a \,|0\rangle = \langle \mathcal{I}_a \rangle \,|0\rangle \ . \tag{3.2.8}$$

For the Verlinde lines we obtain $\langle \mathcal{I}_a \rangle = S_{a0}/S_{00}$. It was pointed out in [14] that defects that have a quantum dimension not equal to one are in general associated with non-invertible symmetries. Note that in the boundary state representation (3.2.7) the quantum dimension is obtained by $\langle \mathcal{I}_a \rangle = \langle 0 \mid B_a \rangle\rangle$.

Operators like (3.2.2) satisfying the Cardy-Petkova-Zuber [115, 116, 130] conditions can be viewed as topological line-defects. The action of these line-defects can be visualized on the complex plane mapped from the cylinder as in Figure 3.1, where we insert the defect at a particular point in time. We refer to the Hilbert space defined on S^1 for every point in time as the *untwisted* Hilbert space.

The corresponding torus partition function is given by inserting the defect inside the trace over the Hilbert space,

$$Z^a(\tau,\bar{\tau}) = \mathrm{tr}_{\mathcal{H}}[\mathcal{I}_a \, q^{L_0 - \frac{c}{24}} \, \bar{q}^{\bar{L}_0 - \frac{c}{24}}] \ , \tag{3.2.9}$$

where $q = e^{2\pi i \tau}$ with τ being the torus modular parameter. After performing a modular S-transformation, the line-defect now extends in the time direction, and at every point in

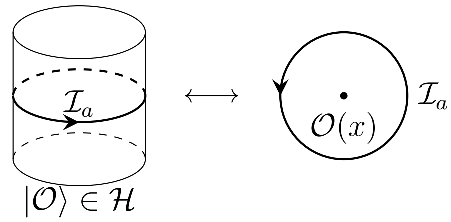

Figure 3.1: Using the state-operator correspondence to depict the action of the line-defect on an operator in the untwisted Hilbert space.

time we obtain the *defect Hilbert space*, $\mathcal{H}_{\mathcal{I}_a}$. The torus partition function is now modified to trace over this defect Hilbert space corresponding to the defect $\mathcal{I}_a$,

$$Z_a(-\tfrac{1}{\tau}, -\tfrac{1}{\bar{\tau}}) = \mathrm{tr}_{\mathcal{H}_{\mathcal{I}_a}}[\tilde{q}^{L_0 - \frac{c}{24}}\ \bar{\tilde{q}}^{\bar{L}_0 - \frac{c}{24}}]\ , \tag{3.2.10}$$

where $\tilde{q} = e^{-2\pi i/\tau}$. Using the S-transformation of the characters, and the fact that the defect commutes with the chiral vertex algebra, we can expand the defect Hilbert space in terms of the characters. The defect partition function can thus be written as

$$Z_a(\tau, \bar{\tau}) = \sum_{b,c} N_{ab}^c\ \chi_b(\tau)\bar{\chi}_c(\bar{\tau})\ , \tag{3.2.11}$$

where the non-negative integers N_{ab}^c encode the degeneracy of the states in $\mathcal{H}_{\mathcal{I}_a}$. Note that even though we started with a diagonal theory, the defect partition function is not necessarily diagonal, i.e. N_{ab}^c need not be a diagonal matrix. This tells us that states in $\mathcal{H}_{\mathcal{I}_a}$ have non-integer spins and correspond to non-local operators attached to the corresponding line $\mathcal{I}_a$.

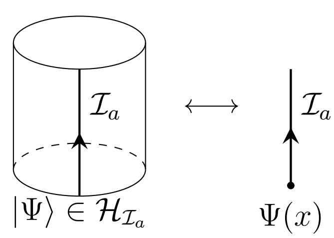

Figure 3.2: States in the defect Hilbert space $\mathcal{H}_{\mathcal{I}_a}$ correspond to non-local operators attached to the line-defect $\mathcal{I}_a$.

An important feature of non-invertible line-defects is the "lasso" effect [14] where, when a topological line-defect is moved past a local operator, one obtains in addition to the symmetry action on the local operator another topological line ending on a defect operator and a junction of topological line operators (see Figure 3.3). The mathematical structure describing symmetry line-defects, defect operators, and their manipulations is called a tube algebra [68].

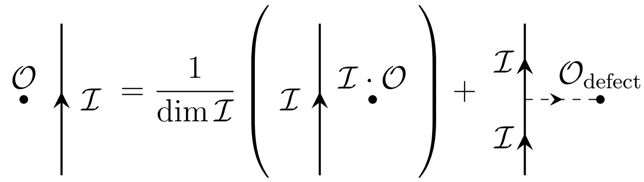

Figure 3.3: Lasso action of a topological line-defect.

3.2.2 Symmetric Orbifold CFT

In this section, we review the symmetric orbifold CFT. Consider N copies of a CFT $\mathcal{M}$ (not necessarily rational). The tensor product CFT has an S_N symmetry that permutes the N copies of the theory. We construct the S_N orbifold CFT by gauging this permutation symmetry. Let's denote the primary operators of the tensor product theory by $\mathcal{O}_I$ where $I = 1, 2, \ldots, N$. The spectrum of the orbifold theory consists of the untwisted sector constructed by taking gauge invariant combinations of operators in the tensor product theory such as

$$\sum_{I=1}^{N} \mathcal{O}_I, \quad \sum_{I,J=1}^{N} \mathcal{O}_I \mathcal{O}_J, \ldots \ . \tag{3.2.12}$$

Modular invariance additionally requires twisted sectors. We introduce the twist operators σ_g labeled by the elements of S_N by

$$\mathcal{O}_I(e^{2\pi i} z)\ \sigma_g(0) = \mathcal{O}_{g \cdot I}(z)\ \sigma_g(0)\ . \tag{3.2.13}$$

These operators introduce non-trivial holonomies for the operators of the seed theory. However, the operators σ_g are not gauge invariant. To define gauge invariant operators we define [123, 124, 137]

$$\sigma_{[g]} \propto \sum_{h \in S_N} \sigma_{h^{-1} g h}\ , \tag{3.2.14}$$

labeled by the conjugacy classes $[g]$ of S_N. The proportionality constant can be fixed by normalizing the two-point function of these operators [124]. A conjugacy class $[g]$ is fixed by giving the number l_i of cycles of length $i = 1, 2, \cdots N$.

$$[g] = 1^{l_1} \cdot 2^{l_2} \cdots N^{l_N} \ , \quad \sum_k k \, l_k = N \ . \tag{3.2.15}$$

Excited states are created by acting with operators of the seed theory on twisted states. For example, consider the non-gauge invariant twist operator σ_g where g is a cycle of length n. Given (3.2.13), the operators of the seed theory have fractional modes

$$\mathcal{O}_I(z) = \frac{1}{n} \sum_m (\mathcal{O}_I)_{\frac{m}{n}} z^{-\frac{m}{n} - h_{\mathcal{O}}} e^{-2\pi i \frac{m}{n}(I-1)} \ . \tag{3.2.16}$$

The modes with fractional indices correspond to excited twist operators. Hence, in the twisted sector corresponding to an element of S_N with a single cycle of length n, there are n subsectors (the vacuum twist operator σ_n and exited states dressed with fractional modes of the operators of the seed theory). More generally, in a twisted sector created by σ_g, twist operators are labeled by the centralizer of g. Thus, the torus partition function can be written as follows [137, 138]

$$Z = \frac{1}{|G|} \sum_{gh=hg} h \underset{g}{\square} (\tau, \bar{\tau}) \ , \tag{3.2.17}$$

where g denotes the twisted sector and h an element of its centralizer. Each term in the sum is equal to

$$h \underset{g}{\square} (\tau, \bar{\tau}) = \mathrm{tr}_{\mathcal{H}_g} \Big(h \, e^{2\pi i \tau (L_0 - \frac{c}{24})} \, e^{-2\pi i \bar{\tau} (\bar{L}_0 - \frac{c}{24})} \Big) \ . \tag{3.2.18}$$

The summation of elements $h \in S_N$ that commute with g imposes the projection onto states that are invariant under the centralizer $C[g]$. Here $|G| = N!$ is the order of S_N. Using the fact that the torus partition function in the individual sectors transforms as follows under modular transformations $\tau \to -\frac{1}{\tau}$

$$h \underset{g}{\square} (\tau, \bar{\tau}) \to g^{-1} \underset{h}{\square} (-\frac{1}{\tau}, -\frac{1}{\bar{\tau}}) \ , \tag{3.2.19}$$

it is straightforward to check that the orbifold partition function is modular invariant.

The spectrum of the twisted sectors can be obtained by expanding the partition function. For a twisted sector labelled by a cycle $[g]$ in (3.2.15), the conformal dimensions h_{CFT} of the universal twisted sector ground state is given by

$$h_{CFT} = \sum_{k=1}^{N} l_k \frac{c_{\text{seed}}}{24}\big(k - \frac{1}{k}\big) \ . \tag{3.2.20}$$

These operators do not depend on the details of the seed CFT. In addition, there are twisted sector states built on primaries in the seed theory with $h_{\text{seed}} > 0$ as well as (fractional) Virasoro descendants, but these states will not play an important role in the following.

Another way [17, 139] to look at the partition function is via a grand canonical generating function. The modular invariant partition function of the seed theory is denoted as $Z(\tau, \bar{\tau})$

$$\sum_N p^N Z_N = \exp[\sum_{k=1}^{\infty} p^k T_k Z(\tau, \bar{\tau})] \ , \tag{3.2.21}$$

where T_k is the Hecke operator

$$T_k Z(\tau, \bar{\tau}) = \frac{1}{k} \sum_{i|k} \sum_{j=0}^{i-1} Z\Big(\frac{k\tau}{i^2} + \frac{j}{i}, \frac{k\bar{\tau}}{i^2} + \frac{j}{i}\Big) \ . \tag{3.2.22}$$

Correlation function of twist operators can be calculated by going to the covering space [121, 123, 124, 140, 141]. Suppose we want to calculate a correlation function of twist operators. Due to (3.2.13), correlation functions of non-gauge invariant operators have branch cuts. The union of the different sheets forms the covering space. Although we consider the orbifold theory on S^2, the covering space does not necessarily have zero genus; its genus is determined by the Riemann–Hurwitz formula [123].

3.3 Universal defects in symmetric orbifolds

We construct the orbifold CFT starting with a tensor product of N copies of a seed theory $\mathcal{M}$ and gauge the S_N symmetry that permutes the N copies. The gauged theory exhibits a quantum symmetry $\text{Rep}(S_N)$[1] [47, 128, 129]. In this section, we construct these universal

[1] Intuitively, this symmetry is generated by the Wilson lines of the S_N gauge field.

topological defects using the projector construction of Petkova and Zuber [115]. In particular, the details of the seed CFT will not play a role in the sense that the defect can be thought of as being built on the trivial topological defect in the seed CFT, which always exists. In addition to these defects, there may be other topological defects coming from the defects of the seed theory itself. We discuss non-universal defects, which are based on nontrivial topological defects in the seed theory, in section 3.5.

3.3.1 Construction

Utilizing the folded permutation brane construction for a topological defect, a universal defect corresponds to the following boundary state in the folded $\mathcal{M}^{\otimes N}/S_N \times \mathcal{M}^{\otimes N}/S_N$ CFT

$$\mid B_R\rangle\rangle = \sum_{[g]} \chi_R([g]) \sum_n \mid n\rangle_{(1),[g]} \otimes \overline{\mid n\rangle}_{(2),[g]} \sum_m \mid m\rangle_{(2),[g]} \otimes \overline{\mid m\rangle}_{(1),[g]} \ , \tag{3.3.1}$$

Here $[g]$ denotes the twisted sector in the $\mathcal{M}^{\otimes N}/S_N$ orbifold labeled by the conjugacy class of S_N. The summation over n, m denotes the sum over all states in the $[g]$-twisted sector including the sum over primaries of the seed theory as well as Virasoro descendants producing an Ishibashi boundary state [133]. The folded boundary state, and thus the defect, is labeled by the choice of representation R of S_N with $\chi_R([g])$ being the character of the conjugacy class $[g]$ in the representation R. Consequently, the boundary state satisfies

$$\left(L_n^{(1)} - \bar{L}_{-n}^{(2)}\right) \mid B_R\rangle\rangle = \left(L_n^{(2)} - \bar{L}_{-n}^{(1)}\right) \mid B_R\rangle\rangle = 0 \ , \tag{3.3.2}$$

where $L_n^{(i)}, i = 1, 2$ are the modes of the stress tensor of the two copies of the $\mathcal{M}^{\otimes N}/S_N$ orbifold after folding. After unfolding, the two copies of the CFT living on half-spaces are separated by the defect operator

$$\mathcal{I}_R = \sum_{[g]} \chi_R([g]) P_{[g]} \bar{P}_{[g]} \ . \tag{3.3.3}$$

The defect is expressed in terms of the identity projectors in the $[g]$-twisted sector satisfying $P_{[g]}^2 = P_{[g]}$ and $P_{[g]} P_{[g']} = 0$ if $[g] \neq [g']$. It is clear from the property of the projectors or the unfolding of the boundary state condition (3.3.2) that the defect is topological, i.e. it commutes with the holomorphic and anti-holomorphic modes of the stress tensor separately.

$$L_n\, \mathcal{I}_R = \mathcal{I}_R\, L_n \ , \qquad \bar{L}_n\, \mathcal{I}_R = \mathcal{I}_R\, \bar{L}_n \ . \tag{3.3.4}$$

Using the properties of the projection operators, one can calculate the fusion product of two defect operators labeled by two representations $R_{1,2}$

$$\begin{aligned}
\mathcal{I}_{R_1}\mathcal{I}_{R_2} &= \sum_{[g]} \chi_{R_1}([g])\chi_{R_2}([g]) P_{[g]}\bar{P}_{[g]} \\
&= \sum_{R_3} \frac{1}{|G|} \sum_{g} \chi_{R_1}(g)\chi_{R_2}(g)\chi_{R_3}(g)^* \mathcal{I}_{R_3} \\
&= \sum_{R_3} N_{R_1 R_2}^{R_3} \mathcal{I}_{R_3} \ .
\end{aligned} \tag{3.3.5}$$

Here $N_{R_1 R_2}^{R_3}$ are the Kronecker coefficients of the decomposition of the tensor product $R_1 \otimes R_2$ into representations R_3. Since S_N for $N > 2$ is a non-abelian group, the topological line-defects include non-invertible ones. This can also be seen from the fact that acting on a state in the $[g]$-twisted sector one has

$$\mathcal{I}_R \mid \Phi_{[g]}\rangle = \chi_R([g]) \mid \Phi_{[g]}\rangle \ . \tag{3.3.6}$$

In particular, this implies that the quantum dimension of a defect $\mathcal{I}_R$ is given by $\langle \mathcal{I}_R \rangle = \chi_R(1) = dim_R$, i.e. the dimension of the representation. In general, for S_N with $N > 2$, apart from the trivial and the alternating (or sign) representation, all other representations have dimensions greater than one, hence giving rise to non-invertible defects.

3.3.2 Modular invariance and defect operators

In this section, we use modular invariance to identify the operators in the defect Hilbert space which can end on topological lines. The starting point is to insert a defect $\mathcal{I}_R$ along the spatial cycle in the torus partition function

$$
\begin{aligned}
Z^R(\tau,\bar{\tau}) &= \frac{1}{|G|}\sum_{gh=hg} tr_{\mathcal{H}_g}\Big(h\, e^{2\pi i\tau(L_0-\frac{c}{24})}\, e^{-2\pi i\bar{\tau}(\bar{L}_0-\frac{c}{24})}\,\mathcal{I}_R\Big)\\
&= \frac{1}{|G|}\sum_{gh=hg}\chi_R([g])\; h\underset{g}{\square}(\tau,\bar{\tau})\ .
\end{aligned}
\tag{3.3.7}
$$

The defect Hilbert space can be obtained by performing a modular transformation $\tau\to-\frac{1}{\tau}=\tau'$, which exchanges the spatial and temporal cycles. Using the modular transformation (3.2.19), the defect partition function is given by

$$
Z_R(\tau',\bar{\tau}') = \frac{1}{|G|}\sum_{gh=hg}\chi_R([g])\; g\underset{h}{\square}(\tau',\bar{\tau}')\ , \tag{3.3.8}
$$

where we used the fact that the characters of S_N are real.

In the orbifold partition function, we decompose the elements h, g which commute $gh = hg$ by labeling the element g by its conjugacy class and h by the element of the centralizer. However, one can do this the other way around, where h labels conjugacy classes and g labels the centralizer of h.

The simplest and most relevant case to the large-N limit is when h corresponds to a single cycle of length $[w]$. The centralizer of such an element is $\mathbb{Z}_w\times S_{N-w}$. The group $\mathbb{Z}_w$ contains elements $1,\omega,\omega^2,\cdots\omega^{w-1}$, where ω is the w-th root of unity. The defect partition function corresponding to the single w-twisted cycle can be written as

$$
Z_{R,[w]} = \frac{1}{\dim C[w]}\;\chi_R(C[w])\; C[w]\underset{[w]}{\square}\ . \tag{3.3.9}
$$

Using the decomposition of $C[w]=\mathbb{Z}_w\times S_{N-w}$ and $\dim C[w] = w(N-w)!$, one gets

$$
Z_{R,[w]} = \frac{1}{(N-w)!}\sum_{g\in S_{N-w}}\frac{1}{w}\Big(\chi_R([1_w\times g])\; 1_w\times g\underset{[w]}{\square} + \sum_{k=1}^{w-1}\chi_R([\omega^k\times g])\;\omega^k\times g\underset{[w]}{\square}\Big)\ . \tag{3.3.10}
$$

To determine the number of defect operators, we want to pick out the ground state contribution of the w-twisted sector from (3.3.10), which has the conformal dimension

$$
h=\bar{h}=\frac{c_{\text{seed}}}{24}\big(w-\frac{1}{w}\big)\ . \tag{3.3.11}
$$

As far as the S_{N-w} permutation is concerned, the sector $[w]$ is untwisted. Consequently, the insertion of $g \in S_{N-w}$ contributes the same factor to the ground state in the defect partition function (3.3.10). The same holds for the 1_w and $\omega^k, k = 1, 2, \cdots w-1$ insertions since these enforce the $h - \bar{h} \in \mathbb{Z}$ projection, which is automatically satisfied for the twisted ground state (3.3.11). This implies that the number of w-twisted defect ground states is simply obtained by setting $\square = 1$ for all terms in the partition function (3.3.10), giving

$$n_w^R = \frac{1}{(N-w)!} \sum_{h' \in S_{N-w}} \frac{1}{w} \sum_{k=0}^{w-1} \chi_R([\omega^k \times h']) \ , \tag{3.3.12}$$

where we included $\omega^0 = 1_w$. A vanishing n_w^R implies that the $\mathcal{I}_R$ defect cannot end on a bare twist operator in the w-twisted sector.

One way to understand the defect operators at the endpoints of topological line-defects is to view these line-defects as open Wilson lines ending on non-gauge invariant operators [129]. A natural proposal for such operators involves using characters to project onto the representation R

$$\sigma_g^R \equiv N_R \sum_{h \in S_N} \chi_R(h)\ \sigma_{h^{-1}gh} \ , \tag{3.3.13}$$

where we pick an element g in the conjugacy class that labels the twisted sector and we focus again on a single cycle of length w. We propose that the $\mathcal{I}_R$ line-defect can end on a defect operator in the $[g]$-twisted sector if (3.3.13) does not vanish. We can decompose the sum over $h \in S_N$ in (3.3.13) into a sum over the centralizer of g and the rest

$$\sigma_g^R \equiv N_R \Big(\sum_{h' \in S_{N-w}} \sum_{k=0}^{w-1} \chi_R([\omega^k \times h'])\sigma_g + \cdots \Big) \ , \tag{3.3.14}$$

where the dots denote summation over other group elements in the conjugacy class of g. Note that the coefficient multiplying σ_g in (3.3.14) is proportional to (3.3.12). Consequently, the vanishing of one implies the vanishing of the other and the criterion for the existence of a defect operator ending on a line-defect is the same. The vanishing of all the terms on the right-hand side of (3.3.13) can be established by conjugating the group element g and using the fact that the characters take the same value on all elements of the same conjugacy class.

It should be noted that for S_N with $N > 4$, the degeneracy of the twisted sector ground states (3.3.12) can be larger than one. For the non-gauge invariant operators in (3.3.13), this can be understood by the fact that the action of S_N on all elements g in a fixed conjugacy class by conjugation $g \to h^{-1}gh$ determines a (generally) reducible representation. The value n_w^R gives the number of times the irreducible representation R appears in this representation.

In the next section we will further test this construction by evaluating correlation functions of defect operators and check the Ward identities following from the non-invertible symmetry $\mathrm{Rep}(S_3)$.

3.4 Example: S_3 symmetric orbifold

We now consider a simple example, the S_3 orbifold theory of a seed CFT $\mathcal{M}$ with central charge c. Upon gauging the S_3 symmetry, a $\mathrm{Rep}(S_3)$ quantum symmetry emerges. The objects of $\mathrm{Rep}(S_3)$ symmetry are topological lines which are labeled by the irreducible representations of S_3.

The symmetric group S_3 is a non-abelian group consisting of permutations of three elements. The group-elements of S_3 are

$$S_3 = \{e, (12), (23), (31), (123), (132)\} \ , \tag{3.4.1}$$

where e is the identity permutation, (12) is a 2-cycle representing the permutation $1 \to 2 \to 1$, (123) is a 3-cycle representing the permutation $1 \to 2 \to 3 \to 1$ and so on. There are three conjugacy classes

$$[e] = \{e\}, \quad [2] = \{(12), (13), (23)\}, \quad [3] = \{(123), (132)\} \ . \tag{3.4.2}$$

The character table of S_3 is given below

$$\begin{array}{c|ccc} & [e] & [2] & [3] \\ \hline \chi_e & 1 & 1 & 1 \\ \chi_A & 1 & -1 & 1 \\ \chi_S & 2 & 0 & -1 \end{array} \tag{3.4.3}$$

where e denotes the trivial representation, A denotes the alternating representation, and S denotes the standard representation.

In this case, the fusion rules of the universal defects defined in (3.3.3) follow from the above character table and read

$$\begin{aligned}
&\mathcal{I}_A \times \mathcal{I}_A = 1, \\
&\mathcal{I}_S \times \mathcal{I}_A = \mathcal{I}_A \times \mathcal{I}_S = \mathcal{I}_S, \\
&\mathcal{I}_S \times \mathcal{I}_S = 1 + \mathcal{I}_A + \mathcal{I}_S \ .
\end{aligned} \tag{3.4.4}$$

We see that the line-defect associated with the standard representation is non-invertible. Using (3.2.14), the gauge invariant ground state operators are

$$\begin{aligned}
\sigma_{[2]} &= \frac{1}{\sqrt{3}}\Big(\sigma_{(12)} + \sigma_{(23)} + \sigma_{(13)}\Big) \ , \\
\sigma_{[3]} &= \frac{1}{\sqrt{2}}\Big(\sigma_{(123)} + \sigma_{(132)}\Big) \ ,
\end{aligned} \tag{3.4.5}$$

where the proportionality constants were fixed by requiring that the two-point functions be normalized to 1. The action of the defects on these operators is summarized in Figure 3.4.

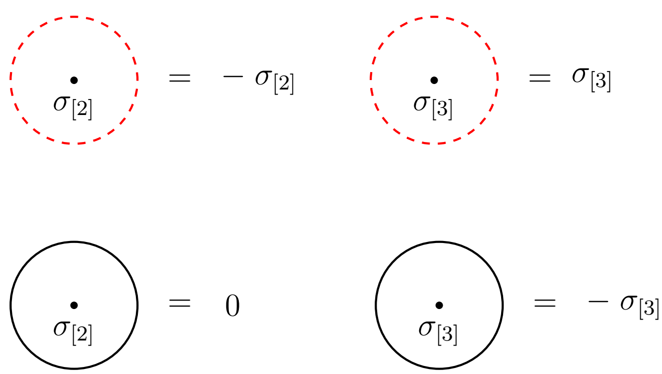

Figure 3.4: Action of the universal line-defects. The red line denotes the invertible sign defect $\mathcal{I}_A$ while the black line denotes the standard defect $\mathcal{I}_S$.

Next, let us discuss the defect Hilbert spaces. From (3.3.13), we observe that there are no two-cycle ground states in $\mathcal{H}_{\mathcal{I}_A}$ and no three-cycle ground states in $\mathcal{H}_{\mathcal{I}_S}$. The twisted ground states in the defect Hilbert space are

$$\begin{aligned}\sigma^S_{[2]} &= N_S\left(2\sigma_{(12)} - \sigma_{(23)} - \sigma_{(13)}\right)\,,\\ \sigma^A_{[3]} &= N_A\left(\sigma_{(123)} - \sigma_{(132)}\right)\,.\end{aligned} \tag{3.4.6}$$

Here, without loss of generality, we choose $\sigma_{(12)}$ and $\sigma_{(123)}$ as representatives of [2] and [3] respectively. The constants N_A, N_S can be fixed by normalizing the two-point correlators of the non-gauge invariant operators with the line-defects inserted to 1. For example, demanding that

$$\langle\ \sigma^S_{[2]} \quad \bullet\!\!-\!\!-\!\!-\!\!-\!\!\bullet\, \sigma^S_{[2]}\ \rangle = N_S^2\left(4\langle\sigma_{(12)}\sigma_{(12)}\rangle + \langle\sigma_{(23)}\sigma_{(23)}\rangle + \langle\sigma_{(13)}\sigma_{(13)}\rangle\right) = 6N_S^2 = 1\,, \tag{3.4.7}$$

gives us $N_S^2 = 1/6$. Similarly, we get $N_A^2 = -1/2$. To show this, we used that the two-point correlator vanishes unless the permutation corresponding to the second twist operator is the inverse of the first [123]. In the above correlator, we implicitly assumed that insertions of the two operators are at the poles of the sphere.

Next, we determine the coefficients in the lasso diagrams. Since the defects are topological, the scaling dimension does not change and the two possible diagrams are shown in Figure 3.5. In the following, we fix the coefficients α and β.

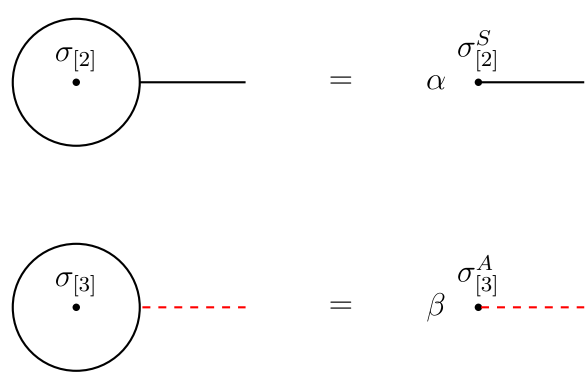

Figure 3.5: Lasso diagrams where the right-hand side is obtained after shrinking the standard defect loop which produces a defect operator.

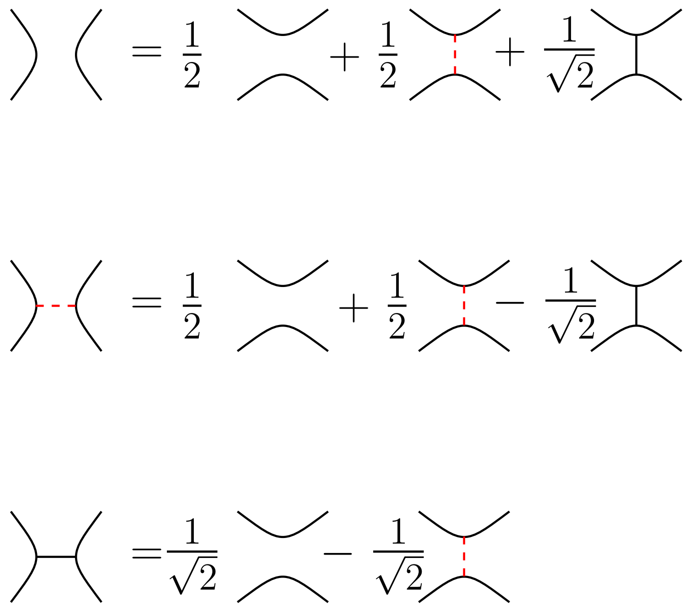

Figure 3.6: F-symbols of $\mathrm{Rep}(S_3)$.

Consider the two-point correlator of the two-cycles encircled by the $\mathcal{I}_S$ line. We can shrink the line-defect to a point by avoiding both operators, which gives us the quantum dimension of the line $\langle \mathcal{I}_S \rangle$. Alternatively, we can make use of the F-symbols [142, 143] in Figure 3.6 corresponding to the crossing relations of $\mathrm{Rep}(S_3)$ to pull the line-defect through the operators and then shrink it to a point. Pictorially, the two ways of shrinking the defect are

$$\langle \sigma_{[2]}\ \sigma_{[2]} \rangle = \frac{1}{\dim S} \langle\ \sigma_{[2]}\ \ \sigma_{[2]}\ \rangle = \frac{1}{2\sqrt{2}} \langle\ \sigma_{[2]} \ \text{———}\ \sigma_{[2]}\ \rangle = \frac{\alpha^2}{2\sqrt{2}} \langle\ \sigma^S_{[2]} \bullet\!\text{———}\!\bullet\ \sigma^S_{[2]}\ \rangle\ , \tag{3.4.8}$$

Requiring that the correlators on both sides are normalized to 1, we get $\alpha^2 = 2\sqrt{2}$. Similarly, for the two-point correlator of the three-cycle ground states,

$$\begin{aligned}\langle \sigma_{[3]}\ \sigma_{[3]} \rangle = \frac{1}{\dim S} \langle\ \sigma_{[3]}\ \ \sigma_{[3]}\ \rangle &= \frac{1}{4} \langle\ \sigma_{[3]}\ \ \ \sigma_{[3]}\ \rangle + \frac{1}{4} \langle\ \sigma_{[3]} \text{- - - - -} \sigma_{[3]}\ \rangle \\ &= \frac{1}{4} \langle \sigma_{[3]}\ \sigma_{[3]} \rangle + \frac{\beta^2}{4} \langle\ \sigma^A_{[3]} \bullet\!\text{- - - - -}\!\bullet\ \sigma^A_{[3]}\ \rangle\ ,\end{aligned} \tag{3.4.9}$$

leads to $\beta^2 = 3$.

We can now obtain selection rules for the three-point correlators in the presence of the line-defects. The only non-trivial three-point correlators of bare twist operators are $\langle \sigma_{[2]}\sigma_{[2]}\sigma_{[3]} \rangle$ and $\langle \sigma_{[3]}\sigma_{[3]}\sigma_{[3]} \rangle$. To illustrate the procedure we focus on the former. As in the case of two-point functions, the locations of the operators in the three-point correlators are fixed using the $SL(2, \mathbb{R})$ symmetry. Consider a line-defect $\mathcal{I}_S$ encircling only $\sigma_{[3]}$. This is equivalent to encircling both the $\sigma_{[2]}$ operators on the sphere as illustrated in Figure 3.7. The second line in the figure is obtained by using the F-symbols in Figure 3.6 and the lasso diagram in Figure 3.5. The correlator $\langle \sigma_{[2]}\sigma_{[2]}\sigma_{[3]} \rangle$ can be expanded using (3.4.5) as follows

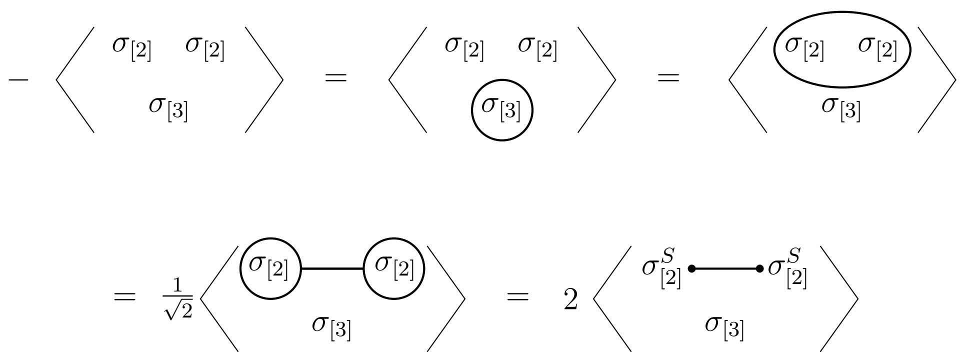

Figure 3.7: The Ward identity associated with $\mathcal{I}_S$ wrapping $\sigma_{[3]}$. We can shrink the line-defect the other way on the sphere which gives the correlator with both the $\sigma_{[2]}$ encircled.

$$\begin{aligned} -\langle \sigma_{[2]}\sigma_{[2]}\sigma_{[3]} \rangle &= \frac{-1}{3\sqrt{2}} \langle\, (\sigma_{(12)} + \sigma_{(23)} + \sigma_{(13)})(\sigma_{(12)} + \sigma_{(23)} + \sigma_{(13)})(\sigma_{(123)} + \sigma_{(132)})\, \rangle \\ &= -\sqrt{2}\, C_{223}\ , \end{aligned} \tag{3.4.10}$$

where we have defined $C_{223} \equiv \langle \sigma_{(12)}\sigma_{(23)}\sigma_{(123)} \rangle = \langle \sigma_{(12)}\sigma_{(13)}\sigma_{(132)} \rangle = \langle \sigma_{(23)}\sigma_{(13)}\sigma_{(123)} \rangle$. Meanwhile, the rightmost correlator in the second line of Figure 3.7 can be computed using (3.4.6) as

$$\begin{aligned} 2\langle \sigma^S_{[2]} \bullet\!\!-\!\!\bullet\, \sigma^S_{[2]}\ \sigma_{[3]} \rangle &= 2\,\frac{1}{6}\,\frac{1}{\sqrt{2}} \langle (2\sigma_{(12)} - \sigma_{(23)} - \sigma_{(13)})(2\sigma_{(12)} - \sigma_{(23)} - \sigma_{(13)})(\sigma_{(123)} + \sigma_{(132)}) \rangle \\ &= -\sqrt{2}\, C_{223} = -\langle \sigma_{[2]}\sigma_{[2]}\sigma_{[3]} \rangle\ . \end{aligned} \tag{3.4.11}$$

Hence, using the explicit expressions of non-gauge invariant twist fields, we can check the Ward identity of $\mathcal{I}_S$. Similarly, we can also use these defects to calculate the following correlator

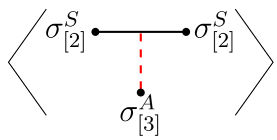

$$= -\frac{\sqrt{3}}{2}\langle \sigma_{[2]}\sigma_{[2]}\sigma_{[3]}\rangle \ . \tag{3.4.12}$$

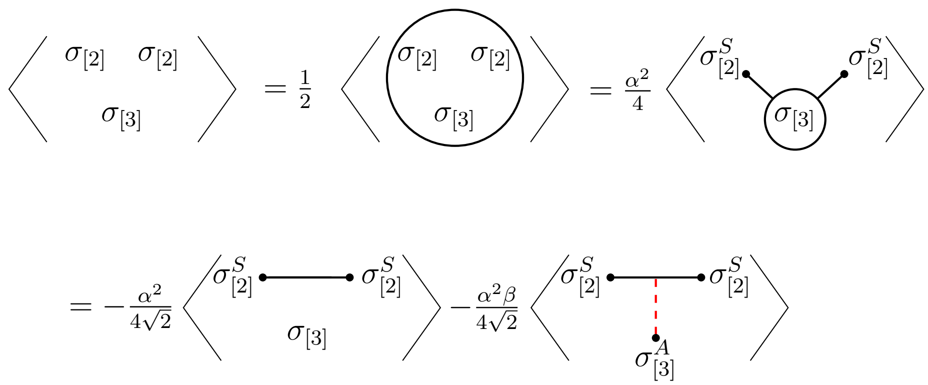

Figure 3.8: The Ward identity associated with $\mathcal{I}_S$ encircling all three operators giving rise to a junction. Shrinking the line-defect by avoiding the operator insertions gives us $\langle \mathcal{I}_S\rangle = 2$.

3.5 Non-universal defects

In section 3.3, we constructed universal defects labeled by an irreducible representation R of the symmetric group S_N. As can be seen from the expression (3.3.3), the defect operator in each twisted sector is proportional to the identity operator and hence does not depend on the details of the seed CFT. Another way to look at this is that the topological defect one starts with, in the seed theory, is the identity or trivial defect. It is an interesting question whether one can start with a nontrivial defect in the seed theory and construct non-universal defects which depend on the details of the seed theory and the topological defects present in it. Similar questions arise in the construction of D-brane states in symmetric orbifolds, as discussed in [144, 145], which we will build upon in the following section.

Here we only construct a simple example of a non-universal defect that is analogous to the "maximally fractional" D-brane of [144]. A twisted sector (3.2.15) in the S_N orbifold theory is labeled by a conjugacy class $[g]$ which is fixed by giving the number l_i of cycles of given length $i = 1, 2, \cdots N$. We focus on diagonal RCFTs discussed in section 3.2.1 as the seed CFT. In particular, we use the defects $\mathcal{I}_a$ in the RCFT defined in (3.2.2). In the tensor product states, we will use the same boundary state labeled by a for all factors to construct a "maximally fractional" defect, which is automatically S_N invariant[2]. In a twisted sector corresponding to a single w cycle, the doubled boundary state is given by

$$\mid B_a\rangle\rangle_{(w)} = \sum_i \frac{S_{ai}}{S_{0i}} \sum_n |i,n\rangle^{(1)}_{(w)} \otimes \overline{|i,n\rangle}^{(2)}_{(w)} \sum_m |i,m\rangle^{(2)}_{(w)} \otimes \overline{|i,m\rangle}^{(1)}_{(w)} , \tag{3.5.1}$$

where the sum over n, m denotes the sum over all the descendants (including fractional Virasoro modes) of the w-twisted sector primary $|i\rangle_{(w)}$. Using these boundary states for single cycles, we can construct a defect boundary state which is labeled by the representation R of S_N as well as the choice of primary a of the RCFT as

$$\mid B_a^R\rangle\rangle = \sum_{[g]\in S_N} \chi_R([g]) \prod_{j=1}^{N} \prod_{k_j=1}^{l_j} \mid B_a\rangle\rangle_{(j)} . \tag{3.5.2}$$

The consistency condition for the topological defects derived by Petkova and Zuber in [115] is equivalent to the Cardy condition for the doubled boundary state (3.5.2). The cylinder amplitude for two defect-boundary states is given by

$$\begin{aligned} Z_{ab}^{R_1R_2}(q) &= \langle\langle B_a^{R_1} \mid q^{L_0^{(1)}+\bar{L}_0^{(1)}-\frac{c}{12}}\, q^{L_0^{(2)}+\bar{L}_0^{(2)}-\frac{c}{12}} \mid B_b^{R_2}\rangle\rangle \\ &= \sum_{[g]\in S_N} \bar{\chi}_{R_1}([g])\, \chi_{R_2}([g]) \prod_{j=1}^{N} \left(\sum_i \frac{S_{ai}^*}{S_{0i}} \frac{S_{bi}}{S_{0i}}\, \chi_i(t/j)\, \chi_i(t/j) \right)^{l_j} . \end{aligned} \tag{3.5.3}$$

The Cardy condition states that under modular transformation to the annulus channel, the partition function has a consistent interpretation as an open string partition function, i.e. the primary representations appear with integer multiplicities. Using the modular transformation of the RCFT characters and the Verlinde formula, one obtains

$$Z_{ab}^{R_1R_2}(\tilde{q}) = \sum_{[g]\in S_N} \bar{\chi}_{R_1}([g])\, \chi_{R_2}([g]) \prod_{j=1}^{N} \Big(\sum_{rs} N_{ab}^{\ \ rs}\, \chi_r(j\tilde{t})\, \chi_s(j\tilde{t}) \Big)^{l_j} , \tag{3.5.4}$$

[2] For discussions on a more general construction of D-branes in symmetric orbifold CFTs see [145].

where $N_{ab}{}^{rs}$ can be expressed in terms of the fusion coefficients n^a_{bc} of the seed RCFT

$$\begin{aligned} N_{ab}{}^{rs} &= \sum_{i,k,j} \frac{S^*_{ai} S_{bi} S_{ik}}{S_{0i}} \frac{S^*_{kj} S_{jr} S_{is}}{S_{0j}} \\ &= \sum_k n^k_{ab} \, n_k{}^{rs} \ . \end{aligned} \tag{3.5.5}$$

Consequently, the $N_{ab}{}^{rs}$ are non-negative integers. The partition function appearing in (3.5.4)

$$Z_{ab}(\tilde{t}) = \sum_{rs} N_{ab}{}^{rs} \, \chi_r(\tilde{t}) \, \chi_s(\tilde{t}) \ , \tag{3.5.6}$$

contains the characters of the folded RCFT with integer multiplicities and can be written as a trace over a Hilbert space $\mathcal{H}_{ab}$ in the doubled tensor product of the seed RCFT. Hence, (3.5.4) can be written as

$$Z^{R_1 R_2}_{ab}(\tilde{q}) = \sum_{[g]\in S_N} \bar{\chi}^{R_1}([g]) \, \chi^{R_2}([g]) \ \mathrm{tr}_{(\mathcal{H}_{ab})^{\otimes N}} \left(g \, \tilde{q}^{L_0 - \frac{c}{24}} \right) \ , \tag{3.5.7}$$

and the character sum projects onto the representations of S_N in the N-fold tensor product of the folded CFT of R_1 and R_2. It follows that the open string partition function will be a sum over states with integer multiplicity. The maximal fractional boundary state (3.5.1) satisfies the Cardy condition and, therefore, defines a consistent topological defect.

It follows from unfolding the boundary state (3.5.2) that the quantum dimension of the maximally fractional defect $\mathcal{I}_{a,R}$ labelled by a, R is given by

$$\langle \mathcal{I}_{a,R} \rangle = \langle 0 \mid B^R_a \rangle\rangle = \chi_R([1]) \left(\frac{S_{a0}}{S_{00}} \right)^N \ , \tag{3.5.8}$$

which is the product of the quantum dimension of the universal defect and the quantum dimensions of the N copies of the topological defect in the RCFT present in the untwisted sector. Similar considerations as presented above determine the fusion coefficients of the defects as well as their defect Hilbert spaces.

The construction of the maximally fractional defects can straightforwardly be extended to other seed CFTs including compact bosons, T^4, and K_3 sigma models (see e.g. [118, 136, 146–150]), where the RCFT defects in (3.5.2) are replaced by topological defects of the seed CFT, which realize more general non-invertible symmetries. We leave the discussion of these defects for future work.

3.6 Large-N symmetric orbifold

In this section, we discuss the universal defects of section 3.3 in the large-N limit. We provide a criterion for a defect to be non-trivial in this limit. Then, we show that there exist representations that pass this criterion. In the next section, we will argue that in the AdS_3/CFT_2 correspondence, these non-trivial defects correspond to topological defects on the worldsheet.

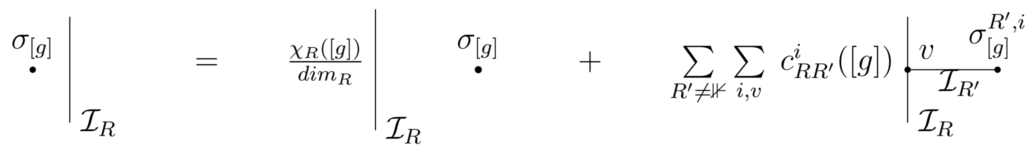

Figure 3.9: Action of the topological defect $\mathcal{I}_R$ on twist operators. The vector v is an element in $\mathrm{Hom}(R \otimes R, R')$. The sum on the right-hand side is over R' with $N_{RR}{}^{R'} \neq 0$. We have omitted the orientation of the defect since all the representations of S_N are real.

Consider the topological defect $\mathcal{I}_R$, the general action on twist operators is shown in Figure 3.9. This depends on the Kronecker coefficients $N_{RR}{}^{R'}$ as well the constants $c^i_{RR'}([g])$. The former determines the representations R' that appear in the sum. In principle, to determine the constants $c^i_{RR'}([g])$ we need to know both the Kronecker coefficients as well as the F-symbols. At present, it is an open problem in mathematics to find explicit expressions for the Kronecker coefficients for arbitrary representations. In fact, it is known that the Kronecker coefficients in general are unbounded for large-N [151].

For a defect to be non-trivial in the large-N limit, it needs to satisfy[3]

$$\lim_{N\to\infty} \frac{\chi_R([g])}{dim_R} < 1 \ . \tag{3.6.1}$$

If this is not the case, in the limit $N \to \infty$ the defect commutes with all the operators and therefore the contributions of non-local operators are zero (see section 2.2.4 of [14]). We conclude that for finite N the contributions of non-local operators on the right-hand side of Figure 3.9 are subleading.

[3]Note the characters satisfy $\chi_R([g]) \leq dim_R$ for any representation.

Let us now comment on what representations lead to non-trivial Ward identities in the large-N limit. Recall that as is the case for the conjugacy classes, representations of S_N are also labeled by partitions of N [4]

$$R: \quad (r_1, r_2, \dots), \quad r_1 + r_2 + \dots = N \ . \tag{3.6.2}$$

We can associate a Young tableau to each representation where the number of boxes in the row i is equal to r_i. For a representation R,[5] the character of a conjugacy class with a single cycle has the following limit [152, 153]

$$\lim_{N\to\infty} \frac{\chi_R([n])}{dim_R} = \sum_i \alpha_i^n - (-1)^n \sum_i \beta_i^n \ , \tag{3.6.3}$$

where $\alpha_i = \lim\limits_{N\to\infty} \frac{r_i}{N}$ is the number of boxes in row i divided by N. Similarly, β_i is the number of boxes in the column i divided by N. As an example, let us look at the standard representation of S_N, which corresponds to the Young tableau

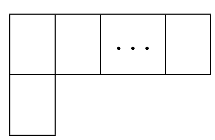

with the corresponding partition being $(N-1, 1)$. We see that

$$\alpha = \lim_{N\to\infty} \left(\frac{N-1}{N}, \frac{1}{N}, 0, 0, \dots \right) = (1, 0, 0, \dots) \ , \tag{3.6.4}$$

and

$$\beta = \lim_{N\to\infty} \left(\frac{2}{N}, \frac{1}{N}, \frac{1}{N} \dots \right) = (0, 0, 0, \dots) \ . \tag{3.6.5}$$

Hence, in the large-N limit $\frac{\chi_S([g])}{dim_S} \to 1$. This can also be derived by calculating the character of the standard representation for finite N using the Frobenius formula. Therefore, we

[4]Here we are using a different notation to label partitions of N compared to section 3.3 where l_i is the number of r_i's that satisfy $r_i = i$.

[5]The representation needs to have a well-defined limit, see for example [152].

conclude that the Ward identities of the standard representations are trivial in the large-N limit and only constrain subleading contributions coming from higher genus covering spaces.

Examples of representations with nontrivial ratio $\frac{\chi_R([g])}{dim_R}$ in the large-N-limit are Young diagrams with two rows and diagrams of hook-shape. For both of the above, the Kronecker coefficients $N_{RR}{}^{R'}$ are known [154–156]. For example, for the Young diagram with two rows

$$\begin{array}{|c|c|c|c|}\hline & & \cdots & \\ \hline & & \cdots & \\ \hline \end{array}$$

we have

$$\alpha = \left(\frac{1}{2}, \frac{1}{2}, 0, \dots\right), \quad \beta = (0, 0, 0, \dots) \ , \tag{3.6.6}$$

and therefore

$$\frac{\chi_R([n])}{dim_R} \to \frac{1}{2^{n-1}} \ . \tag{3.6.7}$$

Thus, we expect the defect corresponding to this representation to be non-trivial in the large-N limit.

3.7 Non-invertible symmetries and AdS$_3$/CFT$_2$ duality

The tensionless limit of the type II $AdS_3 \times S^3 \times \mathcal{M}_4$ background with NS-NS flux is a holographic setup where the non-invertible symmetries of the S_N orbifold CFT are realized. In this section, we take some first steps in constructing the holographic duals of these defects [6].

3.7.1 Tensionless Limit

In recent years, an example of an exact AdS/CFT duality has been established, relating type II string theory on $AdS_3 \times S^3 \times \mathcal{M}_4$ with $k = 1$ units of NS-NS flux to the symmetric orbifold CFT $\mathcal{M}_4^{\otimes N}/S_N$ in the large-N limit. Here, $\mathcal{M}_4$ is the CFT defined by the supersymmetric

[6] See the recent paper [157] for related discussions.

sigma-model with target space T^4 or K_3. The characteristic feature of this duality is that the string theory is defined on highly curved spaces far away from the supergravity limit, yet a tractable worldsheet CFT exists. The worldsheet description is based on a product of a $PSU(1,1|2)$ WZW model times a twisted $\mathcal{M}_4$ sigma model [19, 158]. The agreement of the spectra on the AdS and CFT side was demonstrated in [19, 20], correlation functions were identified in [141, 159], the torus partition function was related to thermal AdS in [160], and D-branes on both sides were related in [144]. The identification of states on both sides relates the vertex operators $\mathcal{O}_h^{(w)}(x)$ for a CFT state in a single cycle twisted sector labeled by w and a seed CFT state labeled by h, to a worldsheet vertex operator $V_h^w(x;z)$ where w now denotes the w-spectral flow sector. This duality relates string amplitudes to the orbifold worldsheet correlation function

$$\begin{aligned}
&\left\langle \mathcal{O}_{h_1}^{(w_1)}(x_1)\, \mathcal{O}_{h_2}^{(w_2)}(x_2) \cdots \mathcal{O}_{h_n}^{(w_n)}(x_n) \right\rangle_{S^2} \\
&= \int_{\mathcal{M}_{g,n}} d\mu \left\langle V_{h_1}^{w_1}(x_1;z_1) V_{h_2}^{w_2}(x_2;z_2) \cdots V_{h_n}^{w_n}(x_n;z_n) \right\rangle_{\Sigma_{g,n}} .
\end{aligned} \tag{3.7.1}$$

The equality of both sides hinges on a remarkable localization property of the string path integral. The integral over the moduli space $\mathcal{M}_{g,n}$ only contributes if a holomorphic covering map exists from the worldsheet $\Sigma_{g,n}$ to the spacetime S^2. In this map, the vertex operator locations z_i on the worldsheet are mapped to the locations x_i of the CFT operators. These points have ramification indices w_i for $i = 1, 2, \cdots, n$. The covering map behaves like

$$\Gamma(z) = x_i + a_i^\Gamma (z - z_i)_i^w + \mathcal{O}\big((z - z_i)^{w_i+1}\big) , \tag{3.7.2}$$

near $z = z_i$ and hence close to z_i describes a w_i-fold cover. The fact that the string worldsheet path integral localizes was shown using worldsheet Ward identities in [21] (see [161–165] for further discussions). In the following, we will focus on correlation functions at leading order in large-N, where both the string worldsheet and the target space are two spheres. This map allows us to reverse engineer the topological defect on the string worldsheet.

We recall that the topological defect operators associated with $\mathrm{Rep}(S_N)$ given in (3.3.3) are projectors on the twisted sectors of the S_N orbifold, weighted by the character of the representation

$$\mathcal{I}_R^{\rm CFT} = \sum_{[g]} \chi_R([g]) P_{[g]} \bar{P}_{[g]} \ . \tag{3.7.3}$$

Single string states created by the vertex operators $V_h^w(x,z)$ in the spectral flow sector w correspond to single cycle twisted states of length w. Limiting ourselves to the single cycle twisted sector, a natural proposal for a worldsheet is the projector

$$\mathcal{I}_R^{\rm ws} = \sum_{w} \chi_R([w]) P_w \bar{P}_w \ , \tag{3.7.4}$$

where P_w is a projector on the w-spectral flow sector and $\chi_R([w])$ is the S_N character of a single cycle conjugacy class of length w in representation R.

Such a projector[7] can be constructed as an operator on the worldsheet using the free field Wakimoto construction [171] of the $SL(2,\mathbb{R})$ part of the worldsheet sigma model. As an initial step, we define $I[C]$ as a contour integral over the worldsheet bosonic field $\Phi(z)$

$$I[C] = -2 \oint_C \frac{dz}{2\pi i}\, \partial_z \Phi \ , \tag{3.7.5}$$

where the contour C is always oriented counterclockwise. The localization of the worldsheet path integral [21, 161, 162], pictorially shown in Figure 3.10, leads to a very special property of the $\partial_z\Phi(z)$ field when inserted in string correlation functions [21]

$$\big\langle \big(-2\partial\Phi(z)\big) V_{h_1}^{w_1}(x_1;z_1)\cdots V_{h_n}^{w_n}(x_n;z_n)\big\rangle = \frac{\partial_z^2\Gamma(z)}{\partial_z\Gamma(z)} \big\langle V_{h_1}^{w_1}(x_1;z_1)\cdots V_{h_n}^{w_n}(x_n;z_n)\big\rangle \ . \tag{3.7.6}$$

The expectation value of $I(C)$ can then be evaluated using the following identity for the covering map Γ

$$\frac{\partial_z^2\Gamma(z)}{\partial_z\Gamma(z)} = \sum_{i=1}^{n} \frac{w_i - 1}{z - z_i} - \sum_{a=1}^{N-1} \frac{2}{z - z_a^*} \ . \tag{3.7.7}$$

Here, z_a are the location of the "secret poles," which in general depend on the location of the CFT operators x_i and are necessary for the existence of the covering map. We have placed

[7] Another proposal for $I[C]$ is the boundary central term $\mathcal{I} = \oint \frac{da}{2\pi i} \frac{\partial_z \gamma}{\gamma}$ [166–170]. This operator gives the winding number of the covering map $\Gamma(z)$, but the winding number is only defined with respect to a base point ($z = 0$ in the given formula) and does not lead to a viable worldsheet version of the topological defect.

the N-th secret pole at $z = \infty$, which is always possible and doing so cancels the background charge of Φ at infinity as discussed in [21]. It is easy to verify that the residue of $\partial_z^2\Gamma/\partial_z\Gamma$ at infinity is zero using the Riemann-Hurwitz formula. The value of $I[C]$ for a given contour can now be determined using the residue theorem.

We can now give a proposal for $\mathcal{I}_R^{\text{ws}}[C]$, i.e. the worldsheet version of the topological defect for contour C

$$\begin{aligned}\mathcal{I}_R^{\text{ws}}[C] &= \sum_w \chi_R(w)\delta_{w-I[C]} \\ &= \sum_{w=1}^{\infty} \chi_R(w) \int_0^{2\pi} \frac{d\alpha}{2\pi} \exp\Big(i\alpha\big(w-1-I[C]\big)\Big) \,. \end{aligned} \tag{3.7.8}$$

Thanks to the localization formula (3.7.6) and (3.7.7), it is easy to see that (3.7.5) evaluates to $w_i - 1$ for a countour which encircles only z_i and is independent of small deformations of the contour. Hence, (3.7.8) is acting like the projector (3.7.4) when encircling a single vertex operator. In particular, if the contour is inserted around a vertex operator in the untwisted sector (this can be the ground state itself), we have $w_i = 1$ and $I[C]$ evaluates to zero and hence $\mathcal{I}_R^{\text{ws}}[C]$ evaluates to $\chi^R([1])$, i.e. the quantum dimension of the operator.

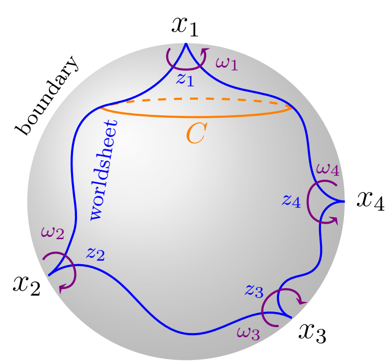

Figure 3.10: Contour C of operator I enclosing a vertex operator localized at x_1.

Consider now a two-point function of twist operators on the boundary. The dual correlator is a two-point function of spectrally flowed vertex operators. It is not too difficult to check that the value of $\mathcal{I}_R^{\text{ws}}[C]$ around any of the two insertions is the same. This is consistent with inserting the corresponding operator $\mathcal{I}_R^{CFT}$ on the boundary around either operators which gives the same value. The more interesting case is when we insert the operator $\mathcal{I}_R^{CFT}$ around a line that does not enclose any operator. This gives the dimension of the representation. On the worldsheet, the corresponding operator $\mathcal{I}_R^{\rm ws}[C]$ will be along a curve with no vertex operator inside giving again the dimension of the representation. However, in this case, the contour integral in $I[C]$ with no poles inside is not equal to the sum of the contour integrals around each of the vertex operators. This is because of the the presence of the secret poles in (3.7.7). On the worldsheet, we interpret this as the result of the lasso effect described in Figure 3.3.

The sign (alternating) defect is an example of an invertible defect for which $\chi^A(w) = (-1)^{w+1}$. When inserted on the boundary, the defect enforces the selection rule that $\sum_i w_i$ is odd. Since the character of the sign representation on single cycles of length w satisfies $\chi_A(w+2) = \chi_A(w)$, we see that $\mathcal{I}_R^{\rm ws}[C]$ is blind to the secret poles (they contribute -2 to the contour integral) and, therefore, the contour integral can be written as a sum of contour integrals around the ramification points reproducing the correct Ward identity on the worldsheet. The same line of reasoning can be applied to the case of three-point functions reproducing the corresponding Ward identities on the worldsheet.

3.7.2 Deformation away from the $k = 1$ and the supergravity limit

Turning on RR-fluxes in the bulk corresponds to deforming the symmetric orbifold CFT by an exactly marginal deformation [165, 172–182]. This deformation is proportional to a two-cycle twist field which we denote by $\sigma_{[2]}$. In the following, we argue that this deformation breaks all the non-invertible universal defects associated with the representations of S_N.

Consider the action of a topological defect $\mathcal{I}_R$ on the twisted state created by $\sigma_{[2]}$

$$\mathcal{I}_R\,|\sigma_{[2]}\rangle = \chi_R([2])\,|\sigma_{[2]}\rangle \ . \tag{3.7.9}$$

The deformation breaks all the defects if and only if $\chi_R([2]) \neq dim_R$. Below we prove that no defect satisfies this and, therefore, all the universal defects are broken in the supergravity limit.

Consider an element g in some representation R. Since all finite groups are unitariazable, this is a $dim_R \times dim_R$ matrix whose eigenvalues satisfy $|\lambda_i| = 1$. Hence,

$$\chi_R(g) = \sum_{i=1}^{dim_R} \lambda_i \ , \quad |\lambda_i| = 1 \ . \tag{3.7.10}$$

We see that $\chi_R(g) = dim_R$ if and only if $\lambda_i = 1 \ \forall \ i$ which is true only for the trivial representation. Hence, we conclude that any marginal deformation involving twist operators breaks all the universal defects. This means that all nontrivial symmetries do not survive the deformation away from the $k = 1$ point.

3.8 Entanglement Entropy and Topological Defects

In this section, we calculate the entanglement entropy for topological defects in symmetric orbifold CFTs using the methods developed for topological defects in rational CFTs in [5, 183, 184]. The defect entropy we calculate can be viewed as a measure of the complexity of the defect. Furthermore, it provides an observable which may be of use in calculating the entanglement entropy holographically using the dual $AdS_3 \times S^4 \times \mathcal{M}_4$ background with the minimal $k = 1$ unit of NS-fivebrane flux [18–21, 127]. Such a calculation may provide a further check on the proposals of the dual of the topological defect operators put forward in [6, 185].

3.8.1 Entanglement entropy and topological defects

In two dimensional CFTs, the simplest example of entanglement entropy is given by considering the theory in its vacuum and a single spatial interval $\mathcal{A}$. The entanglement entropy is then given by the von Neumann entropy of the reduced density matrix $\rho_{\mathcal{A}} = \mathrm{tr}_{\bar{\mathcal{A}}} |0\rangle\langle 0|$, where we trace over the states in the complement of $\mathcal{A}$.

$$S_{\mathcal{A}} = -\,\mathrm{tr}\,\rho_{\mathcal{A}} \ln \rho_{\mathcal{A}} \ . \tag{3.8.1}$$

The replica trick allows the entanglement entropy to be calculated from Rényi entropies

$$S_{\mathcal{A}} = -\partial_K \, \mathrm{tr} \, \rho_{\mathcal{A}}^K \Big|_{K=1} \; . \tag{3.8.2}$$

The K-th Rényi entropy can be calculated by a path integral over a Riemann surface with K sheets, with branch cuts along the interval $\mathcal{A}$ connecting the sheets in a cyclic fashion. The entanglement entropy for the CFT in its ground state can be obtained from the partition function $Z(K)$ over the K-sheeted Riemann surface, by the following expression

$$S_{\mathcal{A}} = \big(1 - \partial_K\big) \ln Z(K) \Big|_{K=1} \; . \tag{3.8.3}$$

In the evaluation of the path integral one has to introduce an ultraviolet cutoff ϵ and the terms which survive the limit of the cutoff going to zero are

$$S_{\mathcal{A}} = \frac{c}{3} \ln \frac{L}{\epsilon} + \ln g_{\mathcal{A}} \; , \tag{3.8.4}$$

where c is the central charge of the CFT. The constant term is not universal in the case of the CFT defined on a real line in the ground state. However, it can become physical in the the presence of a boundary or interface [186–188] and is sometimes called the g-factor or boundary entropy [189]. In the following we would like to calculate this g-factor for topological defects in symmetric orbifold CFTs.

3.8.1.1 Entanglement of symmetric defect

The g-factor (3.8.4) also appears in boundary CFTs, where the partition function of a CFT is defined on an interval of length L, with boundary conditions labeled by a and b at the two ends of the interval.

$$\ln Z = \ln \mathrm{tr} \, e^{-\beta H_{ab}} \sim \ln(g_a g_b) + \frac{c\pi}{6} \frac{L}{\beta} + \cdots \; , \tag{3.8.5}$$

which is valid in the limit $L >> \beta$. After a modular transformation from the open string annulus, the partition function can be viewed as a closed string cylinder between two boundary states

$$Z = \langle\langle a | e^{-L H_{cl}} | b \rangle\rangle \; . \tag{3.8.6}$$

One can extract the g-factors by inserting the ground state and taking the $L \to \infty$ limit. It follows that

$$g_a = \langle 0 | a \rangle\rangle \ . \tag{3.8.7}$$

It has been shown [187] that for an entangling surface $\mathcal{A}$ which starts at the boundary, the g-factor appearing in the entanglement entropy (3.8.4) is given by (3.8.7). So far we have considered a boundary CFT. For a conformal interface, one can use the folding trick [131, 132] where an interface between CFT_1 and CFT_2 is turned into a boundary CFT by folding $\mathrm{CFT}_1 \times \overline{\mathrm{CFT}}_2$, which can be represented by a boundary state $|B\rangle\rangle$. It was argued in [187, 188] that the g-factor for the entanglement entropy for a conformal defect which is symmetric (i.e. in the middle of the entangling region $\mathcal{A}$) is given by (3.8.7), where $| \, a\rangle\rangle$ is the boundary state representing the defect in the folded CFT.

3.8.1.2 Entanglement entropy of defects at the entangling surface

In order to describe the defect located at the boundary of the entangling region $\mathcal{A}$ and its complement (see the left-hand side of Figure 3.11), we can introduce the K sheeted covering map with $z = \ln w$. We introduce a UV cutoff ϵ at the boundary of $\mathcal{A}$ and an IR cutoff

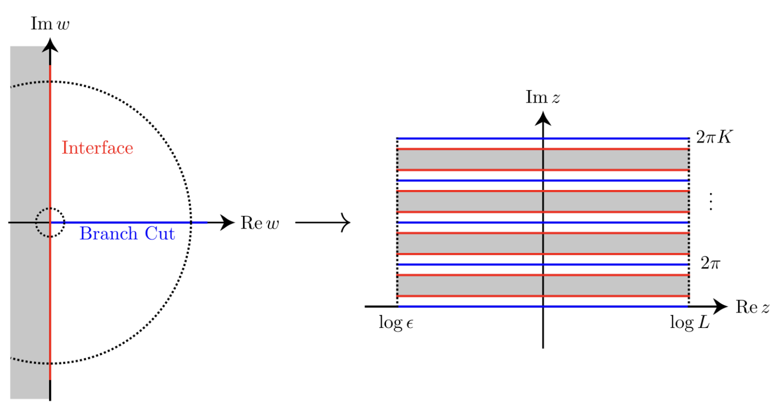

Figure 3.11: Conformal map for the replicated worldsheet for defects at the entangling surface, figure from [5].

L as the length of the branch cut. In general, we have to impose boundary conditions at the cutoff surfaces with the simplest one being to identify the cutoff surfaces periodically, which produces a toroidal worldsheet[8]. It is possible to place a conformal interface at the boundary, which in the replicated surface will turn into K copies of $\mathcal{I}$ and K copies of the conjugate defect $\mathcal{I}^\dagger$ placed equidistant on the torus

$$Z(K) = \mathrm{tr}\Big[\big(\mathcal{I}e^{-tH}\mathcal{I}^\dagger e^{-tH}\big)^K\Big] \ . \tag{3.8.8}$$

The Euclidean time t can be expressed as

$$t = \frac{2\pi^2}{\ln L/\epsilon} \ , \tag{3.8.9}$$

the simplest choice $\epsilon = 1/L$ is made in [183] and the limit $\epsilon \to 0$ corresponds to removing the UV cutoff as well as taking L to be large. For conformal defects, the replica partition function has only been calculated for simple cases such as free bosons and fermions as well as minimal models [183, 193–195]. In all examples, the entanglement entropy behaves as follows[9]

$$S_{\mathcal{A}} = \frac{c_{\text{eff}}}{6}\ln\frac{L}{\epsilon} + \ln g_{\mathcal{A}} \ , \tag{3.8.10}$$

where in general c_{eff} is not the central charge c of the bulk CFT but instead depends, in a complicated fashion, on the details of the conformal interface (see [197] for a recent discussion on universal properties of c_{eff}).

For topological defects, the expression (3.8.8) simplifies since the defects commute with the Hamiltonian and they can be combined

$$Z(K) = \mathrm{tr}\Big[\big(\mathcal{I}\mathcal{I}^\dagger\big)^K e^{-2tKH}\Big] \ . \tag{3.8.11}$$

The entanglement entropy derived from this partition function has the form (3.8.10) with $c_{\text{eff}} = c$. Hence, the leading term in the entanglement entropy does not depend on the

[8]More general conformal boundary conditions have been considered in constructions of symmetry resolved entanglement entropy in [186, 190–192].

[9]The $c_{eff}/6$ differs from (3.8.4) by a factor of 1/2, this is caused by taking the limit $L \to \infty$ and only taking the entanglement of one side of the entangling surface into account, see [196] for a discussion on this issue.

defect and all information is in the sub-leading g-factor which contains information about the ground state degeneracy of the interface. It is the goal of the present section to calculate this quantity for the topological defects in symmetric orbifolds constructed in [6].

3.8.2 Entanglement entropy with symmetric orbifold defect

In this section, we will use the formulas reviewed in subsection 3.8.1 to calculate the entanglement entropy in the presence of the topological defects.

3.8.2.1 Universal defects

Using the folded boundary state (3.3.1), it follows from (3.8.7) that the sub-leading contribution to the entanglement entropy for a symmetrically placed topological defect is given by the logarithm of the g-factor, which in turn is calculated by the overlap of the boundary state with the vacuum

$$g_{\mathcal{A}} = \langle 0 \mid B_R \rangle\rangle = \chi_R(1) = \dim(R) \ . \tag{3.8.12}$$

Note that $g_{\mathcal{A}}$ is given by the quantum dimension of the defect, which is simply the dimension of the irreducible representation R. For conformal defects, this result is only valid for the symmetrically placed defect. For topological defects, we can move them away from the middle and the result will not change unless we come very close to the boundary of the entangling region.

Note, however, that this is not true for the topological defect at the boundary of the entangling surface as discussed in subsection 3.8.1. For the universal topological defects, one finds

$$\begin{aligned} Z(K) &= \mathrm{tr}\Big[\mathcal{I}^{2K} e^{-2KtH}\Big] \\ &= \sum_{[g]} \big[\chi_R([g])\big]^{2K} \,\mathrm{tr}\left(P_{[g]}\bar{P}_{[g]} e^{-2KtH}\right) \ , \end{aligned} \tag{3.8.13}$$

where we used the reality of the characters which implies that $\mathcal{I}^\dagger = \mathcal{I}$. The modular parameter is given by

$$\tau = i\frac{2\pi K}{\ln \frac{L}{\epsilon}} \ . \tag{3.8.14}$$

The partition function can be expressed as a sum over twisted sectors

$$Z(K) = \frac{1}{|G|}\sum_{hg=gh}\left[\chi_R([g])\right]^{2K} h\underset{g}{\Box}(\tau,\bar{\tau}) \ . \tag{3.8.15}$$

We can view this as a summation over twisted sectors labeled by g and a projection on S_N invariant states implemented by h, where h runs over the centralizer of g, i.e. all elements which commute with g. Taking the cutoff $L \to \infty$ implies that $\tau \to 0$, so we have to perform a modular transformation of the torus partition function

$$Z(K) = \frac{1}{|G|}\sum_{g}\sum_{h\in C[g]}\left[\chi_R([g])\right]^{2K} g^{-1}\underset{h}{\Box}(-\frac{1}{\tau},-\frac{1}{\bar{\tau}}) \ . \tag{3.8.16}$$

Note that the limit $\tau \to 0$ implies that the argument of the modular transformed partition function behaves as $-\frac{1}{\tau} \to \infty$. Hence, the partition function is dominated by the sector with the primary of the lowest conformal dimension. For the symmetric orbifold, this is the untwisted vacuum sector.

Note that in the centralizer $C[g]$ of any element $g \in S_N$, the identity is always present since it trivially commutes with any element. Hence, the partition function in the $\tau \to 0$ limit is dominated by the untwisted sector

$$\lim_{\tau\to 0} Z(K) \sim \lim_{\tau\to 0}\sum_{g\in S_N}\frac{1}{|G|}\left[\chi_R([g])\right]^{2K} g\underset{1}{\Box}(-\frac{1}{\tau},-\frac{1}{\bar{\tau}}) \ , \tag{3.8.17}$$

where we also used the reality of the character to replace g^{-1} by g in the torus partition function. In the limit $\tau \to 0$ each term in the partition function contributes the same leading term, which is independent of g.

$$\begin{aligned}\lim_{\tau\to 0} g\underset{1}{\Box}(-\frac{1}{\tau},-\frac{1}{\bar{\tau}}) &= e^{-\frac{2\pi i}{\tau}(-\frac{c}{24})}e^{\frac{2\pi i}{\bar{\tau}}(-\frac{c}{24})} + \cdots \\ &= \exp\left(\frac{c}{12}\frac{1}{K}\ln\frac{L}{\epsilon}\right)\left\{1 + \mathcal{O}(e^{-\frac{1}{K}\ln\frac{L}{\epsilon}})\right\} \ ,\end{aligned} \tag{3.8.18}$$

where the central charge is $c = Nc_{seed}$.

The argument for this is as follows: the modular invariant partition function of the seed theory is $Z(\tau, \bar{\tau})$. Consider an element $g \in S_N$ which is given by k cycles of lengths $n_1, n_2, \cdots n_k$ with $\sum_k n_k = N$. In the tensor product theory, the partition function with g inserted is

$$g\underset{1}{\square}(-\frac{1}{\tau}, -\frac{1}{\bar{\tau}}) = \prod_{i=1}^{k} Z_{seed}(-n_i\frac{1}{\tau}, -n_i\frac{1}{\bar{\tau}}) \ . \tag{3.8.19}$$

In the limit $\tau \to 0$ the partition function of the seed theory is dominated by the vacuum contribution

$$\begin{aligned}
\lim_{\tau\to 0} g\underset{1}{\square}(-\frac{1}{\tau}, -\frac{1}{\bar{\tau}}) &\sim \prod_{i=1}^{k} e^{-\frac{2\pi i}{\tau} n_i c_{seed}/24} e^{\frac{2\pi i}{\bar{\tau}} n_i c_{seed}/24} \\
&\sim e^{-\frac{2\pi i}{\tau} N c_{seed}/24} e^{\frac{2\pi i}{\bar{\tau}} N c_{seed}/24} \\
&\sim \exp\left(\frac{c}{12}\frac{1}{K}\ln\frac{L}{\epsilon}\right) ,
\end{aligned} \tag{3.8.20}$$

where we used $\sum_i n_i = N$. Putting these ingredients together we obtain

$$\lim_{\tau\to 0} \ln Z(K) = \frac{c}{12}\frac{1}{K}\ln\frac{L}{\epsilon} + \ln\Big(\sum_{g\in\sigma}\frac{1}{|G|}\big[\chi_R([g])\big]^{2K}\Big) \ . \tag{3.8.21}$$

Consequently, the entanglement entropy in the limit where L is very large can be calculated using (3.8.3) and one obtains

$$S_A = \frac{c}{6}\ln\frac{L}{\epsilon} + (1-\partial_K)\ln\Big(\sum_{g\in G}\frac{1}{|G|}\big[\chi_R([g])\big]^{2K}\Big)\ |_{K=1} \ . \tag{3.8.22}$$

This expression can be simplified using the orthogonality formula of characters and the fact that characters of S_N are real

$$\frac{1}{|G|}\sum_g \chi_R([g])^* \chi_S([g]) = \delta_{RS} \ . \tag{3.8.23}$$

We arrive at the final expression for the entanglement entropy of a topological defect at the entangling surface.

$$S_A = \frac{c}{6}\ln\frac{L}{\epsilon} - \sum_g \frac{1}{|G|}\big[\chi_R([g])\big]^2 \ln\Big(\big[\chi_R([g])\big]^2\Big) \ . \tag{3.8.24}$$

Note that the expression for the g-factor is considerably more complicated than the symmetric one (3.8.12) which is not surprising since most of the entanglement is localized close to the boundary of the entangling surface.

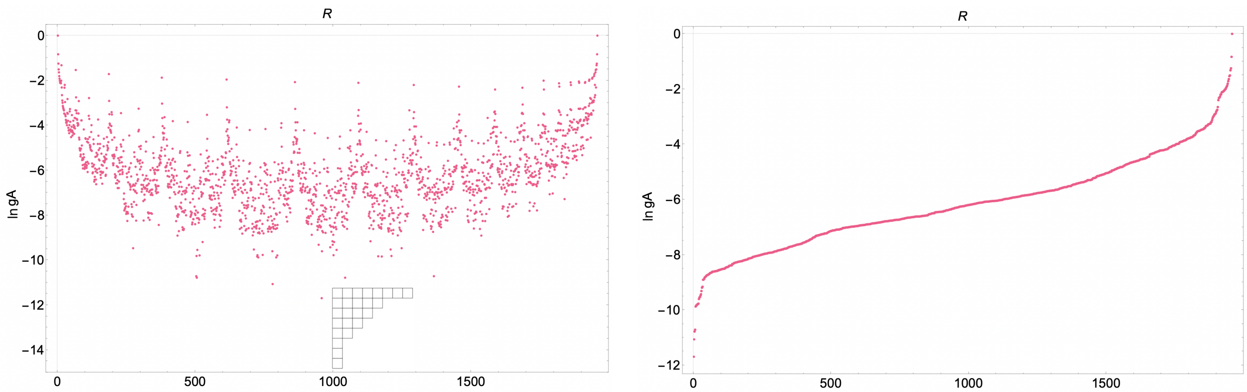

(a) Defect entropy $\ln g_{\mathcal{A}}$ for $N = 25$.

(b) $\ln g_{\mathcal{A}}$ sorted by magnitude for $N = 25$

Figure 3.12: Universal defect entropy for the irreducible representations of S_{25}.

We can evaluate the defect entropy from the character table of S_N and the number of elements in each conjugacy class, which can be calculated using the GAP software package [198] for large values of N. In Figure 3.12 we present the results for two cases of $N = 25$ for which there are 1958 irreducible representations. In the plot on the left the representations are dominance ordered, i.e. for two partitions λ, μ of N, one has $\lambda \trianglerighteq \mu$ if $\lambda_1 + \lambda_2 + \cdots + \lambda_i \geq \mu_1 + \mu_2 + \cdots + \mu_i$ for all i. In addition, we give the Young diagram associated with the representation which has the largest absolute value of $\ln g_{\mathcal{A}}$. In the plot on the right, we plot $\ln g_{\mathcal{A}}$ in order of magnitude. In Figure 3.13 we present the same plots for $N = 35$, for which there are 14883 irreducible representations.

We can recognize a $\mathbb{Z}_2$ symmetry in these plots due to the fact that in general a new irreducible representation can be obtained from an irreducible representation by acting with the one-dimensional alternating representation. The characters of these two representations differ only by signs. Since the characters in the formula (3.8.24) appear squared, we get the same $g_{\mathcal{A}}$ for both representations.

We can obtain a bound on the defect entropy $\ln g_{\mathcal{A}}$ given in (3.8.24) using the fact that

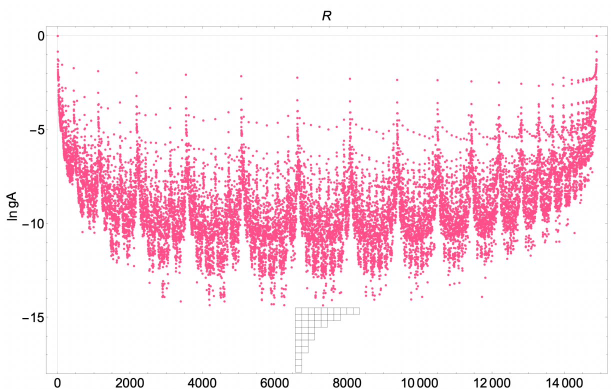

(a) Defect entropy $\ln g_{\mathcal{A}}$ for $N = 35$.

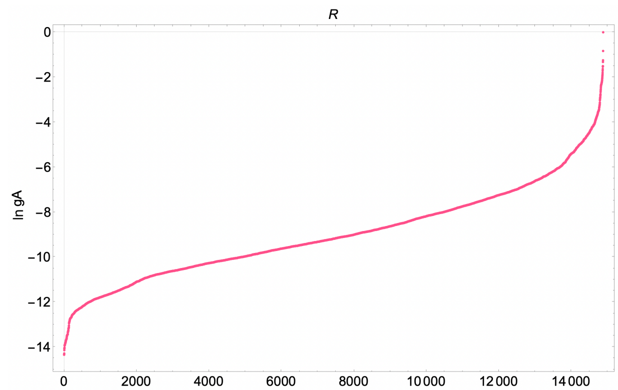

(b) $\ln g_{\mathcal{A}}$ sorted by magnitude for $N = 35$

Figure 3.13: Universal defect entropy for the irreducible representations of S_{35}.

$\chi_R(g) \leq \chi_R(1)$ for all $g \in S_N$

$$\begin{aligned} \sum_g \frac{1}{|G|} \left[\chi_R([g])\right]^2 \ln\Big([\chi_R([g])]^2\Big) &\leq \sum_g \frac{1}{|G|} \left[\chi_R([g])\right]^2 \ln\Big([\chi_R(1)]^2\Big) \\ &\leq 2\ln\Big(\dim(R)\Big) \ , \end{aligned} \tag{3.8.25}$$

where we used character orthogonality (3.8.23) as well as $\chi_R(1) = \dim(R)$. In [199] an asymptotic bound for the dimension of the representation $\dim(R)$ was derived

$$\ln\Big(\dim(R)\Big) \leq N \ln N - N - c\sqrt{N} \ , \tag{3.8.26}$$

where c is a constant $c \sim 2.5651$. This result bounds the absolute value of the defect entropy. Numerical evaluation for $N \leq 35$ seems to indicate that this bound is not very strong and it is an interesting question whether a stronger bound exists, but we have not been able to find one in the mathematics literature.

3.8.2.2 Non-universal defects

For the non-universal defect, the defect symmetric entropy is given by taking the logarithm of the g-factor for the folded boundary state (3.5.2)

$$g_{R,a} = \langle 0 \mid B_a^R \rangle\rangle = \chi_R(1) \left(\frac{S_{a0}}{S_{00}}\right)^N \ , \tag{3.8.27}$$

which follows from the fact that in the untwisted sector we have N copies of the RCFT defect.

For the calculation of the entanglement entropy at the defect, we have to evaluate the replicated partition function (3.8.11) with the defect $\mathcal{I}$ which is obtained from unfolding the folded boundary state (3.5.1). Writing down the complete partition function is somewhat cumbersome due to the summation over the centralizer of g, but we should note that following the same strategy for calculating the entanglement as in subsection 3.8.2.1 still applies and the leading contribution is obtained from the partition function in the $h = 1$ sector, before modular transformation, which gets mapped to the dominant untwisted sector after modular transformation

$$Z(K) = \sum_g \frac{1}{|G|} \big(\chi_R([g])\big)^{2K} \prod_{j=1}^{N} \left(\sum_i \left| \frac{S_{ai}}{S_{0i}} \right|^{2K} \chi_i(\frac{\tau}{j}) \bar{\chi}_i(\frac{\bar{\tau}}{j}) \right)^{l_j} + \cdots \,. \tag{3.8.28}$$

The limit $\tau \to 0$ of Z is evaluated by an S-modular transformation using the transformation of the RCFT characters given in section 3.2.1.

$$\lim_{\tau\to 0} Z(K) \sim \lim_{\tau\to 0} \sum_g \frac{1}{|G|} \big(\chi_R([g])\big)^{2K} \prod_{j=1}^{N} \left(\sum_{i,k,\bar{k}} \left| \frac{S_{ai}}{S_{0i}} \right|^{2K} S_{ik}\; S^*_{i\bar{k}}\; \chi_k(-j\frac{1}{\tau}) \bar{\chi}_{\bar{k}}(-j\frac{1}{\bar{\tau}}) \right)^{l_j} + \cdots \,. \tag{3.8.29}$$

The dominant contribution in the $\tau \to 0$ limit in (3.8.29) comes from the vacuum character χ_0, which behaves like $q^{-\frac{c_{seed}}{24}} \bar{q}^{-\frac{c_{seed}}{24}}$ as $q \to 0$. Using this expansion, and the fact that $\sum_i l_j = N$ for all permutations $g \in S_N$, one obtains

$$\lim_{\tau\to 0} Z(K) \sim \sum_g \frac{1}{|G|} \big(\chi_R([g])\big)^{2K} \Big(\sum_i |S_{ai}|^{2K} |S_{0i}|^{2-2K} \Big)^N \exp\big(\frac{c}{12}\frac{1}{K} \ln \frac{L}{\epsilon}\big) + \cdots \,. \tag{3.8.30}$$

Taking the logarithm produces three terms

$$\lim_{\tau\to 0} \ln Z(K) = \frac{c}{12}\frac{1}{K} \ln\frac{L}{\epsilon} + \ln\Big(\sum_{g\in\sigma} \frac{1}{|G|} \big[\chi^R([g])\big]^{2K} \Big) + N \ln\Big(\sum_i |S_{ai}|^{2K} |S_{0i}|^{2-2K} \Big) + \cdots \,. \tag{3.8.31}$$

Consequently, the entanglement entropy in the limit where L is very large can be calculated using (3.8.3) and one obtains

$$S_A = \frac{c}{6}\ln\frac{L}{\epsilon} - \sum_g \frac{1}{|G|}\left[\chi_R([g])\right]^2 \ln\left(\left[\chi_R([g])\right]^2\right) - N\sum_i |S_{ai}|^2 \ln\left(\left|\frac{S_{ai}}{S_{0i}}\right|^2\right) \ , \qquad (3.8.32)$$

where we have repeated the calculation of subsection 3.8.2.1 to obtain the second term and used the unitarity and symmetry of the modular S matrix, in particular $\sum_j |S_{aj}|^2 = 1$ as in [5, 184]. It is interesting that for the "maximally fractional" universal defect, the defect entropy $\ln g_{\mathcal{A}}$ is the sum of the contribution of the universal defect (3.8.24) and N times the contribution of the RCFT topological defect [5, 184]. This together with the result for the symmetric entanglement entropy (3.8.27) indicates that the maximally fractional defect can be in some sense viewed as a product of the RCFT and symmetric orbifold defect.

3.9 Discussion

In this work, we investigated certain aspects of the universal topological defects of the symmetric orbifold CFT $\mathcal{M}^{\otimes N}/S_N$. These defects are universal in the sense that they do not depend on the details of the seed CFT, and exist in any S_N orbifold theory. Using modular transformations of torus partition function, we determined universal defect operators on which the topological lines can end. These operators are built on the twisted sector ground states. These states are derived from the vacuum of the seed CFT and hence do not depend on the details of the seed CFT other than the central charge and the conjugacy class labeling the twisted sector.

The non-invertibility of the symmetry leads to Ward identities which relate correlation functions of local operators to (sums of) correlation functions of defect and local operators with lines as well as junctions inserted. We illustrated this in the simplest example which exhibits non-ivertible symmetries, namely the S_3 symmetric orbifold.

In addition, we constructed an example of a non-universal defect which is built from a topological defect in the seed CFT (which we took to be diagonal RCFTs with Verlinde lines). This "maximally" fractional defect satisfies the Cardy constraints and it would be interesting to see whether more general solutions (maybe along the lines of similar constructions for

D-branes in symmetric orbifolds in [145]) are possible. The maximally fractional defect we constructed in the present paper can be, in some sense, viewed as a product of the RCFT and symmetric orbifold defects.

We provided a criterion that determined which universal defects are non-trivial in the large-N limit. This was possible due to the known asymptotic behavior of S_N characters. It would be particularly interesting to study the Ward identities of non-trivial defects in the large-N limit. At this moment, this task looks daunting since there are no explicit expressions for both the F-symbols as well as the Kronecker coefficients of S_N to our knowledge.

The universal defects of the orbifold CFT are interesting in the context of $\mathrm{AdS}_3/\mathrm{CFT}_2$ correspondence. We argued that these defects correspond to defects on the worldsheet, a case distinct from previous examples where boundary topological defects correspond to D-branes in the bulk. This is a peculiarity of the tensionless limit. This idea has appeared recently in other works [157, 200]. On the boundary, passing an operator though a topological defect generally produces non-local operators. It would be interesting to understand the holographic dual of these operators.

Away from the orbifold point, we showed that the universal defects are broken explicitly by a marginal deformation. Hence, these defects do not generally exist in the supergravity limit. It would be interesting to understand what happens when the deformation parameter is infinitesimal and what role these softly broken defects might play in holography.

In this work, we focused on the tensionless limit with $k = 1$. This corresponds to the smallest possible radius for AdS_3. For higher values of k, it is believed that the boundary theory is tensored with a Liouville factor but remains an orbifold CFT [170]. Hence, we expect our universal defects to be present for higher values of k as well. It would be interesting to understand the holographic dual of the universal defects in the large k limit where semi-classical supergravity computations are more reliable.

We also calculated the entanglement entropy of a single interval in the presence of universal and non-universal topological defects. For symmetric placement, the defect entropy is the logarithm of the quantum dimension. For a defect at the entangling surface, it depends on the characters of S_N and, for non-universal defects, on the modular S matrix of the seed RCFT. We evaluated the universal defect entropy numerically for $N \leq 35$.

CHAPTER 4

Quantum Field Theory in Non-Integer Dimensions

4.1 Introduction and summary

The goal. Chiral gauge theories are famously difficult to analytically continue away from integer dimensions, an obstacle first raised in the context of dimensional regularization [201–203]. There, the motivation for extending $d \in \mathbb{N}$ to $d \in \mathbb{C}$ was that such a continuation is an extremely convenient regulator, massively simplifying computations. For vector-like theories, this continuation was promptly solved, but chiral theories, which involve the matrix $\gamma^\star$, required significant extra work. Arguably, a completely satisfactory treatment, especially in the context of supersymmetric theories [204, 205], is still lacking. That being said, various working prescriptions are known: for example, one can use the standard 't Hooft-Veltman trick, where we split our spacetime into two submanifolds, the "transverse" and "parallel" directions, and define $\gamma^\star$ only with respect to the latter. For instance, if we were working in $d = 2 + \epsilon$, we would typically declare that

$$\begin{aligned} \{\gamma^\star, \gamma^\mu\} &= 0 \qquad \mu = 1, 2 \\ [\gamma^\star, \gamma^\mu] &= 0 \qquad \mu \neq 1, 2 \end{aligned} \tag{4.1.1}$$

This is all well and good if we are interested in eventually taking $d \to 2$, but not otherwise: if we use this continuation in d, and take $d \to 4$ instead, the answer we would get would differ from the correct one as computed directly in $d = 4$. In other words, 't Hooft-Veltman-like prescriptions are only useful for an infinitesimal neighborhood around a given $d \in \mathbb{N}$.

Here we are more ambitious and would like to extend various theories to a *non-*

infinitesimal subset of the complex d plane, in the sense that we want a family of QFTs, labeled by $d \in \mathbb{C}$, which exactly matches the corresponding QFT when we take *several distinct* $d \in \mathbb{N}$. In other words, a small patch around some specific $d \in \mathbb{N}$ is not enough for us: we want some open set in $\mathbb{C}$ that contains at least a couple of distinct integer dimensions d, with agreement when restricted to those. 't Hooft-Veltman-like prescriptions like the one above are insufficient for this.

Motivation. There are various motivations for this endeavor. First, a better understanding of this continuation for generic d instead of d close to some specified integer might help us in coming up with better prescriptions for dim-reg, perhaps eventually leading to a completely satisfactory treatment of SUSY theories.

But, beyond practical reasons like dim-reg, a proper continuation of QFT to fractional d has attracted significant attention in recent years, see e.g. [206–229] for a very incomplete list of examples. Before we try to define this continuation more precisely, let us spend a few paragraphs explaining some of the reasons why this operation is interesting in the first place.

For us, the fundamental reason is structural: analytic continuation of discrete parameters allows us to meaningfully connect different QFTs in the space of theories. For example, we intuitively tend to think of $2d$ Ising and $3d$ Ising as "the same theory", just at different values of d. On the other hand, one would never say that $2d$ Ising is the same theory as, say, $3d$ ABJM. The reason the former QFTs are "the same" but the latter are not is that the parameter d in Ising can be continued to $d \in \mathbb{C}$, and observables become analytic functions of this variable[1]. This is the same reason we think of the $O(N)$ model as "the same theory", just at different values of N: this makes sense only because the parameter N can be analytically continued[2]. This is not just a question of academic interest, but has important practical implications:

- The ϵ expansion [239] explicitly assumes that the $d = 3$ and $d = 4$ theories are con-

[1]Throughout this paper we will use "analytic" to actually mean "meromorphic".

[2]See e.g. [230–238] for some recent literature on analytic continuation of N.

nected in the space of QFTs. The fact that this technique works at all relies on analytic continuation in d. Indeed, unless there is "something" in between Ising_4 and Ising_3, this expansion would be entirely meaningless. For example, one would never expect to be able to solve graphene by expanding, say, Banks-Zaks around $d = 4$.

- The large N expansion explicitly assumes that the $O(N)$ theory and the $O(N+1)$ theory are connected in the space of QFTs. As before, one would never expect a $1/N$ expansion to work for a random sequence of QFTs, say, something like $T(1) = \text{Ising}$, $T(2) = SU(2) + \psi_{\text{adj}}$, $T(3) = \text{abelian Higgs}$, etc. This expansion works for $O(N)$, but not for $T(N)$, precisely because the former make up a sequence that is analytic in N.

The goal of the analytic continuation program is to make this intuition rigorous: in what precise sense are these theories connected to each other in the space of QFTs? Is this continuation unique? And what does the interpolation teach us about the individual QFTs?

Another common motivation is that analytic continuation in d leads to controlled violations of unitarity [240], making them a very nice playground for studying non-unitary QFT. For instance, [241] examines the free energy in QED in continuous dimension in order to scrutinize the F-theorem [242, 243], which in principle is only proven to hold in unitary theories [244]. More generally, the fundamental principles of the conformal bootstrap program are rather agnostic to the concrete value of d, and the formalism itself appears particularly well adapted to treating this integer as a continuous parameter [245].

Yet another reason it is worth our while to explore this continuation is that much of the emergent phenomena in QCD-like theories that we usually care about, such as non-perturbative symmetry breaking, infrared dualities, confinement, etc., are present in many examples in different integer dimensions [12, 13, 246–279]. If we were able to extend these theories to fractional d, we could try to track these phenomena as we go from one integer dimension to another, which would likely teach us quite a bit about the concrete mechanisms behind these features in our original, integer-dimensional gauge theories.

As a concrete example, there are in the literature various instances of gauge theories that confine in $d = 4$ (see e.g. [280]), but deconfine in $d = 3$ (see e.g. [281, 282]). In this case, one could guess that there is a confinement/deconfinement transition at some $d^\star \in [3, 4]$, which could shed some light on the dynamics of the analogous transition in real-world QCD.

A related example is the fact that the critical number of flavors for which there is symmetry breaking, $N_f^\star$, is meaningful in both $d = 3$ and $d = 4$, but in principle these two numbers are independent [283]. By extending QCD to fractional d we get an interpolation between $N_f^\star(d = 4)$ and $N_f^\star(d = 3)$, potentially connecting these two quantities. With some wishful thinking, it might be possible that connecting these two objects could lead to a better understanding of both[3].

So, with these motivations in mind, here we reconsider the problem of extending a given QFT to $d \in \mathbb{C}$. As mentioned above, this problem is particularly tricky for chiral theories but, at least naively, one would expect that vector-like theories can be continued without significant complications. In this work we point out that, already for vector-like theories, this continuation is very subtle and, despite what some partial results might suggest, still an open problem.

Complications. In section 4.2 we will discuss much more carefully the various options for how this analytic continuation is defined in the first place. For the purposes of this summary, let us settle for a vague, aspirational prescription: compute things for general $d \in \mathbb{N}$ and, if the answer is "uniform in d", declare that the result is also true when $d \in \mathbb{C}$.

The main obstruction to naive prescriptions like the one above is the existence of *low-rank exceptions*: situations where observables are not in fact "uniform in d". The simplest example where this shows up is the free, massless Dirac fermion. Consider the scalar $\bar\psi\psi$; its first few correlation functions are all unremarkable: for example, the two-point function equals $\langle \bar\psi\psi(x)\bar\psi\psi(0)\rangle \propto 1/x^{2(d-1)}$. This result has an obvious continuation to $d \in \mathbb{C}$.

The three- and four-point functions of $\bar\psi\psi$ are also both uniform in d, but something interesting happens for the five-point function. By brute-force computation one can check

[3] As a simple example, [284] used the known value $N_f^\star(d = 2) = \infty$ to improve their estimate of $N_f^\star(d = 3)$.

that it vanishes for all integers $d \geq 4$, but it is non-zero in three dimensions:

$$\langle \bar{\psi}\psi(x_1) \cdots \bar{\psi}\psi(x_5) \rangle \propto \delta_{3,d} \tag{4.1.2}$$

(see (4.2.12) for the actual $d = 3$ expression). What should its continuation to $d \in \mathbb{C}$ be? The answer is far from obvious, at least to us: the integer sequence $\delta_{3,d}$ has no canonical continuation to $d \in \mathbb{C}$. (There are infinitely many functions that interpolate this sequence, but there is no criterion that singles out a specific choice.)

The phenomenon above is in fact quite generic in QFT: most correlation functions have a qualitative, discrete change in behavior at some finite $d \in \mathbb{N}$, which complicates any naive attempts at making $d \in \mathbb{C}$. We next explain the main mechanism for this discontinuity in d.

Consider the n-point function of some scalar operator $\mathcal{O}(x)$:

$$\langle \mathcal{O}(x_1) \cdots \mathcal{O}(x_n) \rangle \tag{4.1.3}$$

We assume that our family of QFTs is invariant under translations and rotations, i.e., the special euclidean group $\mathrm{SE}(d) = SO(d) \ltimes \mathbb{R}^d$. This symmetry then implies that this correlator is defined on $\mathrm{Conf}_n(\mathbb{R}^d)/\mathrm{SE}(d)$, i.e., it can be expressed in terms of scalars constructed out of $v_i = x_i - x_{i+1}$.

What are these scalars, specifically? If the number of insertions is small enough, the ring of $SO(d)$-invariants is generated by the matrix of inner products $g_{ij} = v_i \cdot v_j$. But if the number of v_i's is at least as large as the dimension of $\mathbb{R}^d$, there is one more piece of $SO(d)$-invariant information that is not captured by g_{ij}, namely the orientation defined by the basis $v_1, \ldots, v_d$. In other words, in this case the ring of $SO(d)$-invariants is generated by g_{ij} together with $\varepsilon = \mathrm{sign}(\det(v_1, \ldots, v_d))$. Therefore, one can generically write

$$\langle \mathcal{O}(x_1) \cdots \mathcal{O}(x_n) \rangle = \begin{cases} \mathcal{S}^{\text{even}}_{d,n}(g_{ij}) + \varepsilon \mathcal{S}^{\text{odd}}_{d,n}(g_{ij}) & d \leq n-1 \\ \\ \mathcal{S}^{\text{even}}_{d,n}(g_{ij}) & d > n-1 \end{cases} \tag{4.1.4}$$

for some functions $\mathcal{S}$ (even/odd refer to the intrinsic parity, see below). This is an example of a small-d exception we mentioned above. For fixed n, there is a discontinuous change between $d \leq n-1$ and $d > n-1$, which means that the correlation function cannot be uniform in d: to the extent that there is a meaningful continuation to $d \in \mathbb{C}$, there should be some sort of jump around $d \approx n-1$.

Things are a little nicer if we assume that the theory also has reflection symmetry, namely that it is invariant under the full euclidean group $\mathrm{ISO}(d) = O(d) \ltimes \mathbb{R}^d$. In this case, correlation functions of *parity-even* scalars are defined on $\mathrm{Conf}_n(\mathbb{R}^d)/\mathrm{ISO}(d)$. Importantly, ε is parity-odd, and therefore it cannot appear in their correlation functions. In other words, $\mathrm{Conf}_n(\mathbb{R}^d)/\mathrm{ISO}(d)$ is coordinatized by the Gram matrix g_{ij} alone. In the notation above, the n-point function equals $\mathcal{S}^{\text{even}}_{d,n}(g_{ij})$ for all d. As there is no fundamental change in behavior as we vary the number of spacetime dimensions, there is hope that a nice continuation to $d \in \mathbb{C}$ might exist.

Parity-odd operators, on the other hand, are less constrained than parity-even ones. Under a parity transformation, the n-point function picks up the sign $(-1)^n$. Therefore, if n is even, this *forbids* the presence of ε, but if n is odd, it *forces* its presence instead. Therefore, the case of n even should be uniform in d, but the case of odd n is again discontinuous: the correlation function must vanish if $d > n-1$. This explains why the two-point function of the parity-odd operator $\bar{\psi}\psi$ was well-defined for $d \in \mathbb{C}$, but the five-point function was $\propto \delta_{3,d}$.

The final conclusion is, then, that generic operators in $SO(d)$-invariant theories, and parity-odd operators in $O(d)$-invariant theories, present discrete, qualitative changes in behavior as we vary $d \in \mathbb{N}$, and uniform answers only emerge for sufficiently large d. In the naive approach to analytic continuation, observables become analytic in d only after we ignore by hand low-rank exceptions. In an intuitive sense, the low d behavior is non-perturbative in $1/d$. Needless to say, at the end of the day we only care about QFTs in low dimension anyway, which makes the problem both hard and interesting.

Let us mention for completeness that, for more general QFTs where the symmetry group is neither $SO(d)$ nor $O(d)$, but some more complicated global form of $\mathfrak{so}(d)$, the question is whether the representation theory of this global group is stable or not, i.e., whether there are low-rank isomorphisms in $\mathrm{Rep}(G)$. For example, in the case of $G = SO(d)$ one has the low-rank isomorphism $\wedge^d[\mathbf{1}] \cong \mathbf{1}$, which allows for the exceptional scalar $\det(v_1, \ldots, v_d)$. We will discuss this in more detail in section 4.2.2.

An important incarnation of the subtleties associated with small d exceptions is the following. Say, for example, that we are interested in a perturbative theory defined for general d, whose spectrum contains a pair of scalar operators $\mathcal{O}_1$ and $\mathcal{O}_2$. If their scaling dimensions are different, then these operators cannot mix, and we can compute loop corrections independently. But if the scaling dimensions depend on d, and there is some $d^\star$ for which there is level crossing, then perturbation theory breaks down around $d \approx d^\star$, and we must switch to degenerate perturbation theory (see e.g. [285, 286]). This typically gives rise to branch points close to $|d| = d^\star$. So far, this is standard CFT phenomena.

The striking fact is that this phenomenon can occur even if $\mathcal{O}_1$ and $\mathcal{O}_2$ have different spin. For example, a rank-2 anti-symmetric field $f_{\mu\nu}$ is different from a vector v_μ for generic d, but the isomorphism $[\mathbf{1}, \mathbf{1}] \cong [\mathbf{1}]$ in $SO(3)$ means that these two fields have the same spin in three dimensions, and therefore they can once again mix. Low-d accidental spin degeneracy is rather common, and our general expectation is that analytically continued QFTs will develop branch cuts all over the complex d plane.

We can see this explicitly in the main example we will be looking at in this paper: QCD with gauge group G and fermions ψ in some representation $R \in \mathrm{Rep}(G)$. We will take the limit of large R in order to be able to access CFT data reliably.

In section 4.3 we will compute the scaling dimension of the defect operator ψ to leading order in $1/\dim(R)$. To tree level $\Delta^{(0)}(\psi) = (d-1)/2$, and the first correction is

$$\Delta^{(1)}(\psi) = \frac{4(d-1)^2\Gamma(d-2)}{d\Gamma(d/2)^3\Gamma(1-d/2)} \frac{\dim(G)}{\dim(R)} \tag{4.1.5}$$

This quantity admits a natural continuation in d.

On the other hand, for the scaling dimension of the local operator $\bar{\psi}\psi$, the first correction turns out to be

$$\Delta^{(1)}(\bar{\psi}\psi) = \frac{4(d-1)^2\Gamma(d-2)}{d\Gamma(d/2)^3\Gamma(1-d/2)} \left(2 - \frac{d-4}{d-2} \frac{\mathrm{tr}[\gamma^{\alpha\mu\nu}]\,\mathrm{tr}[\gamma_{\alpha\mu\nu}]}{\mathrm{tr}[1]^2}\right) \frac{\dim(G)}{\dim(R)} \tag{4.1.6}$$

We find the structure $\mathrm{tr}[\gamma^{\alpha\mu\nu}]\,\mathrm{tr}[\gamma_{\alpha\mu\nu}]$, which vanishes for all integers $d \neq 3$, but is non-zero for $d = 3$. Unlike $\Delta(\psi)$, this scaling dimension doesn't have an obvious analytic continuation in d.

As emphasized above, the obstruction to analyticity in d is the existence of low rank exceptions, in this case the exception being the $3d$ isomorphism $[\mathbf{1},\mathbf{1},\mathbf{1}] \cong \mathbf{1}$, which allows $\mathrm{tr}[\gamma_{\mu\nu\rho}]$ to be non-zero.

The usual way to recover analyticity in the literature is to declare that $\mathrm{tr}[\gamma_{\mu_1\cdots\mu_n}] \equiv 0$ for all $d \in \mathbb{C}$. If we do this, the scaling dimension above becomes

$$\widehat{\Delta}^{(1)}(\bar{\psi}\psi) = \frac{8(d-1)^2\Gamma(d-2)}{d\Gamma(d/2)^3\Gamma(1-d/2)}\frac{\dim(G)}{\dim(R)} \tag{4.1.7}$$

where the hat signifies that this holds only for *generic* $d \in \mathbb{N}$, but not necessarily for *all* $d \in \mathbb{N}$. This formula is now analytic in d, and it agrees with $\Delta^{(1)}$ for all integers $d > 3$, but it gives the wrong answer when $d = 3$. Therefore, this prescription fails to provide a good analytic continuation: $\widehat{\Delta}^{(1)}$ is not a good interpolation of QCD_d for $d \in \mathbb{C}$, since it disagrees with the honest answer as computed directly in $d = 3$.

Does this mean analytic continuation is not possible? Is there any way to work with analytic objects $\widehat{\Delta}^{(1)}$, while at the same time to recover the correct answer $\Delta^{(1)}$ when $d \in \mathbb{N}$?

In fact, analytic continuation is possible, but the mechanism is not immediately obvious. To simplify the notation, let us omit the $\dim(G)/\dim(R)$ factors (or, equivalently, let us take $G = U(1)$). Then, the correct answer in $d = 3$ is $\Delta^{(1)} = 256/3\pi^2$, as given by (4.1.6) with $\mathrm{tr}[\gamma^{\alpha\mu\nu}]\,\mathrm{tr}[\gamma_{\alpha\mu\nu}]/\,\mathrm{tr}[1]^2 = -3!$. On the other hand, the analytic expression (4.1.7) evaluated at $d = 3$ reads $\widehat{\Delta}^{(1)} = -128/3\pi^2$, which is of course wrong.

The resolution is the following. Close to $d = 3$, the operator $\bar{\psi}\psi$ becomes degenerate with $\bar{\psi}\gamma_{\mu\nu\rho}\psi$. This is impossible for generic d, since these operators have different spin, but in three dimensions one has the low-rank exception $\gamma_{\mu\nu\rho} \propto \epsilon_{\mu\nu\rho}$, and therefore these become the exact same operator. Hence, intuitively speaking, these operators can mix for d close to 3.

If we compute the correction $\Delta^{(1)}$ for $\bar{\psi}\gamma_{\mu\nu\rho}\psi$, and force it to be analytic by dropping by hand the odd traces $\mathrm{tr}[\gamma_{\mu_1\cdots\mu_n}]$, we find

$$\widehat{\Delta}^{(1)}(\bar{\psi}\gamma_{\mu\nu\rho}\psi) = \frac{8(d-4)\Gamma(d+2)}{d^2(d-2)^2\Gamma(d/2)^3\Gamma(1-d/2)} \tag{4.1.8}$$

If we now take $d = 3$, we find $\widehat{\Delta}^{(1)}(\bar{\psi}\gamma_{\mu\nu\rho}\psi) = 256/3\pi^2$, which is the correct answer for $\Delta^{(1)}(\bar{\psi}\psi)$. In this way, we recover the correct scaling dimension, as computed honestly in $d = 3$, from an object $\widehat{\Delta}^{(1)}$ that is analytic. But do note that (4.1.8) disagrees with $\Delta^{(1)}(\bar{\psi}\psi)$ at $d = 2$, so one should not think of this expression as the correct analytic continuation of $\Delta^{(1)}(\bar{\psi}\psi)$ for all $d \in \mathbb{C}$: this branch is only correct for d close to 3.

This last statement will perhaps be more clear if we plot the analytic dimensions $\widehat{\Delta}^{(1)}(\bar{\psi}\gamma_{\mu_1\cdots\mu_n}\psi)$ for $d \in \mathbb{R}$: where the red dots correspond to the honest value of $\Delta^{(1)}(\bar{\psi}\psi)$ as

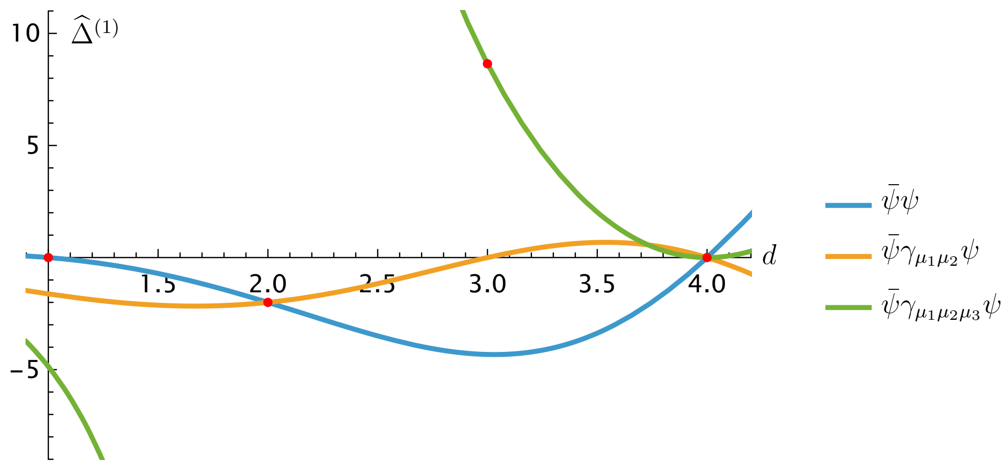

Figure 4.1: The leading $1/N_f$ corrections $\widehat{\Delta}^{(1)}$ to the scaling dimensions of $\bar{\psi}\psi$, $\bar{\psi}\gamma_{\mu_1\mu_2}\psi$, and $\bar{\psi}\gamma_{\mu_1\mu_2\mu_3}\psi$ as functions of the spacetime dimension d.

computed in integer d, using the rigorous gamma matrix traces in that dimension, without throwing away odd traces. The solid lines, on the other hand, correspond to $\widehat{\Delta}^{(1)}$, i.e., they are the analytic scaling dimensions that arise after setting $\mathrm{tr}[\gamma_{\mu\nu\rho}] \equiv 0$ by hand. This picture makes it clear that all red dots agree with *some* analytic branch, but no branch is correct for *all* dots.

To order $1/\dim(R)$ the expression for $\Delta(\bar{\psi}\psi)$ only includes the trace $\mathrm{tr}[\gamma_{\mu\nu\rho}]$, which is why this quantity requires only one new branch, around $d = 3$. To order in $1/\dim(R)^2$ one finds a new trace $\text{tr}[\gamma_{\mu\nu\rho\sigma\tau}]\,\text{tr}[\gamma^{\mu\nu\rho\sigma\tau}]$ in the honest, general d expression for $\Delta(\bar{\psi}\psi)$. As before, we can make $\Delta^{(2)}$ analytic in d by dropping these odd traces, producing an expression $\widehat{\Delta}^{(2)}(\bar{\psi}\psi)$ that agrees with $\Delta^{(2)}(\bar{\psi}\psi)$ for all $d > 5$, but fails otherwise. One can anyway recover the correct answer at $d = 5$ by considering the operator $\bar{\psi}\gamma_{\mu\nu\rho\sigma\tau}\psi$, which becomes isomorphic to $\bar{\psi}\psi$ when $d = 5$; this gives rise to a new branch, defined around this integer. The "all orders" exact answer $\Delta(\bar{\psi}\psi)$ involves infinitely many branches, one adapted to each odd d, as a result of the infinitely many exceptional traces $\text{tr}[\gamma_{\mu_1\cdots\mu_n}]$.

To the extent that a continuation of chiral quantities is well-defined, we expect operators like $\bar{\psi}\gamma^\star\psi$ to present discontinuities at the *even* integers, as a result of the exceptional traces $\text{tr}[\gamma^\star\gamma_{\mu_1\cdots\mu_n}]$. We do not explore these chiral quantities further here.

In a general CFT, there is no single expression for $\Delta(\mathcal{O})$ that is both analytic in d and that agrees with the correct, honest answer for all $d \in \mathbb{N}$. Instead, there is an infinite family of expressions $\widehat{\Delta}(\mathcal{O}_i)$, where $\mathcal{O}_i$ are all the operators that become isomorphic to $\mathcal{O}$ at some $d \in \mathbb{N}$. These $\widehat{\Delta}$'s are defined by ignoring by hand low-rank exceptions and, as such, they are all analytic in d. But at the same time, they also capture the correct value of $\Delta(\mathcal{O})$ for those integer dimensions d in which $\mathcal{O}_i = \mathcal{O}$. This allows us to have our cake and eat it too: we can work with analytic objects $\widehat{\Delta}$ which, at the same time, contain all the same information as the honest Δ's. The only price one has to pay is that one has to choose the correct branch adapted to each $d \in \mathbb{N}$.

Presumably, a similar branched structure exists for all CFT data, and not just scaling dimensions. We leave a more thorough analysis of this for future work; the confusing five-point function of $\bar{\psi}\psi$ (cf. (4.1.2)) should be a good place to start.

If the flavor symmetry of the theory has a stable representation theory (e.g., if we consider parity-even operators in an $O(d)$-invariant QFT), then there are no low-rank isomorphisms, and hence no spin degeneracy. In this case, quantities like $\Delta(\mathcal{O})$ are single-valued; this is why "simple theories" like Wilson-Fisher have scaling dimensions that are analytic in d.

The plan for the rest of this paper is as follows. In section 4.2 we make an attempt at defining the problem more precisely, and we also describe some of the complications that arise in a general QFT. In section 4.3 we illustrate these observations by computing a few observables in a specific theory, viz. QCD. In section 4.4 we study analogous observables in the QED Gross–Neveu–Yukawa model, including the effects of four-fermion interactions. In section 4.5 we finish with some open problems and general speculations.

4.2 Generalities

In this section we try to set up the problem of analytic continuation more systematically and precisely.

4.2.1 Definition (or lack thereof)

Let us begin with the important clarification that we do not claim every QFT admits analytic continuation, nor that this continuation is necessarily unique. For example, it might be the case that Chern-Simons theories are stuck to $d = 3$, but it might also be the case that some clever re-writing allows us to define them for general $d \in \mathbb{C}$. However unlikely the second one might sound, either option is logically possible, and we make no claim either way.

As for uniqueness, this depends on how one formulates the question. For example, $3d$ Maxwell should admit several natural extensions away from $d = 3$: it is connected to $4d$ Maxwell in the obvious way, but also to a $4d$ compact scalar, since $f_{\mu\nu} \leftrightarrow \epsilon_{\mu\nu\sigma}\partial^\sigma\phi$ in $d = 3$. More generally, analytic continuation of a given QFT_d is always relative to a choice of target at $d\pm1$, it is not an intrinsic operation one can perform on a specific QFT. Whenever we talk about analytic continuation in d, we must choose a sequence of QFTs defined for multiple integers $d \in \mathbb{N}$, and then ask whether they can be interpolated via $d \in \mathbb{C}$.

In fact, if uniqueness is to hold at all, it can only do so if we have a target for *all* $d \in \mathbb{N}$, and not just for a few consecutive integers. Indeed, assume that a certain computation produces the expression $\delta^{\mu\nu}\delta_{\mu\nu}$. The obvious analytic continuation is that $\delta^{\mu\nu}\delta_{\mu\nu} = d$. But if we only require the continuation to give the right answer for $d = 2$ and $d = 3$, then we can write $\delta^{\mu\nu}\delta_{\mu\nu} = f(d)$ where $f(d)$ is any analytic function that satisfies $f(2) = 2$, $f(3) = 3$.

There are infinitely many such functions, and therefore this construction is not unique. Only if we impose $f(d) = d$ for all $d \in \mathbb{N}$ (together with some further constraints on the growth of f in the complex plane) is the equality $f(d) = d$ for all $d \in \mathbb{C}$ unique.[4] This is of course a simplified version of the well-known theorem [287] that the usual rules of dim-reg lead to a unique analytic continuation only if we require them to be correct for *all* $d \in \mathbb{N}$.

An analogous statement holds for continuation of flavor symmetries: we need to specify an *infinite* sequence of $O(N)$-symmetric QFTs to analytically continue N. Any finite collection of QFTs can always be made part of infinitely many sequences, and they can all be used to define continuations. As will hopefully become clear as we go on, analytic continuation in N and in d are not entirely independent operations, and there are many conceptual similarities. As a very simple example, note that upon compactification (on a sufficiently symmetric manifold), the Lorentz group becomes a flavor symmetry.

With this in mind, a very rough, intuitive definition could look something like this. Given an infinite sequence of QFTs defined for all $d \in \mathbb{N}$, one computes a certain observable, such as a scaling dimension Δ_d, for all $d \in \mathbb{N}$. Then, if this sequence is sufficiently well-behaved in some sense (such as having bounded forward differences), then it has a unique analytic continuation to complex d, and we declare that this is the observable the QFT computes at fractional d.

Of course this is too vague to be an actual definition. For starters, a QFT is not just a collection of numbers $\{\Delta\}$, but a much richer structure that implies infinitely many coherence relations between them. Unfortunately, the honest answer is that we don't have a general definition. We can mention a few special cases here where a working definition exists, but we will spend the rest of this paper explaining some of the obstructions associated to this operation and why the problem is still very much open.

[4]The precise statement is the following. Say we have a quantity $f(d)$ defined for multiple integers $S \subsetneq \mathbb{N}$, and we wish to continue it to some analytic function on some open, connected set $D \subset \mathbb{C}$ that contains these integers. Is this continuation unique? The answer is clearly *no*: we can always shift $f(d)$ by, say, $\sin(\pi d)$. The only situation where we can guarantee uniqueness is when S has an accumulation point in D. And the only accumulation point in $\mathbb{N}$ (as embedded in the Riemann sphere $\mathbb{C} \cup \{\infty\}$) is $d = \infty$. Therefore, the only way to ensure that $f(d)$ has a unique continuation is to assume that it is defined for all sufficiently large $d \in \mathbb{N}$.

One situation where rigorous analytic continuation to fractional d may be possible is for QFTs that admit a lattice discretization [288–298]. These can put on a lattice whose continuum limit has fractional Hausdorff dimension, and this gives a non-perturbative definition of the field theory at that $d \in \mathbb{R}$. A natural question is whether this continuum limit always exists, whether it is unique, and whether the result is actually analytic in d. We do not know the answer to any of these questions. Another important issue is how to define this continuation in theories that do not admit a nice discretization; as we shall see, fermions are particularly subtle in fractional dimension, precisely for the same reason these objects refuse to sit peacefully on a lattice.

As for analytic continuation directly in the continuum, we only know how to define this in perturbative settings. For example, the $O(N)$ model admits a $1/N$ expansion, and this perturbative series happens to be analytic in d. Indeed, the large N expansion is organized in terms of Feynman integrals, and these admit a general definition of analytic continuation [287].

So, to summarize:

- We do not have a general definition of analytic continuation in d, nor in N. There are some cases where one can give a working prescription, but these are very non-generic and it is not clear if the result is always well-defined and unique.

- If a general definition exists at all, it will only lead to a unique extension if we choose an *infinite* sequence of QFTs as our starting point. This holds both for analytic continuation of d and N.

- Not every infinite sequence admits a continuation. Indeed, there is no reason to expect a random sequence like $T(1)$ = Ising, $T(2) = SU(2) + \psi_{\text{adj}}$, $T(3)$ = abelian Higgs, etc. to admit a meaningful interpolation.

4.2.2 Kinematics

As above, there is no general definition of analytic continuation of a QFT to $d \in \mathbb{C}$. We can try to make some progress by disentangling the dynamics from the kinematics. Namely, here we would like to understand the representation theory of the Lorentz group at fractional d. We begin with the Lorentz group being $O(d)$, and then explain why other global forms such as $SO(d)$ and $Spin(d)$ do not really have a satisfactory continuation.

Orthogonal group $O(d)$. We first recall some basic facts about $\mathrm{Rep}(O(d))$ [299]. When d is odd, any irreducible representation can be specified by an $SO(d)$ irreducible representation $\lambda \in \mathrm{Rep}(SO(d))$, together with a choice of intrinsic parity $\pm$. When d is even, $SO(d)$ has a $\mathbb{Z}_2$ outer automorphism C that permutes the last two Dynkin labels. Then, if λ is fixed by this action, it induces two representations of $O(d)$ which take the same form as before, $(\lambda, \pm)$. If $\lambda \in \mathrm{Rep}(SO(d))$ is not fixed by C, only the direct sum $\lambda + \lambda^{\mathsf{C}}$ induces an $O(d)$ representation. We call $(\lambda, +)$ a true tensor and $(\lambda, -)$ a pseudo-tensor. For representations of type $\lambda + \lambda^{\mathsf{C}}$, there is no intrinsic parity (the two choices for this sign are exchanged by electric-magnetic duality).

We now explain what the analogue of $\mathrm{Rep}(O(d))$ in the case of fractional d is. The precise mathematical framework to understand groups of continuous rank is that of Deligne categories [300]; see [238] for a physics-oriented presentation. Here we simply summarize some facts about Deligne categories without providing precise definitions; see the references for more details.

In short, an irreducible representation of $O(d)$ at fractional d is a simple object in the category $\widetilde{\mathrm{Rep}}(O(d))$. Such objects are labeled by terminating sequences of non-negative integers, which play the role of the usual Dynkin labels for integer d.

For convenience we will denote these sequences via the associated Young diagram. For example, the vector of $\widetilde{\mathrm{Rep}}(O(d))$ corresponds to the sequence $[\mathbf{1}] = (1, 0, \dots)$. It becomes a true vector of $O(d)$ when $d \in \mathbb{N}$; we will explain how to recover pseudo-tensors below.

The dimension of a given object in $\widetilde{\mathrm{Rep}}(O(d))$ can be obtained by plugging its Dynkin labels into the regular Weyl formula of $O(d)$ for increasing values of $d \in \mathbb{N}$; this produces an integer sequence of polynomial growth which, by standard arguments, has a unique analytic continuation to $d \in \mathbb{C}$. For example, the vector representation of $O(d)$ has dimension $1, 2, 3, \dots$ for $d = 1, 2, 3, \dots$, and this has a unique analytic continuation to the Riemann sphere, namely $f(d) = d$. Then, the dimension of the object labeled by $(1, 0, \dots)$ is $\dim([\mathbf{1}]) = d$ for all $d \in \mathbb{C}$.

Conversely, any sequence of true-tensor representations of $O(d)$ that share the same Young diagram for all $d \in \mathbb{N}$ defines an object in the Deligne category above. We will call such sequences *stable*. An example of an unstable sequence is $S^d[\mathbf{1}]$: this has d boxes, which increases as we increase d. The dimension of this sequence is $\dim(S^d[\mathbf{1}]) = \binom{2d-1}{d} - \binom{2d-3}{d-2}$, which grows like $\sim 2^{2d}$, too fast to have a good, unique continuation to $d \in \mathbb{C}$. The category $\widetilde{\mathrm{Rep}}(O(d))$ only describes stable sequences, precisely because these, and only these, have a unique analytic continuation to complex d.

Let us stress that the Deligne category above is not the "Rep" of anything: there is no structure $O(d), d \in \mathbb{C}$, whose category of representations coincides with $\widetilde{\mathrm{Rep}}(O(d))$. In order to talk about $O(d)$ at fractional d we do not literally consider a Lie group of complex rank; instead, it is enough to understand $O(d)$ for all $d \in \mathbb{N}$. (Intuitively, $\widetilde{\mathrm{Rep}}(O(d))$ is a regularized version of the representation category of the direct limit $O(\infty)$.)

The objects in $\widetilde{\mathrm{Rep}}(O(d))$ can be composed, which generalizes the usual notion of tensor product of representations. In practice, composition looks exactly like regular tensor products as computed in any $O(d)$ for $d \in \mathbb{N}$ large enough to fit the representations. For example,

$$[\mathbf{1}, \mathbf{1}] \times [\mathbf{1}, \mathbf{1}] = \mathbf{1} + [\mathbf{1}, \mathbf{1}] + [\mathbf{2}] + [\mathbf{2}, \mathbf{2}] + [\mathbf{2}, \mathbf{1}, \mathbf{1}] + [\mathbf{1}, \mathbf{1}, \mathbf{1}, \mathbf{1}] \tag{4.2.1}$$

holds for all integers $d \geq 11$, and therefore it is also true in $\widetilde{\mathrm{Rep}}(O(d))$.

The category $\widetilde{\mathrm{Rep}}(O(d))$ allows us to meaningfully talk about tensor fields at fractional d. An important question is how it relates to $\mathrm{Rep}(O(d))$ when d happens to be an integer. These are not identical on the nose since, for example, $\wedge^4[\mathbf{1}]$ is a non-trivial object in $\widetilde{\mathrm{Rep}}(O(d))$ for any d, but it is the zero object in $\mathrm{Rep}(O(3))$. The short answer is that, if $d \in \mathbb{N}$, there is an equivalence of categories $\mathrm{Rep}(O(d)) \cong \widetilde{\mathrm{Rep}}(O(d))/\mathcal{I}$ where $\mathcal{I}$ is the collection of "negligible morphisms" — the quotient kills all objects in $\widetilde{\mathrm{Rep}}(O(d))$ that are trivial in $\mathrm{Rep}(O(d))$.

A followup question is what happens to the pseudo-tensors of $O(d)$, which are not naturally described by $\widetilde{\mathrm{Rep}}(O(d))$. The answer is that they "reappear" when we quotient by the null representations above. To see this, note that any pseudo-tensor can equivalently be written as the product of a true tensor and the Levi-Civita symbol. For example $([\mathbf{2}], -) \cong ([\mathbf{2}, \mathbf{1}], +)$ when $d = 3$, $([\mathbf{2}], -) \cong ([\mathbf{2}, \mathbf{1}, \mathbf{1}], +)$ when $d = 4$, etc. Therefore, for any fixed $d \in \mathbb{N}$, the pseudo-tensor $([\mathbf{2}], -)$ is described by a certain object in $\widetilde{\mathrm{Rep}}(O(d))$: $[\mathbf{2}, \mathbf{1}]$ when $d = 3$, $[\mathbf{2}, \mathbf{1}, \mathbf{1}]$ when $d = 4$, etc.

In this sense, the Deligne category is not "missing" any $O(d)$ representation: for any fixed $d \in \mathbb{N}$, there is some object in $\widetilde{\mathrm{Rep}}(O(d))$ that descends to any given pseudo-tensor. But at the same time there is no meaningful way to talk about pseudo-tensors for $d \in \mathbb{C} \setminus \mathbb{N}$. As far as this categorical framework is concerned, only true tensors make sense for general $d \in \mathbb{C}$; pseudo-tensors only reappear when $d \in \mathbb{N}$. (An analogous statement holds for representations of type $\lambda + \lambda^{\mathsf{C}}$. These do not correspond to any object in $\widetilde{\mathrm{Rep}}(O(d))$ but, for any given $d \in \mathbb{N}$, there is some object that descends to $\lambda + \lambda^{\mathsf{C}}$. An example of a tensor of this type is the $(d/2)$-form. This does not correspond to an object in $\widetilde{\mathrm{Rep}}(O(d))$ since its Dynkin labels are $(0, \ldots, 0, 2, 0) \oplus (0, \ldots, 0, 0, 2)$, which does not have a meaningful direct limit, this is not a terminating sequence. But this $(d/2)$-form does have an image when $d \in \mathbb{N}$: $\wedge^2[\mathbf{1}]$ when $d = 4$, $\wedge^3[\mathbf{1}]$ when $d = 6$, etc.)

In conclusion, the category $\widetilde{\mathrm{Rep}}(O(d))$ captures all representations of $O(d)$ and, for stable, true tensors, it gives their canonical continuation to $d \in \mathbb{C}$. We can anticipate that, in QFT, pseudo-tensors and tensors whose spin depends on d (say, some field that transforms as $S^d[\mathbf{1}]$) will both fight back if we try to continue them to fractional d. Only fields that are true tensors and that define stable sequences as we vary $d \in \mathbb{N}$ should have a nice analytic continuation. So for example, the generalization of free Maxwell where the gauge field is a p-form should be amenable to analytic continuation for any fixed p, but if we want a generalization of the theta term, we should take $p = d/2$, in which case the theory will likely protest.

Other groups: $SO(d), Spin(d)$, etc. Let us now discuss what goes wrong if we try to repeat this story for other global forms of the Lorentz group. For example, say that we try to define a putative $\widetilde{\mathrm{Rep}}(SO(d))$ via stable sequences of $SO(d)$ representations, i.e., we assume that its simple objects are again labeled by terminating sequences of non-negative integers. One problem with this is that, unlike $\widetilde{\mathrm{Rep}}(O(d))$, our naive $\widetilde{\mathrm{Rep}}(SO(d))$ is actually missing some representations. In the case of $O(d)$ we explained that there is no simple object in $\widetilde{\mathrm{Rep}}(O(d))$ that corresponds to the $(d/2)$-form but, for any fixed $d \in \mathbb{N}$, this representation does have an image: $\wedge^2[\mathbf{1}]$ when $d = 4$, $\wedge^3[\mathbf{1}]$ when $d = 6$, etc. On the other hand, in the case of $SO(d)$, this $(d/2)$-form is actually reducible, and we can break it into the self-dual and anti-self-dual parts. These irreducible pieces do not have an image in our $\widetilde{\mathrm{Rep}}(SO(d))$ at all. (And indeed, it was already noticed in the early days of dim-reg that (anti-)self-dual fields are especially tricky to analytically continue [301].)

Another problem with this naive definition is that certain operations, like tensor products, are non-analytic in d. For example, consider the decomposition (4.2.1). This equation is true in $SO(d)$ for all $d \geq 11$, and therefore we would guess that it is also true in $\widetilde{\mathrm{Rep}}(SO(d))$ for all $d \in \mathbb{C}$. But then, we would conclude that $[\mathbf{1},\mathbf{1}] \times [\mathbf{1},\mathbf{1}]$ contains only one singlet for any $d \in \mathbb{C}$, which is actually false: in $SO(4)$ one has $\wedge^4[\mathbf{1}] \cong \mathbf{1}$, and therefore there are two singlets when $d = 4$. In a formal sense, objects like $\mathrm{Hom}(R_1, R_2)$ in the would-be category $\widetilde{\mathrm{Rep}}(SO(d))$ are discontinuous in d, due to low-rank exceptions.

In fact, the same non-analyticity would occur in $\widetilde{\mathrm{Rep}}(O(d))$ if we insisted that this category should describe pseudo-tensors as well. Indeed, one has $([\mathbf{1},\mathbf{1}],-) \times ([\mathbf{1},\mathbf{1}],+) = (\mathbf{1},-) + (\wedge^4[\mathbf{1}],-) + \cdots$ in $O(d)$ for all $d \geq 11$, which would imply that there are no singlets for any $d \in \mathbb{C}$, which is actually false: when $d = 4$, there is one singlet, since in this case $(\wedge^4[\mathbf{1}],-) \cong (\mathbf{1},+)$. True tensors are stable, pseudo-tensors are not.

Finally, let us consider the $Spin(d)$ form of the Lorentz group. This group has the same issues as $SO(d)$: self-dual and anti-self-dual representations are not captured by terminating sequences of Dynkin labels at all, and low-rank exceptions make tensor products non-analytic in d. One could wonder if $Pin(d)$ might fare better, since $O(d)$ does admit a continuation as opposed to $SO(d)$. The answer is *no, not really*: pinor representations are also not captured by terminating sequences of Dynkin labels. Indeed, this representation has Dynkin labels $(0,\dots,0,1)$ for odd d, and $(0,\dots,0,1,0)\oplus(0,\dots,0,0,1)$ for even d, and these sequences do not have a meaningful direct limit. Pinors are unstable representations. For example, their dimension $2^{\lfloor d/2\rfloor}$ is non-polynomial in d and, as such, it does not have a well-defined, unique continuation to $d\in\mathbb{C}$[5].

As a well-known example of the complications associated to pinors, consider the trace $\mathrm{tr}[\gamma^{\mu\nu\rho}]$. If we compute this for small values of d, we find

$$
\begin{aligned}
d=2:&\ \mathrm{tr}[\gamma^{\mu\nu\rho}]=0\\
d=3:&\ \mathrm{tr}[\gamma^{\mu\nu\rho}]=2i\epsilon^{\mu\nu\rho}\\
d=4:&\ \mathrm{tr}[\gamma^{\mu\nu\rho}]=0\\
d=5:&\ \mathrm{tr}[\gamma^{\mu\nu\rho}]=0\\
&\ \vdots
\end{aligned}
\tag{4.2.2}
$$

whose stable limit is $\mathrm{tr}[\gamma^{\mu\nu\rho}]=0$. This is the standard 't Hooft-Veltman prescription for this trace; while correct around $d=4$, it gives the wrong answer for the small rank exception $d=3$. This means that if we use this continuation for $d\in\mathbb{C}$, we will necessarily get the wrong answer when we take $d\to3$. More generally, all prescriptions for fermions in fractional dimension found in the literature ignore by hand low-rank exceptions that occur below $d=4$, which means that they will necessarily fail for small enough d. If our only goal is to continue to an infinitesimal neighborhood of $d=4$, this is not the end of the world, but

[5] A possible formalization of these facts, suggested to us by Justin Kulp, is the following. As above, $\widetilde{\mathrm{Rep}}(O(d))$ is the correct category to talk about stable representations. On the other hand, unstable representations are not objects in this category. But, the fact that unstable representations can be tensored to produce stable ones (e.g., the square of a pinor is $1+[\mathbf{1}]+\wedge^2[\mathbf{1}]+\cdots$) means that these large representations should be objects in a module category of $\widetilde{\mathrm{Rep}}(O(d))$, i.e., what we are missing is some version of $\widetilde{\mathrm{Rep}}(\mathrm{Cliff}(d))$ as a module over $\widetilde{\mathrm{Rep}}(O(d))$. See also [302] (and in particular the discussion around footnote 8).

if we want a continuation to $d \in \mathbb{C}$ that gives the correct answer when $d = 3$ or $d = 2$, we cannot drop small d exceptions, and we have to work harder.

Back to physics. We should note here that the fact that the representation theory of $O(d)$ is well-defined for non-integer d does not imply that analytic continuation of $O(d)$-symmetric QFTs is necessarily easy. For example, scalar fields transform according to the trivial representation of $O(d)$, which is stable. But, out of these scalars, one can construct more complicated tensors, including unstable ones. Indeed, consider the evanescent operators of [240], given by $R_p := \mathrm{tr}_{\wedge^p[\mathbf{1}]}[M]$, where $M_{\mu\nu} = \partial_\mu \partial_\nu \phi$. The representations $\wedge^p[\mathbf{1}]$ are all well-defined for $d \in \mathbb{C}$. But if we take d to be an integer, then the operators with $p > d$ are all null. As such, their continuation to fractional d is rather subtle: for example, they often have negative norm [240].

For QFTs that are invariant under $SO(d)$ only, things are even less straightforward. The lack of a proper $\widetilde{\mathrm{Rep}}(SO(d))$ category means that parity-breaking QFTs cannot be continued to complex d, at least not if we want to use the framework of Deligne categories as above. Of course, in physics we never let the lack of a rigorous framework stop us. We should try to continue such theories anyway; if the results are consistent, then a suitable generalization of Deligne categories must exist.

In this paper we will only study vector-like theories, but with a focus on parity-odd operators. Such representations are unstable from the point of view of $\widetilde{\mathrm{Rep}}(O(d))$, and therefore they should present the same obstructions as generic operators in a chiral theory. For example, much like $\mathrm{Hom}_{SO(d)}([\mathbf{1},\mathbf{1}] \times [\mathbf{1},\mathbf{1}], \mathbf{1}) = \delta_{d,4}\mathbb{C}$ is non-analytic in d due to the $SO(4)$ low-rank isomorphism $\wedge^4[\mathbf{1}] \cong \mathbf{1}$, one also has $\mathrm{Hom}_{O(d)}(([\mathbf{1},\mathbf{1}],+) \times ([\mathbf{1},\mathbf{1}],-), \mathbf{1}) = \delta_{d,4}\mathbb{C}$ due to the $O(4)$ low-rank isomorphism $(\wedge^4[\mathbf{1}],-) \cong (\mathbf{1},+)$. These low-rank exceptions will force us to go beyond the current framework of analytic continuation in QFT.

For completeness, let us mention that this whole discussion also goes through for analytic continuation of flavor (or gauge) symmetry groups. For example, an $O(N)$ symmetry should allow for a somewhat straightforward continuation of N, but an $SO(N)$ symmetry will likely be harder to define. For a general symmetry group, its Deligne interpolating category is well defined if its representation theory is stable; the best understood examples [238] are $U(N)$, $Sp(N)$ and S_N. For example, the fact that $\widetilde{\mathrm{Rep}}(U(N))$ exists but $\widetilde{\mathrm{Rep}}(SU(N))$ does not is related to the well-known fact that mesons in planar QCD are much easier to understand than baryons [303]. The latter are unstable in the sense above: while $[\mathbf{1}] \otimes \overline{[\mathbf{1}]}$ contains a singlet for any number of colors, there is no finite power of $[\mathbf{1}]$ that yields a singlet in "$\widetilde{\mathrm{Rep}}(SU(N))$". Unstable representations are non-perturbative in $1/N$, and they obstruct any naive attempts at analytic continuation of this parameter. (Similarly, the existence of $\widetilde{\mathrm{Rep}}(S_N)$ is related to the success of operations like the replica trick and the symmetric product orbifold).

4.2.3 A simple example: free fermions

As we reviewed above, fields transforming in unstable representations of the Lorentz group are particularly adverse to analytic continuation, (s)pinors being the most important example. Does this mean fermionic theories cannot be analytically continued to $d \in \mathbb{C}$? We believe a meaningful continuation is possible, although we will explain here some of the obstructions one has to overcome, and then describe our best attempts at doing so.

Here we will frame the discussion in the context of free Dirac fermions. We will perform a few computations in this QFT and then ask whether the result admits a meaningful continuation or not. This is an extended version of the toy model discussed in the introduction; readers interested in the interacting case only can safely skip to section 4.3.

A simple observable one can consider is the free energy of this system. This quantity is given by [304]

$$\log Z = 2^{\lfloor d/2 \rfloor + 2 - d} \sum_{n=1}^{\infty} \frac{(-1)^{n+1}}{n} \sinh(n/2T)^{1-d} \tag{4.2.3}$$

Does this admit a meaningful continuation to complex d? The factor $2^{\lfloor d/2 \rfloor}$ doesn't seem to like $d \notin \mathbb{N}$, but this is obviously a moot point: we could just as well ask about the free energy *per fermionic degree of freedom*, which simply amounts to dividing the expression above by this awkward factor. The resulting object does admit a perfectly healthy continuation to complex d. (And note that one can extract some interesting physics already for this extremely simple observable: for example, the limits $T \to 0$ and $d \to 1$ do not commute. This reflects the fact that the ground state is discontinuous at $d = 1$: there is only one vacuum for $d > 1$, but two vacua at $d = 1$.)

Are there observables for which analytic continuation is not possible? A potential example is the following. Give the fermion a mass m, and couple it to a background $U(1)$ gauge field A. At energies below m we can integrate out the fermion, producing a local effective action for A [305, 306]:

$$\begin{aligned} S_{\text{eff}}(A) &\supset \operatorname{Tr}\log(\not{\partial} + m + i\not{A}) \\ &= \operatorname{Tr}\log(\not{\partial} + m) + \operatorname{Tr}\left[\frac{1}{\not{\partial}+m} i\not{A}\right] - \frac{1}{2}\operatorname{Tr}\left[\frac{1}{\not{\partial}+m} i\not{A} \frac{1}{\not{\partial}+m} i\not{A}\right] + \cdots \end{aligned} \tag{4.2.4}$$

The parity-even part of this effective action is straightforward. For example, at the quadratic level $\mathcal{O}(A^2)$, it reads[6]

$$S_{\text{eff}}^{\text{even}}(A) \supset \frac{1}{2}\int_k A_\mu(k) A_\nu(-k) \int_p \operatorname{tr}[S(p)\gamma^\mu S(p+k)\gamma^\nu]_{\text{even}} \tag{4.2.5}$$

where

$$\begin{aligned} \operatorname{tr}[S(p)\gamma^\mu S(p+k)\gamma^\nu]_{\text{even}} &= \frac{-1}{(p^2+m^2)((p+k)^2+m^2)}\big(\operatorname{tr}[\not{p}\gamma^\mu(\not{p}+\not{k})\gamma^\nu] - m^2\operatorname{tr}[\gamma^\mu\gamma^\nu]\big) \\ \operatorname{tr}[S(p)\gamma^\mu S(p+k)\gamma^\nu]_{\text{odd}} &= \frac{-im}{(p^2+m^2)((p+k)^2+m^2)}\big(\operatorname{tr}[\not{p}\gamma^\mu\gamma^\nu] + \operatorname{tr}[\gamma^\mu(\not{p}+\not{k})\gamma^\nu]\big) \end{aligned} \tag{4.2.6}$$

Evaluating the trace and performing the p integral[7], we learn that the heavy fermion simply generates a renormalization of the would-be gauge coupling:

$$S_{\text{eff}}^{\text{even}}(A) \supset 2^{\lfloor d/2 \rfloor}\frac{\Gamma(2-d/2)}{3(4\pi)^{d/2}}|m|^{d-4}\int_k \frac{1}{2}A_\mu(k)(k^\mu k^\nu - k^2\delta^{\mu\nu})A_\nu(-k) \tag{4.2.7}$$

[6] We denote momentum integrals by $\int_k := \int \frac{\mathrm{d}^d k}{(2\pi)^d}$ and the free fermion propagator by $S(p) = \frac{1}{i\not{p}+m}$.

[7] Here we neglect the question of whether such momentum integrals converge in the first place. While very important in general, and even more so in the context of varying d, this issue is orthogonal to the one we are trying to address here. So below we just cut off the integrals at $p = \Lambda$ and consider $m \gg \Lambda \gg k$, and throw away subleading terms like Λ/m.

Up to the inconsequential factor $2^{\lfloor d/2 \rfloor}$, this admits a natural analytic continuation to $d \in \mathbb{C}$.

The parity-odd part in $S_{\text{eff}}(A)$ is a very different story. For example, at the linear level $\mathcal{O}(A)$ we find

$$\begin{aligned} S_{\text{eff}}^{\text{odd}}(A) &\supset i \int_k A_\mu(k) \int_p \operatorname{tr}[S(p)\gamma^\mu] \\ &= i \operatorname{tr}[\gamma^\mu] \operatorname{sign}(m)|m|^{d-1} \frac{\Gamma(1-d/2)}{(4\pi)^{d/2}} \int_k A_\mu(k) \end{aligned} \tag{4.2.8}$$

Now, while the coefficient $\frac{\Gamma(1-d/2)}{(4\pi)^{d/2}}$ admits a meaningful continuation to $d \in \mathbb{C}$, things are not so simple for the trace $\operatorname{tr}[\gamma^\mu]$. In $d = 1$ this is just $\operatorname{tr}[\gamma^\mu] = \pm 1$, and we obtain the well-known $1d$ Chern-Simons term that arises when integrating out a heavy fermion: $S_{\text{eff}}^{\text{odd}}(A) \supset \frac{i}{2} \operatorname{sign}(m) \int A$. If d is an integer different from 1, this trace vanishes instead. So, for general $d \in \mathbb{N}$, the effective action contains a Kronecker delta $\delta_{d,1}$, and there is no natural way to analytically continue such an object to fractional d. Similarly, at the quadratic level we find something proportional to $\operatorname{tr}[\gamma^{\mu\nu\rho}] \propto \delta_{d,3}\epsilon^{\mu\nu\rho}$, for which there is no obvious analytic continuation either. And of course the pattern continues: there is a $5d$ Chern-Simons term at the cubic level, etc.

So even for this very simple theory, which is free and vector-like, it is not entirely clear how to continue away from integer dimensions. Some questions, like the free energy, are well-defined for $d \in \mathbb{C}$; some others, like the free energy in presence of an external field, not quite so. And we see that the main obstruction is the existence of low-rank exceptions. Indeed, the even part of $S_{\text{eff}}(A)$ only involves traces of an even number of gammas, and these are the same for all d; but the odd part involves traces with an odd number of gammas, and those vanish unless the number of insertions equals the number of spacetime dimensions. In other words, $S_{\text{eff}}^{\text{even}}(A)$ has a stable limit (and it agrees with it) but $S_{\text{eff}}^{\text{odd}}(A)$ does not.

One could complain that the issue with this analysis is that we are trying to analytically continue an object, $S_{\text{eff}}(A)$, which is a function of a *vector* field, and it is sort of meaningless to talk about non-trivial tensors in fractional dimension anyway; only scalars are to be continued. This is not entirely true since, as we explained above, stable tensor fields make sense in fractional dimension, and vectors are stable. But in any case, there are complications for scalar questions as well, as we explain next.

For simplicity let us turn off A and let us set the fermion mass to zero, and consider the correlation functions of $\bar{\psi}\psi$. This operator is parity-odd[8], so we might expect the same difficulties as above; but crucially, it is a Lorentz scalar, so if we find any obstacles to analytically continuing its correlators, those will be harder to dismiss. We can begin with its expectation value, which is given by

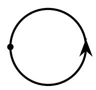

$$\begin{aligned} &= -\lim_{x\to 0} \mathrm{tr}[S(x)] \\ &= \frac{\Gamma(d/2)}{2\pi^{d/2}}\,\mathrm{tr}[\gamma_\mu]\lim_{x\to 0}\frac{x^\mu}{x^d} \end{aligned} \tag{4.2.9}$$

which contains once again the problematic $\mathrm{tr}[\gamma_\mu]$ factor. This trace vanishes for all integers $d > 1$. But in $d = 1$ the trace is non-zero and we find $\langle\bar{\psi}\psi\rangle = \frac{1}{2}\delta_{1,d}$. Again, it is unclear how this should be analytically continued in d.

There is a simple explanation for this discontinuity at $d = 1$. This operator has scaling dimension $\Delta(\bar{\psi}\psi) = d - 1$. For $d > 1$, this is non-zero, and its *vev* is forced to vanish by the (unbroken) scaling symmetry. But in $d = 1$ the scaling dimension vanishes, and this operator becomes degenerate with the identity, which allows for mixing of these operators, explaining why $\bar{\psi}\psi$ is allowed to acquire a *vev*. This mixing is a discontinuous process and we should not be alarmed by it. In $d = 1$ we could define a different operator by subtracting the contribution of the identity, namely by normal ordering $:\!\bar{\psi}\psi\!: = \bar{\psi}\psi - 1/2$, which now has vanishing *vev*. Apparently, the reasonable analytic continuation of this expectation value is $\langle\bar{\psi}\psi\rangle = 0$ for all d, including $d = 1$. This is a bit misleading: the combination $\bar{\psi}\psi - 1/2$ doesn't make sense above $d = 1$, since $\bar{\psi}\psi$ has non-zero Δ (more precisely, this combination is not a conformal primary). So we either work with $\bar{\psi}\psi$, which has a discontinuous *vev*, or with the discontinuous object $\bar{\psi}\psi - \delta_{1,d}/2$, which has continuous *vev*. Either way, this bilinear operator is simply non-analytic in d around $d = 1$.

[8]Parity here refers to reflections, namely flipping the sign of a *single* spatial coordinate, say, x_1. This acts as $\psi \mapsto \gamma_1\psi$ and $\bar{\psi} \mapsto -\bar{\psi}\gamma_1$ (the relative sign is inherited from the Lorentzian identification $\bar{\psi} = \psi^\dagger\gamma^0$). The usual mass term $\bar{\psi}\psi$ is odd under reflections. In even dimensions, one can also consider $\bar{\psi}\gamma^\star\psi$, which is even.

Are there any further discontinuities in $\bar{\psi}\psi$ at higher d? We can answer this question by looking at its connected five-point function

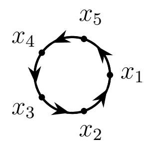

$$+ \text{ permutations} \tag{4.2.10}$$

for a total of $4! = 24$ permutations. The first permutation is proportional to

$$\left(\prod_{i=1}^{5} \frac{(x_i - x_{i+1})_{\mu_i}}{|x_i - x_{i+1}|^d}\right) \operatorname{tr}[\gamma^{\mu_1}\gamma^{\mu_2}\gamma^{\mu_3}\gamma^{\mu_4}\gamma^{\mu_5}] \tag{4.2.11}$$

We can use the Clifford relation to write the product of five gammas as the fully anti-symmetrized product $\gamma^{\mu_1\mu_2\mu_3\mu_4\mu_5}$, plus terms with three gammas, $\gamma^{\mu_1\mu_2\mu_3}\delta^{\mu_4\mu_5}$ (plus permutations), and terms with a single gamma, $\gamma^{\mu_1}\delta^{\mu_2\mu_3}\delta^{\mu_4\mu_5}$ (plus permutations). The fully anti-symmetric term $\gamma^{\mu_1\mu_2\mu_3\mu_4\mu_5}$ vanishes due to translation invariance, since we only have four linearly independent vectors to contract it with. So the final answer is that the five-point function is proportional to various combinations of the x_i's contracted with $\operatorname{tr}[\gamma^{\mu\nu\rho}] \propto \delta_{3,d}$ and with $\operatorname{tr}[\gamma^{\mu}] \propto \delta_{1,d}$. Although not obvious from this discussion, the overall coefficient is non-zero, i.e., the various combinations do not cancel each other out[9].

The conclusion of this little exercise is that this correlation function vanishes for all $d \in \mathbb{N}$ except for $d = 3$. Then, the stable limit of this correlation function is that it vanishes for all $d \in \mathbb{C}$, and we again discover a non-analytic behavior of $\bar{\psi}\psi$, this time not only at $d = 1$, but also at $d = 3$. It is not hard to imagine that the seven-point function is proportional to the trace of five gammas, giving rise to a discontinuity at $d = 5$, etc. Not only is the *vev* of $\bar{\psi}\psi$ discontinuous as a function of d, so are its higher correlation functions.

For future reference we mention that, if we were interested in *quartic* operators such as $(\bar{\psi}\psi)^2$, then there are well-known subtleties such as the existence of operators of the

[9]The full expression is too large to include here. If we take the simplifying configuration $x_1 = (0,0,0)$, $x_2 = (0,0,a)$, $x_3 = (0,0,1)$, $x_4 = (0,b,0)$, $x_5 = (c,0,0)$, and take the the limit $a \to 0, b \to \infty$ so that the result fits in a single line, we find

$$b^5|a|\langle\bar{\psi}\psi(x_1)\cdots\bar{\psi}\psi(x_5)\rangle = i\,\operatorname{sign}(c)\left(\frac{1}{c^2} - \frac{|c|}{(1+c^2)^{3/2}}\right) \tag{4.2.12}$$

up to factors of 2π. This is of course odd under parity, as required, but crucially non-zero.

form [307, 308]

$$\mathscr{O}_n := \bar{\psi}\gamma^{\mu_1\cdots\mu_n}\psi\,\bar{\psi}\gamma_{\mu_1\cdots\mu_n}\psi \tag{4.2.13}$$

These are scalars and degenerate with $(\bar{\psi}\psi)^2$, so these operator will generically mix. In integer dimensions, the operators with $n > d$ vanish by anti-symmetry. But in fractional dimension these are independent and non-trivial, and one must consider them together with the original quartic [284, 309, 310]. The quartics with $n > d$ are evanescent: non-trivial when $d \notin \mathbb{N}$, but null when $d \in \mathbb{N}$. The difficulty in defining traces of gamma matrices in non-integer dimension also shows up in $\mathscr{O}_n$; for example, the OPE of $\bar{\psi}\psi$ with the quartics above is

$$\bar{\psi}\psi(x)\,\mathscr{O}_n(0) \sim \frac{1}{x^{2(d-1)}}\,\mathrm{tr}[\gamma_{\mu_1\cdots\mu_n}]\bar{\psi}\gamma^{\mu_1\cdots\mu_n}\psi + \cdots \tag{4.2.14}$$

Without a prescription for $\mathrm{tr}[\gamma_{\mu_1\cdots\mu_n}]$ in fractional dimension, we are somewhat forced to admit that OPEs are discontinuous as a function of d, even for scalar operators as we are considering here.

Clearly, even free theories present some difficulties in defining a meaningful continuation in d. In the reminder of this paper we will study interacting theories instead. But before doing that, this might be a good point to pause and discuss our conventions for gamma matrices in fractional dimension.

4.2.3.1 Gamma matrices

Integer dimension. For integer d we define the Clifford algebra as

$$\gamma^\mu\gamma^\nu + \gamma^\nu\gamma^\mu = 2\delta^{\mu\nu} \tag{4.2.15}$$

It is a well-known fact that, if d is an integer and $\delta^{\mu\nu}$ denotes the standard metric on $\mathbb{R}^d$, then the Clifford algebra admits an (essentially unique) irreducible matrix representation, of dimension $2^{\lfloor d/2 \rfloor}$ (see e.g. [311]). For the discussion below we don't need to assume that the matrix representation has been chosen to be irreducible. In fact, when a QFT contains N_f fermions, one might as well declare that the theory has a *single* fermion that transforms under the reducible representation that consists of N_f copies of the irreducible one. This latter perspective is notationally more convenient, especially in the case of fractional d.

The Clifford relation (4.2.15) implies the usual reduction identities, such as

$$\begin{aligned} \gamma^\mu \gamma_\mu &= d \\ \gamma^\mu \gamma^\nu \gamma_\mu &= (2-d)\gamma^\nu \end{aligned} \tag{4.2.16}$$

etc. Similarly, one can also take the matrix trace of the Clifford relation, which yields the usual trace identities

$$\begin{aligned} \mathrm{tr}[\gamma^\mu \gamma^\nu] &= \delta^{\mu\nu}\,\mathrm{tr}[1] \\ \mathrm{tr}[\gamma^\mu \gamma^\nu \gamma^\rho \gamma^\sigma] &= (\delta^{\mu\nu}\delta^{\rho\sigma} - \delta^{\mu\rho}\delta^{\nu\sigma} + \delta^{\mu\sigma}\delta^{\nu\rho})\,\mathrm{tr}[1] \end{aligned} \tag{4.2.17}$$

etc.

Traces over the odd part of Clifford are a little less well-behaved. First, we can use the Clifford relation to write a product of gamma matrices as their full anti-symmetrization, plus products of fewer matrices. For example,

$$\gamma_\mu \gamma_\nu \gamma_\rho = \gamma_{\mu\nu\rho} + \gamma_\mu \delta_{\nu\rho} - \gamma_\nu \delta_{\mu\rho} + \gamma_\rho \delta_{\mu\nu} \tag{4.2.18}$$

where $\gamma_{\mu\nu\rho} := \frac{1}{3!}(\gamma_\mu\gamma_\nu\gamma_\rho \pm \text{permutations})$. Therefore, we only need to work out traces of fully anti-symmetrized gammas $\mathrm{tr}[\gamma_{\mu_1\cdots\mu_n}]$ since more general products can always be reduced to these.

As is well-known, $\mathrm{tr}[\gamma_{\mu_1\cdots\mu_n}]$ vanishes unless n is equal to d and is also odd. This follows from the basic identity

$$\gamma_\alpha \gamma^{\mu_1\cdots\mu_n}\gamma^\alpha = (-1)^n(d-2n)\gamma^{\mu_1\cdots\mu_n} \tag{4.2.19}$$

together with cyclicity. When this trace is non-zero, it equals $\pm i^{(n-1)/2}\epsilon_{\mu_1\cdots\mu_n}\,\mathrm{tr}[1]$. The sign is arbitrary, since $\pm\gamma^\mu$ both satisfy the Clifford algebra. This sign can be understood as a choice of orientation; it does not affect the even part of the algebra, which is why both choices lead to the same representation of $Spin(d)$.

Fractional d. As explained in subsection 4.2.2, fractional d does not literally mean that the rank of $O(d)$ is fractional. Instead, we are instructed to look at the Deligne category $\widetilde{\mathrm{Rep}}(O(d))$. Unfortunately, the fermionic version $\widetilde{\mathrm{Rep}}(Pin(d))$ is not actually well-defined: pinor representations are unstable.

We of course do not want to admit defeat either, so let us push through anyway. Intuitively, fractional d should look something like $\mathrm{Rep}(Pin(\infty))$. We will not try to make this precise, but we do ask: is there any sense in which the various formulas like (4.2.16) and (4.2.17) have a direct limit? If not in the rigorous mathematical sense, at least in a more practical one?

In fact, some formulas do admit a meaningful stabilization. For example, the relation $\gamma^\mu\gamma^\nu\gamma_\mu = (2-d)\gamma^\nu$ is true for all $d \in \mathbb{N}$, and therefore it makes sense to claim that it is also true when $d \in \mathbb{C}$. In order to make this rigorous one would have to specify what type of object γ^μ is when $d \in \mathbb{C}$. We will not let these minutiae distract us too much; in practice, one can regard these matrices as elements of a formal algebra of symbols subject to the Clifford relation.

What about the identity $\mathrm{tr}[\gamma^\mu\gamma^\nu] = \delta^{\mu\nu}\,\mathrm{tr}[1]$? This equation is again true for all $d \in \mathbb{N}$, so it is tempting to once again declare that it is also true when $d \in \mathbb{C}$. This is not entirely immediate though:

- If we think of the γ^μ's as living in a certain algebra of symbols, then this trace identity formally follows from the Clifford relation, as long as "tr" satisfies linearity $\mathrm{tr}[\lambda A + \mu B] = \lambda\,\mathrm{tr}[A] + \mu\,\mathrm{tr}[B]$ and cyclicity $\mathrm{tr}[AB] = \mathrm{tr}[BA]$. But this is not actually well-defined, since there is no sense in which such an algebra has a finite-dimensional representation, and therefore there is no reason a trace acting on it should exist.

- Relatedly, the trace relation looks stable when written in terms of $\mathrm{tr}[1]$. But if we replace this factor by $2^{\lfloor d/2 \rfloor}$, the identity no longer looks particularly nice, since this sequence does not have a unique analytic continuation.

One can formally fix both problems at the same time by writing instead $\mathrm{tr}[\gamma^\mu\gamma^\nu]/\,\mathrm{tr}[1] =$

$\delta^{\mu\nu}$. Now, the *l.h.s.* can be thought of as a "regularized trace", one that has a finite $d \to \infty$ limit, and the *r.h.s.* is a perfectly well-defined, stable tensor. In practice, this just means that the trace relations over the even part of the Clifford algebra are all correct at fractional d, but with the understanding that the factor $\mathrm{tr}[1]$ is to be left as is, instead of replacing it by $2^{\lfloor d/2 \rfloor}$ or some interpolation thereof.

This last comment actually has an important corollary. When we work with Dirac fermions in a certain integer-dimensional QFT, we take ψ to transform according to a pinor representation of the Lorentz group. Such a representation is always given by a certain number of copies of the irreducible, $2^{\lfloor d/2 \rfloor}$-dimensional representation, and we define N_f to be this number. In other words, "number of fermions" in a given QFT simply means how many copies of the smallest Dirac representation appear in our theory. In fractional d, there is no such "smallest" representation, and therefore no canonical definition of N_f. The object that plays the role of N_f is $\mathrm{tr}[1]$, where the trace refers to a sum over both flavor and spin indices. If one wishes to specialize our general-d formulas to a given $d \in \mathbb{N}$, the dictionary is

$$\mathrm{tr}[1] = N_f \times 2^{\lfloor d/2 \rfloor} \tag{4.2.20}$$

If $d \notin \mathbb{N}$, there is no canonical way to disentangle spin and flavor, and the only meaningful operation is tracing over both, at the same time. Therefore, in the same way N_f normally labels families of fermionic QFTs, in fractional dimension it is $\mathrm{tr}[1]$ what labels such families.

The traces over the odd part of Clifford are again less well-behaved. Indeed, the identity $\mathrm{tr}[\gamma_{\mu_1\cdots\mu_n}] = \pm\delta_{n,d} i^{(n-1)/2} \epsilon_{\mu_1\cdots\mu_n} \mathrm{tr}[1]$ implies that (for fixed n) these traces all vanish for sufficiently large d, and therefore their stable limit is that they vanish for all $d \in \mathbb{C}$. But of course setting them to zero does not lead to a good analytic continuation, since they miss the low-rank exceptions where these traces are occasionally non-zero.

For the time being, we will simply leave the odd traces unspecified. That is to say, in the same way the factor $\mathrm{tr}[1]$ is not meant to be continued to $d \in \mathbb{C}$, but just carried along, the odd traces $\mathrm{tr}[\gamma_{\mu_1\cdots\mu_n}]$ will also be left as is. As we shall see, one can get very far without ever trying to write down a specific formula for these traces.

The rules above are enough to have a working theory of fermions in fractional dimension. Our general philosophy is that, if one wants to be on the safe side when working with gamma matrices, the parameter d is always an integer, there is no such a thing as $\gamma^\mu \in Pin(d)$ for $d \in \mathbb{C}$. Instead, one computes observables using formulas that are true for all $d \in \mathbb{N}$, and analytically continues the answer, not the intermediate steps. (It goes without saying, this last part is still very non-trivial, and not even necessarily well-defined; here we are just kicking the can down the road.)

Conversely, if one insists on trying to work with formal symbols defined for all $d \in \mathbb{C}$, one runs into many well-known paradoxes. Let us describe a few of them here for illustration purposes. In the discussion below we abandon our general philosophy that one should only talk about γ^μ for integer d, and assume that these exist at fractional d as well.

If γ^μ is a valid object at fractional d, and "tr" is a valid operation acting on it, then we must admit the existence of a symbol $\mathrm{tr}[\gamma^\mu]$. This is non-zero for $d = 1$, and therefore we cannot just claim that $\mathrm{tr}[\gamma^\mu] = 0$ for all $d \in \mathbb{C}$. For example, it might be the case that

$$\mathrm{tr}[\gamma^\mu]\,\mathrm{tr}[\gamma_\mu] \stackrel{?}{=} \frac{1}{\Gamma(d)\Gamma(2-d)} \tag{4.2.21}$$

or some other analytic function of d that equals $\delta_{1,d}$ when $d \in \mathbb{N}$.

One can in fact give a formal argument to determine $\mathrm{tr}[\gamma_\mu]$ for fractional d. First, note that this symbol satisfies the identity

$$\mathrm{tr}[\gamma_\rho]\delta_{\mu\nu} = \mathrm{tr}[\gamma_\mu]\delta_{\nu\rho} = \mathrm{tr}[\gamma_\nu]\delta_{\mu\rho} \tag{4.2.22}$$

as can be checked by taking the trace of (4.2.18) and using cyclicity. By contracting μ and ν one finds $d\,\mathrm{tr}[\gamma_\rho] = \mathrm{tr}[\gamma_\rho]$ which implies that either $d = 1$ or $\mathrm{tr}[\gamma_\rho] = 0$. This is of course the correct answer for integer d, but also appears to follow from the Clifford relation for fractional d as well. Therefore, if we take the point of view that gamma matrices for fractional d are well-defined as formal symbols, and that their traces are meaningful as formal operations that satisfy linearity and cyclicity, then $\mathrm{tr}[\gamma_\rho]$ is identically zero at fractional d. In other words, the only possible value we can assign to this symbol that is compatible with the standard properties of "tr" is $\mathrm{tr}[\gamma^\mu]\,\mathrm{tr}[\gamma_\mu] = \delta_{1,d}$, which is non-analytic in d.

Of course, another solution to $d\,\mathrm{tr}[\gamma_\rho] = \mathrm{tr}[\gamma_\rho]$ is $\mathrm{tr}[\gamma_\rho] = \infty$, which is perhaps the only logical trace for an object that is not trace class. This also nicely matches the intuition that fractional d is formally equivalent to infinite d.

The identity (4.2.22), while admittedly rather weird, seems to be required for consistency of momentum integrals. For example, we typically say that, under the integral sign, $k^\mu k^\mu \to \frac{1}{d}\delta^{\mu\nu}k^2$, since $\delta^{\mu\nu}$ is the only tensor that has the right index structure. But if we admit that $\mathrm{tr}[\gamma_\mu]$ is a valid tensor, one should aslo allow for $\mathrm{tr}[\gamma_\mu]\,\mathrm{tr}[\gamma_\nu]$, which technically is also a symmetric rank-2 tensor. The identity (4.2.22) implies that these are not independent structures: indeed, multiplying both sides by $\mathrm{tr}[\gamma_\nu]$, we find $\mathrm{tr}[\gamma_\mu]\,\mathrm{tr}[\gamma_\nu] = \delta_{\mu\nu}\,\mathrm{tr}[\gamma_\rho]\,\mathrm{tr}[\gamma^\rho]$. So at the very least, these formal manipulations do not interfere with the standard rules of analytic continuation of loop integrals.

While the argument above concerns the trace of a single gamma, the same pattern occurs for any odd number of gammas. For example, once again using Clifford plus cyclicity, one can check that

$$\delta_{\mu\rho}\,\mathrm{tr}[\gamma_{\nu\sigma\tau}] + \delta_{\nu\sigma}\,\mathrm{tr}[\gamma_{\mu\rho\tau}] + \delta_{\mu\tau}\,\mathrm{tr}[\gamma_{\nu\rho\sigma}] - \delta_{\nu\rho}\,\mathrm{tr}[\gamma_{\mu\sigma\tau}] - \delta_{\mu\sigma}\,\mathrm{tr}[\gamma_{\nu\rho\tau}] - \delta_{\nu\tau}\,\mathrm{tr}[\gamma_{\mu\rho\sigma}] = 0 \tag{4.2.23}$$

Contracting μ and ρ simplifies to $(d-3)\,\mathrm{tr}[\gamma_{\nu\sigma\tau}] = 0$, which again implies that this trace vanishes unless $d = 3$. The general statement is that the trace of n gamma matrices, where n is odd, is proportional to $\delta_{n,d}$, even if d is fractional.

Moreover, if we insist that these traces make sense at $d \in \mathbb{C}$, there are some further questions one must reckon with. For example, is the operator $\mathrm{tr}[\gamma_\mu]\bar{\psi}\gamma^\mu\psi$ a Lorentz scalar? If the symbol $\mathrm{tr}[\gamma_\mu]$ defines a valid expression with a free Lorentz index, we should be able to contract it with other free Lorentz indices to construct scalars. More generally, one would guess that $\bar{\psi}\psi$ is infinitely degenerate with operators of the form

$$\mathrm{tr}[\gamma_{\mu_1\cdots\mu_n}]\bar{\psi}\gamma^{\mu_1\cdots\mu_n}\psi, \qquad n \text{ odd} \tag{4.2.24}$$

We will term these operators *extraneous*. They are similar in spirit to the evanescent operators (4.2.13) we encountered in the previous subsection, and it is tempting to ascribe the various discontinuities in $\bar{\psi}\psi$ to their existence.

These extraneous operators appear in the OPE of the evanescent quartics. For example, consider the quadratic $\bar\psi\psi$, and compute its OPE with a generic quartic $\bar\psi\Gamma\psi\,\bar\psi\bar\Gamma\psi$ for a pair of arbitrary matrices $\Gamma, \bar\Gamma$. The double contractions give

$$\begin{aligned}\bar\psi\psi(x)\,\bar\psi\Gamma\psi\bar\psi\bar\Gamma\psi(0) &\supset \operatorname{tr}[S(x)^2\Gamma]\bar\psi\bar\Gamma\psi + \operatorname{tr}[S(x)^2\bar\Gamma]\bar\psi\Gamma\psi + \bar\psi\bar\Gamma S(x)^2\Gamma\psi - \bar\psi\Gamma S(x)^2\bar\Gamma\psi \\ &\propto \frac{1}{x^{2(d-1)}}\big(\operatorname{tr}[\Gamma]\bar\psi\bar\Gamma\psi + \operatorname{tr}[\bar\Gamma]\bar\psi\Gamma\psi + \bar\psi[\bar\Gamma,\Gamma]\psi\big)\end{aligned} \tag{4.2.25}$$

If we now take $\Gamma = \gamma_{\mu_1\cdots\mu_n}$ and $\bar\Gamma = \gamma^{\mu_1\cdots\mu_n}$, the OPE becomes

$$\bar\psi\psi(x)\,\mathscr{O}_n(0) \supset \frac{1}{x^{2(d-1)}}\operatorname{tr}[\gamma_{\mu_1\cdots\mu_n}]\bar\psi\gamma^{\mu_1\cdots\mu_n}\psi \tag{4.2.26}$$

Therefore, if we admit the existence of the evanescent operators $\mathscr{O}_n$, it seems somewhat unavoidable to accept the existence of extraneous operators as well.

All of these paradoxes go away if we agree that the gamma matrices are only defined for integer d, and the analytic continuation is not defined by literally working in $Pin(d)$ for $d \in \mathbb{C}$, but rather we should study $Pin(d)$ for all $d \in \mathbb{N}$, and (roughly speaking) take the direct limit $Pin(\infty)$.

In this work we are only concerned with vector-like theories, and we don't have much to say about the chirality matrix $\gamma^\star$. This matrix is even more subtle than the regular gamma matrices. For example, while $\operatorname{tr}[\gamma_{\mu\nu\rho}]$ is hard to define for $d \in \mathbb{C}$, at least it has a $d \to \infty$ limit: this trace vanishes for all sufficiently large d. This limit misses the $d = 3$ low-rank exception, but at least it exists. On the other hand, $\operatorname{tr}[\gamma^\star]$ oscillates between 0 (for even d) and $\operatorname{tr}[1]$ (for odd d), and therefore it does not even have a limit.

It appears to us that, if an analytic continuation of $\gamma^\star$ is possible at all, it will hardly be unique. For example, if we define for integer d

$$\gamma^\star := i^{d(d-1)/2}\gamma^1\cdots\gamma^d \tag{4.2.27}$$

where the factor of i is included to make $\gamma^\star$ hermitian, then it follows that

$$\begin{aligned}(\gamma^\star)^2 &= 1 \\ \gamma_\mu\gamma^\star\gamma^\mu &= (-1)^{d+1}d\gamma^\star\end{aligned} \tag{4.2.28}$$

etc. The factor $(-1)^{d+1}$ does not have a unique, canonical continuation to $d \in \mathbb{C}$. Assuming that these equations make sense in fractional d for *some* choice of analytic continuation, then upon taking the formal trace one finds $(-1)^{d+1}\,\mathrm{tr}[\gamma^\star] = \mathrm{tr}[\gamma^\star]$. Therefore, if our choice of analytic continuation for $(-1)^{d+1}$ is such that it differs from 1 for $d \notin \mathbb{N}$, then we must once again conclude that $\mathrm{tr}[\gamma^\star]$ vanishes when $d \notin \mathbb{N}$, and this trace is again non-analytic in d. Of course, similar conclusions hold for traces containing $\gamma^\star$ and one or more insertions of γ^μ's.

One can use $\gamma^\star$ to construct further evanescent operators, such as $\bar{\psi}(1-(-1)^{(d^2-1)/8}\gamma^\star)\psi$. Perhaps one has to take these into account as well. We will not explore the matrix $\gamma^\star$ any further in this chapter.

4.3 A case study: QCD

Here we will illustrate the general discussion from the previous section in one particularly interesting example: vector-like massless QCD. Needless to say, this theory is the prototypical example of a strongly-coupled QFT. In order to recover computational control we will be working in the large N_f limit, in which the strongly-coupled, low-energy fixed point becomes tractable as a series expansion in $1/N_f$. We have no insights as to what a non-perturbative definition should look like.

We use the standard large-N_f expansion and compare the result with the known dynamics of the theory in $d = 1, 2, 3, 4$.

In order to simplify the notation, let us restrict ourselves to the abelian case for now; we will point out the modifications required for general gauge group below. The lagrangian of the theory in Euclidean signature is given by

$$L = \frac{1}{4e^2} f^{\mu\nu} f_{\mu\nu} - \bar{\psi}\gamma^\mu(\partial_\mu + i a_\mu)\psi + \text{gauge-fixing} \tag{4.3.1}$$

As far as the large N_f expansion is concerned, this Lagrangian describes a flow between the free CFT $e^2 \to 0$ and the interacting CFT $e^2 \to \infty$. The engineering dimension of e^2 is

$4-d$, and therefore the direction of the flow depends on whether d is larger or smaller than 4. The interesting case is of course $d \leq 4$, but in order to talk about analytic continuation in d we must choose a target QFT for all $d \in \mathbb{N}$, and therefore we will also care about this theory for $d > 4$. For simplicity we will use language adapted to $d < 4$, namely we will call the $e^2 \to 0$ fixed point the "high energy" theory and the $e^2 \to \infty$ fixed point the "low energy" one, even though these roles are exchanged for $d > 4$. The low-energy theory is non-perturbative in e^2 but weakly-coupled in $1/N_f$.

The Feynman rules of this theory at the low-energy fixed point are

 $= -i\dfrac{\not{p}}{p^2}$

 $= \dfrac{g}{p^{d-2}}(\delta^{\mu\nu} + \xi p^\mu p^\nu / p^2)$ (4.3.2)

together with the usual vertex $-i\gamma^\mu$. Here, g is the effective coupling

$$g := \frac{(4\pi)^{d/2}}{\mathrm{tr}[1]} \frac{2\Gamma(d-2)}{\Gamma(2-d/2)\Gamma(d/2-1)^2} \frac{d-1}{d-2} \tag{4.3.3}$$

where $\mathrm{tr}[1] = 2^{\lfloor d/2 \rfloor} N_f$. Note that, in position space, the photon propagator is

$$\begin{aligned} &\int_k e^{ikx} \frac{g}{k^{d-2}}(\delta_{\mu\nu} + \xi k_\mu k_\nu / k^2) \\ &\quad = \frac{2}{(4\pi)^{d/2}\Gamma(d/2)} \frac{g}{x^2}((d-2+\xi)\delta_{\mu\nu} - 2\xi x_\mu x_\nu / x^2) \end{aligned} \tag{4.3.4}$$

which has the same $1/x^2$ scaling as its $d = 4$ counterpart. This implies that $\Delta(f_{\mu\nu}) = 2$, which is below the unitarity bound $d-2$ for all $d > 4$. The $d > 4$ CFTs are all non-unitary.

We will compute the following observables to leading order in $g \sim 1/N_f$:

- The expectation value of W for various closed contours, where W denotes a Wilson line:

$$W(\gamma) = \exp\left(i \oint_\gamma a\right) \tag{4.3.5}$$

- The scaling dimension of ψ. By this we mean the exponent in the two-point function

$$\langle \bar{\psi}(x) W \psi(0) \rangle \propto x^{-2\Delta(\psi)} \tag{4.3.6}$$

where W is a Wilson line connecting x to 0. This x dependence arises for a straight Wilson line, since we want the geometry to preserve scale invariance.

- The scaling dimension of $\bar{\psi}\psi$, namely the exponent in

$$\langle\bar{\psi}\psi(x)\bar{\psi}\psi(0)\rangle \propto x^{-2\Delta(\bar{\psi}\psi)} \tag{4.3.7}$$

We will then try to analytically continue these observables to $d \in \mathbb{C}$.

Another observable that would be particularly instructive to study in the future is the magnetic current $\star f$. As above, this satisfies $\Delta(\star f) = 2$, which saturates the unitarity bound, in agreement with its being conserved. This operator is parity-odd, which means that it is an unstable representation of $O(d)$, i.e., its continuation to fractional d is much more involved than f itself. See for example [312] for some very interesting results concerning magnetic operators in fractional dimension.

4.3.1 Wilson lines

In this section we sketch the computation of the expectation value of Wilson lines along various closed contours [313]. This is textbook material by now so we will be superficial; the main point we want to illustrate here is that these expectation values admit a well-defined analytic continuation in d.

As mentioned above, we begin with the case of abelian gauge group, and generalize to arbitrary gauge group afterward.

The expectation value is given by the usual cluster expansion

$$\langle e^{i\oint a}\rangle = e^{-\frac{1}{2}\oint\oint\langle aa\rangle + \frac{1}{4!}\oint\oint\oint\oint\langle aaaa\rangle_c + \cdots} \tag{4.3.8}$$

To leading order in $1/N_f$ we simply keep the first term. So we need to line-integrate the propagator $\Delta_{\mu\nu} = \langle a_\mu a_\nu\rangle$ along the contour of interest:

$$\log\langle W(\gamma)\rangle = -\frac{1}{2}\oint\!\!\oint_{\gamma\times\gamma} \mathrm{d}x^\mu\,\mathrm{d}y^\nu\,\Delta_{\mu\nu}(x-y) \tag{4.3.9}$$

For the actual computations we use two different regulators: analytic regularization $\frac{1}{x^2} \to \frac{\mu^2}{(\mu^2 x^2)^\alpha}$ (with μ some arbitrary scale) and point-splitting regularization, where we deform one integration contour via $\gamma \to \gamma + \epsilon$. We can gain different insights from each of these two options.

In this discussion we will write the photon propagator as $\Delta_{\mu\nu} = \frac{\delta_{\mu\nu}}{x^2}$, which accounts for multiple situations:

- If we multiply by $\frac{e^2}{4\pi^2}$ we obtain free Maxwell in $4d$. This will be a useful cross-check for our computations.
- If we multiply by $\frac{4g}{(4\pi)^{d/2}\Gamma(d/2-1)}$, we obtain the low-energy fixed point of QED$_d$ to leading order in $1/N_f$.
- If we replace $\frac{1}{x^2} \to \frac{\mu^2}{(\mu^2 x^2)^\alpha}$ and take $\alpha \to d/2-1$ instead of $\alpha \to 1$, we obtain the high-energy fixed point of QED$_d$ instead of the low-energy one. The associated short-distance coupling is $e^2 = \mu^{4-d} \frac{4\pi^{d/2}}{\Gamma(d/2-1)}$.

Let us first explain why we are allowed to use $\Delta_{\mu\nu} \propto \frac{\delta_{\mu\nu}}{x^2}$, without the ξ-dependent part, instead of the more general $\Delta_{\mu\nu} \propto \frac{1}{x^2}((d-2+\xi)\delta_{\mu\nu} - 2\xi x_\mu x_\nu / x^2)$ (cf. (4.3.4)). A formal proof of gauge invariance is as follows. To leading order in $1/N_f$, we need to integrate the propagator along a (flat) closed 2-manifold of the form $\gamma \times \gamma$, where γ is the support of W. Then, under the integral sign, we can replace $x_\mu x_\nu \to \frac{1}{2}\delta_{\mu\nu} x^2$, which means that $(d-2+\xi)\delta_{\mu\nu} - 2\xi x_\mu x_\nu / x^2 \to (d-2)\delta_{\mu\nu}$, and the answer is ξ-independent. A perhaps better argument is to note that, in momentum space

$$\oint_\gamma \mathrm{d}x^\mu \oint_\gamma \mathrm{d}y^\nu \Delta_{\mu\nu}(x-y) = \int_k \Delta_{\mu\nu}(k) V^\mu(\gamma, k) V^\nu(\gamma, -k) \tag{4.3.10}$$

where the eikonal factor V^μ is

$$V^\mu(\gamma, k) := \int_\gamma \mathrm{d}x^\mu \; e^{-ikx} \tag{4.3.11}$$

Then, the gauge part of (4.3.10) is proportional to $k_\mu V^\mu = \int_\gamma \mathrm{d}(e^{-ikx})$, which vanishes for a closed loop. Note that either of these arguments goes through even in the presence of a regulator, such as replacing $\frac{1}{x^2} \to \frac{\mu^2}{(\mu^2 x^2)^\alpha}$ or shifting one of the integration contours via $\gamma \to \gamma + \epsilon$. So this justifies the claim that we are allowed to simply use $\Delta_{\mu\nu} = \frac{\delta_{\mu\nu}}{x^2}$.

We begin with a circle geometry, $x = (R\cos\theta, R\sin\theta)$. Then, $\mathrm{d}x^\mu \mathrm{d}y_\mu = R^2\cos(\theta - \theta')\mathrm{d}\theta\mathrm{d}\theta'$ and so, in analytic regularization,

$$
\begin{aligned}
\log\langle W(\bigcirc)\rangle &= -\frac{1}{2}\frac{\mu^2 R^2}{(2\mu^2 R^2)^\alpha}\int_0^{2\pi}\mathrm{d}\theta\int_0^{2\pi}\mathrm{d}\theta'\frac{\cos(\theta-\theta')}{(1-\cos(\theta-\theta'))^\alpha} \\
&= -\frac{1}{2}\frac{\mu^2 R^2}{(2\mu^2 R^2)^\alpha}2\pi\left(-2^{\alpha+1}\pi\frac{\Gamma(1-2\alpha)}{\Gamma(2-\alpha)\Gamma(-\alpha)}\right)
\end{aligned}
\tag{4.3.12}
$$

Taking $\alpha \to 1$ we find $\log\langle W\rangle = \pi^2$, while $\alpha \to d/2-1$ leads to $\log\langle W\rangle = (\mu R)^{4-d}\frac{2\pi^2\Gamma(3-d)}{\Gamma(1-d/2)\Gamma(3-d/2)}$. This implies, for our large N_f QED$_d$ problem, that[10]

$$
\log\langle W(\bigcirc)\rangle = \begin{cases} \dfrac{4\pi^2 g}{(4\pi)^{d/2}\Gamma(d/2-1)} & R \gg e^{2/(d-4)} \\ e^2 R^{4-d}\dfrac{\pi^{2-d/2}\Gamma(3-d)\Gamma(d/2-1)}{2\Gamma(1-d/2)\Gamma(3-d/2)} & R \ll e^{2/(d-4)} \end{cases}
\tag{4.3.13}
$$

For $d < 4$, which is the regime where the theory is UV free and has an interesting IR fixed point, the log of the expectation value vanishes at short distances, implying that the UV defect entropy is zero. On the other hand, the long-distance answer is positive. This is not incompatible with the g-theorem [314], since here we are dealing with a bulk RG flow, not a defect one.

As a check of the result above, we note that the $\alpha \to 1$ limit of (4.3.12), when multiplied by $\frac{e^2}{4\pi^2}$, yields the well-known free Maxwell answer $\langle W(\bigcirc)\rangle = \exp(e^2/4)$.

Furthermore, if we take $d = 1$ in (the first line of) the general expression (4.3.13), we find $\log\langle W\rangle = -2/N_f$, while if we take $d = 2$ we find $\log\langle W\rangle = 0$. These agree with computations performed directly in $d = 1, 2$.

We can reuse the results above to easily get the answer for general gauge group. Say we take the Wilson line to be in a representation ρ of G; then, to tree level, the expectation

[10] The UV limit in $d = 3$ is special because R^{4-d} becomes R, which is linear and hence a counterterm. In this case one has to expand around $\alpha = d/2 - 1$ and keep the subleading term as well. The result is the usual $R\log(\mu R)$ behavior.

value the loop is simply $\mathrm{tr}_\rho[1] = \dim(\rho)$. To next order we replace $\Delta_{\mu\nu} \to \Delta_{\mu\nu}\delta^{ab}$, where a, b are adjoint indices, and we also take a trace over ρ. In other words, we replace

$$\begin{aligned}\langle aa\rangle &\to \mathrm{tr}_\rho[\langle aa\rangle] \\ &= \mathrm{tr}_\rho[t^a t^b]\delta_{ab}\langle aa\rangle_{\mathrm{QED}} \\ &= T(\rho)\dim(G)\langle aa\rangle_{\mathrm{QED}}\end{aligned} \tag{4.3.14}$$

Therefore, the expectation value for non-abelian G reads

$$\log(\langle W_\rho(\bigcirc)\rangle/\dim(\rho)) = \log\langle W(\bigcirc)\rangle_{\mathrm{QED}} \times \frac{T(\rho)\dim(G)}{\dim(\rho)T(R)} + \mathcal{O}(N_f^{-2}) \tag{4.3.15}$$

where $T(R)$ arises because the effective coupling is $g_{\mathrm{QCD}} = g_{\mathrm{QED}} \times \frac{1}{T(R)}$.

Again, if we take $d = 1$ we recover the answer derived independently in QCD_1. If we take $d = 2$, both answers vanish to order $1/N_f$. In any case, the main conclusion is that (4.3.13) admits a meaningful continuation to $d \in \mathbb{C}$.

For future reference let us sketch the same result but in point-splitting regularization, where we add a small shift to one of the integration contours. The easiest way to do this is to push the second integration off the plane, so that $x = (R\cos\theta, R\sin\theta, 0)$ and $y = (R\cos\theta', R\sin\theta', \epsilon)$. This yields

$$-\frac{1}{2}\int_0^{2\pi} \mathrm{d}\theta \int_0^{2\pi} \mathrm{d}\theta' \, \frac{R^2\cos(\theta-\theta')}{2R^2 - 2R^2\cos(\theta-\theta') + \epsilon^2} \tag{4.3.16}$$

which evaluates to $-\frac{\pi^2 R}{|\epsilon|} + \pi^2 + \mathcal{O}(\epsilon)$. The divergence is just $-\frac{\pi}{|\epsilon|}$ times the perimeter $2\pi R$, so it can be canceled by a local counterterm along the line. The finite part agrees with the analytic computation from before.

A mild complaint for this regulator is that it requires a third direction, so it doesn't work if $d < 3$. It is in fact possible to point-split while keeping the two contours on the same plane; the only way to do this, without having the contours intersect at all, is to shrink one of them by a small amount. In other words, we take $x = (R\cos\theta, R\sin\theta)$ and

$y = ((R+\epsilon)\cos\theta', (R+\epsilon)\sin\theta')$. Then,

$$
\begin{aligned}
\log\langle W(\bigcirc)\rangle &= -\frac{1}{2}\iint_0^{2\pi} \frac{R(R+\epsilon)\cos(\theta-\theta')\,\mathrm{d}\theta\,\mathrm{d}\theta'}{(R\sin\theta-(R+\epsilon)\sin\theta')^2+(R\cos\theta-(R+\epsilon)\cos\theta')^2} \\
&= -\frac{1}{2}2\pi\times\begin{cases}\frac{2\pi R^2}{2R\epsilon+\epsilon^2} & \epsilon>0 \\ -\frac{2\pi(R+\epsilon)^2}{2R\epsilon+\epsilon^2} & \epsilon<0\end{cases} \\
&= -\frac{\pi^2 R}{|\epsilon|}+\begin{cases}\frac{1}{2}\pi^2 & \epsilon>0 \\ \frac{3}{2}\pi^2 & \epsilon<0\end{cases}+\mathcal{O}(\epsilon)
\end{aligned}
\tag{4.3.17}
$$

The singularity is $-\frac{\pi^2 R}{|\epsilon|}$ as before, but the finite part appears ambiguous: it depends on whether we shrink the second contour or we expand it. This of course makes no sense, the finite part should be scheme-independent. The resolution is that a local counterterm shifts the expectation value by something proportional to the length of the line, but in this case we have two lengths, $2\pi R$ and $2\pi(R+\epsilon)$. So we split the difference and write the result as $-\frac{\pi}{2|\epsilon|}\times 2\pi(R+\epsilon/2)+\pi^2+\mathcal{O}(\epsilon)$, where we once again read the finite, scheme-independent part as π^2. (Equivalently, we can also take the symmetric limit $\lim_{\epsilon\to 0}=\frac{1}{2}(\lim_{\epsilon\to 0^+}+\lim_{\epsilon\to 0^-})$, for the same answer).

As a final comment, we remark that we found the scheme-independent part of $\langle W\rangle$ for a circular geometry to be independent of the radius R. This is of course as expected, since a circle has a single scale, and a conformal line has no scales of its own, and therefore there is no dimensionless ratio the expectation value could depend on. Below we will consider a rectangular geometry which has two scales, and we will find that $\langle W\rangle$ is a non-trivial function of their ratio. Another simple geometry with two scales is the ellipse, say with axes (a,b), for which we find $\log\langle W\rangle = -\frac{2\pi a}{|\epsilon|}E(1-b^2/a^2)+\frac{1}{2}\pi^2(b/a+a/b)+\mathcal{O}(\epsilon)$, where E is the complete elliptic integral of the second kind. The singularity is once again $-\frac{\pi}{2|\epsilon|}$ times the length of the line, and the finite part $\pi^2(a/b+b/a)$ is a non-trivial function of the dimensionless ratio a/b. For $a=b$ we recover the circle answer π^2.

We now move on to the rectangular geometry that measures the potential energy between two probe charges:

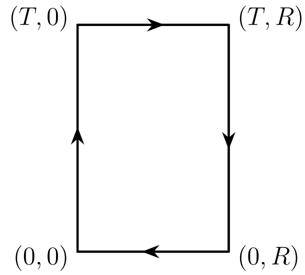

(4.3.18)

We use both regularizations. We begin with y being the straight line between $(0,0)$ and $(T,0)$, while x is the whole rectangle; we will then add the other pieces of the y path. We parametrize $y(\tau') = (\tau'(T+2\epsilon)-\epsilon, -\epsilon)$, with $\tau' \in [0,1]$, as well as

$$x(\tau) = \begin{cases} (4\tau T, 0) & 0<\tau<1/4 \\ (T, (4\tau-1)R) & 1/4<\tau<1/2 \\ ((-4\tau+3)T, R) & 1/2<\tau<3/4 \\ (0, (-4\tau+4)R) & 3/4<\tau<1 \end{cases} \tag{4.3.19}$$

Then, $\mathrm{d}x^\mu \mathrm{d}y_\mu = 4T(T+2\epsilon)(\Theta(0<\tau<1/4) - \Theta(1/2<\tau<3/4))\mathrm{d}\tau\mathrm{d}\tau'$ and so this segment contributes

$$\begin{aligned} &-2T^2\int_0^{1/4}\mathrm{d}\tau\int_0^1\mathrm{d}\tau'\frac{\mu^2}{(\mu^2T^2(4\tau-\tau')^2)^\alpha} \\ &\quad + 2T^2\int_{1/2}^{3/4}\mathrm{d}\tau\int_0^1\mathrm{d}\tau'\frac{\mu^2}{(\mu^2(T^2(-4\tau-\tau'+3)^2+R^2)^\alpha} \\ &\quad = \mu^{2(1-\alpha)}\bigg(T^2R^{-2\alpha}\,{}_2F_1(\tfrac{1}{2},\alpha;\tfrac{3}{2};-\tfrac{T^2}{R^2}) \\ &\quad + \frac{1}{2(\alpha-1)}\big[-R^{2(1-\alpha)} + (R^2+T^2)^{1-\alpha} + \tfrac{1}{1-2\alpha}T^{2(1-\alpha)}\big]\bigg) \\ &\quad = -\frac{1}{2(\alpha-1)} + 1 + \frac{T}{R}\arctan\frac{T}{R} + \frac{1}{2}\log\frac{\mu^2R^2T^2}{R^2+T^2} + \mathcal{O}(\alpha-1) \end{aligned} \tag{4.3.20}$$

in analytic regularization, and

$$
\begin{aligned}
-2T(T+2\epsilon) & \int_0^{1/4} \mathrm{d}\tau \int_0^1 \mathrm{d}\tau' \frac{1}{(4\tau T - \tau'(T+2\epsilon)+\epsilon)^2+\epsilon^2} \\
& + \int_{1/2}^{3/4} \mathrm{d}\tau \int_0^1 \mathrm{d}\tau' \frac{1}{(R+\epsilon)^2 + (T(4\tau+\tau'-3)+2\tau'\epsilon-\epsilon)^2} \\
& = -\frac{\pi T}{2|\epsilon|} + \frac{\pi T}{4R} + 1 + \frac{1}{2}\log\frac{T^2R^2}{2(T^2+R^2)\epsilon^2} \\
& + \frac{T}{2R}(\arctan(T/R) - \arctan(R/T)) + \begin{cases} -\pi/4 & \epsilon > 0 \\ +3\pi/4 & \epsilon < 0 \end{cases}
\end{aligned}
\tag{4.3.21}
$$

in point-splitting regularization.

Adding the other three segments amounts adding the same expression with $T \leftrightarrow R$, and multiplying by 2, so all in all

$$
\log\langle W(\square)\rangle = 2\frac{T}{R}\arctan\frac{T}{R} + \log\frac{\mu^2R^2T^2}{R^2+T^2} + (R \leftrightarrow T) \tag{4.3.22}
$$

for the analytic regularization approach, after absorbing the $\frac{1}{2(\alpha-1)}$ pole into a corner counterterm. The point-splitting result, after removing the $-\frac{\pi(T+R)}{|\epsilon|}$ pole into a perimeter counterterm, is in fact identical to this, thanks to standard arctan identities.

So both approaches yield the same answer, but they both introduce a dependence on the arbitrary scale μ. This dependence is somewhat artificial in that the rescaling $\mu \to \lambda\mu$ can be removed by a corner counterterm $\log(\lambda)$, so the result doesn't depend on μ in a measurable way. But at the same time it is not possible to remove this dependence, which means that the configuration breaks the $1d$ scale invariance of the line (the more precise statement is that this is a trace anomaly, see e.g. [315]). This is in fact the cusp anomalous dimension of the line, as we elaborate on below.

Note that in analytic regularization, the circle and rectangle both had no need for a perimeter counterterm. On the other hand, in point-splitting, the circle had a divergence $-\frac{\pi^2 R}{|\epsilon|}$, while the rectangle had a divergence $-\frac{\pi(T+R)}{|\epsilon|}$; these are both equal to $-\frac{\pi}{2|\epsilon|} \times$ length, so the same counterterm fixes both. This is of course as expected: for a fixed choice of scheme, we should find the same counterterm for any geometry, since counterterms are local and thus do not care about the shape of the line. In other words, if two geometries have different linear divergences, it would not be possible to fix both at the same time, and the observable would be inconsistent. It is reassuring that the circle and rectangle lead to the same counterterm, for both choices of regularization.

Note also that if we take the $T \gg R$ limit of the above, we find $V(R) = -\pi/R + \mathcal{O}(\log T)$ which, after multiplying by $\frac{e^2}{4\pi^2}$, becomes $V(R) = -\frac{e^2}{4\pi R}$, which is the usual Coulomb potential of free $4d$ Maxwell. On the other hand, for our large N_f QED$_d$ problem,

$$V(R) = -\frac{4\pi g}{(4\pi)^{d/2}\Gamma(d/2-1)}\frac{1}{R} \qquad R \gg e^{2/(d-4)} \tag{4.3.23}$$

and therefore we learn that these theories are all Coulomb-like. This is of course the only R dependence compatible with scale invariance, so this result is simply telling us that the Wilson line is conformal.

We end this discussion with a quick analysis of the cusp, which we parametrize by two segments $x = (s, 0)$ and $x = (s\cos\phi, s\sin\phi)$, where $s \in (0, \infty)$:

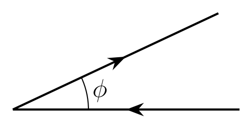

(4.3.24)

We are more cavalier than before, and simply cutoff the s integral at short and long distances; we find the same divergences as before, plus a new type, namely the cusp. This comes from the crossed terms where x is horizontal and y is oblique:

$$-\frac{1}{2} \times 2 \times \int_\infty^0 \mathrm{d}s \int_0^\infty \mathrm{d}s' \frac{\cos\phi}{(s - s'\cos\phi)^2 + (s'\sin\phi)^2} - (\text{same, with } \phi = \pi) \tag{4.3.25}$$

where we subtract the $\phi = \pi$ term so that the cusp dimension of a straight line vanishes.

We interpret s and s' as the proper times of the probe charges, and – as one often does when using Schwinger's parametrization – change variables into the "total proper time" $\tau = s + s' \in (0, \infty)$, and the "relative proper time" $q = \frac{s}{s+s'} \in (0, 1)$. The Jacobian is simply τ, so this integral simplifies to

$$\begin{aligned} &\int_\epsilon^L \frac{\mathrm{d}\tau}{\tau} \int_0^1 \mathrm{d}q \, \frac{\cos\phi}{(q-(1-q)\cos\phi)^2 + (1-q)^2\sin^2\phi} - (\cdots) \\ &= \big(1 + 2\cot(\phi)\arctan(\cot(\phi/2))\big)\log\frac{L}{\epsilon} \end{aligned} \tag{4.3.26}$$

whence $\Gamma_{\text{cusp}}(\phi) = -(1 + 2\cot(\phi)\arctan(\cot(\phi/2))) \equiv ([\phi] - \pi)\cot(\phi - \pi) - 1$, where $[\phi] = \phi$ mod 2π.

The rectangle has four cusps, each contributing a factor of

$$\big(1 + 2\cot(\phi)\arctan(\cot(\phi/2))\big)\Big|_{\phi=\pi/2} \times \log L \equiv +\log(L) \tag{4.3.27}$$

This is in agreement with our earlier computation (4.3.22), where we found $\cdots + 2\log(R^2)$.

We note that the cusp dimension above satisfies $\Gamma_{\text{cusp}}(\phi) < 0, \Gamma'_{\text{cusp}}(\phi) > 0, \Gamma''_{\text{cusp}}(\phi) < 0$, in agreement with the general analysis of [315]. For our QED_d problem, we are to multiply this function by $\frac{4g}{(4\pi)^{d/2}\Gamma(d/2-1)}$, which is positive for all $2 < d < 4$, so these inequalities are still satisfied. This is not entirely obvious, since [315] explicitly assumes unitarity, which is not present in fractional d. Of course, the loss of unitarity does not show up in any of the simple observables we look at in this paper, so it is not entirely surprising that our $\Gamma_{\text{cusp}}(\phi)$ behaves as if the theory was unitary. Indeed, as pointed out at the beginning of this subsection, to leading order in $1/N_f$ the photon propagator in QED_d has the same x dependence as the propagator of $4d$ free Maxwell, which is of course unitary. So the only non-trivial statement is that the coefficient that connects these two propagators is positive for all $2 < d < 4$.

In any case, we note that $\frac{4g}{(4\pi)^{d/2}\Gamma(d/2-1)}$ is positive for $2 < d < 4$, but actually vanishes in $d = 2, 4$. For $d = 4$ this simply reflects the fact that the "infrared fixed point" of QED_4 is essentially free. For $d = 2$, it is due to the fact that, while the Wilson line defines a conformal defect for generic d, it becomes topological in $d = 2$: it becomes a Verlinde line of $SO(\dim R)_1/G_{T(R)}$.

The factor $\frac{4g}{(4\pi)^{d/2}\Gamma(d/2-1)}$ becomes negative for $d < 2$, and the potential $V(R)$ and the cusp $\Gamma_{\text{cusp}}(\phi)$ become positive. While our general analysis should perhaps not be trusted all that much below $d < 2$ (for example, does it even make sense to talk about the cusp angle ϕ if we have fewer than two directions?), above we found that the $d \to 1$ limit of the general d formulas does give the same answer as the direct $d = 1$ computation, so let us indulge. One possible interpretation for the change of sign in $\frac{4g}{(4\pi)^{d/2}\Gamma(d/2-1)}$ is that this factor is actually the norm of the field strength $f_{\mu\nu}$, namely

$$\begin{aligned}\langle \partial_{[\rho}a_{\mu]}(x)\partial_{[\sigma}a_{\nu]}(0)\rangle &= -g\int_p e^{ipx}\frac{p_{[\sigma}\delta_{\nu][\rho}p_{\mu]}}{p^{d-2}} \\ &= \frac{16g}{(4\pi)^{d/2}\Gamma(d/2-1)}\frac{x_{[\sigma}\delta_{\nu][\rho}x_{\mu]}}{x^6}\end{aligned} \tag{4.3.28}$$

The fact that $f_{\mu\nu}$ has negative norm below $d=2$ can be understood as the statement that this field carries $d-2$ degrees of freedom, this being the dimension of the vector representation of $SO(d-2)$ (which is itself the little group of massless, helicity 1 particles in d dimensions).

4.3.2 Quarks

In this subsection we sketch the computation of $\langle\bar{\psi}(x)W\psi(0)\rangle$, with W is a straight Wilson line connecting x to 0. We again are rather brief, as we shall encounter no surprises. By conformal invariance, this correlation function is proportional to $x^{-2\Delta(\psi)}$ where, to tree level, $\Delta^{(0)}(\psi)=(d-1)/2$. Below we compute the $1/N_f$ correction to this scaling dimension.

Our goal is to isolate the log divergence in this correlation function, from whose coefficient we can read off $\Delta^{(1)}$. The log divergence is associated with scale-less integrals, and we introduce the notation

$$\mathscr{L} := \int_k \frac{1}{k^d} \equiv \frac{1}{(4\pi)^{d/2}\Gamma(d/2)}\log(\Lambda^2) \tag{4.3.29}$$

for those.

For this geometry, the eikonal factor (cf. (4.3.10)) reads

$$V^\mu(x,k) = \int_x^0 \mathrm{d}z^\mu e^{-ikz} = ix^\mu\frac{1-e^{-ikx}}{kx} \tag{4.3.30}$$

which, diagrammatically, we will denote as the insertion of an external source coupled to the photon: $\otimes\!\!\sim\!\!\sim$. Note that, unlike before, here $k_\mu V^\mu$ does not vanish, since the contour is not closed; instead, $k_\mu V^\mu = i(1-e^{-ikx})$. This will cancel the gauge dependent part of the undress correlator $\langle\bar{\psi}(x)\psi(0)\rangle$.

There are three diagrams that contribute to this two-point function to leading order; we evaluate them in turn:

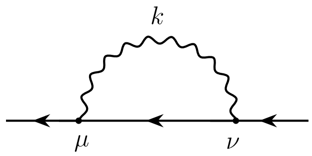

$$
\begin{aligned}
&= -\int_{pk} e^{ipx} S(p)\gamma^\mu S(p+k)\gamma^\nu S(p)\Delta_{\mu\nu}(k) \\
&= ig\int_p e^{ipx} S(p)\gamma^\mu\gamma^\alpha\left[\int_k \frac{p_\alpha + k_\alpha}{k^{d-2}(p+k)^2}(\delta_{\mu\nu} + \xi\frac{k_\mu k_\nu}{k^2})\right]\gamma^\nu S(p) \\
&= -g\left[\frac{(d-2)^2}{d} + \xi\right] S(x)\mathscr{L}
\end{aligned}
\tag{4.3.31}
$$

Next,

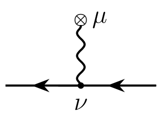

$$
\begin{aligned}
&= -\int_{pk} e^{ipx} V^\mu(x,-k) S(p)\gamma^\nu S(p+k)\Delta_{\mu\nu}(k) \\
&= g\int_p e^{ipx} S(p)\gamma^\nu\left[\int_k V^\mu(x,-k) S(p+k)\frac{1}{k^{d-2}}(\delta_{\mu\nu} + \xi\frac{k_\mu k_\nu}{k^2})\right]
\end{aligned}
\tag{4.3.32}
$$

We isolate the log divergence by focusing on the various degeneration limits. For this integral there are two: p large with $p+k$ fixed, and the other way around. These are equal to each other, so we consider one and multiply the answer by 2. For the remaining integral, we note that, by Lorentz covariance, we can write

$$
\int_k V^\mu(x,-k) S(k)\frac{1}{k^{d-2}}(\delta_{\mu\nu} + \xi\frac{k_\mu k_\nu}{k^2}) = -i(\gamma_\nu f(x^2) + x_\nu \not{x} g(x^2))
\tag{4.3.33}
$$

for some scalar functions f, g defined by

$$
\delta_{\alpha\nu} f(x^2) + x_\alpha x_\nu g(x^2) = \int_k V^\mu(x,-k)\frac{k_\alpha}{k^d}(\delta_{\mu\nu} + \xi\frac{k_\mu k_\nu}{k^2})
\tag{4.3.34}
$$

Therefore, the diagram can be simplified into

$$
\begin{aligned}
&= 2ig\int_p e^{ipx} S(p)\int_k V^\mu(x,-k)\frac{k_\mu}{k^d}(1+\xi) \\
&= 2g\int_p e^{ipx} S(p)\int_k (1 - e^{ikx})\frac{1}{k^d}(1+\xi) \\
&= 2g(1+\xi) S(x)\mathscr{L}
\end{aligned}
\tag{4.3.35}
$$

Finally, the last diagram contributing to this two-point function is

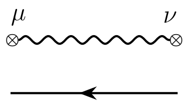

$$\begin{aligned} &= -\frac{1}{2}S(x)\int_k V^\mu(x,-k)V^\nu(x,k)\Delta_{\mu\nu}(k) \\ &= -\frac{1}{2}gS(x)\int_k V^\mu(x,-k)V^\nu(x,k)\frac{1}{k^{d-2}}(\delta_{\mu\nu}+\xi\frac{k_\mu k_\nu}{k^2}) \end{aligned} \tag{4.3.36}$$

where $1/2$ is a symmetry factor. The gauge part is straightforward, since $k_\mu V^\mu \propto 1-e^{ikx}$, which is easily integrated:

$$\begin{aligned} \int_k V^\mu(x,-k)V^\nu(x,k)\frac{1}{k^{d-2}}\xi\frac{k_\mu k_\nu}{k^2} &= \xi\int_k (1-e^{ikx})(1-e^{-ikx})\frac{1}{k^d} \\ &= 2\xi\mathscr{L} \end{aligned} \tag{4.3.37}$$

On the other hand, the physical part equals

$$-\frac{1}{2}gS(x)\int_k \frac{x^2}{(kx)^2}(1-e^{ikx})(1-e^{-ikx})\frac{1}{k^{d-2}} \tag{4.3.38}$$

In order to evaluate this integral, we define

$$h(s) := \int_k \frac{1}{(kx)^2}(1-e^{ikxs})(1-e^{-ikxs})\frac{1}{k^{d-2}} \tag{4.3.39}$$

and note that the integral we are after is $h(1)$. On the other hand, if we differentiate this twice, we find

$$h''(s) = \int_k (e^{ikxs}+e^{-ikxs})\frac{1}{k^{d-2}} \tag{4.3.40}$$

This is just (twice) the position-space scalar propagator, namely $h''(s) = \frac{8}{(4\pi)^{d/2}\Gamma(d/2-1)}\frac{1}{(sx)^2}$. Therefore, integrating twice, we derive

$$h(s) = -\frac{8\log(s)}{x^2(4\pi)^{d/2}\Gamma(d/2-1)} + c_1(x) + c_2(x)s \tag{4.3.41}$$

where c_1, c_2 are constants of integration. Furthermore, from the definition of $h(s)$, it is clear that a rescaling of s can be compensated by a rescaling of x, which means that $\log(s)$ must be accompanied by $\frac{1}{2}\log(x^2)$, with the same coefficient. Therefore, the physical part evaluates to

$$-gS(x)((2-d)\mathscr{L} + \#\Lambda|x|) \tag{4.3.42}$$

where the second term comes from $c_2(x)$. This term, proportional to the length of the line, is a perimeter counterterm, and we simply drop it. So, all in all, this diagram contributes

$$g(d-2-\xi)S(x)\mathscr{L} \tag{4.3.43}$$

Adding up all contributions, we see that the ξ-dependent part nicely cancels, while the physical parts add up to

$$gS(x)\mathscr{L} \times 4\frac{d-1}{d} \tag{4.3.44}$$

whence

$$\Delta(\psi) = \frac{d-1}{2} - g\frac{2(d-1)}{(4\pi)^{d/2}\Gamma(d/2+1)} + \mathcal{O}(g^2) \tag{4.3.45}$$

We can check this in various special cases. The anomalous dimension vanishes in $d=1$, it equals $-\frac{1}{2N_f}$ in $d=2$, $-\frac{32}{3\pi^2 N_f}$ in $d=3$, and vanishes in $d=4$. The first three agree with known low-dimensional results. The fourth simply says that our IR CFT becomes free in $4d$ which, in a rough sense, corresponds to the logarithmic running $e^2 \to 0$ in QED$_4$.

As another simple check, taking the trace of (4.3.44) gives the $\mathcal{O}(N_f^0)$ correction to the *vev* $\langle\bar\psi\psi\rangle$. This is easily seen to vanish for all d, including $d=1$, in agreement with $\langle\bar\psi\psi\rangle = \frac{1}{2}N_f$ being tree-level exact in $d=1$.

Furthermore, the general d answer (4.3.45) also agrees with [316].

Finally, we describe the generalization to non-abelian gauge groups. The first change is that the effective coupling becomes $g_{\rm QCD} = g_{\rm QED} \times \frac{1}{T(R)}$. Furthermore, the gluon propagator becomes $\Delta_{\rm QCD} = \Delta_{\rm QED}\delta^{ab}$, where a, b are color indices, and the vertex acquires a factor of t^a_R. This gives an extra factor of $(t^a t^a)_{ij} = T(R)\frac{\dim(G)}{\dim(R)}\delta_{ij}$. Thus the final result in QCD is equal to the QED one multiplied by $\frac{\dim(G)}{\dim(R)}$, in agreement with known results in integer dimensions.

4.3.3 Mesons

In this subsection we study bilinear operators of the form $\bar\psi\Gamma\psi$, where Γ is some matrix in spinor-flavor space. In particular, we will be interested in the correlation function $\langle\bar\psi\Gamma\psi\,\bar\psi\bar\Gamma\psi\rangle$

where $\Gamma, \bar{\Gamma}$ are in principle distinct matrices, assumed hermitian for concreteness. We begin with $G = U(1)$, and generalize to QCD afterwards.

To tree level this correlator is given by

$$\langle \bar{\psi}\Gamma\psi(p)\, \bar{\psi}\bar{\Gamma}\psi(-p)\rangle = \tag{4.3.46}$$

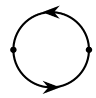

$+$

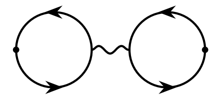

The first diagram will show up quite often, so we give it a name: $M(\Gamma, \bar{\Gamma})$. It evaluates to

$$\begin{aligned} M(\Gamma, \bar{\Gamma}) &:= -\int_q \mathrm{tr}[S(q)\Gamma S(q+p)\bar{\Gamma}] \\ &= \frac{1}{g}\frac{1}{2(d-2)}\frac{\mathrm{tr}[\gamma^\alpha\Gamma\gamma^\beta\bar{\Gamma}]}{\mathrm{tr}[1]}\frac{-\delta_{\alpha\beta}p^2 + (2-d)p_\alpha p_\beta}{p^{4-d}} \end{aligned} \tag{4.3.47}$$

In this notation, the second diagram is equal to

$$-M(\Gamma, \gamma^\mu)\Delta_{\mu\nu}(p)M(\gamma^\nu, \bar{\Gamma}) \tag{4.3.48}$$

We note that

$$M(\Gamma, \gamma^\mu) = \frac{1}{g}\frac{1}{\mathrm{tr}[1]}\frac{\mathrm{tr}[\Gamma\gamma^\mu]p^2 - p^\mu\,\mathrm{tr}[\Gamma \not{p}]}{p^{4-d}} \tag{4.3.49}$$

which vanishes when contracted with p_μ, i.e., this structure is transverse. This implies that the ξ-dependent part in $M(\Gamma, \gamma^\mu)\Delta_{\mu\nu}(p)$ drops out, and the correlation function is gauge invariant, as one would expect. So to summarize, to tree level this correlation function is

$$\langle \bar{\psi}\Gamma\psi(p)\, \bar{\psi}\bar{\Gamma}\psi(-p)\rangle = M(\Gamma, \bar{\Gamma}) - \frac{g}{p^{d-2}}M(\Gamma, \gamma^\mu)M(\gamma_\mu, \bar{\Gamma}) \tag{4.3.50}$$

Let us evaluate this explicitly for a few special cases. First, when $\Gamma = \gamma^\rho$, the corresponding bilinear is the gauge current $\bar{\psi}\gamma^\rho\psi$; for this, we find

$$\langle \bar{\psi}\gamma^\rho\psi\, \bar{\psi}\bar{\Gamma}\psi\rangle = M(\gamma^\rho, \bar{\Gamma}) - \frac{g}{p^{d-2}}M(\gamma^\rho, \gamma^\mu)M(\gamma_\mu, \bar{\Gamma}) \tag{4.3.51}$$

which, using (4.3.49), becomes

$$\begin{aligned} &= M(\gamma^\rho, \bar{\Gamma}) - \frac{\delta^{\rho\mu}p^2 - p^\mu p^\rho}{p^2}M(\gamma_\mu, \bar{\Gamma}) \\ &\equiv 0 \end{aligned} \tag{4.3.52}$$

Therefore, we learn that the correlation function $\langle\bar\psi\gamma^\rho\psi\,\bar\psi\bar\Gamma\psi\rangle$ vanishes for any choice of $\bar\Gamma$. This is in fact the expected result: the gauge current $\bar\psi\gamma^\rho\psi$ is a null operator, since the equations of motion imply

$$\frac{1}{e^2}\partial_\mu f^{\mu\nu}=\bar\psi\gamma^\nu\psi \tag{4.3.53}$$

which becomes $\bar\psi\gamma^\nu\psi\equiv 0$ in the low energy limit $e^2\to\infty$. (If we were to repeat the computation of $\langle\bar\psi\gamma^\rho\psi\,\bar\psi\bar\Gamma\psi\rangle$ using the full photon propagator $\frac{e^2\delta_{\mu\nu}}{p^2(1-e^2\Pi)}$ instead of the low energy one $-\frac{\delta_{\mu\nu}}{p^2\Pi}$, we would find that the correlator decays exponentially $\langle\bar\psi\gamma^\rho\psi(x)(\cdots)\rangle\sim\exp(-\mu|x|)$, where $\mu\sim(N_fe^2)^{1/(4-d)}$ with e the short-distance dimensionful coupling. Therefore, the gauge current creates the higher-d analogue of the Coleman-Schwinger boson; it defines a massive operator and it decouples in the low energy effective theory).

Let us now consider $\Gamma=\bar\Gamma=1$. Then, we find

$$\langle\bar\psi\psi(p)\,\bar\psi\psi(-p)\rangle=M(1,1)-\frac{g}{p^{d-2}}M(1,\gamma^\mu)M(\gamma_\mu,1) \tag{4.3.54}$$

which, using (4.3.49), becomes

$$\langle\bar\psi\psi(p)\,\bar\psi\psi(-p)\rangle=-\frac{1}{g}\frac{d-1}{d-2}\frac{1}{p^{2-d}}-\frac{1}{g}\frac{1}{\operatorname{tr}[1]^2}\frac{1}{p^{4-d}}(\operatorname{tr}[\gamma_\mu]\operatorname{tr}[\gamma^\mu]p^2-p^\mu p^\nu\operatorname{tr}[\gamma_\mu]\operatorname{tr}[\gamma_\nu]) \tag{4.3.55}$$

From the p scaling we read off $\Delta^{(0)}=d-1$, as expected. But we also encounter the usual $\operatorname{tr}[\gamma_\mu]$ issue. At this point we could just declare that only $\Delta^{(0)}$ is meaningful, and the overall coefficient is scheme-dependent anyway, so it doesn't really matter if we fail to analytically continue it. But in order to compute $\Delta^{(1)}$ we will have to divide the $\mathcal{O}(g^0)$ result by this $\mathcal{O}(g^{-1})$ one, and therefore we cannot really sweep this issue under the rug. Perhaps more importantly, unless we manage to simplify the factor $p^\mu p^\nu$ into $p^2\delta^{\mu\nu}$, the expression above seems to be in tension with Lorentz invariance, which requires the correlator of scalar operators to be a function of p^2 only.

The simplest way to deal with this awkward structure is to note that, for integer d, the trace $\operatorname{tr}[\gamma_\mu]$ is only non-zero when $d=1$. But when $d=1$, the two terms in $\operatorname{tr}[\gamma_\mu]\operatorname{tr}[\gamma^\mu]p^2-p^\mu p^\nu\operatorname{tr}[\gamma_\mu]\operatorname{tr}[\gamma_\nu]$ are actually equal to each other, and they cancel each other out. Therefore, this structure vanishes for all $d\in\mathbb{N}$, and the correct analytic continuation is that it vanishes for all $d\in\mathbb{C}$.

If we insist that γ_μ must make sense at fractional d, then we can reach the same conclusion via a more elaborate argument. In this case, we need the formal identity (4.2.22) (namely $\mathrm{tr}[\gamma_\rho]\delta_{\mu\nu} = \mathrm{tr}[\gamma_\mu]\delta_{\nu\rho} = \mathrm{tr}[\gamma_\nu]\delta_{\mu\rho}$). Contracting this identity with $\mathrm{tr}[\gamma_\mu]$ yields $\mathrm{tr}[\gamma_\rho]\,\mathrm{tr}[\gamma_\nu] = \mathrm{tr}[\gamma_\mu]\,\mathrm{tr}[\gamma^\mu]\delta_{\nu\rho}$, which again implies that the two terms $\mathrm{tr}[\gamma_\mu]\,\mathrm{tr}[\gamma^\mu]p^2$ and $p^\mu p^\nu\,\mathrm{tr}[\gamma_\mu]\,\mathrm{tr}[\gamma_\nu]$ are equal to each other.

Whatever argument one likes best, the end result is very simple:

$$\langle \bar\psi\psi(p)\,\bar\psi\psi(-p)\rangle = -\frac{1}{g}\frac{d-1}{d-2}\frac{1}{p^{2-d}} \tag{4.3.56}$$

Let us now consider the first non-trivial $1/N_f$ correction. This is given by the diagrams

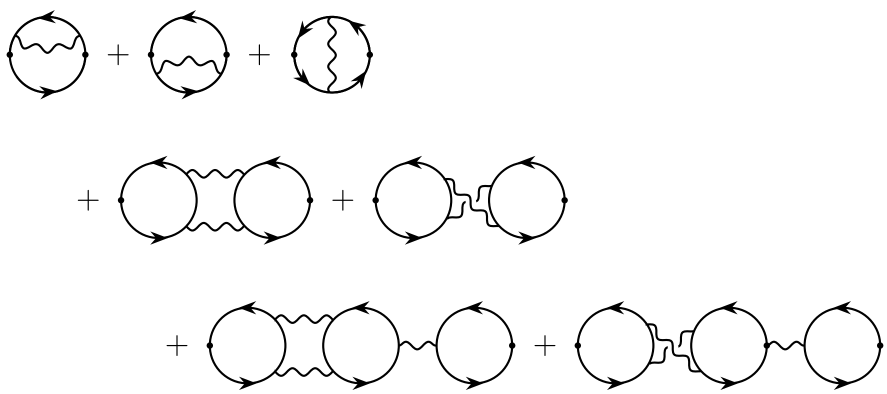

(4.3.57)

We will call these three lines the "one-loop", "two-loop", and "three-loop" diagrams, respectively (even though they are all of order $\mathcal{O}(N_f^0)$).

Our task is to isolate the log divergence in these Feynman integrals. In particular, logs are associated with scale-less integrals, and we denote those by

$$\mathscr{L} := \int_k \frac{1}{k^d} \equiv \frac{1}{(4\pi)^{d/2}\Gamma(d/2)}\log(\Lambda^2) \tag{4.3.58}$$

Let us go ahead and evaluate (4.3.57). The first and second one-loop diagrams are the simplest: they are equal to each other, and also almost identical to the trace of (4.3.31). Specifically, they both equal

$$\begin{aligned} -\int_q \mathrm{tr}[(4.3.31)\bar\Gamma S(q+p)\Gamma] &= g\left[\frac{(d-2)^2}{d}+\xi\right]\mathscr{L}\int_q \mathrm{tr}[S(q)\bar\Gamma S(q+p)\Gamma] \\ &= -g\left[\frac{(d-2)^2}{d}+\xi\right]\mathscr{L} M(\Gamma,\bar\Gamma) \end{aligned} \tag{4.3.59}$$

The third one-loop diagram is also relatively straightforward: it equals

$$\int_{qk} \operatorname{tr}[\Gamma S(q)\gamma^\mu S(q+k)\bar{\Gamma} S(q+k+p)\gamma^\nu S(q+p)]\Delta_{\mu\nu}(k) \tag{4.3.60}$$

We can extract the log divergence by looking at the limit $p \to 0$; we can do this in two ways, either we set $S(q+k+p) \to S(q+k)$ or $S(q+p) \to S(q)$. Adding up these two singularities, we find

$$\frac{g\mathscr{L}}{d} M(\gamma^\mu\gamma^\alpha\bar{\Gamma}\gamma_\alpha\gamma_\mu, \Gamma) + g\mathscr{L}\xi M(\bar{\Gamma}, \Gamma) + (\Gamma \leftrightarrow \bar{\Gamma}) \tag{4.3.61}$$

The one-loop diagrams, after cutting open the photon line, determine the tree-level value of the four-point function $\langle a_\mu\, a_\nu\, \bar{\psi}\Gamma\psi\, \bar{\psi}\bar{\Gamma}\psi\rangle$. Therefore, they should be gauge invariant by themselves. And indeed, adding up twice (4.3.59) (for the first two diagrams) plus (4.3.61) (for the third), the ξ-dependent factors cancel out, as required.

Next, we evaluate the two-loop diagrams. As a useful first step, let us cut open the photon lines and focus on the left half of these diagrams, i.e., let us compute the three-point function $\langle a_\mu\, a_\nu\, \bar{\psi}\Gamma\psi\rangle$, as given by the diagrams

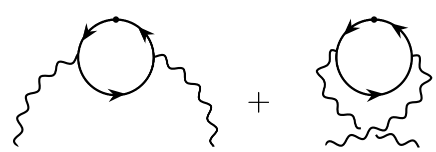

(4.3.62)

These evaluate to

$$\int_q \operatorname{tr}[S(q+p)\Gamma S(q)\gamma^\mu S(q+k+p)\gamma^\nu] + \begin{pmatrix} \mu \leftrightarrow \nu \\ k \leftrightarrow -k-p \end{pmatrix} \tag{4.3.63}$$

This integral is given by some complicated function of the dimensionless ratio p^2/k^2; we will consider the limit $p^2 \ll k^2$, in which case we can evaluate the integral analytically:

$$= -\frac{2i}{g}\frac{(d-1)(d-4)}{d-2}\frac{1}{k^{4-d}}\frac{\operatorname{tr}[\Gamma\gamma^{[\mu}\not{k}\gamma^{\nu]}]}{\operatorname{tr}[1]}(1+\mathcal{O}(p^2/k^2)) \tag{4.3.64}$$

Note that this vanishes when contracted with k_μ, as required by gauge invariance. (We also mention that, being a three-point function, the full p^2/k^2 dependence is determined from this expression and the general constraints of conformal invariance; this dependence is somewhat obscured in momentum space, and we will not need it anyway, so this limit $p^2 \ll k^2$ is enough for our purposes.)

We can now evaluate the two-loop diagrams:

$$\begin{aligned}\int_{qk\ell} &\mathrm{tr}[S(q+p)\Gamma S(q)\gamma^\mu S(q+p+k)\gamma^\nu] \\ &\times \mathrm{tr}[S(\ell+p)\gamma^\sigma S(k+p+\ell)\gamma^\rho S(\ell)\bar{\Gamma}] \\ &\times \Delta_{\mu\rho}(k+p)\Delta_{\nu\sigma}(k) + \text{cross-channel}\end{aligned} \tag{4.3.65}$$

As before, we isolate the log divergence by looking at the limit $p \to 0$; we can do this in either of the first two lines. When we take $p = 0$, say, in the first line, we end up with the same integral as in (4.3.64). Then, the fact that that integral is transverse means that these two diagrams add up to something ξ-independent as well.

Plugging (4.3.64) into our two-loop integral, we find

$$-\frac{2ig}{\mathrm{tr}[1]}\frac{(d-1)(d-4)}{d-2}\int_{k\ell}\frac{\mathrm{tr}[\Gamma\gamma^{[\mu}\not{k}\gamma^{\nu]}]}{k^d}\,\mathrm{tr}[S(\ell+p)\gamma_\nu S(k+p+\ell)\gamma_\mu S(\ell)\bar{\Gamma}] + (\Gamma \leftrightarrow \bar{\Gamma}) \tag{4.3.66}$$

The k integral is now elementary:

$$\begin{aligned}= \frac{2g\mathscr{L}}{\mathrm{tr}[1]}\frac{(d-1)(d-4)}{d(d-2)}&(\mathrm{tr}[\Gamma\gamma^\alpha\gamma^{[\mu}\gamma^{\nu]}] - \delta^{\mu\alpha}\,\mathrm{tr}[\Gamma\gamma^\nu] + \delta^{\nu\alpha}\,\mathrm{tr}[\Gamma\gamma^\mu]) \\ &\int_\ell \mathrm{tr}[S(\ell+p)\gamma_\nu\gamma_\alpha\gamma_\mu S(\ell)\bar{\Gamma}] + (\Gamma \leftrightarrow \bar{\Gamma})\end{aligned} \tag{4.3.67}$$

which simplifies to

$$= -\frac{2g\mathscr{L}}{\mathrm{tr}[1]}\frac{(d-1)(d-4)}{d(d-2)}\,\mathrm{tr}[\Gamma\gamma^{\alpha\mu\nu}]M(\bar{\Gamma}, \gamma_{\alpha\mu\nu}) + (\Gamma \leftrightarrow \bar{\Gamma}) \tag{4.3.68}$$

Finally, we evaluate the three-loop diagrams. These are actually the easiest: the left side of these diagrams is identical to the two-loop diagrams we just computed, with $\bar{\Gamma} \to \gamma^\rho$, and the right side of these diagrams is $\Delta_{\rho\sigma}M(\gamma^\sigma, \bar{\Gamma})$. But the two-loop diagrams (4.3.68) are easily seen to vanish when we replace $\bar{\Gamma} \to \gamma^\rho$, since both $\mathrm{tr}[\bar{\Gamma}\gamma^{\alpha\mu\nu}]$ and $M(\bar{\Gamma}, \gamma_{\alpha\mu\nu})$ vanish when we perform this replacement. Therefore, the three-loop diagrams are zero. (One can reach this same conclusion from charge-conjugation symmetry.)

To summarize, the first non-trivial correction to the $\langle \bar{\psi}\Gamma\psi\,\bar{\psi}\bar{\Gamma}\psi\rangle$ correlation function is

$$\begin{aligned}\frac{g\mathscr{L}}{d}\Bigg(&-(d-2)^2 M(\Gamma, \bar{\Gamma}) + M(\gamma^\mu\gamma^\alpha\bar{\Gamma}\gamma_\alpha\gamma_\mu, \Gamma) \\ &- \frac{2}{\mathrm{tr}[1]}\frac{(d-1)(d-4)}{(d-2)}\,\mathrm{tr}[\Gamma\gamma^{\alpha\mu\nu}]M(\bar{\Gamma}, \gamma_{\alpha\mu\nu})\Bigg) + (\Gamma \leftrightarrow \bar{\Gamma})\end{aligned} \tag{4.3.69}$$

As mentioned earlier, this should vanish if any of the insertions is a gauge current, i.e., if, say, $\Gamma = \gamma^\rho$. And indeed, for this choice of Γ the first term is easily seen to cancel against the second, while the third vanishes on its own.

Let us now take $\Gamma = \bar{\Gamma} = 1$. Then, we find

$$\begin{aligned}\frac{4(d-1)g\mathscr{L}}{d}&\left(2M(1,1) + \frac{1}{\mathrm{tr}[1]}\frac{d-4}{d-2}\,\mathrm{tr}[\gamma^{\alpha\mu\nu}]M(1,\gamma_{\alpha\nu\mu})\right)\\ &= -\frac{4(d-1)\mathscr{L}}{d}\frac{d-1}{d-2}\frac{1}{p^{2-d}}\left(2 - \frac{d-4}{d-2}\frac{\mathrm{tr}[\gamma^{\alpha\mu\nu}]\,\mathrm{tr}[\gamma_{\alpha\mu\nu}]}{\mathrm{tr}[1]^2}\right)\end{aligned} \tag{4.3.70}$$

Adding the tree-level result (4.3.56) to the one-loop result (4.3.70), we conclude that

$$\langle\bar{\psi}\psi(p)\,\bar{\psi}\psi(-p)\rangle \propto 1 + \frac{4(d-1)g\mathscr{L}}{d}\left(2 - \frac{d-4}{d-2}\frac{\mathrm{tr}[\gamma^{\alpha\mu\nu}]\,\mathrm{tr}[\gamma_{\alpha\mu\nu}]}{\mathrm{tr}[1]^2}\right) + \mathcal{O}(g^2) \tag{4.3.71}$$

from where we read off $\Delta^{(1)}$ as

$$\Delta^{(1)}(\bar{\psi}\psi) = -\frac{g}{(4\pi)^{d/2}\Gamma(d/2)}\frac{4(d-1)}{d}\left(2 - \frac{d-4}{d-2}\frac{\mathrm{tr}[\gamma^{\alpha\mu\nu}]\,\mathrm{tr}[\gamma_{\alpha\mu\nu}]}{\mathrm{tr}[1]^2}\right) \tag{4.3.72}$$

As a check, let us consider a few special cases of this. If $d = 1$, we get $\Delta^{(1)} = 0$. If $d = 2$, we get $\Delta^{(1)} = -1/N_f$. If $d = 3$, we use $\frac{\mathrm{tr}[\gamma^{\alpha\mu\nu}]\,\mathrm{tr}[\gamma_{\alpha\mu\nu}]}{\mathrm{tr}[1]^2} = -3!$ to get $\Delta^{(1)} = 128/3\pi^2 N_f$. These agree with known results in integer dimensions. If $d = 4$ we once again get $\Delta^{(1)} = 0$, as expected.

Before we discuss the result above more thoroughly, let us quickly mention the non-abelian case. As in previous subsections, all diagrams considered here stay the same, and we just multiply by the usual color factor $\dim(G)/\dim(R)$. The only exception is that the gluonic line in (4.3.46) acquires corrections due to ghosts and self-interactions, which contribute to order $\mathcal{O}(N_f^0)$. But as we argued below (4.3.55), this diagram does not contribute to $\bar{\psi}\psi$, so this does not affect our analysis above. Taking our QED result and multiplying by $\dim(G)/\dim(R)$ matches the $d = 1, 2, 3$ expectations.

How should we think of (4.3.72) at fractional d? If we believe equation (4.2.23) for fractional d, and thus also its implication that $(d-3)\,\mathrm{tr}[\gamma_{\alpha\mu\nu}] \equiv 0$, then we would conclude that the second term is exactly zero for all $d \neq 3$, and this scaling dimension is discontinuous there.

This conclusion is not actually precise enough. The correct interpretation of (4.3.72) for $d \in \mathbb{C}$ requires us to think about (a regularized version of) $\mathrm{Rep}(Pin(\infty))$ more carefully. Before we do that, we would like to mention the more naive approach which, while ultimately not well-defined, yields some amusing results.

For the naive approach, we assume that γ^μ makes sense for $d \in \mathbb{C}$, and that its various traces are non-zero, analytic functions of d. If this is the case, we must reckon with the extraneous operators in (4.2.24); these are formally scalars, and have the same tree-level scaling dimension as $\bar\psi\psi$, and therefore we must solve a (infinite-dimensional) degenerate perturbation theory problem. We don't think this is the correct perspective, and therefore we won't dwell on this too much. But as an illustration, let us truncate the extraneous operators to the subset $\{\bar\psi\psi, \mathrm{tr}[\gamma_{\rho\sigma\tau}]\bar\psi\gamma^{\rho\sigma\tau}\psi\}$. Now, take the general formula (4.3.69) and plug in $\Gamma = \bar\Gamma = 1 + \chi\,\mathrm{tr}[\gamma_{\rho\sigma\tau}]\gamma^{\rho\sigma\tau}$ for some coefficient χ, to be chosen below. Then, one finds

$$\begin{aligned}\langle\bar\psi\Gamma\psi(p)\,\bar\psi\bar\Gamma\psi(-p)\rangle = M(\Gamma,\bar\Gamma) - \frac{4g\mathscr{L}}{d}\Bigg((d-4)\left\{4 + \frac{\chi^{-1} - 6\,\mathrm{tr}[1]}{\mathrm{tr}[1]}\frac{d-1}{d-2}\right\}M(\bar\Gamma,\Gamma) \\ - \left\{6(d-3) + \frac{\chi^{-1} - 6\,\mathrm{tr}[1]}{\mathrm{tr}[1]}\frac{(d-1)(d-4)}{(d-2)}\right\}M(1,\Gamma)\Bigg)\end{aligned} \tag{4.3.73}$$

The point of (4.3.73) is the following: if we choose the coefficient χ such that the term proportional to $M(1,\Gamma)$ vanishes, namely

$$\chi^{-1} \equiv -\frac{12}{(d-4)(d-1)}\,\mathrm{tr}[1] \tag{4.3.74}$$

then the two-point function becomes

$$\langle\bar\psi\Gamma\psi(p)\,\bar\psi\bar\Gamma\psi(-p)\rangle = M(\Gamma,\bar\Gamma)\left(1 + \frac{8(d-1)g\mathscr{L}}{d} + \mathcal{O}(g^2)\right) \tag{4.3.75}$$

from which we can read off $\Delta^{(1)}$ as

$$\Delta^{(1)}\big(\bar\psi(1+\chi\,\mathrm{tr}[\gamma_{\rho\sigma\tau}]\gamma^{\rho\sigma\tau})\psi\big) = -\frac{8(d-1)g}{d(4\pi)^{d/2}\Gamma(d/2)} \tag{4.3.76}$$

This is now analytic in d. But if we take $d = 3$, we get $-64/3\pi^2 N_f$, instead of the correct answer $128/3\pi^2 N_f$. The reason for this is that, if we take $d = 3$, the operator in parentheses in (4.3.76) actually vanishes. Indeed, in $d=3$ one has $\mathrm{tr}[\gamma_{\rho\sigma\tau}]\gamma^{\rho\sigma\tau} = -6\,\mathrm{tr}[1]$, and therefore

$$\left(-\frac{12}{(d-4)(d-1)}\,\mathrm{tr}[1]\right)^{-1} \mathrm{tr}[\gamma_{\rho\sigma\tau}]\gamma^{\rho\sigma\tau} \xrightarrow{d\to 3} -1 \tag{4.3.77}$$

So in this approach, we would conclude that we either work with the operator $\bar\psi\psi$, whose scaling dimension is discontinuous at $d=3$, or with an operator $\bar\psi(1+\chi\,\mathrm{tr}[\gamma_{\rho\sigma\tau}]\gamma^{\rho\sigma\tau})\psi$ whose dimension is analytic in d, but the operator itself is discontinuous, and it becomes null at $d=3$. Furthermore, there is no scalar operator in QED$_3$ with dimension $-64/3\pi^2 N_f$, so the formula (4.3.76) does not match anything in the physical theory[11]. This is reminiscent of various results in the literature, where one observes that continuous families of CFTs, when particularized to concrete values of the parameter, appear to contain operators that are not present if one began with that choice of the parameter, see e.g. [223, 226, 227] for recent examples.

We now explain what we believe is a more fruitful perspective – this being that one should be working in "Rep($Pin(\infty)$)". In short, we will try to work with *stable* quantities, namely we will ignore low d exceptions and only use formulas that are correct for *all* sufficiently large $d \in \mathbb{N}$. In particular, all traces over the even part of the Clifford algebra are stable, while the traces over the odd part will be replaced by their stable limit, i.e., they will be declared to be zero. This last prescription is correct at large enough d, but wrong at small $d \in \mathbb{N}$, and therefore we will have to fix the low rank exceptions by hand, in a systematic way.

Note that declaring that odd traces are zero is formally equivalent, as we did in the discussion of $\bar\psi(1+\chi\,\mathrm{tr}[\gamma_{\mu\nu\sigma}]\gamma^{\mu\nu\sigma})\psi$, to adding suitable extraneous operators with coefficients chosen so that these traces cancel out. The notion of a direct limit makes this precise.

In any event, once we declare that all traces with an odd number of gammas vanish, we

[11]Intriguingly, there is one bilinear in QED$_3$ with this scaling dimension: the adjoint scalar $\bar\psi_i\psi^j$ − trace, which has $\Delta^{(1)} = -64/3\pi^2$ [317, 318]. This is not a flavor singlet, so this operator is distinct from our $\bar\psi\psi$. It is not clear to us if this is just a coincidence, but we do mention that, as explained around (4.2.20), the notion of flavor quantum numbers is somewhat ambiguous in fractional dimension, so it is conceivable that the singlet and the adjoint get mixed up somehow. It would be interesting to study the interplay between flavor symmetries and analytic continuation of d more carefully in the future.

can easily write down expressions for scaling dimensions that are analytic in d. The issue is that these formulas will yield the wrong answer for small d, as these expressions are missing the contribution of these traces that we set to zero by hand. The obvious question is whether we can harmonize the two approaches and write down observables that are both analytic in d and correct for all $d \in \mathbb{N}$, and not just for large enough d.

A hint toward realizing this goal is to notice that $\bar{\psi}\gamma_{\mu_1\cdots\mu_n}\psi$ is a rank-n anti-symmetric tensor only *generically*, but not always. For example, $\bar{\psi}\gamma_{\mu_1\mu_2\mu_3}\psi$ is actually a scalar when $d = 3$. More generally, the low-rank exceptions where $\mathrm{tr}[\gamma_{\mu_1\cdots\mu_n}]$ is non-zero are precisely the situations where these fermion bilinars are actually scalars.

This means that if we want to understand the scalar operator $\bar{\psi}\psi$ at low d, we must also consider the higher-rank forms $\bar{\psi}\gamma_{\mu_1\cdots\mu_n}\psi$ as well, since the latter are sometimes scalars too. In a formal sense, in fractional d we must allow for something like mixing of Lorentz tensors of different spin, since at exceptional values of d, these representations become isomorphic.

So, with this insight in mind, let us compute $\Delta(\bar{\psi}\gamma_{\mu_1\cdots\mu_n}\psi)$ to leading order in $1/N_f$. For this we can just reuse our general formulas (4.3.50), (4.3.69) and simply plug in $\Gamma = \bar{\Gamma} = \gamma_{\mu_1\cdots\mu_n}$. For generic d these formulas will involve, much like in the case of $\bar{\psi}\psi$, traces of an odd number of gammas. The stable limit of these dimensions is easily worked out, the answer being

$$\begin{aligned}
\widehat{\Delta}(\bar{\psi}\psi) &= 1 - \frac{8(d-1)}{d}\frac{g}{(4\pi)^{d/2}\Gamma(d/2)} \\
\widehat{\Delta}(\bar{\psi}\gamma_\mu\psi) &= 0 \\
\widehat{\Delta}(\bar{\psi}\gamma_{\mu_1\mu_2}\psi) &= 1 + \frac{8(d-3)}{d}\frac{g}{(4\pi)^{d/2}\Gamma(d/2)} \\
\widehat{\Delta}(\bar{\psi}\gamma_{\mu_1\mu_2\mu_3}\psi) &= 1 - \frac{8(d-4)(d+1)}{d(d-2)}\frac{g}{(4\pi)^{d/2}\Gamma(d/2)}
\end{aligned} \tag{4.3.78}$$

etc. Here, the hat means that this scaling dimension refers to the direct limit $d \to \infty$, i.e., these expressions are only correct for large enough d, and they fail at small $d \in \mathbb{N}$, since they ignore traces that are actually non-zero sometimes. The vanishing of $\widehat{\Delta}(\bar{\psi}\gamma_\mu\psi)$ simply reflects the fact that this bilinear is the gauge current and hence a null operator. We will forget about this bilinear from now on.

As a quick check of the result above note that, if we take $d = 4 - 2\epsilon$ and expand at small ϵ, we find

$$\begin{aligned}
\widehat{\Delta}(\bar\psi\psi) &= 3 - 2\epsilon + \frac{1}{\mathrm{tr}[1]}\left(-18\epsilon + 15\epsilon^2 + \tfrac{35}{2}\epsilon^3 + (\tfrac{83}{4} - 36\zeta(3))\epsilon^4 + \cdots\right) \\
\widehat{\Delta}(\bar\psi\gamma_{\mu_1\mu_2}\psi) &= 3 - 2\epsilon + \frac{1}{\mathrm{tr}[1]}\left(6\epsilon - 13\epsilon^2 - \tfrac{9}{2}\epsilon^3 + (\tfrac{7}{4} + 12\zeta(3))\epsilon^4 + \cdots\right) \\
\widehat{\Delta}(\bar\psi\gamma_{\mu_1\mu_2\mu_3}\psi) &= 3 - 2\epsilon + \frac{1}{\mathrm{tr}[1]}\left(30\epsilon^2 + 13\epsilon^3 - \tfrac{35}{2}\epsilon^4 + \cdots\right)
\end{aligned} \tag{4.3.79}$$

in perfect agreement with the corresponding ϵ expansion. The reason these two computations match is that the ϵ expansion of [309] uses the 't Hooft-Veltman prescription that is adapted to a neighborhood of $d = 4$, in which traces with an odd number of gammas do vanish.

The key point of (4.3.78) is the following. If we take $\widehat{\Delta}(\bar\psi\psi)$ and plug in $d = 3$, we find $1 - \frac{64}{3\pi^2 N_f}$, which differs from the correct answer as computed directly in $d = 3$, namely $1 + \frac{128}{3\pi^2 N_f}$. On the other hand, in $d = 3$ the operator $\bar\psi\gamma_{\mu_1\mu_2\mu_3}\psi$ is a scalar and, if we take $\widehat{\Delta}(\bar\psi\gamma_{\mu_1\mu_2\mu_3}\psi)$ and plug in $d = 3$, we do get the correct answer, i.e., $1 + \frac{128}{3\pi^2 N_f}$. That being said, the formula for $\widehat{\Delta}(\bar\psi\gamma_{\mu_1\mu_2\mu_3}\psi)$ gives the wrong answer for $d = 2$, while the formula for $\widehat{\Delta}(\bar\psi\psi)$ gives the correct answer in this dimension. So neither $\widehat{\Delta}(\bar\psi\psi)$ nor $\widehat{\Delta}(\bar\psi\gamma_{\mu_1\mu_2\mu_3}\psi)$ matches the honest $\Delta(\bar\psi\psi)$ for all $d \in \mathbb{N}$, but they do each give the correct answer for some specific $d \in \mathbb{N}$. The graph on page 107 plots the functions (4.3.78).

To leading order in $1/N_f$ the operator $\bar\psi\psi$ only picks up the trace $\mathrm{tr}[\gamma_{\mu_1\mu_2\mu_3}]$, which is why we find one extra branch adapted to $d = 3$. To higher orders in $1/N_f$ one finds higher odd traces $\mathrm{tr}[\gamma_{\mu_1\cdots\mu_n}]$, and therefore there are infinitely many branches for $\Delta(\bar\psi\psi)$, each adapted to a neighborhood of a given odd d. The analytic continuation of d for a generic QFT does not live on $\mathbb{C}$, but rather on some infinite cover thereof; only on such cover are observables truly analytic. It would be interesting to try and make this statement mathematically rigorous, especially in relation to analytic continuation of other discrete parameters, like the number of colors in large N_c gauge theories.

An important aspect that should be considered more carefully is that the factor of $\frac{g}{(4\pi)^{d/2}\Gamma(d/2)}$ in (4.3.78) is $\sim \frac{2^d}{\mathrm{tr}[1]}\sin(\pi d/2)\mathcal{O}(1/\sqrt{d})$ at large d. This grows with d and therefore the $\Delta^{(1)}$ correction is larger than the tree-level result $\Delta^{(0)}$ for sufficiently large d, and the large-N_f expansion breaks down. In other words, our result for $\Delta(\bar\psi\psi)$ is only reliable in the limit $2^{\lfloor d/2\rfloor}N_f \gg 2^d$. This puts any notion of uniqueness into question since, as we argued, analytic continuation can only possibly be unique if we impose "nice behavior" at $d\to\infty$. For fixed N_f, the inequality $2^{\lfloor d/2\rfloor}N_f \gg 2^d$ is always disobeyed for sufficiently large d, and therefore it is impossible to establish whether our result is unique or not. It appears to us that, ultimately, the topic of uniqueness in analytic continuation of QFTs can only be addressed in non-perturbative settings.

4.4 QED$_d$ Gross–Neveu–Yukawa model at large N_f

We now add a Gross–Neveu–Yukawa interaction to large-N_f QED$_d$, as studied in the previous section. The purpose is to understand how the branch structure discussed above is modified by the additional interaction. We consider the Euclidean action [319, 320]

$$\mathcal{L} = \sum_{i=1}^{N_f}\left[-\bar\psi_i\gamma^\mu(\partial_\mu + iA_\mu)\psi_i + \phi\,\bar\psi_i\psi_i\right] + \frac{1}{4e^2}F_{\mu\nu}^2 + \frac{N_f}{2u^2}(\partial_\mu\phi)^2 + N_f\lambda_0^2\phi^4 \tag{4.4.1}$$

and take the large-N_f limit with e^2N_f, u, and λ_0 held fixed.

The scalar field is normalized so that its bare propagator is

$$G_\phi^{\text{bare}}(p) = \frac{u^2}{N_f p^2} \tag{4.4.2}$$

At large N_f, the leading correction to the scalar two-point function comes from the fermion bubble

$$\Sigma(p) = \int_\ell \operatorname{tr}\left[\frac{\not p + \not\ell}{(p+l)^2}\frac{\not\ell}{\ell^2}\right] = -\frac{1}{2}\operatorname{tr}[1]\,\kappa_d(1,1)|p|^{d-2} \tag{4.4.3}$$

In $d=3$, this gives $\Sigma(p) = -N_f|p|/8$ when $\operatorname{tr}[1] = 2N_f$. The effective scalar propagator is therefore

$$\begin{aligned} G_\phi^{\text{eff}}(p) &= \left[\left(G_\phi^{\text{bare}}(p)\right)^{-1} - \Sigma(p)\right]^{-1} \\ &= \left[\frac{N_f p^2}{u^2} + \frac{1}{2}\operatorname{tr}[1]\,\kappa_d(1,1)|p|^{d-2}\right]^{-1} \end{aligned} \tag{4.4.4}$$

For $2<d<4$, the fermion bubble dominates in the infrared, and hence

$$G_\phi(p) = \frac{h}{|p|^{d-2}} + \cdots, \qquad h := \frac{2}{\operatorname{tr}[1]\kappa_d(1,1)} \tag{4.4.5}$$

Here, the dots denote corrections subleading in the large-N_f infrared expansion. Thus, in the infrared, the effective scalar propagator has the same large-N_f scaling as the gauge-field propagator.

The Feynman rules relevant for the leading $1/N_f$ computation are

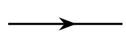

$$= S(p) = -i\frac{\not{p}}{p^2}$$

$$= \Delta_{\mu\nu}(p) = \frac{g}{p^{d-2}}\left(\delta^{\mu\nu} + \xi\frac{p^\mu p^\nu}{p^2}\right) \tag{4.4.6}$$

$$= G(p) = \frac{h}{p^{d-2}}$$

where g is the same effective coupling as defined in (4.3.3). The gauge and scalar vertices are[12]

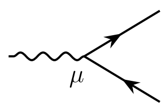

$$= -i\gamma^\mu,$$

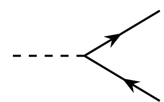

$$= 1 \tag{4.4.7}$$

4.4.1 Fermion bilinears

We now consider bilinears $\bar{\psi}\Gamma\psi$ and use the notation $M(\Gamma, \bar{\Gamma})$ of Sec. 4.3 for the corresponding fermion bubble. At leading order, the connected two-point function receives one new contribution, namely scalar exchange. Thus, the connected two-point function is given by

$$\langle\bar{\psi}\Gamma\psi(p)\,\bar{\psi}\bar{\Gamma}\psi(-p)\rangle = \tag{4.4.8}$$

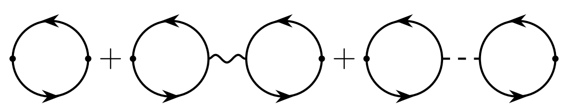

which combine to give

$$\langle\bar{\psi}\Gamma\psi(p)\,\bar{\psi}\bar{\Gamma}\psi(-p)\rangle_{\text{tree}} = M(\Gamma, \bar{\Gamma}) - \frac{g}{p^{d-2}}M(\Gamma, \gamma^\mu)M(\gamma_\mu, \bar{\Gamma}) + \frac{h}{p^{d-2}}M(\Gamma, 1)M(1, \bar{\Gamma}) \tag{4.4.9}$$

As before, $M(\Gamma, \gamma^\mu)$ is transverse, so the ξ-dependent part of the photon propagator drops out.

For the scalar bilinear $\Gamma = \bar{\Gamma} = 1$, one has

$$M(1, 1) = -\frac{1}{2}\,\mathrm{tr}[1]\,\kappa_d(1, 1)|p|^{d-2}, \qquad M(1, \gamma^\mu) = 0. \tag{4.4.10}$$

[12]The quartic interaction is irrelevant for $d < 4$, and we will not include it in the leading large-N_f analysis.

The first and the third terms in (4.4.8) therefore cancel,

$$\langle \bar{\psi}\psi(p)\, \bar{\psi}\psi(-p)\rangle_{\text{tree}} = 0 \tag{4.4.11}$$

Thus, the leading connected correlator of the scalar bilinear vanishes. This is just the statement that, at the critical point, the inverse effective scalar propagator is generated by the same fermion bubble that appears in $M(1,1)$.

In what follows, this vanishing connected correlator will not be used as the starting point for extracting an anomalous dimension. Rather, to compare with the pure QED result for $\Gamma = \bar{\Gamma} = 1$, we focus on the logarithmic corrections to the one-particle-irreducible bilinear two-point function, namely the fermion bubble.[13]

At the next order in the large-N_f expansion, the logarithmic correction to the 1PI bilinear two-point function receives contributions from three classes of diagrams: pure gauge-exchange diagrams, pure scalar-exchange diagrams, and mixed gauge-scalar diagrams. The pure gauge-exchange contribution is the same as in the pure QED$_d$ calculation above. We discuss the last two classes in turn.

We first consider the scalar-exchange contribution to the logarithmic part of the 1PI bilinear two-point function. Equivalently, this is the Gross–Neveu–Yukawa part of the calculation with the gauge field turned off. The relevant diagrams are the scalar analogues of the diagrams considered in pure QED$_d$

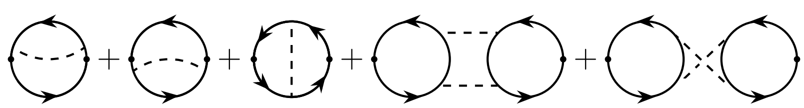

(4.4.12)

The first two diagrams are self-energy insertions on the fermion lines, the third diagram is the vertex correction, and the last two diagrams contain two scalar exchanges. Similarly, the logarithmic terms can be extracted using the same momentum-region argument as in the pure QED$_d$ calculation. Keeping only the relevant large momentum regions gives the logarithmic contribution to the 1PI bilinear two-point function.

[13] Since the leading connected correlator in this channel vanishes after scalar exchange is included, the $\mathscr{L}$ term in the 1PI bubble is not a correction to a nonzero leading two-point function of $\bar{\psi}\psi$. Therefore, the usual extraction of an anomalous dimension from a logarithmic correction to a two-point function does not directly apply.

The scalar correction to the fermion propagator gives

$$\int_k S(p)S(k+p)S(p)G(k) = -h\frac{d-2}{d}\mathscr{L}\, S(p) \tag{4.4.13}$$

Thus, the first two diagrams contribute

$$-2h\frac{d-2}{d}\mathscr{L}\, M(\Gamma,\bar{\Gamma}) \tag{4.4.14}$$

The third diagram gives

$$-\frac{h}{d}\mathscr{L}\, M(\Gamma,\gamma^\alpha\bar{\Gamma}\gamma_\alpha) + (\Gamma\leftrightarrow\bar{\Gamma}) \tag{4.4.15}$$

The logarithmic contributions from the last two diagrams cancel. The scalar contribution to the logarithmic correction is therefore

$$\left(-h\frac{d-2}{d}\mathscr{L}\, M(\Gamma,\bar{\Gamma}) - \frac{h}{d}\mathscr{L}\, M(\Gamma,\gamma^\alpha\bar{\Gamma}\gamma_\alpha)\right) + (\Gamma\leftrightarrow\bar{\Gamma}) \tag{4.4.16}$$

For the scalar bilinear $\Gamma=\bar{\Gamma}=1$, this becomes

$$-\frac{4h(d-1)}{d}\,\mathscr{L}\, M(1,1) \tag{4.4.17}$$

There are also mixed diagrams, with one gauge exchange and one scalar exchange

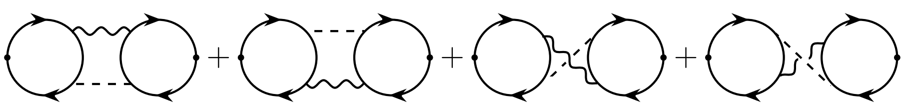

(4.4.18)

For general bilinear insertions Γ and $\bar{\Gamma}$, the mixed diagrams are gauge invariant by themselves. Indeed, the ξ-dependent part of the photon propagator is proportional to

$$k_\mu k_\alpha\left[M(\Gamma,\gamma^\mu\gamma^\alpha) - M(\Gamma,\gamma^\alpha\gamma^\mu)\right] \tag{4.4.19}$$

which vanishes. We may therefore keep only the transverse part of the photon propagator.

After extracting the logarithmic contribution, the mixed diagrams give

$$\mathcal{M}_{\text{mix}} = \frac{4(d-3)gh\,\kappa_d(1,1)\mathscr{L}}{d}\, M(\Gamma,\gamma^{\mu\alpha})\ \mathrm{tr}[\bar{\Gamma}\gamma_{\alpha\mu}] + (\Gamma\leftrightarrow\bar{\Gamma}) \tag{4.4.20}$$

For $\Gamma=\bar{\Gamma}=1$, this term vanishes by using $\mathrm{tr}[\gamma_{\alpha\mu}]=0$. Thus, the mixed diagrams do not contribute to the scalar bilinear at this order.

The gauge contribution is the same one found in the pure QED_d calculation. Combining the scalar, gauge, and mixed contributions, the logarithmic correction to the 1PI bilinear two-point function is

$$\begin{aligned}&\left(-h\frac{d-2}{d}\mathscr{L}\,M(\Gamma,\bar{\Gamma})-\frac{h}{d}\mathscr{L}\,M(\Gamma,\gamma^{\alpha}\bar{\Gamma}\gamma_{\alpha})\right)\\&\quad+\frac{g\mathscr{L}}{d}\bigg(-(d-2)^2M(\Gamma,\bar{\Gamma})+M(\gamma^{\mu}\gamma^{\alpha}\bar{\Gamma}\gamma_{\alpha}\gamma_{\mu},\Gamma)\\&\qquad\qquad-\frac{2}{\mathrm{tr}[1]}\frac{(d-1)(d-4)}{d-2}\,\mathrm{tr}[\Gamma\gamma^{\alpha\mu\nu}]M(\bar{\Gamma},\gamma_{\alpha\mu\nu})\bigg)\\&\quad+\frac{4(d-3)gh\,\kappa_d(1,1)\mathscr{L}}{d}M(\Gamma,\gamma^{\mu\alpha})\,\mathrm{tr}[\bar{\Gamma}\gamma_{\alpha\mu}]+(\Gamma\leftrightarrow\bar{\Gamma}).\end{aligned}\tag{4.4.21}$$

This formula is the QED_d–GNY analogue of the logarithmic 1PI meson result in the pure gauge theory.

For the scalar bilinear $\Gamma=\bar{\Gamma}=1$, the mixed term vanishes, and one finds

$$M(1,1)\mathscr{L}\left[-\frac{4h(d-1)}{d}+\frac{4g(d-1)}{d}\left(2-\frac{d-4}{d-2}\frac{\mathrm{tr}\,(\gamma^{\alpha\mu\nu})\,\mathrm{tr}\,(\gamma_{\alpha\mu\nu})}{\mathrm{tr}(1)^2}\right)\right]\tag{4.4.22}$$

Thus, the scalar channel in the QED_d–GNY model inherits the same low-rank obstruction as in pure QED_d. For generic d the odd trace is absent in the stable limit, while at $d=3$ it is nonzero and changes the logarithmic coefficient. The Yukawa interaction shifts the scalar part of the 1PI correction, but it does not remove the branch structure associated with the exceptional identity $\gamma_{\mu\nu\rho}\sim\epsilon_{\mu\nu\rho}$ in three dimensions.

We close with a caution about the interpretation of this result. The combination of a vanishing leading connected correlator and a nonzero logarithm in the 1PI kernel may look like a logarithmic CFT. This is not the right conclusion yet. In the GNY theory, $\bar{\psi}\psi$ belongs to a scalar-singlet sector containing operators such as ϕ, ϕ^3, and $\partial^2\phi$. These operators are not all independent, since the scalar equation of motion relates them. Thus, the correct question is not whether the single object $\bar{\psi}\psi$ has a logarithmic two-point function. One must first quotient by the equation-of-motion relation and then separate descendant directions from primary directions. Only on this reduced space of independent scalar primaries does it make sense to ask whether the dilatation operator is diagonalizable, or instead has a Jordan block. We will not carry out this operator-mixing problem here.

4.5 Conclusions and future directions

In this paper we have argued that analytic continuation in the number of spacetime dimensions d is a meaningful operation, but one that is also remarkably subtle.

We showed that, if we think of d as living in $\mathbb{C}$, then correlation functions, OPEs, and scaling dimensions of generic operators are all discontinuous, even in theories as simple as the free fermion CFT. On the other hand, we provided evidence that analyticity is recovered if we consider some infinite cover of $\mathbb{C}$, although this last perspective definitely warrants a much more thorough study.

A simple application of our results is the following. The QCD theory we studied in section 4.3 is known to be dual to a WZW model when $d = 2$ (see e.g. [321]). Then, the analytic continuation in d we constructed can be interpreted as one specific choice for analytic continuation of this $2d$ theory (see e.g. [322, 323] for somewhat recent efforts for such problem). The rank of the WZW model is N_f, so we only have a continuation for large rank. The question of how to construct a non-perturbative continuation is still open, of course.

As stressed in the introduction, analytic continuation in d requires a choice of target for all $d \in \mathbb{N}$, i.e., it is not an operation that is intrinsically defined for a QFT that lives in one specific d. That being said, some families might not have a meaningful continuation if we insist on having a target for *all* $d \in \mathbb{N}$, but the continuation might exist if we content ourselves with having a target for some congruence class in $\mathbb{N}$. As a simple illustration, the integer sequence $a_n = (-1)^n$ does not have a nice continuation to the complex $n \in \mathbb{C}$ plane, but if we unzip $\mathbb{N}$ into the even and odd integers, then we do get two healthy continuations, namely $a_n = 1$ and $a_n = -1$. In this sense, it might be the case that some QFT that is naturally defined for $d = 3$ might fail to have a nice continuation if we insist that we want all $d \in \mathbb{N}$, but the continuation might be well-defined if we only require a target at $d \in 2\mathbb{N} + 1$.

For example, because of Bott periodicity, fermions might have a nicer continuation in d if we consider the eight cases $d \in 8\mathbb{N} + k$, $k \in \{0, \ldots, 7\}$ separately. This would allow us, for example, to analytically continue Majorana fermions.

An interesting family of QFTs one might want to analytically continue in d is Chern-Simons(-matter) theories. In the same way we set up the analytic continuation of QED/QCD via the $1/N_f$ expansion, in CS one can perform a $1/k$ expansion, which one could use to try and define a continuation perturbatively. This continuation in d should present all the same subtleties we explored here[14], and likely many more. As before, defining this continuation requires a choice of target for an infinite family of $d \in \mathbb{N}$; here one natural choice is to take the d-dimensional Chern-Simons form for all $d \in 2\mathbb{N}+1$.

Although we do not have anything sharp to say about this, it should be useful to think about the complications induced by $\operatorname{tr}[\gamma_{\mu_1\cdots\mu_n}]$ in the language of von Neumann algebras. Indeed, if $Pin(d)$ for fractional d is morally $Pin(\infty)$, then we should perhaps think of the γ^μ's for fractional d as operators acting on some infinite-dimensional space, and their trace should be regularized somehow (while preserving all the properties required by QFT, namely Lorentz invariance, linearity and cyclicity). Looking at our various expressions for $\Delta(\bar\psi\psi)$, we see that observables always depend on these traces via the quotient $\operatorname{tr}[\gamma_{\mu_1\cdots\mu_n}]/\operatorname{tr}[1]$, i.e., these are indeed regularized traces, if only formally.

Another aspect that invites further analysis is the connection between analytic continuation of d and of N. One simple remark in this context is that the difficulty in defining traces of γ^μ in fractional d can be reformulated entirely in the language of analytic continuation of flavor symmetries. Indeed, the gamma matrices can equivalently be thought of as Majorana fermions in an auxiliary $0+1d$ system, in terms of which $\operatorname{tr}[\gamma_\mu\gamma_\nu\cdots] = \langle\Psi_\mu\Psi_\nu\cdots\rangle$.[15] As far

[14] As we mentioned before, generic operators in a chiral theory should behave similarly to parity-odd operators in a vector-like theory. For example, we saw that in regular QCD the parity-odd operator $\bar\psi\psi$ was rather subtle at fractional d, but the gauge sector (Wilson lines) were perfectly well-behaved. Once we give up reflection symmetry, the gauge sector should become subtle as well. For instance, without this symmetry, the most general photon two-point function compatible with gauge invariance is $\Pi_{\mu\nu}(p) = (p^2\delta_{\mu\nu} - p_\mu p_\nu)\Pi^{\text{even}}(p^2) + ip^\sigma \operatorname{tr}[\gamma_{\mu\nu\sigma}]\Pi^{\text{odd}}(p^2)$. Therefore, if CS theories admit continuation in d at all, the gauge sector will acquire a branched structure in d similar to the one in $\bar\psi\psi$ discussed in this paper.

[15] The fact that $\operatorname{tr}[\gamma_{\mu_1\cdots\mu_n}]$ is non-zero only when $n = d$ has a simple interpretation in this language: the correlation function vanishes due to the d Ramond zero-modes, unless we insert the same number of Ψ's.

as these Majorana fermions is concerned, the group $Pin(d)$ is a flavor symmetry.[16]

Let us also emphasize that the obstructions to analyticity in d or N are always due to low rank exceptions. Indeed, the direct limit of a representation is always analytic, by construction, since this limit is defined by considering only the asymptotic behavior in $d, N \to \infty$, which is smooth. In this sense, the non-analyticity reflects features that are non-perturbative in $1/d$ or $1/N$. It would be nice to understand this better, specifically by drawing insights developed in the context of large N_c gauge theories. (There, unstable representations are usually called "heavy" or "large".)

Let us finally go back to one of the original motivations we mentioned in the introduction, namely dim-reg in the context of supersymmetry. Our main conclusion is that analytic continuation in d is very subtle; therefore, if we only care about this operation as a simplifying device for loop computations, then we have nothing to offer: the rigorous way to analytically continue requires more work than dim-reg saves. Conversely, if one is interested in this continuation for its own sake (e.g., can we find an interpolation between $d = 3$ and $d = 4$ Seiberg-like dualities?), then unfortunately we also have reasons to be pessimistic: supersymmetry itself is, in a sense, a low d exception. It is not clear to us how to set up a healthy SUSY target for all $d \in \mathbb{N}$. We leave this possibility open for now.

[16]More precisely, the flavor symmetry is $O(d)$; the double-cover $Pin(d)$ appears because the vacua of these fermions realize the symmetry projectively. This is just the statement that this flavor symmetry has a 't Hooft anomaly. Note that the correlation functions of Ψ^μ present unstable behavior even though this operator transforms under the vector representation of $O(d)$, which is stable; this happens because the ground state of the theory is itself unstable.

[1] M. Anderson. Leading order corrections to the Nambu action. *Phys. Rev. D*, 51:2863–2871, 1995.

[2] Malcolm R. Anderson, Filipe Bonjour, Ruth Gregory, and John Stewart. Effective action and motion of a cosmic string. *Phys. Rev. D*, 56:8014–8028, 1997.

[3] Joan Elias Miró, Andrea L. Guerrieri, Aditya Hebbar, João Penedones, and Pedro Vieira. Flux Tube S-matrix Bootstrap. *Phys. Rev. Lett.*, 123(22):221602, 2019.

[4] Adwait Gaikwad, Victor Gorbenko, and Andrea L. Guerrieri. QCD worldsheet axion from the bootstrap. *JHEP*, 01:090, 2024.

[5] Michael Gutperle and John D. Miller. A note on entanglement entropy for topological interfaces in RCFTs. *JHEP*, 04:176, 2016.

[6] Michael Gutperle, Yan-Yan Li, Dikshant Rathore, and Konstantinos Roumpedakis. Non-invertible symmetries in S_N orbifold CFTs and holography. 5 2024.

[7] Michael Gutperle, Yan-Yan Li, Dikshant Rathore, and Konstantinos Roumpedakis. A note on entanglement entropy and topological defects in symmetric orbifold CFTs. 6 2024.

[8] Diego Delmastro, Yan-Yan Li, and Dikshant Rathore. Does QFT make sense in non-integer dimensions? 7 2026.

[9] Ofer Aharony and Zohar Komargodski. The Effective Theory of Long Strings. *JHEP*, 05:118, 2013.

[10] Sergei Dubovsky, Raphael Flauger, and Victor Gorbenko. Effective String Theory Revisited. *JHEP*, 09:044, 2012.

[11] Joan Elias Miró and Andrea Guerrieri. Dual eft bootstrap: Qcd flux tubes, 2021.

[12] N. Seiberg and E. Witten. Electric-magnetic duality, monopole condensation, and confinement in n=2 supersymmetric yang-mills theory. *Nuclear Physics B*, 426(1):19–52, 1994.

[13] N. Seiberg. Electric - magnetic duality in supersymmetric nonAbelian gauge theories. *Nucl. Phys. B*, 435:129–146, 1995.

[14] Chi-Ming Chang, Ying-Hsuan Lin, Shu-Heng Shao, Yifan Wang, and Xi Yin. Topological Defect Lines and Renormalization Group Flows in Two Dimensions. *JHEP*, 01:026, 2019.

[15] Zohar Komargodski, Kantaro Ohmori, Konstantinos Roumpedakis, and Sahand Seifnashri. Symmetries and strings of adjoint QCD_2. *JHEP*, 03:103, 2021.

[16] Clay Cordova and Kantaro Ohmori. Non-Invertible Chiral Symmetry and Exponential Hierarchies. 5 2022.

[17] Robbert Dijkgraaf, Gregory W. Moore, Erik P. Verlinde, and Herman L. Verlinde. Elliptic genera of symmetric products and second quantized strings. *Commun. Math. Phys.*, 185:197–209, 1997.

[18] Matthias R. Gaberdiel, Rajesh Gopakumar, and Chris Hull. Stringy AdS_3 from the worldsheet. *JHEP*, 07:090, 2017.

[19] Matthias R. Gaberdiel and Rajesh Gopakumar. Tensionless string spectra on AdS_3. *JHEP*, 05:085, 2018.

[20] Lorenz Eberhardt, Matthias R. Gaberdiel, and Rajesh Gopakumar. The Worldsheet Dual of the Symmetric Product CFT. *JHEP*, 04:103, 2019.

[21] Lorenz Eberhardt, Matthias R. Gaberdiel, and Rajesh Gopakumar. Deriving the $\mathrm{AdS}_3/\mathrm{CFT}_2$ correspondence. *JHEP*, 02:136, 2020.

[22] E. B. Bogomolny. Stability of Classical Solutions. *Sov. J. Nucl. Phys.*, 24:449, 1976.

[23] M. K. Prasad and Charles M. Sommerfield. An Exact Classical Solution for the 't Hooft Monopole and the Julia-Zee Dyon. *Phys. Rev. Lett.*, 35:760–762, 1975.

[24] Jose D. Edelstein, Carlos Nunez, and Fidel Schaposnik. Supersymmetry and Bogomolny equations in the Abelian Higgs model. *Phys. Lett. B*, 329:39–45, 1994.

[25] Davide Gaiotto, Anton Kapustin, Nathan Seiberg, and Brian Willett. Generalized Global Symmetries. *JHEP*, 02:172, 2015.

[26] Thomas T. Dumitrescu and Amey P. Gaikwad. Phases of giant magnetic vortex strings, 2025.

[27] A. A. Abrikosov. On the Magnetic properties of superconductors of the second group. *Sov. Phys. JETP*, 5:1174–1182, 1957.

[28] Holger Bech Nielsen and Poul Olesen. Vortex-line models for dual strings. *Nuclear Physics B*, 61:45–61, 1973.

[29] N. S. Manton and P. Sutcliffe. *Topological solitons*. Cambridge Monographs on Mathematical Physics. Cambridge University Press, 2004.

[30] Erick J. Weinberg. *Classical solutions in quantum field theory: Solitons and Instantons in High Energy Physics*. Cambridge Monographs on Mathematical Physics. Cambridge University Press, 9 2012.

[31] H. J. de Vega and F. A. Schaposnik. A Classical Vortex Solution of the Abelian Higgs Model. *Phys. Rev. D*, 14:1100–1106, 1976.

[32] Erick J. Weinberg. Classical solutions in quantum field theories. *Ann. Rev. Nucl. Part. Sci.*, 42:177–210, 1992.

[33] Steven Weinberg. *The quantum theory of fields. Vol. 2: Modern applications*. Cambridge University Press, 8 2013.

[34] David Tong. Tasi lectures on solitons, 2005.

[35] Erick J. Weinberg. Multivortex solutions of the ginzburg-landau equations. *Phys. Rev. D*, 19:3008–3012, May 1979.

[36] Clifford Henry Taubes. Arbitrary N: Vortex Solutions to the First Order Landau-Ginzburg Equations. *Commun. Math. Phys.*, 72:277–292, 1980.

[37] Lev Davidovich Landau and E. M. Lifshits. *Quantum Mechanics: Non-Relativistic Theory*, volume v.3 of *Course of Theoretical Physics*. Butterworth-Heinemann, Oxford, 1991.

[38] Sergei Dubovsky, Raphael Flauger, and Victor Gorbenko. Evidence from Lattice Data for a New Particle on the Worldsheet of the QCD Flux Tube. *Phys. Rev. Lett.*, 111(6):062006, 2013.

[39] Sergei Dubovsky and Victor Gorbenko. Towards a Theory of the QCD String. *JHEP*, 02:022, 2016.

[40] Y. Burnier and K. Zuleta. Effective action of a five-dimensional domain wall. *JHEP*, 05:065, 2009.

[41] S. Mandelstam. Vortices and Quark Confinement in Nonabelian Gauge Theories. *Phys. Rept.*, 23:245–249, 1976.

[42] Gerard 't Hooft. Gauge Fields with Unified Weak, Electromagnetic, and Strong Interactions. In *1975 High-Energy Particle Physics Divisional Conference of EPS (includes 8th biennial conf on Elem. Particles)*, 9 1975.

[43] N. Seiberg and Edward Witten. Monopoles, duality and chiral symmetry breaking in N=2 supersymmetric QCD. *Nucl. Phys. B*, 431:484–550, 1994.

[44] N. Seiberg and Edward Witten. Electric - magnetic duality, monopole condensation, and confinement in N=2 supersymmetric Yang-Mills theory. *Nucl. Phys. B*, 426:19–52, 1994. [Erratum: Nucl.Phys.B 430, 485–486 (1994)].

[45] Ying-Hsuan Lin and Shu-Heng Shao. Duality Defect of the Monster CFT. *J. Phys. A*, 54(6):065201, 2021.

[46] Ryan Thorngren and Yifan Wang. Fusion Category Symmetry I: Anomaly In-Flow and Gapped Phases. 12 2019.

[47] Ryan Thorngren and Yifan Wang. Fusion Category Symmetry II: Categoriosities at $c = 1$ and Beyond. 6 2021.

[48] Mendel Nguyen, Yuya Tanizaki, and Mithat Ünsal. Semi-Abelian gauge theories, non-invertible symmetries, and string tensions beyond N-ality. *JHEP*, 03:238, 2021.

[49] Yichul Choi, Clay Cordova, Po-Shen Hsin, Ho Tat Lam, and Shu-Heng Shao. Noninvertible duality defects in 3+1 dimensions. *Phys. Rev. D*, 105(12):125016, 2022.

[50] Justin Kaidi, Kantaro Ohmori, and Yunqin Zheng. Kramers-Wannier-like Duality Defects in (3+1)D Gauge Theories. *Phys. Rev. Lett.*, 128(11):111601, 2022.

[51] Yichul Choi, Clay Cordova, Po-Shen Hsin, Ho Tat Lam, and Shu-Heng Shao. Non-invertible Condensation, Duality, and Triality Defects in 3+1 Dimensions. 4 2022.

[52] Konstantinos Roumpedakis, Sahand Seifnashri, and Shu-Heng Shao. Higher Gauging and Non-invertible Condensation Defects. 4 2022.

[53] Lakshya Bhardwaj, Lea Bottini, Sakura Schafer-Nameki, and Apoorv Tiwari. Non-Invertible Higher-Categorical Symmetries. 4 2022.

[54] Jeremias Aguilera Damia, Riccardo Argurio, and Luigi Tizzano. Continuous Generalized Symmetries in Three Dimensions. 6 2022.

[55] Guillermo Arias-Tamargo and Diego Rodriguez-Gomez. Non-Invertible Symmetries from Discrete Gauging and Completeness of the Spectrum. 4 2022.

[56] Yui Hayashi and Yuya Tanizaki. Non-invertible self-duality defects of Cardy-Rabinovici model and mixed gravitational anomaly. *JHEP*, 08:036, 2022.

[57] Justin Kaidi, Gabi Zafrir, and Yunqin Zheng. Non-invertible symmetries of $\mathcal{N} = 4$ SYM and twisted compactification. *JHEP*, 08:053, 2022.

[58] Andrea Antinucci, Giovanni Galati, and Giovanni Rizi. On Continuous 2-Category Symmetries and Yang-Mills Theory. 6 2022.

[59] Yichul Choi, Ho Tat Lam, and Shu-Heng Shao. Non-invertible Time-reversal Symmetry. 8 2022.

[60] Yichul Choi, Ho Tat Lam, and Shu-Heng Shao. Non-invertible Global Symmetries in the Standard Model. 5 2022.

[61] Thomas Bartsch, Mathew Bullimore, Andrea E. V. Ferrari, and Jamie Pearson. Non-invertible Symmetries and Higher Representation Theory I. 8 2022.

[62] Ben Heidenreich, Jacob McNamara, Miguel Montero, Matthew Reece, Tom Rudelius, and Irene Valenzuela. Non-invertible global symmetries and completeness of the spectrum. *JHEP*, 09:203, 2021.

[63] Clay Cordova, Kantaro Ohmori, and Tom Rudelius. Generalized Symmetry Breaking Scales and Weak Gravity Conjectures. 2 2022.

[64] Tzu-Chen Huang, Ying-Hsuan Lin, and Sahand Seifnashri. Construction of two-dimensional topological field theories with non-invertible symmetries. *JHEP*, 12:028, 2021.

[65] Vladimir Bashmakov, Michele Del Zotto, and Azeem Hasan. On the 6d Origin of Non-invertible Symmetries in 4d. 6 2022.

[66] Francesco Benini, Christian Copetti, and Lorenzo Di Pietro. Factorization and global symmetries in holography. 3 2022.

[67] Jeremias Aguilera Damia, Riccardo Argurio, and Eduardo Garcia-Valdecasas. Non-Invertible Defects in 5d, Boundaries and Holography. 7 2022.

[68] Ying-Hsuan Lin, Masaki Okada, Sahand Seifnashri, and Yuji Tachikawa. Asymptotic density of states in 2d CFTs with non-invertible symmetries. 8 2022.

[69] Pierluigi Niro, Konstantinos Roumpedakis, and Orr Sela. Exploring non-invertible symmetries in free theories. *JHEP*, 03:005, 2023.

[70] Clay Cordova and Kantaro Ohmori. Quantum Duality in Electromagnetism and the Fine-Structure Constant. 7 2023.

[71] Tom Rudelius and Shu-Heng Shao. Topological Operators and Completeness of Spectrum in Discrete Gauge Theories. *JHEP*, 12:172, 2020.

[72] Kansei Inamura. Topological field theories and symmetry protected topological phases with fusion category symmetries. *JHEP*, 05:204, 2021.

[73] Mendel Nguyen, Yuya Tanizaki, and Mithat Ünsal. Noninvertible 1-form symmetry and Casimir scaling in 2D Yang-Mills theory. *Phys. Rev. D*, 104(6):065003, 2021.

[74] Lakshya Bhardwaj, Sakura Schafer-Nameki, and Jingxiang Wu. Universal Non-Invertible Symmetries. *Fortsch. Phys.*, 70(11):2200143, 2022.

[75] Justin Kaidi, Kantaro Ohmori, and Yunqin Zheng. Symmetry TFTs for Non-invertible Defects. *Commun. Math. Phys.*, 404(2):1021–1124, 2023.

[76] Shi Chen and Yuya Tanizaki. Solitonic Symmetry beyond Homotopy: Invertibility from Bordism and Noninvertibility from Topological Quantum Field Theory. *Phys. Rev. Lett.*, 131(1):011602, 2023.

[77] Vladimir Bashmakov, Michele Del Zotto, Azeem Hasan, and Justin Kaidi. Non-invertible symmetries of class S theories. *JHEP*, 05:225, 2023.

[78] Clay Cordova, Sungwoo Hong, Seth Koren, and Kantaro Ohmori. Neutrino Masses from Generalized Symmetry Breaking. 11 2022.

[79] Yichul Choi, Ho Tat Lam, and Shu-Heng Shao. Non-invertible Gauss law and axions. *JHEP*, 09:067, 2023.

[80] Ryo Yokokura. Non-invertible symmetries in axion electrodynamics. 12 2022.

[81] Lakshya Bhardwaj, Sakura Schafer-Nameki, and Apoorv Tiwari. Unifying constructions of non-invertible symmetries. *SciPost Phys.*, 15(3):122, 2023.

[82] Lakshya Bhardwaj, Lea E. Bottini, Sakura Schafer-Nameki, and Apoorv Tiwari. Non-invertible symmetry webs. *SciPost Phys.*, 15(4):160, 2023.

[83] Thomas Bartsch, Mathew Bullimore, Andrea E. V. Ferrari, and Jamie Pearson. Non-invertible Symmetries and Higher Representation Theory II. 12 2022.

[84] Anuj Apte, Clay Cordova, and Ho Tat Lam. Obstructions to gapped phases from noninvertible symmetries. *Phys. Rev. B*, 108(4):045134, 2023.

[85] Justin Kaidi, Emily Nardoni, Gabi Zafrir, and Yunqin Zheng. Symmetry TFTs and anomalies of non-invertible symmetries. *JHEP*, 10:053, 2023.

[86] Masataka Koide, Yuta Nagoya, and Satoshi Yamaguchi. Noninvertible symmetries and boundaries in four dimensions. *Phys. Rev. D*, 108(6):065009, 2023.

[87] Jeremias Aguilera Damia, Riccardo Argurio, Francesco Benini, Sergio Benvenuti, Christian Copetti, and Luigi Tizzano. Non-invertible symmetries along 4d RG flows. *JHEP*, 02:084, 2024.

[88] Lakshya Bhardwaj and Sakura Schafer-Nameki. Generalized Charges, Part II: Non-Invertible Symmetries and the Symmetry TFT. 5 2023.

[89] Marieke van Beest, Philip Boyle Smith, Diego Delmastro, Zohar Komargodski, and David Tong. Monopoles, Scattering, and Generalized Symmetries. 6 2023.

[90] Craig Lawrie, Xingyang Yu, and Hao Y. Zhang. Intermediate defect groups, polarization pairs, and noninvertible duality defects. *Phys. Rev. D*, 109(2):026005, 2024.

[91] Shi Chen and Yuya Tanizaki. Solitonic symmetry as non-invertible symmetry: cohomology theories with TQFT coefficients. 7 2023.

[92] Clay Cordova, Po-Shen Hsin, and Carolyn Zhang. Anomalies of Non-Invertible Symmetries in (3+1)d. 8 2023.

[93] Andrea Antinucci, Francesco Benini, Christian Copetti, Giovanni Galati, and Giovanni Rizi. Anomalies of non-invertible self-duality symmetries: fractionalization and gauging. 8 2023.

[94] Valentin Benedetti, Horacio Casini, and Javier M. Magan. ABJ anomaly as a U(1) symmetry and Noether's theorem. 9 2023.

[95] Yichul Choi, Matthew Forslund, Ho Tat Lam, and Shu-Heng Shao. Quantization of Axion-Gauge Couplings and Noninvertible Higher Symmetries. *Phys. Rev. Lett.*, 132(12):121601, 2024.

[96] Yuta Nagoya and Soichiro Shimamori. Non-invertible duality defect and non-commutative fusion algebra. *JHEP*, 12:062, 2023.

[97] Masaki Okada and Yuji Tachikawa. Non-invertible symmetries act locally by quantum operations. 3 2024.

[98] Naoto Kan, Kohki Kawabata, and Hiroki Wada. Symmetry fractionalization and duality defects in Maxwell theory. 4 2024.

[99] Fabio Apruzzi, Ibrahima Bah, Federico Bonetti, and Sakura Schafer-Nameki. Noninvertible Symmetries from Holography and Branes. *Phys. Rev. Lett.*, 130(12):121601, 2023.

[100] Iñaki García Etxebarria. Branes and Non-Invertible Symmetries. *Fortsch. Phys.*, 70(11):2200154, 2022.

[101] Jonathan J. Heckman, Max Hubner, Ethan Torres, Xingyang Yu, and Hao Y. Zhang. Top down approach to topological duality defects. *Phys. Rev. D*, 108(4):046015, 2023.

[102] Jonathan J. Heckman, Max Hübner, Ethan Torres, and Hao Y. Zhang. The Branes Behind Generalized Symmetry Operators. *Fortsch. Phys.*, 71(1):2200180, 2023.

[103] Marieke van Beest, Dewi S. W. Gould, Sakura Schafer-Nameki, and Yi-Nan Wang. Symmetry TFTs for 3d QFTs from M-theory. *JHEP*, 02:226, 2023.

[104] Muldrow Etheredge, Inaki Garcia Etxebarria, Ben Heidenreich, and Sebastian Rauch. Branes and symmetries for $\mathcal{N} = 3$ S-folds. *JHEP*, 09:005, 2023.

[105] Ibrahima Bah, Enoch Leung, and Thomas Waddleton. Non-invertible symmetries, brane dynamics, and tachyon condensation. *JHEP*, 01:117, 2024.

[106] Markus Dierigl, Jonathan J. Heckman, Miguel Montero, and Ethan Torres. R7-branes as charge conjugation operators. *Phys. Rev. D*, 109(4):046004, 2024.

[107] Antoine Bourget, Andrés Collinucci, and Sakura Schafer-Nameki. Generalized Toric Polygons, T-branes, and 5d SCFTs. 1 2023.

[108] Fabio Apruzzi, Federico Bonetti, Dewi S. W. Gould, and Sakura Schafer-Nameki. Aspects of Categorical Symmetries from Branes: SymTFTs and Generalized Charges. 6 2023.

[109] Florent Baume, Jonathan J. Heckman, Max Hübner, Ethan Torres, Andrew P. Turner, and Xingyang Yu. SymTrees and Multi-Sector QFTs. 10 2023.

[110] Mirjam Cvetič, Jonathan J. Heckman, Max Hübner, and Ethan Torres. Generalized symmetries, gravity, and the swampland. *Phys. Rev. D*, 109(2):026012, 2024.

[111] Jonathan J. Heckman, Max Hübner, and Chitraang Murdia. On the Holographic Dual of a Topological Symmetry Operator. 1 2024.

[112] Riccardo Argurio, Francesco Benini, Matteo Bertolini, Giovanni Galati, and Pierluigi Niro. On the Symmetry TFT of Yang-Mills-Chern-Simons theory. 4 2024.

[113] Hao Y. Zhang. K-theoretic Global Symmetry in String-constructed QFT and T-duality. 4 2024.

[114] Erik P. Verlinde. Fusion Rules and Modular Transformations in 2D Conformal Field Theory. *Nucl. Phys. B*, 300:360–376, 1988.

[115] V. B. Petkova and J. B. Zuber. Generalized twisted partition functions. *Phys. Lett. B*, 504:157–164, 2001.

[116] V. B. Petkova and J. B. Zuber. The Many faces of Ocneanu cells. *Nucl. Phys. B*, 603:449–496, 2001.

[117] Jurg Frohlich, Jurgen Fuchs, Ingo Runkel, and Christoph Schweigert. Kramers-Wannier duality from conformal defects. *Phys. Rev. Lett.*, 93:070601, 2004.

[118] Jurg Frohlich, Jurgen Fuchs, Ingo Runkel, and Christoph Schweigert. Duality and defects in rational conformal field theory. *Nucl. Phys. B*, 763:354–430, 2007.

[119] Jurgen Fuchs, Ingo Runkel, and Christoph Schweigert. TFT construction of RCFT correlators 1. Partition functions. *Nucl. Phys. B*, 646:353–497, 2002.

[120] Lance J. Dixon, Jeffrey A. Harvey, C. Vafa, and Edward Witten. Strings on Orbifolds. *Nucl. Phys. B*, 261:678–686, 1985.

[121] Lance J. Dixon, Daniel Friedan, Emil J. Martinec, and Stephen H. Shenker. The Conformal Field Theory of Orbifolds. *Nucl. Phys. B*, 282:13–73, 1987.

[122] Antal Jevicki, Mihail Mihailescu, and Sanjaye Ramgoolam. Gravity from CFT on S**N(X): Symmetries and interactions. *Nucl. Phys. B*, 577:47–72, 2000.

[123] Oleg Lunin and Samir D. Mathur. Correlation functions for M**N / S(N) orbifolds. *Commun. Math. Phys.*, 219:399–442, 2001.

[124] Ari Pakman, Leonardo Rastelli, and Shlomo S. Razamat. Diagrams for Symmetric Product Orbifolds. *JHEP*, 10:034, 2009.

[125] Juan Martin Maldacena. The Large N limit of superconformal field theories and supergravity. *Adv. Theor. Math. Phys.*, 2:231–252, 1998.

[126] Nathan Seiberg and Edward Witten. The D1 / D5 system and singular CFT. *JHEP*, 04:017, 1999.

[127] G. Giribet, C. Hull, M. Kleban, M. Porrati, and E. Rabinovici. Superstrings on AdS_3 at $k = 1$. *JHEP*, 08:204, 2018.

[128] Cumrun Vafa. Quantum Symmetries of String Vacua. *Mod. Phys. Lett. A*, 4:1615, 1989.

[129] Yuji Tachikawa. On gauging finite subgroups. *SciPost Phys.*, 8(1):015, 2020.

[130] John L. Cardy. Boundary Conditions, Fusion Rules and the Verlinde Formula. *Nucl. Phys. B*, 324:581–596, 1989.

[131] Masaki Oshikawa and Ian Affleck. Boundary conformal field theory approach to the critical two-dimensional Ising model with a defect line. *Nucl. Phys. B*, 495:533–582, 1997.

[132] C. Bachas, J. de Boer, R. Dijkgraaf, and H. Ooguri. Permeable conformal walls and holography. *JHEP*, 06:027, 2002.

[133] Nobuyuki Ishibashi. The Boundary and Crosscap States in Conformal Field Theories. *Mod. Phys. Lett. A*, 4:251, 1989.

[134] Andreas Recknagel. Permutation branes. *JHEP*, 04:041, 2003.

[135] Nadav Drukker, Davide Gaiotto, and Jaume Gomis. The Virtue of Defects in 4D Gauge Theories and 2D CFTs. *JHEP*, 06:025, 2011.

[136] Clay Cordova and Giovanni Rizi. Non-Invertible Symmetry in Calabi-Yau Conformal Field Theories. 12 2023.

[137] Robbert Dijkgraaf, Cumrun Vafa, Erik P. Verlinde, and Herman L. Verlinde. The Operator Algebra of Orbifold Models. *Commun. Math. Phys.*, 123:485, 1989.

[138] Albrecht Klemm and Michael G. Schmidt. Orbifolds by Cyclic Permutations of Tensor Product Conformal Field Theories. *Phys. Lett. B*, 245:53–58, 1990.

[139] Juan Martin Maldacena, Gregory W. Moore, and Andrew Strominger. Counting BPS black holes in toroidal Type II string theory. 3 1999.

[140] Konstantinos Roumpedakis. Comments on the S_N orbifold CFT in the large N-limit. *JHEP*, 07:038, 2018.

[141] Andrea Dei and Lorenz Eberhardt. Correlators of the symmetric product orbifold. *JHEP*, 01:108, 2020.

[142] Daniel Barter, Jacob Bridgeman, and Ramona Wolf. Computing associators of endomorphism fusion categories. *SciPost Physics*, 13(2):029, 2022.

[143] Lakshya Bhardwaj, Lea E. Bottini, Daniel Pajer, and Sakura Schäfer-Nameki. Gapped Phases with Non-Invertible Symmetries: (1+1)d. 10 2023.

[144] Matthias R. Gaberdiel, Bob Knighton, and Jakub Vošmera. D-branes in $AdS_3 \times S^3 \times T^4$ at k = 1 and their holographic duals. *JHEP*, 12:149, 2021.

[145] Alexandre Belin, Shovon Biswas, and James Sully. The spectrum of boundary states in symmetric orbifolds. *JHEP*, 01:123, 2022.

[146] Jurgen Fuchs, Matthias R. Gaberdiel, Ingo Runkel, and Christoph Schweigert. Topological defects for the free boson CFT. *J. Phys. A*, 40:11403, 2007.

[147] Constantin P. Bachas. On the Symmetries of Classical String Theory. In *workshop on Quantum Mechanics of Fundamental Systems: the Quest for Beauty and Simplicity: Dedicated to Claudio Bunster on the occasion of his 60th birthday*, pages 17–26, 2009.

[148] Costas Bachas, Ilka Brunner, and Daniel Roggenkamp. A worldsheet extension of O(d,d:Z). *JHEP*, 10:039, 2012.

[149] Ilka Brunner, Nils Carqueville, and Daniel Plencner. Orbifolds and topological defects. *Commun. Math. Phys.*, 332:669–712, 2014.

[150] Sriram Bharadwaj, Pierluigi Niro, and Konstantinos Roumpedakis. to appear.

[151] Igor Pak and Greta Panova. On the complexity of computing kronecker coefficients, 2015.

[152] Alexei Borodin and Grigori Olshanski. *Representations of the Infinite Symmetric Group*. Cambridge University Press, 11 2016.

[153] Andrei Okounkov. On the representations of the infinite symmetric group, 1998.

[154] Jeffrey B Remmel. A formula for the kronecker products of schur functions of hook shapes. *Journal of Algebra*, 120(1):100–118, 1989.

[155] Jeffrey B. Remmel and Tamsen Whitehead. On the Kronecker product of Schur functions of two row shapes. *Bulletin of the Belgian Mathematical Society - Simon Stevin*, 1(5):649 – 683, 1994.

[156] Mercedes H. Rosas. The kronecker product of schur functions indexed by two-row shapes or hook shapes, 2000.

[157] Jonathan J. Heckman, Jacob McNamara, Miguel Montero, Adar Sharon, Cumrun Vafa, and Irene Valenzuela. On the Fate of Stringy Non-Invertible Symmetries. 1 2024.

[158] Nathan Berkovits, Cumrun Vafa, and Edward Witten. Conformal field theory of AdS background with Ramond-Ramond flux. *JHEP*, 03:018, 1999.

[159] Andrea Dei, Matthias R. Gaberdiel, Rajesh Gopakumar, and Bob Knighton. Free field world-sheet correlators for AdS_3. *JHEP*, 02:081, 2021.

[160] Lorenz Eberhardt. Partition functions of the tensionless string. *JHEP*, 03:176, 2021.

[161] Bob Knighton, Sean Seet, and Vit Sriprachyakul. Spectral flow and localisation in AdS_3 string theory. 12 2023.

[162] N. M. McStay and R. A. Reid-Edwards. Symmetries and covering maps for the minimal tension string on $AdS_3 \times S^3 \times T^4$. *JHEP*, 04:048, 2024.

[163] Yasuaki Hikida and Volker Schomerus. Engineering Perturbative String Duals for Symmetric Product Orbifold CFTs. 12 2023.

[164] Wolfgang Lerche. Gromov-Witten/Hilbert versus AdS3/CFT2 Correspondence. 10 2023.

[165] Bob Knighton and Vit Sriprachyakul. Unravelling $\mathrm{AdS}_3/\mathrm{CFT}_2$ near the boundary. 4 2024.

[166] Amit Giveon, D. Kutasov, and Nathan Seiberg. Comments on string theory on AdS(3). *Adv. Theor. Math. Phys.*, 2:733–782, 1998.

[167] David Kutasov and Nathan Seiberg. More comments on string theory on AdS(3). *JHEP*, 04:008, 1999.

[168] Amit Giveon and David Kutasov. Notes on AdS(3). *Nucl. Phys. B*, 621:303–336, 2002.

[169] Jihun Kim and Massimo Porrati. On the central charge of spacetime current algebras and correlators in string theory on AdS_3. *JHEP*, 05:076, 2015.

[170] Lorenz Eberhardt and Matthias R. Gaberdiel. String theory on AdS_3 and the symmetric orbifold of Liouville theory. *Nucl. Phys. B*, 948:114774, 2019.

[171] Minoru Wakimoto. Fock representations of the affine lie algebra A1(1). *Commun. Math. Phys.*, 104:605–609, 1986.

[172] Benjamin A. Burrington, Amanda W. Peet, and Ida G. Zadeh. Operator mixing for string states in the d1-d5 cft near the orbifold point. *Physical Review D*, 87(10), May 2013.

[173] Matthias R. Gaberdiel, Cheng Peng, and Ida G. Zadeh. Higgsing the stringy higher spin symmetry. *JHEP*, 10:101, 2015.

[174] Bin Guo and Samir D. Mathur. Lifting of level-1 states in the d1d5 cft. *Journal of High Energy Physics*, 2020(3), March 2020.

[175] Christoph A Keller and Ida G Zadeh. Conformal perturbation theory for twisted fields. *Journal of Physics A: Mathematical and Theoretical*, 53(9):095401, February 2020.

[176] Lorenz Eberhardt. A perturbative CFT dual for pure NS–NS AdS_3 strings. *J. Phys. A*, 55(6):064001, 2022.

[177] Bruno Balthazar, Amit Giveon, David Kutasov, and Emil J. Martinec. Asymptotically free $\mathrm{AdS}_3/\mathrm{CFT}_2$. *JHEP*, 01:008, 2022.

[178] Luis Apolo, Alexandre Belin, Suzanne Bintanja, Alejandra Castro, and Christoph A. Keller. Deforming symmetric product orbifolds: a tale of moduli and higher spin currents. *Journal of High Energy Physics*, 2022(8), August 2022.

[179] Marc-Antoine Fiset, Matthias R. Gaberdiel, Kiarash Naderi, and Vit Sriprachyakul. Perturbing the symmetric orbifold from the worldsheet. *JHEP*, 07:093, 2023.

[180] Lorenz Eberhardt. A perturbative cft dual for pure ns–ns ads3 strings. *Journal of Physics A: Mathematical and Theoretical*, 55(6):064001, January 2022.

[181] Matthias R. Gaberdiel, Rajesh Gopakumar, and Beat Nairz. Beyond the Tensionless Limit: Integrability in the Symmetric Orbifold. 12 2023.

[182] Sergey Frolov and Alessandro Sfondrini. Comments on Integrability in the Symmetric Orbifold. 12 2023.

[183] Kazuhiro Sakai and Yuji Satoh. Entanglement through conformal interfaces. *JHEP*, 12:001, 2008.

[184] Enrico M. Brehm, Ilka Brunner, Daniel Jaud, and Cornelius Schmidt-Colinet. Entanglement and topological interfaces. *Fortsch. Phys.*, 64(6-7):516–535, 2016.

[185] Bob Knighton, Vit Sriprachyakul, and Jakub Vošmera. Topological defects and tensionless holography. 6 2024.

[186] John L. Cardy. Boundary conformal field theory. 11 2004.

[187] Tatsuo Azeyanagi, Andreas Karch, Tadashi Takayanagi, and Ethan G. Thompson. Holographic calculation of boundary entropy. *JHEP*, 03:054, 2008.

[188] Marco Chiodaroli, Michael Gutperle, and Ling-Yan Hung. Boundary entropy of supersymmetric Janus solutions. *JHEP*, 09:082, 2010.

[189] Ian Affleck and Andreas W. W. Ludwig. Universal noninteger 'ground state degeneracy' in critical quantum systems. *Phys. Rev. Lett.*, 67:161–164, 1991.

[190] Kantaro Ohmori and Yuji Tachikawa. Physics at the entangling surface. *J. Stat. Mech.*, 1504:P04010, 2015.

[191] Giuseppe Di Giulio, René Meyer, Christian Northe, Henri Scheppach, and Suting Zhao. On the boundary conformal field theory approach to symmetry-resolved entanglement. *SciPost Phys. Core*, 6:049, 2023.

[192] Yuya Kusuki, Sara Murciano, Hirosi Ooguri, and Sridip Pal. Symmetry-resolved entanglement entropy, spectra & boundary conformal field theory. *JHEP*, 11:216, 2023.

[193] Yuji Satoh. On supersymmetric interfaces for string theory. *JHEP*, 03:072, 2012.

[194] Enrico M. Brehm and Ilka Brunner. Entanglement entropy through conformal interfaces in the 2D Ising model. *JHEP*, 09:080, 2015.

[195] Michael Gutperle and John D. Miller. Entanglement entropy at holographic interfaces. *Phys. Rev. D*, 93(2):026006, 2016.

[196] Andreas Karch, Zhu-Xi Luo, and Hao-Yu Sun. Universal relations for holographic interfaces. *JHEP*, 09:172, 2021.

[197] Andreas Karch, Yuya Kusuki, Hirosi Ooguri, Hao-Yu Sun, and Mianqi Wang. Universal Bound on Effective Central Charge and Its Saturation. 4 2024.

[198] The GAP Group. *GAP – Groups, Algorithms, and Programming, Version 4.13.0*, 2024.

[199] Vershik, Anatolii Moiseevich and Kerov, Sergei Vasil'evich. Asymptotic theory of characters of the symmetric group. *Functional analysis and its applications*, 15(4):246–255, 1981.

[200] Justin Kaidi, Yuji Tachikawa, and Hao Y. Zhang. On a class of selection rules without group actions in field theory and string theory. 1 2024.

[201] C. G. Bollini and J. J. Giambiagi. Dimensional Renormalization: The Number of Dimensions as a Regularizing Parameter. *Nuovo Cim. B*, 12:20–26, 1972.

[202] G. 't Hooft and M. Veltman. Regularization and renormalization of gauge fields. *Nuclear Physics B*, 44(1):189–213, 1972.

[203] G. M. Cicuta and E. Montaldi. Analytic renormalization via continuous space dimension. *Lett. Nuovo Cim.*, 4:329–332, 1972.

[204] Warren Siegel. Supersymmetric dimensional regularization via dimensional reduction. *Physics Letters B*, 84(2):193–196, 1979.

[205] W. Siegel. Inconsistency of supersymmetric dimensional regularization. *Physics Letters B*, 94(1):37–40, 1980.

[206] Simone Giombi, Grigory Tarnopolsky, and Igor R. Klebanov. On C_J and C_T in Conformal QED. *JHEP*, 08:156, 2016.

[207] Kenan Diab, Lin Fei, Simone Giombi, Igor R. Klebanov, and Grigory Tarnopolsky. On C_J and C_T in the Gross–Neveu and O(N) models. *J. Phys. A*, 49(40):405402, 2016.

[208] Andrea Cappelli, Lorenzo Maffi, and Satoshi Okuda. Critical Ising Model in Varying Dimension by Conformal Bootstrap. *JHEP*, 01:161, 2019.

[209] Simone Giombi, Richard Huang, Igor R. Klebanov, Silviu S. Pufu, and Grigory Tarnopolsky. The $O(N)$ Model in $4 < d < 6$: Instantons and complex CFTs. *Phys. Rev. D*, 101(4):045013, 2020.

[210] Johan Henriksson. The critical O(N) CFT: Methods and conformal data. *Phys. Rept.*, 1002:1–72, 2023.

[211] Simone Giombi, Elizabeth Helfenberger, and Himanshu Khanchandani. Line defects in fermionic CFTs. *JHEP*, 08:224, 2023.

[212] Benoit Sirois. Navigating through the O(N) archipelago. *SciPost Phys.*, 13(4):081, 2022.

[213] Zheng Zhou and Yin-Chen He. Slightly broken higher-spin current in bosonic and fermionic QED in the large-N limit. *SciPost Phys.*, 15(2):072, 2023.

[214] Johan Henriksson, Stefanos R. Kousvos, and Marten Reehorst. Spectrum continuity and level repulsion: the Ising CFT from infinitesimal to finite ε. *JHEP*, 02:218, 2023.

[215] Claudio Bonanno, Andrea Cappelli, Mikhail Kompaniets, Satoshi Okuda, and Kay Joerg Wiese. Benchmarking the Ising universality class in $3 \leq d < 4$ dimensions. *SciPost Phys.*, 14(5):135, 2023.

[216] Shai M. Chester and Ning Su. Upper critical dimension of the 3-state Potts model. *Phys. Rev. D*, 111(12):L121701, 2025.

[217] Qingjun Jin, Ke Ren, Gang Yang, and Rui Yu. Is Yang-Mills theory unitary in fractional spacetime dimensions? *Sci. China Phys. Mech. Astron.*, 67(7):271011, 2024.

[218] Qingjun Jin, Ke Ren, Gang Yang, and Rui Yu. Gluonic evanescent operators: negative-norm states and complex anomalous dimensions. *JHEP*, 09:151, 2024.

[219] Marten Reehorst, Slava Rychkov, Benoit Sirois, and Balt C. van Rees. Bootstrapping frustrated magnets: the fate of the chiral $\mathrm{O}(N) \times \mathrm{O}(2)$ universality class. *SciPost Phys.*, 18(2):060, 2025.

[220] Simone Giombi and Anurag Pendse. Line Defects with a Cusp in Fermionic CFTs. 11 2025.

[221] Elia de Sabbata, Nadav Drukker, and Andreas Stergiou. Transdimensional defects. *JHEP*, 08:187, 2025.

[222] Johan Henriksson. The tricritical Ising CFT and conformal bootstrap. *JHEP*, 08:031, 2025.

[223] Bernardo Zan. On the Wilson-Fisher fixed point in the limit of integer spacetime dimensions. 1 2026.

[224] Ludo Fraser-Taliente. Local CFTs extremise F. 4 2026.

[225] Li-Yuan Chiang, David Poland, and Gordon Rogelberg. Moments in the CFT Landscape. 3 2026.

[226] Fabiana De Cesare and Slava Rychkov. Disturbing News About the d=2+epsilon Expansion. *PTEP*, 2025(9):093B02, 2025.

[227] Fabiana De Cesare and Slava Rychkov. Disturbing news about the d=2+epsilon expansion II. Assessing the recombination scenario. 2 2026.

[228] Yongwei Guo and Zhijin Li. Central charges C_J and C_T in QED_d-GNY model and scalar QED_d. 6 2026.

[229] Shi Chen, Aleksey Cherman, and Robert D. Pisarski. Does Hot QCD Have a Conformal Manifold in the Chiral Limit? *Phys. Rev. Lett.*, 137(6):061903, 2026.

[230] John Cardy. Logarithmic conformal field theories as limits of ordinary CFTs and some physical applications. *J. Phys. A*, 46:494001, 2013.

[231] Victor Gorbenko and Bernardo Zan. Two-dimensional O(n) models and logarithmic CFTs. *JHEP*, 10:099, 2020.

[232] Nikita Nekrasov. Analytic continuation and supersymmetry. *Proc. Symp. Pure Math.*, 107:167–178, 2024.

[233] Kasia Budzik, Harish Murali, and Pedro Vieira. Following Black Hole States. 6 2023.

[234] Weiguang Cao, Xiaochuan Lu, and Tom Melia. Constraints on the spectrum of field theories with non-integer $O(N)$ symmetry from quantum evanescence. *SciPost Phys. Core*, 7:055, 2024.

[235] Jesper Lykke Jacobsen, Rongvoram Nivesvivat, and Hubert Saleur. On currents in the $O(n)$ loop model. *SciPost Phys.*, 16(4):111, 2024.

[236] Paul Roux, Jesper Lykke Jacobsen, Sylvain Ribault, and Hubert Saleur. Critical spin chains and loop models with $PSU(n)$ symmetry. *SciPost Phys.*, 18(1):033, 2025.

[237] Jaychandran Padayasi, Abijith Krishnan, Max A. Metlitski, Ilya A. Gruzberg, and Marco Meineri. The extraordinary boundary transition in the 3d O(N) model via conformal bootstrap. *SciPost Phys.*, 12(6):190, 2022.

[238] Damon J. Binder and Slava Rychkov. Deligne Categories in Lattice Models and Quantum Field Theory, or Making Sense of $O(N)$ Symmetry with Non-integer N. *JHEP*, 04:117, 2020.

[239] Kenneth G. Wilson and Michael E. Fisher. Critical exponents in 3.99 dimensions. *Phys. Rev. Lett.*, 28:240–243, 1972.

[240] Matthijs Hogervorst, Slava Rychkov, and Balt C. van Rees. Unitarity violation at the Wilson-Fisher fixed point in 4-ϵ dimensions. *Phys. Rev. D*, 93(12):125025, 2016.

[241] Simone Giombi, Igor R. Klebanov, and Grigory Tarnopolsky. Conformal QED$_d$, F-Theorem and the ϵ Expansion. *J. Phys. A*, 49(13):135403, 2016.

[242] Daniel L. Jafferis, Igor R. Klebanov, Silviu S. Pufu, and Benjamin R. Safdi. Towards the F-Theorem: N=2 Field Theories on the Three-Sphere. *JHEP*, 06:102, 2011.

[243] Igor R. Klebanov, Silviu S. Pufu, and Benjamin R. Safdi. F-Theorem without Supersymmetry. *JHEP*, 10:038, 2011.

[244] H. Casini and Marina Huerta. On the RG running of the entanglement entropy of a circle. *Phys. Rev. D*, 85:125016, 2012.

[245] Sheer El-Showk, Miguel Paulos, David Poland, Slava Rychkov, David Simmons-Duffin, and Alessandro Vichi. Conformal Field Theories in Fractional Dimensions. *Phys. Rev. Lett.*, 112:141601, 2014.

[246] Julian Schwinger. Gauge invariance and mass. ii. *Phys. Rev.*, 128:2425–2429, Dec 1962.

[247] Sidney Coleman. More about the massive schwinger model. *Annals of Physics*, 101(1):239–267, 1976.

[248] G. 't Hooft. A two-dimensional model for mesons. *Nuclear Physics B*, 75(3):461–470, 1974.

[249] Curtis G. Callan, Nigel Coote, and David J. Gross. Two-dimensional yang-mills theory: A model of quark confinement. *Phys. Rev. D*, 13:1649–1669, Mar 1976.

[250] Sidney Coleman. Quantum sine-gordon equation as the massive thirring model. *Phys. Rev. D*, 11:2088–2097, Apr 1975.

[251] Edward Witten. Nonabelian Bosonization in Two-Dimensions. *Commun. Math. Phys.*, 92:455–472, 1984.

[252] Robert D. Pisarski. Chiral-symmetry breaking in three-dimensional electrodynamics. *Phys. Rev. D*, 29:2423–2426, May 1984.

[253] Thomas Appelquist, Daniel Nash, and L. C. R. Wijewardhana. Critical behavior in (2+1)-dimensional qed. *Phys. Rev. Lett.*, 60:2575–2578, Jun 1988.

[254] Thomas W. Appelquist, Mark Bowick, Dimitra Karabali, and L. C. R. Wijewardhana. Spontaneous chiral-symmetry breaking in three-dimensional qed. *Phys. Rev. D*, 33:3704–3713, Jun 1986.

[255] Thomas Appelquist and Daniel Nash. Critical behavior in (2+1)-dimensional qcd. *Phys. Rev. Lett.*, 64:721–724, Feb 1990.

[256] A.M. Polyakov. Quark confinement and topology of gauge theories. *Nuclear Physics B*, 120(3):429–458, 1977.

[257] T. Banks, R. Myerson, and J. Kogut. Phase transitions in abelian lattice gauge theories. *Nuclear Physics B*, 129(3):493–510, 1977.

[258] Jorge V. José, Leo P. Kadanoff, Scott Kirkpatrick, and David R. Nelson. Renormalization, vortices, and symmetry-breaking perturbations in the two-dimensional planar model. *Phys. Rev. B*, 16:1217–1241, Aug 1977.

[259] C. Dasgupta and B. I. Halperin. Phase transition in a lattice model of superconductivity. *Phys. Rev. Lett.*, 47:1556–1560, Nov 1981.

[260] Ian Affleck, Michael Dine, and Nathan Seiberg. Dynamical Supersymmetry Breaking in Supersymmetric QCD. *Nucl. Phys. B*, 241:493–534, 1984.

[261] Nathan Seiberg and Edward Witten. Gauge dynamics and compactification to three-dimensions. In *Conference on the Mathematical Beauty of Physics (In Memory of C. Itzykson)*, pages 333–366, 6 1996.

[262] Kenneth A. Intriligator and N. Seiberg. Mirror symmetry in three-dimensional gauge theories. *Phys. Lett. B*, 387:513–519, 1996.

[263] Ofer Aharony. Baryons, monopoles and dualities in Chern-Simons-matter theories. *JHEP*, 02:093, 2016.

[264] Y. Nambu and G. Jona-Lasinio. Dynamical model of elementary particles based on an analogy with superconductivity. i. *Phys. Rev.*, 122:345–358, Apr 1961.

[265] G. 't Hooft. Symmetry breaking through bell-jackiw anomalies. *Phys. Rev. Lett.*, 37:8–11, Jul 1976.

[266] Sidney Coleman and Edward Witten. Chiral-symmetry breakdown in large-n chromodynamics. *Phys. Rev. Lett.*, 45:100–102, Jul 1980.

[267] C. Vafa and E. Witten. Restrictions on symmetry breaking in vector-like gauge theories. *Nuclear Physics B*, 234(1):173–188, 1984.

[268] Cumrun Vafa and Edward Witten. Parity conservation in quantum chromodynamics. *Phys. Rev. Lett.*, 53:535–536, Aug 1984.

[269] Kenneth G. Wilson. Confinement of quarks. *Phys. Rev. D*, 10:2445–2459, Oct 1974.

[270] S. Mandelstam. Ii. vortices and quark confinement in non-abelian gauge theories. *Physics Reports*, 23(3):245–249, 1976.

[271] N. Seiberg and E. Witten. Monopoles, duality and chiral symmetry breaking in n = 2 supersymmetric qcd. *Nuclear Physics B*, 431(3):484–550, 1994.

[272] C. Montonen and D. Olive. Magnetic monopoles as gauge particles? *Physics Letters B*, 72(1):117–120, 1977.

[273] P. Goddard, J. Nuyts, and D. Olive. Gauge theories and magnetic charge. *Nuclear Physics B*, 125(1):1–28, 1977.

[274] Nathan Seiberg. Five-dimensional SUSY field theories, nontrivial fixed points and string dynamics. *Phys. Lett. B*, 388:753–760, 1996.

[275] Kenneth A. Intriligator, David R. Morrison, and Nathan Seiberg. Five-dimensional supersymmetric gauge theories and degenerations of Calabi-Yau spaces. *Nucl. Phys. B*, 497:56–100, 1997.

[276] Edward Witten. Some comments on string dynamics. In *STRINGS 95: Future Perspectives in String Theory*, pages 501–523, 7 1995.

[277] Edward Witten. Solutions of four-dimensional field theories via M-theory. *Nucl. Phys. B*, 500:3–42, 1997.

[278] Cumrun Vafa and Edward Witten. A Strong coupling test of S duality. *Nucl. Phys. B*, 431:3–77, 1994.

[279] Fabiana De Cesare, Lorenzo Di Pietro, and Marco Serone. Five-dimensional CFTs from the epsilon-expansion. *Phys. Rev. D*, 104(10):105015, 2021.

[280] Kenneth A. Intriligator and N. Seiberg. Lectures on supersymmetric gauge theories and electric-magnetic duality. *Nucl. Phys. B Proc. Suppl.*, 45BC:1–28, 1996.

[281] Vladimir Bashmakov, Jaume Gomis, Zohar Komargodski, and Adar Sharon. Phases of $\mathcal{N} = 1$ theories in $2 + 1$ dimensions. *JHEP*, 07:123, 2018.

[282] Jaume Gomis, Zohar Komargodski, and Nathan Seiberg. Phases Of Adjoint QCD_3 And Dualities. *SciPost Phys.*, 5(1):007, 2018.

[283] Zohar Komargodski and Nathan Seiberg. A symmetry breaking scenario for QCD_3. *JHEP*, 01:109, 2018.

[284] Lorenzo Di Pietro, Zohar Komargodski, Itamar Shamir, and Emmanuel Stamou. Quantum Electrodynamics in d=3 from the epsilon Expansion. *Phys. Rev. Lett.*, 116(13):131601, 2016.

[285] G. P. Korchemsky. On level crossing in conformal field theories. *JHEP*, 03:212, 2016.

[286] Alexander N. Manashov and Leonid A. Shumilov. Correction exponents in the chiral Heisenberg model at $1/N^2$: singular contributions and operator mixing. *Eur. Phys. J. C*, 86(6):648, 2026.

[287] John C. Collins. *Renormalization : An Introduction to Renormalization, the Renormalization Group and the Operator-Product Expansion*, volume 26 of *Cambridge Monographs on Mathematical Physics*. Cambridge University Press, Cambridge, 1984.

[288] Masuo Suzuki. Phase transition and fractals. *Progress of Theoretical Physics*, 69(1):65–76, 01 1983.

[289] Y Gefen, A Aharony, and B B Mandelbrot. Phase transitions on fractals. i. quasi-linear lattices. *Journal of Physics A: Mathematical and General*, 16(6):1267, apr 1983.

[290] Y Gefen, A Aharony, Y Shapir, and B B Mandelbrot. Phase transitions on fractals. ii. sierpinski gaskets. *Journal of Physics A: Mathematical and General*, 17(2):435, feb 1984.

[291] Y Gefen, A Aharony, and B B Mandelbrot. Phase transitions on fractals. iii. infinitely ramified lattices. *Journal of Physics A: Mathematical and General*, 17(6):1277, apr 1984.

[292] E. Pytte. Monte carlo study of ising spin dynamics on a fractal lattice. *Phys. Rev. B*, 34:2060(R)–2063(R), Aug 1986.

[293] J.C. Le Guillou and J. Zinn Justin. Accurate critical exponents for ising like systems in non-integer dimensions. In J.C. LE GUILLOU and J. ZINN-JUSTIN, editors, *Large-Order Behaviour of Perturbation Theory*, volume 7 of *Current Physics–Sources and Comments*, pages 559–564. Elsevier, 1990.

[294] G. Eyink. Quantum Field Theory Models on Fractal Space-time. 1: Introduction and Overview. *Commun. Math. Phys.*, 125:613–636, 1989.

[295] Pascal Monceau and Michel Perreau. Critical behavior of the ising model on fractal structures in dimensions between one and two: Finite-size scaling effects. *Phys. Rev. B*, 63:184420, Apr 2001.

[296] Arnab Kar and S. G. Rajeev. Scalar Quantum Field Theory on Fractals. *Annals Phys.*, 327:102–117, 2012.

[297] Hangmo Yi. Quantum critical behavior of the quantum ising model on fractal lattices. *Physical Review E*, 91(1), January 2015.

[298] Beni Yoshida and Aleksander Kubica. Quantum criticality from Ising model on fractal lattices. 4 2014.

[299] Roe Goodman and Nolan R. Wallach. Symmetry, representations, and invariants. Graduate Texts in Mathematics. Springer, 2009.

[300] Pierre Deligne. La categorie des representations du groupe symetrique st, lorsquet n'est pas un entier naturel. *Algebraic groups and homogeneous spaces*, 01 2007.

[301] Michiel Bos. An example of dimensional regularization with antisymmetric tensors. *Annals of Physics*, 181(2):177–197, 1988.

[302] Davide Gaiotto, Suriyah Rajalingam Kannagi, and Sergio Sanjurjo. D-branes and the planar limit of Chern-Simons theory. Link invariants. *JHEP*, 03:194, 2026.

[303] Edward Witten. Baryons in the 1/N Expansion. *Nucl. Phys. B*, 160:57–115, 1979.

[304] Nathan Benjamin, Jaeha Lee, Hirosi Ooguri, and David Simmons-Duffin. Universal asymptotics for high energy CFT data. *JHEP*, 03:115, 2024.

[305] A. N. Redlich. Parity violation and gauge noninvariance of the effective gauge field action in three dimensions. *Phys. Rev. D*, 29:2366–2374, May 1984.

[306] S. Deser, R. Jackiw, and S. Templeton. Three-dimensional massive gauge theories. *Phys. Rev. Lett.*, 48:975–978, Apr 1982.

[307] Alessandro Bondi, Guiseppe Curci, Giampiero Paffuti, and Paolo Rossi. Metric and central charge in the perturbative approach to two dimensional fermionic models. *Annals of Physics*, 199(2):268–339, 1990.

[308] Michael J. Dugan and Benjamín Grinstein. On the vanishing of evanescent operators. *Physics Letters B*, 256(2):239–244, 1991.

[309] Lorenzo Di Pietro and Emmanuel Stamou. Scaling dimensions in QED3 from the epsilon-expansion. *JHEP*, 12:054, 2017.

[310] Lorenzo Di Pietro and Emmanuel Stamou. Operator mixing in the epsilon-expansion: Scheme and evanescent-operator independence. *Phys. Rev. D*, 97(6):065007, 2018.

[311] Marcus Berg, Cecile DeWitt-Morette, Shangjr Gwo, and Eric Kramer. The Pin groups in physics: C, P, and T. *Rev. Math. Phys.*, 13:953–1034, 2001.

[312] Shai M. Chester, Mark Mezei, Silviu S. Pufu, and Itamar Yaakov. Monopole operators from the $4-\epsilon$ expansion. *JHEP*, 12:015, 2016.

[313] A.M. Polyakov. Gauge fields as rings of glue. *Nuclear Physics B*, 164:171–188, 1980.

[314] Gabriel Cuomo, Zohar Komargodski, and Avia Raviv-Moshe. Renormalization Group Flows on Line Defects. *Phys. Rev. Lett.*, 128(2):021603, 2022.

[315] Gabriel Cuomo, Yin-Chen He, and Zohar Komargodski. Impurities with a cusp: general theory and 3d Ising. *JHEP*, 11:061, 2024.

[316] J. A. Gracey. Electron mass anomalous dimension at O(1/(Nf(2)) in quantum electrodynamics. *Phys. Lett. B*, 317:415–420, 1993.

[317] Michael Hermele, T. Senthil, and Matthew P. A. Fisher. Erratum: Algebraic spin liquid as the mother of many competing orders [phys. rev. b 72, 104404 (2005)]. *Phys. Rev. B*, 76:149906, Oct 2007.

[318] Shai M. Chester and Silviu S. Pufu. Anomalous dimensions of scalar operators in QED_3. *JHEP*, 08:069, 2016.

[319] Rufus Boyack, Ahmed Rayyan, and Joseph Maciejko. Deconfined criticality in the qed_3 gross-neveu-yukawa model: The $1/n$ expansion revisited. *Phys. Rev. B*, 99:195135, May 2019.

[320] Lukas Janssen and Yin-Chen He. Critical behavior of the qed_3-gross-neveu model: Duality and deconfined criticality. *Phys. Rev. B*, 96:205113, Nov 2017.

[321] Diego Delmastro, Jaume Gomis, and Matthew Yu. Infrared phases of 2d QCD. *JHEP*, 02:157, 2023.

[322] Ruochen Ma and Chong Wang. Theory of deconfined pseudocriticality. *Phys. Rev. B*, 102(2):020407, 2020.

[323] Adam Nahum. Note on Wess-Zumino-Witten models and quasiuniversality in 2+1 dimensions. *Phys. Rev. B*, 102(20):201116, 2020.